

Methods in
Molecular Biology 1195

Springer Protocols

Kursad Turksen *Editor*

Epidermal Cells

Methods and Protocols

Third Edition

 Humana Press

METHODS IN MOLECULAR BIOLOGY

Series Editor
John M. Walker
School of Life Sciences
University of Hertfordshire
Hatfield, Hertfordshire, AL10 9AB, UK

For further volumes:
<http://www.springer.com/series/7651>

Epidermal Cells

Methods and Protocols

Third Edition

Edited by

Kursad Turksen

*Ottawa Hospital Research Institute,
Ottawa, ON, Canada*

 **Humana Press**

Editor

Kursad Turksen
Ottawa Hospital Research Institute
Spratt Centre for Stem Cell Research
Regenerative Medicine Program
Ottawa, ON, Canada

ISSN 1064-3745 ISSN 1940-6029 (electronic)
ISBN 978-1-4939-1223-0 ISBN 978-1-4939-1224-7 (eBook)
DOI 10.1007/978-1-4939-1224-7
Springer New York Heidelberg Dordrecht London

Library of Congress Control Number: 2014941687

© Springer Science+Business Media New York 2014

This work is subject to copyright. All rights are reserved by the Publisher, whether the whole or part of the material is concerned, specifically the rights of translation, reprinting, reuse of illustrations, recitation, broadcasting, reproduction on microfilms or in any other physical way, and transmission or information storage and retrieval, electronic adaptation, computer software, or by similar or dissimilar methodology now known or hereafter developed. Exempted from this legal reservation are brief excerpts in connection with reviews or scholarly analysis or material supplied specifically for the purpose of being entered and executed on a computer system, for exclusive use by the purchaser of the work. Duplication of this publication or parts thereof is permitted only under the provisions of the Copyright Law of the Publisher's location, in its current version, and permission for use must always be obtained from Springer. Permissions for use may be obtained through RightsLink at the Copyright Clearance Center. Violations are liable to prosecution under the respective Copyright Law.

The use of general descriptive names, registered names, trademarks, service marks, etc. in this publication does not imply, even in the absence of a specific statement, that such names are exempt from the relevant protective laws and regulations and therefore free for general use.

While the advice and information in this book are believed to be true and accurate at the date of publication, neither the authors nor the editors nor the publisher can accept any legal responsibility for any errors or omissions that may be made. The publisher makes no warranty, express or implied, with respect to the material contained herein.

Printed on acid-free paper

Humana Press is a brand of Springer
Springer is part of Springer Science+Business Media (www.springer.com)

Preface

Since the development of the first set of conditions supportive of epidermal cell culture by Howard Green's lab more than three decades ago, the field of epidermal biology has advanced tremendously. This latest edition of epidermal cell protocols underscores these advances in our understanding of epidermal biology. I have gathered updated and new protocols that complement and extend the earlier edition. The inclusion of protocols useful for both *in vitro* and *in vivo* studies reflects many useful developments in the field. I am grateful to and sincerely thank all the contributors for their willingness to share and provide details for protocols that will continue to accelerate work in the field.

I also thank Dr. John Walker, the Editor in Chief of the MIMB series, for his vision and support for these volumes.

I am also grateful to Patrick Martin, Editor of Springer's Protocols series, for his support and encouragement in putting together this volume.

A special *thank-you* goes to David Casey for always being there to answer my and contributors' questions; this helped tremendously with the timely completion of this volume.

Ottawa, ON, Canada

Kursad Turksen

Contents

<i>Preface</i>	<i>v</i>
<i>Contributors</i>	<i>ix</i>
1 Differentiation of Human Induced Pluripotent Stem Cells into a Keratinocyte Lineage..... <i>Igor Kogut, Dennis R. Roop, and Ganna Bilousova</i>	1
2 Differentiation of Epidermal Keratinocytes from Human Embryonic Stem Cells..... <i>Fahad K. Kidwai, Tong Cao, and Kai Lu</i>	13
3 Protocol for Serial Cultivation of Epithelial Cells Without Enzymes or Chemical Compounds..... <i>Dongxia Ye and Antonio Peramo</i>	23
4 Growth and Differentiation of HaCaT Keratinocytes..... <i>Van G. Wilson</i>	33
5 Transgene Delivery to Cultured Keratinocytes via Replication-Deficient Adenovirus Vectors..... <i>Vincent P. Ramirez and Brian J. Aneskievich</i>	43
6 Analyzing the Global Chromatin Structure of Keratinocytes by MNase-Seq..... <i>Jason M. Rizzo and Satrajit Sinha</i>	49
7 Analysis and Meta-analysis of Transcriptional Profiling in Human Epidermis..... <i>Claudia Mimoso, Ding-Dar Lee, Jiri Zavadil, Marjana Tomic-Canic, and Miroslav Blumenberg</i>	61
8 Compound Screening and Transcriptional Profiling in Human Primary Keratinocytes: A Brief Guideline..... <i>Raphaela Rid, Harald Hundsberger, and Kamil Önder</i>	99
9 Preparation of Primary Cultures of Mouse Epidermal Keratinocytes and the Measurement of Phospholipase D Activity..... <i>Lakiea J. Bailey, Vivek Choudhary, Purnima Merai, and Wendy B. Bollag</i>	111
10 Lipid Rafts and Detergent-Resistant Membranes in Epithelial Keratinocytes..... <i>Kathleen P. McGuinn and Mý G. Mahoney</i>	133
11 MMP-2, -9 and TIMP-1, -2 Assays in Keratinocyte Cultures..... <i>Takashi Kobayashi</i>	145
12 Reactive Oxygen Species (ROS) Protection via Cysteine Oxidation in the Epidermal Cornified Cell Envelope..... <i>Wilbert P. Vermeij and Claude Backendorf</i>	157
13 Modified Methods for Growing 3-D Skin Equivalents: An Update..... <i>Rebecca Lamb and Carrie A. Ambler</i>	171

14	A Novel Three-Dimensional Cell Culture Method to Analyze Epidermal Cell Differentiation In Vitro.	183
	<i>Toji Okugawa and Yobei Hirai</i>	
15	Reconstruction of Normal and Pathological Human Epidermis on Polycarbonate Filter.	191
	<i>Evelyne De Vuyst, Céline Charlier, Séverine Giltaire, Valérie De Glas, Catherine Lambert de Rouvroit, and Yves Poumay</i>	
16	Methods for the Preparation of an Autologous Serum-Free Cultured Epidermis and for Autografting Applications.	203
	<i>John J. Wille, Jeremy J. Burdge, and Jong Y. Park</i>	
17	Human Keratinocyte Cultures in the Investigation of Early Steps of Human Papillomavirus Infection.	219
	<i>Laura M. Griffin, Louis Cicchini, Tao Xu, and Dohun Pyeon</i>	
18	Preparation and Delivery of 4-Hydroxy-Tamoxifen for Clonal and Polyclonal Labeling of Cells of the Surface Ectoderm, Skin, and Hair Follicle.	239
	<i>Christine Chevalier, Jean-François Nicolas, and Anne-Cécile Petit</i>	
19	Microdissection and Visualization of Individual Hair Follicles for Lineage Tracing Studies.	247
	<i>Inês Sequeira, Emilie Legué, Suzanne Capgras, and Jean-François Nicolas</i>	
20	Isolation and Characterization of a Stem Cell Side-Population from Mouse Hair Follicles.	259
	<i>Paula L. Miliiani de Marval, Sun Hye Kim, and Marcelo L. Rodriguez-Puebla</i>	
21	Multiscale Mathematical Modeling and Simulation of Cellular Dynamical Process.	269
	<i>Shinji Nakaoka</i>	
22	Erratum to: Differentiation of Human Induced Pluripotent Stem Cells into a Keratinocyte Lineage.	285
	<i>Igor Kogut, Dennis R. Roop, and Ganna Bilousova</i>	
23	Erratum to: Reactive Oxygen Species (ROS) Protection via Cysteine Oxidation in the Epidermal Cornified Cell Envelope.	287
	<i>Wilbert P. Vermeij and Claude Backendorf</i>	
24	Erratum to: Human Keratinocyte Cultures in the Investigation of Early Steps of Human Papillomavirus Infection.	289
	<i>Laura M. Griffin, Louis Cicchini, Tao Xu, and Dohun Pyeon</i>	
	<i>Index</i>	291

Contributors

- CARRIE A. AMBLER • *School of Biological and Biomedical Sciences, Durham University, Durham, UK; Biophysical Sciences Institute, Durham University, Durham, UK*
- BRIAN J. ANESKIEVICH • *Graduate Program in Pharmacology & Toxicology, Department of Pharmaceutical Sciences, School of Pharmacy, University of Connecticut, Storrs, CT, USA*
- CLAUDE BACKENDORF • *University of Leiden, Leiden, The Netherlands*
- LAKIEA J. BAILEY • *Department of Physiology, Georgia Regents University, Augusta, GA, USA*
- GANNA BILOUSOVA • *Department of Dermatology, University of Colorado, Aurora, CO, USA; Charles C. Gates Center for Regenerative Medicine and Stem Cell Biology, University of Colorado, Aurora, CO, USA*
- MIROSLAV BLUMENBERG • *The RO Perelman Department of Dermatology, NYU Cancer Institute, NYU Langone Medical Center, New York, NY, USA; Department of Biochemistry and Molecular Pharmacology, NYU Cancer Institute, NYU Langone Medical Center, New York, NY, USA*
- WENDY B. BOLLAG • *Department of Physiology, Georgia Regents University, Augusta, GA, USA; Charlie Norwood VA Medical Center, Augusta, GA, USA*
- JEREMY J. BURDGE • *Wound Care Clinic, Grant Hospital, Columbus, OH, USA*
- TONG CAO • *Oral Sciences Disciplines, Faculty of Dentistry, National University of Singapore, Singapore, Singapore*
- SUZANNE CAPGRAS • *CNRS, URA2578, Unité de Biologie Moléculaire du Développement, Institut Pasteur, Paris, France*
- CÉLINE CHARLIER • *Cell and Tissue Laboratory, URPHYM, Namur Research Institute for Life Sciences, University of Namur, Namur, Belgium*
- CHRISTINE CHEVALIER • *CNRS, URA2578, Unité de Biologie Moléculaire du Développement, Institut Pasteur, Paris, France*
- VIVEK CHOUDHARY • *Department of Physiology, Georgia Regents University, Augusta, GA, USA; Charlie Norwood VA Medical Center, Augusta, GA, USA*
- LOUIS CICCINI • *School of Medicine, University of Colorado, Aurora, CO, USA*
- VALÉRIE DE GLAS • *Cell and Tissue Laboratory, URPHYM, Namur Research Institute for Life Sciences, University of Namur, Namur, Belgium*
- EVELYNE DE VUYST • *Cell and Tissue Laboratory, URPHYM, Namur Research Institute for Life Sciences, University of Namur, Namur, Belgium*
- SÉVERINE GILTAIRE • *Cell and Tissue Laboratory, URPHYM, Namur Research Institute for Life Sciences, University of Namur, Namur, Belgium*
- LAURA M. GRIFFIN • *School of Medicine, University of Colorado, Aurora, CO, USA*
- YOHEI HIRAI • *Department of Bioscience, School of Science and Engineering, Kwansei Gakuin University, Sanda, Japan*
- HARALD HUNDSBERGER • *Department of Medical and Pharmaceutical Biotechnology, University of Applied Sciences, Krems, Austria*
- FAHAD K. KIDWAI • *Oral Sciences Disciplines, Faculty of Dentistry, National University of Singapore, Singapore, Singapore*

- SUN HYE KIM • *Department of Molecular Biomedical Sciences, Center for Comparative Medicine & Translational Research, North Carolina State University, Raleigh, NC, USA; Center for Human Health & the Environment, North Carolina State University, Raleigh, NC, USA*
- TAKASHI KOBAYASHI • *Department of Dermatology, Chiba Medical Center, Teikyo University, Ichihara, Japan*
- IGOR KOGUT • *Department of Dermatology, University of Colorado, Aurora, CO, USA; Charles C. Gates Center for Regenerative Medicine and Stem Cell Biology, University of Colorado, Aurora, CO, USA*
- REBECCA LAMB • *School of Biological and Biomedical Sciences, Durham University, Durham, UK*
- CATHERINE LAMBERT DE ROUVROIT • *Cell and Tissue Laboratory, URPHYM, Namur Research Institute for Life Sciences, University of Namur, Namur, Belgium*
- DING-DAR LEE • *The RO Perelman Department of Dermatology, NYU Cancer Institute, NYU Langone Medical Center, New York, NY, USA; Department of Biochemistry and Molecular Pharmacology, NYU Cancer Institute, NYU Langone Medical Center, New York, NY, USA; Department of Dermatology, Taipei Veterans General Hospital, Faculty of Medicine, National Yang-Ming University, Taipei, Taiwan*
- EMILIE LEGUÉ • *CNRS, URA2578, Unité de Biologie Moléculaire du Développement, Institut Pasteur, Paris, France*
- KAI LU • *Institute for Integrated Cell-Material Sciences, Kyoto University, Kyoto, Japan*
- Mÿ G. MAHONEY • *Department of Dermatology and Cutaneous Biology, Thomas Jefferson University, Philadelphia, PA, USA; Department of Biochemistry and Molecular Biology, Thomas Jefferson University, Philadelphia, PA, USA*
- KATHLEEN P. MCGUINN • *Department of Dermatology and Cutaneous Biology, Thomas Jefferson University, Philadelphia, PA, USA*
- PURNIMA MERAI • *Department of Physiology, Georgia Regents University, Augusta, GA, USA*
- PAULA L. MILIANI DE MARVAL • *Department of Molecular Biomedical Sciences, Center for Comparative Medicine & Translational Research, North Carolina State University, Raleigh, NC, USA; Center for Human Health & the Environment, North Carolina State University, Raleigh, NC, USA*
- CLAUDIA MIMOSO • *The RO Perelman Department of Dermatology, NYU Cancer Institute, NYU Langone Medical Center, New York, NY, USA; Department of Biochemistry and Molecular Pharmacology, NYU Cancer Institute, NYU Langone Medical Center, New York, NY, USA*
- SHINJI NAKAOKA • *Laboratory for Mathematical Modeling of Immune System, RIKEN Center for Integrative Medical Science Center (IMS-RCAI), Yokohama, Kanagawa, Japan*
- JEAN-FRANÇOIS NICOLAS • *CNRS, URA2578, Unité de Biologie Moléculaire du Développement, Institut Pasteur, Paris, France*
- YOJI OKUGAWA • *Department of Bioscience, School of Science and Engineering, Kwansei Gakuin University, Sanda, Japan*
- KAMIL ÖNDER • *Division of Molecular Dermatology, Department of Dermatology, Paracelsus Private Medical University Salzburg, Salzburg, Austria*
- JONG Y. PARK • *Division of Cancer Prevention and Control, Moffitt Cancer Center, Tampa, FL, USA*
- ANTONIO PERAMO • *Department of Surgery, University of Michigan, Ann Arbor, MI, USA*

- ANNE-CÉCILE PETIT • CNRS, URA2578, *Unité de Biologie Moléculaire du Développement, Institut Pasteur, Paris, France*
- YVES POUMAY • *Cell and Tissue Laboratory, URPHYM, Namur Research Institute for Life Sciences, University of Namur, Namur, Belgium*
- DOHUN PYEON • *School of Medicine, University of Colorado, Aurora, CO, USA*
- VINCENT P. RAMIREZ • *Graduate Program in Pharmacology & Toxicology, Department of Pharmaceutical Sciences, School of Pharmacy, University of Connecticut, Storrs, CT, USA*
- RAPHAELA RID • *Division of Molecular Dermatology, Department of Dermatology, Paracelsus Private Medical University Salzburg, Salzburg, Austria*
- JASON M. RIZZO • *Department of Biochemistry, Center of Excellence in Bioinformatics and Life Sciences, State University of New York, Buffalo, NY, USA*
- MARCELO L. RODRIGUEZ PUEBLA • *Department of Molecular Biomedical Sciences, Center for Comparative Medicine & Translational Research, North Carolina State University, Raleigh, NC, USA; Center for Human Health & the Environment, North Carolina State University, Raleigh, NC, USA*
- DENNIS R. ROOP • *Department of Dermatology, University of Colorado, Aurora, CO, USA; Charles C. Gates Center for Regenerative Medicine and Stem Cell Biology, University of Colorado, Aurora, CO, USA*
- INÈS SEQUEIRA • CNRS, URA2578, *Unité de Biologie Moléculaire du Développement, Institut Pasteur, Paris, France*
- SATRAJIT SINHA • *Department of Biochemistry, Center of Excellence in Bioinformatics and Life Sciences, State University of New York, Buffalo, NY, USA*
- MARJANA TOMIC-CANIC • *Wound Healing and Regenerative Medicine Research Program, Department of Dermatology and Cutaneous Surgery, University of Miami, Miami, FL, USA; Hussman Institute of Human Genomics, Miller Medical School, University of Miami, Miami, FL, USA*
- WILBERT P. VERMEIJ • *University of Leiden, Leiden, The Netherlands*
- JOHN J. WILLE • *Department of Cell Biology, Autologenic, Inc., Chesterfield, NJ, USA*
- VAN G. WILSON • *Department of Microbial Pathogenesis and Immunology, College of Medicine, Texas A&M Health Science Center, Bryan, TX, USA*
- TAO XU • *School of Medicine, University of Colorado, Aurora, CO, USA*
- DONGXIA YE • *Shanghai Ninth People's Hospital Affiliated to Medical School of Shanghai Jiaotong University, Shanghai, China*
- JIRI ZAVADIL • *Mechanisms of Carcinogenesis Section, International Agency for Research on Cancer, Lyon, France*

Differentiation of Human Induced Pluripotent Stem Cells into a Keratinocyte Lineage

Igor Kogut, Dennis R. Roop, and Ganna Bilousova

Abstract

Direct reprogramming of somatic cells into induced pluripotent stem cells (iPSCs) provides an opportunity to develop novel personalized treatment options for numerous diseases and to advance current approaches for cell-based drug discoveries and disease modeling. The ability to differentiate iPSCs into relevant cell types is an important prerequisite for the successful development of iPSC-based treatment and modeling strategies. Here, we describe a protocol for the efficient differentiation of human iPSCs into functional keratinocytes. The protocol employs treating iPSCs with retinoic acid and bone-morphogenetic protein-4 to induce differentiation toward a keratinocyte lineage, which is then followed by the growth of differentiated iPSCs on collagen type I- and collagen type IV-coated dishes to enrich for iPSC-derived keratinocytes.

Keywords: Induced pluripotent stem cells, iPSCs, Differentiation, Keratinocytes, Retinoic acid, Bone-morphogenetic protein-4

Abbreviations

ColI	Type I collagen
ColIV	Type IV collagen
ESC	Embryonic stem cell
iPSC	Induced pluripotent stem cell
Krt14	Keratin 14
RA	Retinoic acid
BMP4	Bone-morphogenetic protein-4

1 Introduction

The discovery that the ectopic expression of selected transcription factors can reprogram somatic cells into embryonic stem cell (ESC)-like cells, termed induced pluripotent stem cells (iPSCs), has opened up a new era in research and therapy (1–5). The iPSC technology addresses many obstacles associated with the use of ESCs, including ethical concerns, and allows for the generation of

patient-specific pluripotent stem cells, which can be genetically corrected, differentiated into adult lineages, and returned to the same patient as an autograft (6–9). In addition to genetic disorders, the iPSC technology can be applicable to tissue regeneration, basic science research of human development, and disease modeling. However, before iPSC-based approaches are successfully implemented into the clinic, efficient protocols for the differentiation of iPSCs into relevant cell types need to be developed.

In this chapter, we describe a protocol for the efficient differentiation of human iPSCs into keratinocytes, which may potentially be applicable for cell transplantation in the clinic and for modeling inherited skin diseases, such as the epidermolysis bullosa (EB) subtypes and congenital ichthyoses (10–12). The protocol has been adapted from our previously published work (13) on the differentiation of mouse iPSCs into keratinocytes as well as studies published by other groups on the differentiation of human ESCs and iPSCs into epithelial and keratinocyte lineages (14, 15) with modifications. The resulting iPSC-derived keratinocyte-like cells express the markers specific to authentic basal layer keratinocytes, such as keratin 14 (Krt14) and keratin 5 (Krt5), and are able to reconstitute a normal stratified epidermis when grafted onto an immunodeficient mouse. The protocol requires the seeding of iPSCs onto Geltrex (Gibco) and collagen type I (ColI)-coated dishes followed by the combined treatment with retinoic acid (RA) to induce iPSC differentiation into an ectodermal fate (16) and with bone-morphogenetic protein-4 (BMP4) to block the commitment toward a neural fate (17). In addition, we discovered that growth on collagen type IV (ColIV)- and ColI-coated dishes, which mimics the environment of the basal layer of the skin, improves the efficiency of differentiation to a keratinocyte fate. To enrich for keratinocyte stem cells that are positive for Krt14, a keratin marker confirming commitment of the ectoderm to a keratinocyte fate, we exploit the ability of Krt14-positive cells to rapidly attach to ColI/ColIV-coated surfaces (18).

The methodology for iPSC differentiation toward a keratinocyte lineage relies primarily on the ability to maintain long-term human keratinocyte cultures. Therefore, before initiating this iPSC differentiation protocol, we recommend establishing the growth conditions for culturing normal human keratinocytes that allow for their maintenance in culture for at least 6–10 passages. We found that commercially available CnT-07 medium or EpiLife medium supplemented with EpiLife Defined Growth Supplement (EDGS) promotes more efficient expansion of human keratinocytes seeded onto ColI-coated dishes. The growth of differentiated iPSC-derived cultures under keratinocyte cell culture conditions following the rapid attachment to ColI/ColIV-coated plates allows for the efficient enrichment for Krt14-positive keratinocytes up to 80–90 % (13, 15).

2 Materials

2.1 Coating Tissue Culture Dishes with Geltrex and Coll

1. Collagen, type I: 3 mg/mL solution (Advanced BioMatrix).
2. Geltrex hESC-qualified Reduced Growth Factor Basement Membrane Matrix (Gibco).
3. Dulbecco's Modified Eagle Medium/Nutrient Mixture F-12 (DMEM/F12) (Gibco).
4. 60 mm tissue culture (TC) dishes.

2.2 Plating iPSCs for Differentiation

1. N2B27 medium: Combine DMEM/F12 and Neurobasal medium (Gibco) in a 1:1 ratio and supplement with 0.1 mM nonessential amino acids, 1 mM glutamine, 55 μ M 2-mercaptoethanol (2-ME), N2 supplement (100 \times) (Life Technologies), B27 supplement (50 \times) (Life Technologies), 50 μ g/mL ascorbic acid, 0.05 % bovine serum albumin (BSA), 50 U/mL penicillin–streptomycin, 100 ng/mL basic FGF (Life Technologies), and 10 μ g/mL Y27632 (Sigma-Aldrich).
2. Dispase (BD).

2.3 Differentiation of iPSCs with RA and BMP4

1. 1 mM stock solution of all-trans RA (Sigma-Aldrich) reconstituted in dimethyl sulfoxide (DMSO).
2. 25 μ g/ μ L stock solution of human BMP4 (R&D Systems) reconstituted in sterile 4 mM HCl containing 0.1 % BSA.
3. Defined keratinocyte serum-free medium (DKSFM) (Gibco) supplemented with 50 U/mL penicillin–streptomycin. DKSFM is sold as a kit containing DKSFM basal medium and DKSFM growth supplement.
4. 1 \times PBS.
5. CnT-07 epidermal keratinocyte medium (CELLnTEC) containing 50 U/mL penicillin–streptomycin. CnT-07 is sold as a kit containing CnT basal medium and supplements A, B, and C.

2.4 Rapid Attachment and Culturing of iPSC-Derived Keratinocytes

1. 100 mm tissue culture dish.
2. Collagen, type IV, powder (Sigma-Aldrich).
3. 0.25 % Glacial acetic acid.
4. Collagen, type I, 3 mg/ml solution (Advanced BioMatrix).
5. CnT-07 (*see* Section 2.3).
6. Accutase (Gibco).
7. 1 \times PBS without Ca²⁺ and Mg²⁺.

2.5 Equipment

1. Biological safety cabinet.
2. 37 °C water bath.
3. 37 °C/5 % CO₂ humidified tissue culture incubator.
4. Centrifuge (room temperature).

3 Methods

3.1 Coating Tissue Culture Dishes with Geltrex and ColI

The procedure is to be performed in a biological safety cabinet using aseptic techniques. Similar to Matrigel, Geltrex matrix solidifies rapidly at room temperature (RT). Therefore; it is recommended to aliquot each new batch of the matrix upon arrival and use pre-chilled pipet tips, racks, and tubes while working with the reagent. We recommend making 50, 100, and 200 μL aliquots and to store them at $-80\text{ }^{\circ}\text{C}$. Use Geltrex at 1:100 dilutions. While the maintenance of feeder-free iPSC cultures requires only Geltrex as a surface coating agent, for iPSC differentiation, the combination of Geltrex and ColI is more efficient to induce the commitment toward a keratinocyte lineage (*see Note 1*). The coating procedure below is described for a 60 mm tissue culture dish. If a larger dish is to be used, adjust the volume of the coating solution accordingly.

1. Remove a 50 μL aliquot of Geltrex from the $-80\text{ }^{\circ}\text{C}$ freezer, and place it on ice in the biological safety cabinet.
2. Add 5 mL of cold sterile DMEM/F12 to a 15 mL conical tube.
3. Use a 1 mL glass pipet, take 1 mL cold DMEM/F12 from the 15 mL conical tube prepared in step 2, and add to the frozen Geltrex. Gently pipet up and down to thaw and dissolve Geltrex. Transfer the dissolved Geltrex to the rest of DMEM/F12 in the 15 mL conical tube prepared in step 2. Pipet to mix diluted Geltrex.
4. Add 50 μL of 3 mg/mL ColI stock solution into diluted Geltrex from step 3. Pipet to mix diluted Geltrex with ColI. Add 4 mL of coating solution into 60 mm dish. Tap or swirl the plate to ensure that the entire surface is coated.
5. Incubate the dish with Geltrex/ColI coating solution at $37\text{ }^{\circ}\text{C}$ in the tissue culture incubator for at least 1 h.
6. Once the coating is complete, leave the coating solution in the dish and proceed with the plating of iPSCs as described in the next subsection (*see Section 3.2*). Alternatively, aspirate the coating solution and add 2 mL of fresh DMEM/F12 into the-coated dish to prevent it from drying before plating the cells.

3.2 Plating iPSCs for Differentiation

Prepare one 60 mm tissue culture dish of feeder-free iPSCs grown to $\sim 70\%$ of confluency (*see Note 2*). Examine cells under a microscope to confirm the absence of contamination and the maintenance of their undifferentiated phenotype. If the cells are stressed or dying, they start to differentiate, presenting themselves as “cobblestone” areas with larger polymorphic cells, and should not be used for the differentiation toward keratinocytes. For iPSC differentiation toward keratinocytes, we recommend a 1:8 split ratio of iPSCs (*see Note 3*).

1. Prewarm N2B27 medium and Dispase in the 37 °C water bath.
2. Using the microscope, confirm that the colonies are ready for passaging. Gently aspirate medium from the dish. Add 2 mL of 1 × PBS, swirl the plate to wash the cells, and gently aspirate PBS.
3. Add 1 mL of Dispase and return the plate to the 37 °C tissue culture incubator for 3–5 min.
4. While the cells are being incubated with Dispase, gently aspirate the Geltrex/ColI coating solution (or DMEM/F12) from step 6 in the Geltrex/ColI coating procedure (*see* Section 3.1) and add 4 mL of complete N2B27 medium into the coated dish.
5. After 3–5-min incubation with Dispase, confirm that the cells are ready to be picked by looking for rolled or folded edges around the colonies.
6. Transfer the plate to the biological safety cabinet, and carefully aspirate Dispase. After the treatment with Dispase, the colonies are very loosely attached to the surface of the dish and may peel off if too much force is used (*see* Note 4).
7. Gently add 2 mL of plain DMEM/F12. Aspirate off the medium, and repeat the wash three times.
8. Add 2 mL of complete N2B27 into the dish, and gently scrape the colonies off the plate. Transfer the cells from the dish into a 15 mL conical tube, and add 6 mL of complete N2B27 to bring the total volume of cell suspension to 8 mL.
9. Gently mix the cell suspension to break large clumps of cells. Transfer 1 mL of the cell suspension to the coated dish prepared in step 3 of the current subsection. Discard or replate the leftover cells using the conditions established for a given laboratory (*see* Note 5).
10. Transfer the newly plated cells to the incubator, and gently shake the plate back and forth and side to side to distribute the cells evenly (*see* Note 6). Incubate the cells overnight in the 37 °C tissue culture incubator.

3.3 Differentiation of iPSCs with RA and BMP4

The differentiation and subculturing of iPSC-derived keratinocytes are to be performed in a biological safety cabinet using aseptic techniques. The protocol schematic is outlined in Fig. 1. Examine the new plate the day after passaging to confirm the successful attachment of iPSCs. If iPSCs start forming colonies (Fig. 2a), proceed with the differentiation protocol below (*see* Note 7).

1. Prewarm complete DKSFM (with antibiotics and DKSFM supplement) in the 37 °C water bath.
2. Add 5 mL of prewarmed DKSFM from the previous step to a 15 mL conical tube, add 5 µL of 1 mM RA to achieve 1 µM final working concentration and 5 µL of 25 µg/µL BMP4 to achieve 25 ng/mL final working concentration, and mix well.

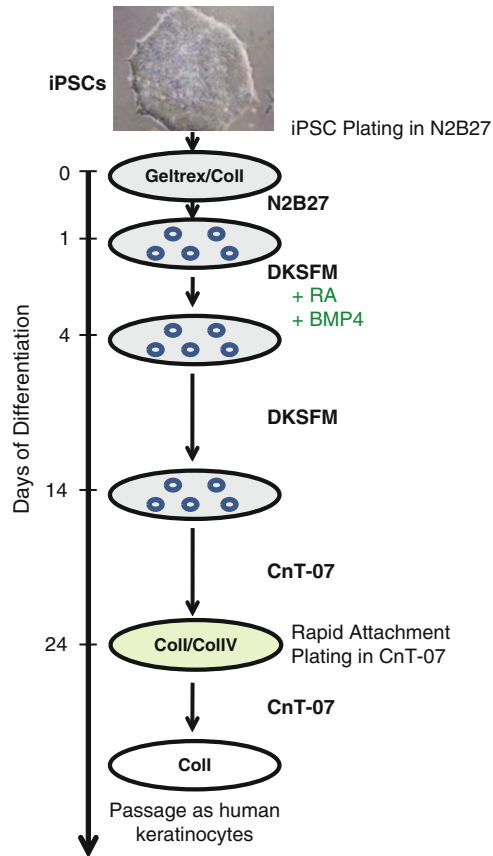


Fig. 1 Schematic representation of the protocol for the differentiation of human iPSCs into a keratinocyte lineage

3. Aspirate off N2B27 medium from the dish with plated iPSCs, wash once with 4 mL of $1 \times$ PBS, and add 4 mL of DKSFM containing $1 \mu\text{M}$ RA and $25 \text{ ng}/\mu\text{L}$ BMP4 from the step above. This is day 1 of differentiation procedure.
4. Transfer the cells to the incubator and incubate for 48 h.
5. Replace the medium with fresh DKSFM containing $1 \mu\text{M}$ RA and $25 \text{ ng}/\mu\text{L}$ BMP4 after 48 h of incubation. Transfer the cell to the incubator for another 48 h.
6. After the second round of 48-h induction (day 4 of differentiation), replace the medium with complete DKSFM without RA and BMP4. Incubate cells in the incubator for 10 days in complete DKSFM, changing medium every other day.
7. On day 14 of differentiation, prepare complete CnT-07 medium by adding antibiotics and provided supplements and prewarm the medium. By this day, the majority of the cells in the outgrown iPSC colony start exhibiting an epithelial-like phenotype (*see* Fig. 2b).

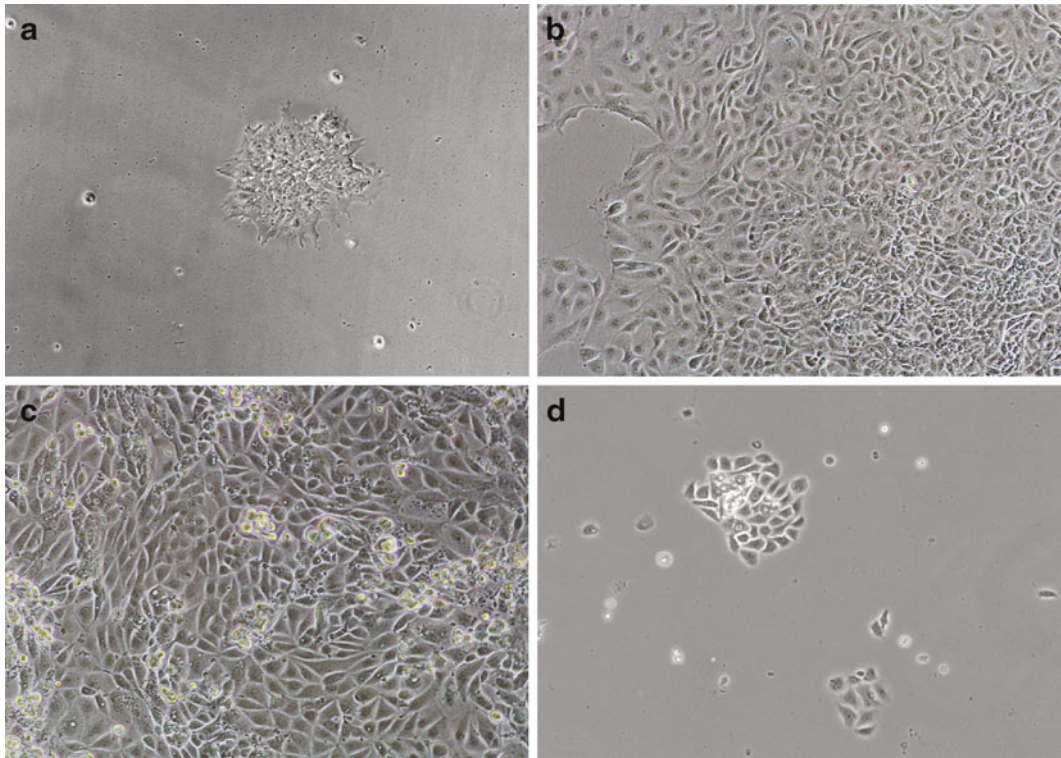


Fig. 2 The stages of iPSC differentiation during keratinocyte derivation. Human iPSCs generated with a modified mRNA-based approach from human neonatal fibroblasts were differentiated into keratinocytes using RA and BMP4. **(a)** Human iPSCs seeded at low density for differentiation on day 1 of differentiation. **(b)** An iPSC colony outgrown on a Geltrex/Coll-coated plate after the combined treatment with RA and BMP4 on day 14 of differentiation. **(c)** An iPSC colony outgrown on a Geltrex/Coll-coated plate on day 24 of differentiation before rapid attachment plating. **(d)** iPSC-derived keratinocytes at passage 1 post rapid attachment plating (day 29 of differentiation, day 5 post rapid attachment). All images were taken with 10× objectives

8. Aspirate off DKSEFM from differentiated cells and replace with 4 mL of complete CnT-07. Incubate the cells in the tissue culture incubator for another 10 days, changing complete CnT-07 every other day.

3.4 Rapid Attachment and Culturing of iPSC-Derived Keratinocytes

On day 24 of differentiation, many cells that migrate away from the outgrown iPSC colony will exhibit a keratinocyte-like phenotype (Fig. 2c) and start expressing p63, a master regulator required for the commitment of the ectoderm to a keratinocyte fate (19, 20), and Krt14 (see Note 8). By this day, the 60 mm dish used for iPSC differentiation is fully confluent and needs to be passaged. To enrich for iPSC-derived keratinocytes during passaging, we perform the rapid attachment of the differentiated iPSC culture to Coll/ColIV-coated plates. We recommend using up to four 100 mm Coll/ColIV-coated tissue culture dishes to

perform the rapid attachment procedure from one 60 mm dish containing differentiated iPSCs. If only one 100 mm dish is to be used, plate one-fourth of the differentiated iPSC culture for the rapid attachment procedure.

3.4.1 Coating Plates with ColI and ColIV

The procedure is to be performed in the biological safety cabinet using aseptic techniques.

1. Reconstitute ColIV powder to a concentration of 2 mg/mL in sterile 0.25 % glacial acetic acid. Dissolve for several hours at 2–8 °C, occasionally swirling. Make aliquots, and store them at –20 °C.
2. Thaw the aliquot of ColIV stock solution (2 mg/mL) very slowly by placing the vial in an ice bucket and keeping it at 4 °C for several hours.
3. Resuspend ColIV stock solution in the appropriate volume (5 mL per each 100 mm dish) of sterile 0.25 % glacial acetic acid to a final working concentration of 7 µg/mL. Add an appropriate volume of ColI stock solution to achieve a final working ColI concentration of 30 µg/mL. Coat the plates by using 5 mL of working solution to cover a 100 mm dish. Incubate the plates at room temperature in the biological safety cabinet for 1 h.
4. Aspirate the liquid from the coated plates, and rinse the dishes once with 5 mL of sterile 1× PBS and once with 5 mL of ddH₂O.
5. Air-dry the washed dishes in the biological safety cabinet. Use plates directly or seal them with Parafilm and store at 4 °C for up to 6 months. To use a previously stored ColIV-coated plate, allow the plate to warm up at room temperature in the biological safety cabinet for at least 1 h prior to plating cells.

3.4.2 Rapid Attachment of iPSC-Derived Keratinocytes

1. On day 24 of differentiation, prewarm complete CnT-07, Accutase, and ColI/ColIV-coated dish(es).
2. Wash the cells with 1× PBS, add 2 mL of Accutase, and incubate in the tissue culture incubator for 5 min (*see Note 9*). Confirm under the microscope that cells start detaching.
3. Add 3 mL of complete Cnt-07, pipet up and down to dislodge the cells, and collect the cell suspension into a 15 mL conical tube. Spin the cells down at 260 × *g* for 5 min, and aspirate the supernatant. Resuspend the pellet in 10 mL of complete Cnt-07 medium, repeat the spin at 260 × *g* for 5 min, and aspirate the supernatant.
4. Resuspend the pellet in 4 mL of complete CnT-07 and pipet up and down to break cell clumps into single cells.

5. Add 9 mL of complete CnT-07 medium into each ColI/ColIV-coated dish, and transfer 1 mL of cell suspension from step 4 above into each ColI/ColIV-coated dish. Allow the cells to attach to the coated dish at room temperature for 15–30 min (*see Note 10*).
6. Carefully aspirate the medium with the floating cells (these are undifferentiated or partially differentiated iPSCs). Do not disturb the attached cells (these are iPSC-derived Krt14-positive cells). Add 10 mL of fresh complete CnT-07 medium into the plate with the attached cells. Let the cells expand in the 37 °C tissue culture incubator, changing the medium every other day. Passage cells as needed (*see Note 11*) with Accutase in CnT-07 or EpiLife (with EDGS supplement) on ColI-coated dishes. After passage 2 or 3 and following the rapid attachment step, the culture should consist of ~90 % of Krt14-positive cells exhibiting a keratinocyte-like phenotype (*see Fig. 2d*). The keratinocyte-like phenotype of the obtained culture can be verified by the standard immunofluorescence analyses for Krt14 expression and by the ability to reconstitute a normal stratified epidermis in organotypic cultures.

4 Notes

1. We initially used growth factor reduced BD Matrigel to plate iPSCs for differentiation. However, the combination of Geltrex and ColI gives a higher yield of keratinocytes upon iPSC differentiation.
2. The provided protocol is optimized for iPSCs generated with an integration-free modified mRNA-based reprogramming approach (21, 22). We maintain iPSCs on either mitomycin C-inactivated human neonatal fibroblasts or Geltrex matrix in N2B27 medium (23) under low O₂ conditions (5 %). While iPSCs are maintained under low-oxygen conditions, the differentiation toward a keratinocyte lineage is performed under atmospheric O₂ (~20 %) in the regular tissue culture incubator. To avoid spontaneous differentiation, the iPSC culture should only be grown to a subconfluent state. Healthy undifferentiated human iPSCs usually form round tight colonies with clear margins (Fig. 2a). Avoid using partially differentiated iPSCs for keratinocyte derivation. Although the provided protocol has been shown to produce functional keratinocytes from human iPSCs generated by an integrating lentivirus approach, there is always a possibility that the partial reactivation of exogenous factors, especially c-Myc and Klf4, may influence the differentiation of these lentivirally derived iPSCs into keratinocytes, and the protocol may require optimizations for this type of iPSCs.

3. While we recommend a 1:4 or a 1:5 split ratio for the maintenance of iPSCs, for their differentiation, iPSCs need to be seeded as small clumps at very low density to allow for enough surface area for the sufficient expansion of differentiating cells. The colonies should be evenly dispersed in the dish. To achieve this, gently shake the dish from side to side and front to back during passaging.
4. If iPSC colonies peel off while being incubated with Dispase, collect Dispase with detached iPSC colonies into a 15 mL conical tube, add plain DMEM/F12 into the dish, gently scrape the remaining colonies off, and transfer the colonies from the dish into the 15 mL conical tube with Dispase and the rest of iPSCs. Spin the cells down at $75 \times g$ for 10 min, and aspirate the supernatant. Gently resuspend the iPSC pellet in plain DMEM/F12, spin the cells down at $75 \times g$ for 10 min, and repeat the wash two times. Proceed with step 9 of Section 3.2.
5. While we regularly use N2B27 medium for the maintenance of human iPSCs, other media can also be used.
6. Do not swirl the dish since the cells tend to cluster in the middle when the dish is being swirled.
7. If the colonies start to differentiate spontaneously, discard the dish and repeat the replating of iPSCs using a fresh iPSC culture.
8. We are able to obtain a maximum of 25–30 % of K14-positive cells in the entire culture before the rapid attachment step. The efficiency of differentiation usually varies from 5 to 30 % among experiments and among iPSC lines.
9. We do not recommend using trypsin at this stage of the protocol.
10. If only a few cells attach, incubate the plate for up to an hour in the 37 °C tissue culture incubator. Alternatively, skip the rapid attachment during the first passage. Instead, split the entire plate of differentiated iPSCs onto four fresh ColI-coated dishes in complete CnT-07. Let the cells reach 60–70 % confluency, and then perform the rapid attachment plating as described in Section 3.4.
11. It may take up to 2 weeks to expand the culture of iPSC-derived keratinocytes post rapid attachment plating. Do not allow the cells to overgrow, since this will induce premature differentiation. Ideally, the cells should be subcultured onto a fresh ColI-coated dish once they reach 60 % confluency. We recommend using Accutase instead of trypsin for keratinocyte passaging.

Acknowledgements

We are grateful for funding support from the National Institutes of Health (R01AR059947 and P30 AR057212), the US Department of Defense (PR110793), the Foundation for Ichthyosis and Related Skin Types (F.I.R.S.T.), and the Dystrophic Epidermolysis Bullosa Research Association (DEBRA) International.

References

1. Takahashi K, Yamanaka S (2006) Induction of pluripotent stem cells from mouse embryonic and adult fibroblast cultures by defined factors. *Cell* 126(4):663–676
2. Takahashi K, Tanabe K, Ohnuki M, Narita M, Ichisaka T, Tomoda K, Yamanaka S (2007) Induction of pluripotent stem cells from adult human fibroblasts by defined factors. *Cell* 131(5):861–872
3. Yu J, Vodyanik MA, Smuga-Otto K, Antosiewicz-Bourget J, Franke JL, Tian S, Nie J, Jonsdottir GA, Ruotti V, Stewart R, Slukvin II, Thomson JA (2007) Induced pluripotent stem cell lines derived from human somatic cells. *Science* 318(5858):1917–1920
4. Okita K, Ichisaka T, Yamanaka S (2007) Generation of germline-competent induced pluripotent stem cells. *Nature* 448(7151):313–317
5. Wernig M, Meissner A, Foreman R, Brambrink T, Ku M, Hochedlinger K, Bernstein BE, Jaenisch R (2007) In vitro reprogramming of fibroblasts into a pluripotent ES-cell-like state. *Nature* 448(7151):318–324
6. Yamanaka S (2007) Strategies and new developments in the generation of patient-specific pluripotent stem cells. *Cell Stem Cell* 1(1):39–49
7. Nishikawa S, Goldstein RA, Nierras CR (2008) The promise of human induced pluripotent stem cells for research and therapy. *Nat Rev Mol Cell Biol* 9(9):725–729
8. Yamanaka S (2009) A fresh look at iPS cells. *Cell* 137(1):13–17
9. Takahashi K (2012) Cellular reprogramming—lowering gravity on Waddington’s epigenetic landscape. *J Cell Sci* 125(Pt 11):2553–2560
10. Khavari PA (1997) Therapeutic gene delivery to the skin. *Mol Med Today* 3(12):533–538
11. DiGiovanna JJ, Robinson-Bostom L (2003) Ichthyosis: etiology, diagnosis, and management. *Am J Clin Dermatol* 4(2):81–95
12. Smith F (2003) The molecular genetics of keratin disorders. *Am J Clin Dermatol* 4(5):347–364
13. Bilousova G, Chen J, Roop DR (2011) Differentiation of mouse induced pluripotent stem cells into a multipotent keratinocyte lineage. *J Invest Dermatol* 131(4):857–864
14. Metallo CM, Ji L, de Pablo JJ, Palecek SP (2008) Retinoic acid and bone morphogenetic protein signaling synergize to efficiently direct epithelial differentiation of human embryonic stem cells. *Stem Cells* 26(2):372–380
15. Itoh M, Kiuru M, Cairo MS, Christiano AM (2011) Generation of keratinocytes from normal and recessive dystrophic epidermolysis bullosa-induced pluripotent stem cells. *Proc Natl Acad Sci U S A* 108(21):8797–8802
16. Bain G, Kitchens D, Yao M, Huettner JE, Gottlieb DI (1995) Embryonic stem cells express neuronal properties in vitro. *Dev Biol* 168(2):342–357
17. Gambaro K, Aberdam E, Virolle T, Aberdam D, Rouleau M (2006) BMP-4 induces a Smad-dependent apoptotic cell death of mouse embryonic stem cell-derived neural precursors. *Cell Death Differ* 13(7):1075–1087
18. Bickenbach JR, Chism E (1998) Selection and extended growth of murine epidermal stem cells in culture. *Exp Cell Res* 244(1):184–195
19. Mills AA, Zheng B, Wang XJ, Vogel H, Roop DR, Bradley A (1999) p63 is a p53 homologue required for limb and epidermal morphogenesis. *Nature* 398(6729):708–713
20. Koster MI, Kim S, Mills AA, DeMayo FJ, Roop DR (2004) p63 is the molecular switch for initiation of an epithelial stratification program. *Genes Dev* 18(2):126–131
21. Warren L, Manos PD, Ahfeldt T, Loh YH, Li H, Lau F, Ebina W, Mandal PK, Smith ZD, Meissner A, Daley GQ, Brack AS, Collins JJ, Cowan C, Schlaeger TM, Rossi DJ (2010) Highly efficient reprogramming to pluripotency and

- directed differentiation of human cells with synthetic modified mRNA. *Cell Stem Cell* 7 (5):618–630
22. Warren L, Ni Y, Wang J, Guo X (2012) Feeder-free derivation of human induced pluripotent stem cells with messenger RNA. *Sci Rep* 2:657
23. Liu Y, Song Z, Zhao Y, Qin H, Cai J, Zhang H, Yu T, Jiang S, Wang G, Ding M, Deng H (2006) A novel chemical-defined medium with bFGF and N2B27 supplements supports undifferentiated growth in human embryonic stem cells. *Biochem Biophys Res Commun* 346 (1):131–139

Differentiation of Epidermal Keratinocytes from Human Embryonic Stem Cells

Fahad K. Kidwai, Tong Cao, and Kai Lu

Abstract

For many years, cell therapies have been hampered by limited availability and inter-batch variability of primary cells. Human embryonic stem cell (hESC) can give rise to specialized cells like keratinocytes and recently emerged as a virtually unlimited source of potential therapeutic cells. However, xenogeneic components in differentiation cocktails have been limiting the clinical potential of hESC-derived keratinocytes (hESCs-Kert). Here, we demonstrated efficient differentiation of H9 human embryonic stem cells (H9-hESCs) into keratinocytes (H9-Kert^{ACC}) in an autogenic co-culture system. We used activin as the main factor to induce keratinocyte differentiation. H9-Kert^{ACC} expressed keratinocyte markers at mRNA and protein levels. Establishment of such animal-free microenvironment for keratinocyte differentiation will accelerate potential clinical application of hESCs.

Keywords: Activin, Co-culture, Differentiation, Epidermal, Human embryonic stem cell, Keratinocyte, Tissue engineering, Xeno-free

1 Introduction

Human embryonic stem cell (hESC)-derived keratinocytes (hESCs-Kert) hold great clinical, industrial, and research potential. Currently, our efforts are focused on the application of hESCs-Kert for regenerative dental medicine and as an in vitro model for industrial research and development.

To date, strategies for inducing hESCs towards the keratinocyte lineage involve the use of xenogeneic components including feeder cells and/or extracellular matrix (ECM) (1–9). Presence of these xenogeneic components in culture environment limits the potential of hESCs due to the risk of transmitting animal pathogens and viral/bacterial infections (10–13). Furthermore, exposure of hESCs to animal components in culture system may cause higher expression of immunogenic agents (e.g., *N*-glycolylneuraminic acid and *N*-acetylneuraminic acid) in hESCs (14, 15). Eradicating or minimizing exposure to xenogeneic components during cultivation and differentiation would enhance hESCs-Kert's potential for clinical application (16, 17).

2 Materials

2.1 Cell Culture and Differentiation

- (a) Mouse embryonic fibroblast medium (mEF medium): 900 ml of Dulbecco's Modified Eagle medium (DMEM) (Sigma) and 100 ml of fetal bovine serum (FBS, Biowest), supplemented with 10 ml of non-essential amino acids solution (Sigma) and 10 ml of penicillin–streptomycin 100× solution (GIBCO/Brl). Stored at 4 °C.
- (b) mEF freezing medium: 70 ml of DMEM and 20 ml of FBS. Stored at 4 °C.
- (c) hESC medium: 1:1 DMEM/F-12, supplemented with 20 % knockout serum replacement, 1 % non-essential amino acid, 1 mM L-glutamine, 4 ng/mL FGF-2, and 0.1 mM β-mercaptoethanol (Sigma, St Louis, MO). Stored at 4 °C.
- (d) Embryoid body medium: 80 % DMEM/F12 and 20 % knock-out serum replacer (KSR), supplemented with 1 % nonessential amino acids, 1 mM L-glutamine, and 0.1 mM β-mercaptoethanol. Stored at 4 °C.
- (e) FAD medium: Mixture of 3:1 of DMEM and Ham's F12 media supplemented with 50 µg/ml ascorbic acid (Sigma), 2 % FBS, 5 µg/ml insulin, 10 ng/ml recombinant human epidermal growth factor, and 0.5 µM of retinoic acid (RA). Stored at 4 °C.
- (f) Defined keratinocyte serum free medium and supplement (DKSF, Invitrogen). Stored at 4 °C.

2.2 Reverse Transcriptase-Polymerase Chain Reaction Analysis and Real-Time RT-PCR

- (a) cDNA reaction mixture: 4 µl of 5× cDNA synthesis buffer, 1 µl of iScript enzyme mixture, 500 ng of mRNA samples, and RNase-free water.
- (b) Real-time reaction mixture: 4 µl of 5× Green GoTaq® Flexi Buffer (Promega), 0.1 µl of GoTaq® Flexi DNA Polymerase (Promega), 1.2 µl of 25 mM MgCl₂ (Promega), 0.4 µl of forward primer (1st BASE), 0.4 µl of reverse primer (1st BASE), 0.4 µl of dNTP (Promega), 12.5 µl of cDNA template 1 µl, distilled and deionized H₂O (ddH₂O).
- (c) Real-time reverse transcriptase-polymerase chain reaction (RT-PCR) master mix: 10 µl of SYBR Green PCR Master Mix, 0.4 µl of forward primer (1st BASE), 0.4 µl of reverse primer (1st BASE), 1 µl of cDNA, 8.2 µl of distilled and deionized H₂O (ddH₂O).
- (d) Primers used in the experiments are listed in Table 1.

2.3 Immunofluorescence Staining and Flow Cytometry

- (a) Fixing solution: 4 % (w/v) paraformaldehyde (Sigma).
- (b) Permeabilization solution: 0.4 % (v/v) Triton X-100 in PBS.

Table 1
Oligonucleotide sequences of primers used in RT-PCR and real-time RT-PCR

Gene	GenBank accession number	Forward primer	Reverse primer	Amplicon size
sox1	NM_005986.2	5'-caa tgcggg gag gagaag tc-3'	5'-ctc tggaccaaactgtgg cg-3'	464
pax 6	NM_000280.3	5'-ggc agg tat tac gag act gg-3'	5'-cct cat ctgaattcttc cg-3'	427
K18	NM_000224.2	5'-ccg tcttgcctgctgatga ct-3'	5'-ggc ctttactctctctctg g-3'	200
p63	NM_001114978.1	5'-gga aaacaatgccc- agac tc-3'	5'-gtg gaatcgtc cag gtg gc-3'	294
k14	NM_000526.4	5'-gac cat tgaggacct gag ga-3'	5'-att gat gtcggcttcac ac-3'	157
hOCT4	NM_001173531.1	5'-cgt gaagctgga- gaaggagaagct g-3'	5'-aag ggcccagcttacacatg ttc-3'	246
Nestin	NM_006617.1	5'-tgaaggcaatcaca- cagg-3'	5'-tgacccaacatgacctctg-3'	136
TERT	NM_001193376.1	5'-agctatgcccggacc- tccat-3'	5'-gcctgcagcaggaggatctt-3'	185
β -actin	NM_001017992.2	5'-avaghgctcgcctt- tgcc-3'	5'-acatgccggagccgttgc-3'	198
β -tubulin iii	NM_001197181.1	5'-gggcattcca- acctt-3'	5'-agctcggcgcctctgtgtag-3'	440

- (c) Washing buffer: 1× PBS supplemented with 0.05 % (v/v) Tween 20.
- (d) Staining buffer: 4 % BSA in PBS.
- (e) Primary antibodies and secondary antibodies used in the experiments are listed in Table 2.
- (f) Slow fade gold anti-fade reagent DAPI (Invitrogen) (dilution factor, 1:100).
- (g) FACS buffer: MACS[®] buffer solution (Miltenyi Biotec).

3 Methods

During embryogenesis, keratinocyte differentiation initiates from the expression of K18⁺ cells in primitive epithelium. Later on, these K18⁺ cells are replaced by p63⁺ keratinocyte progenitor cells (18). It has been reported that expression of p63⁺ results in the induction

Table 2
List of antibodies used in immunofluorescence and flow cytometry

Antibody	Source	Catalog # and company	References
Primary antibody	Mouse anti-human K18	sc-6259 (DC-10) Biotechnology, Santa Cruz, CA, USA	(22)
Primary antibody	Mouse anti-human K14	sc 58724 (LL002), Biotechnology, Santa Cruz, CA, USA	(23)
Primary antibody	Mouse anti-integrin $\alpha 6$	sc-71423 (3H1512), Biotechnology, Santa Cruz, CA, USA	(24)
Primary antibody	Mouse anti-human involucrin	sc-21748 (SY5); Santa Cruz Biotechnology, CA, USA	(25)
Primary antibody	Rabbit anti-human filaggrin	sc-30229 (H-300); Santa Cruz Biotechnology, CA, USA	(26)
Secondary antibody	Alexa Fluor 488 rabbit anti-mouse IgG	A11037; Invitrogen, CA, USA	(21)
Secondary antibody	Alexa Fluor 594 goat anti-rabbit IgG	A11037; Invitrogen, CA, USA	(21)

of genes like Ly6/PLAUR domain-containing 3 (LYPD3), integral membrane 2B, lymphocyte antigen 6 complex (LY6G6C), RAB25 (Ras-related protein Rab-25), nucleoside diphosphate kinase 2 (NME2), insulin-like growth factor-binding protein 3 (IGFBP3), insulin-like growth factor 2 (IGF2), Wnt-related genes, and fibroblast growth factor receptor 2 (FGFR2). These cells subsequently give rise to basal keratinocytes (K14⁺ and integrin alpha 6⁺) cells in stratified epidermis (18, 19).

3.1 Cell Culture and Differentiation

- (a) The National Institutes of Health-registered H9 hESC line (Agreement no. 04-W094, WiCell Research Institute, Madison, WI) was used in this study.
- (b) H9-hESCs were seeded onto mitotically inactivated mEF feeder cells in hESC medium as previously reported (20, Note 1).
- (c) Upon confluence, hESC colonies were treated with 1 mg/ml collagenase IV (GIBCO) for 3 min at 37 °C followed by manual dissection and centrifugation at $200 \times g$ for 5 min in a 15 ml falcon tube.
- (d) The cell pellets were re-suspended in fresh hESC culture medium and seeded on inactivated feeder cells at 1:6 splitting ratio every 5–7 days.
- (e) All cells were cultured at 37 °C with 5 % CO₂ atm and 95 % humidity.

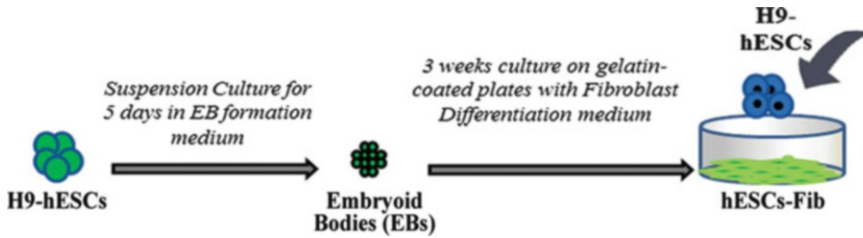


Fig. 1 Schematic diagram showing the establishment of an autogenic microenvironment for hESC cultivation and differentiation. *EB* embryoid body, *hESCs* human embryonic stem cells, *hESCs-Fib* hESC-derived fibroblast

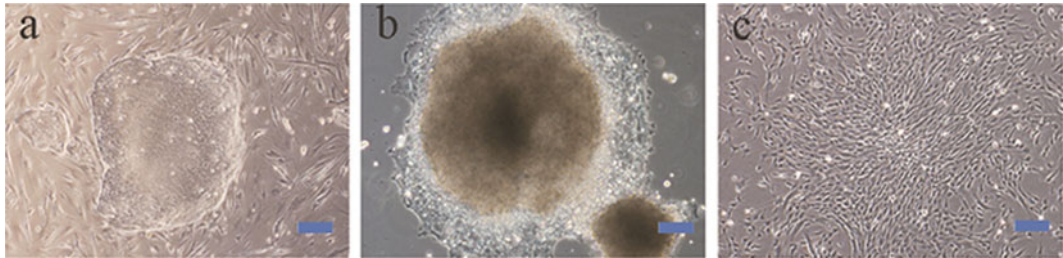


Fig. 2 Phase-contrast images of hESCs-Fib at different stages during derivation. (a) hESCs were kept on mitotically inactivated mouse feeder cells in undifferentiated state. (b) Seeding of embryoid bodies on gelatin-coated plates. Differentiation to hESCs-Fib initiated from the periphery of the embryoid body outgrowth. (c) hESCs-Fib at passage 2 showing fibroblast-like morphology. Scale bar = 100 μm

- (f) The medium was changed daily. All media and reagents were obtained from Invitrogen unless otherwise stated.
- (g) For the establishment of autogenic co-culture system (ACC system), hESCs were differentiated into fibroblast (hESCs-Fib) by dissociating hESCs into clumps under 1 mg/ml collagenase type IV treatment. Cells were then transferred to non-adherent 6-well culture plates in embryoid body medium. After 5 days in suspension culture, hESCs were differentiated into embryoid bodies (EBs, Fig. 1). EBs are three-dimensional aggregates of hESCs.
- (h) hESC-derived EBs were seeded on 0.1 % gelatin-coated 75 cm^2 plates in a DMEM-FBS medium for 3 weeks. The cells at this stage were named as hESCs-Fib passage 0 (Fig. 2).
- (i) hESCs-Fib passage 0 were sequentially passaged until homogeneous morphology was obtained.
- (j) hESCs-Fib were grown for ten passages. hESCs-Fib passage 8 were mitotically inactivated and plated onto the gelatin-coated 6-well plate at approximately 1.4×10^5 cells per well followed by hESC seeding on the next day.

- (k) The hESCs–hESCs-Fib ACC system was kept in hESC medium for 2–3 days before the start of differentiation (Figs. 1 and 2c).
- (l) For keratinocyte differentiation in the ACC system, hESC medium was replaced by FAD medium for 20 days. Additionally, 25 ng/ml of activin was supplemented between day 9 and 11 (3 days in total). After 20 days, the differentiated cells were detached and seeded on human collagen type IV-coated flasks and kept in DSFM without activin and RA. Cells at this stage were named as hESCs-Kert (Fig. 3a).
- (m) hESCs-Kert culture were maintained in DKSF.
- (n) A keratinocyte cell line, HaCaT, was taken as control (control cell line).

**3.2 Reverse
Transcriptase-
Polymerase Chain
Reaction Analysis
and Real-Time RT-PCR**

hESCs-Kert were characterized at mRNA level (Fig. 3b).

- (a) Cells were harvested and spun down at $300 \times g$ for 5 min.
- (b) Supernatant was removed, and cells were washed with PBS.
- (c) Pelleted hESCs-Fib were subjected to RNA extraction using RNeasy Mini Kit (Qiagen), following the manufacturer's instruction.
- (d) RNA concentration was read by Nanodrop ND-1000 spectrophotometer (Nanodrop technologies).
- (e) For cDNA synthesis, 500 ng of total mRNA per 20 μ l reaction volume of each sample was reverse-transcribed into cDNA using iScript cDNA synthesis Kit (Bio-Rad).
- (f) cDNA synthesis was carried out in athermal cycler (MyCyclerTM BioRad) under the following condition: 5 min at 25 °C, 30 min at 42 °C, 5 min at 85 °C, and held at 4 °C. The obtained cDNA samples were subjected to PCR amplification for 35 cycles (denaturing at 95 °C for 30 s; annealing for 45 s; extension at 72 °C for 60 s, followed by final extension at 72 °C for 10 min, and held at 4 °C).
- (g) β -actin was used as loading control.
- (h) Amplified PCR products were loaded onto 2 % agarose gel and subjected to electrophoresis for 35 min at 65 V.
- (i) DNA bands were visualized by ultraviolet (UV) illumination, and images were captured under a universal hood II (BioRad).
- (j) For real-time RT-PCR, reactions were performed using SYBR Green PCR Master Mix (Applied Biosystems) on a StepOne-PlusTM real-time RT-PCR system (Applied Biosystems).
- (k) β -actin was used as the reference gene for mRNA gene expression analyses.

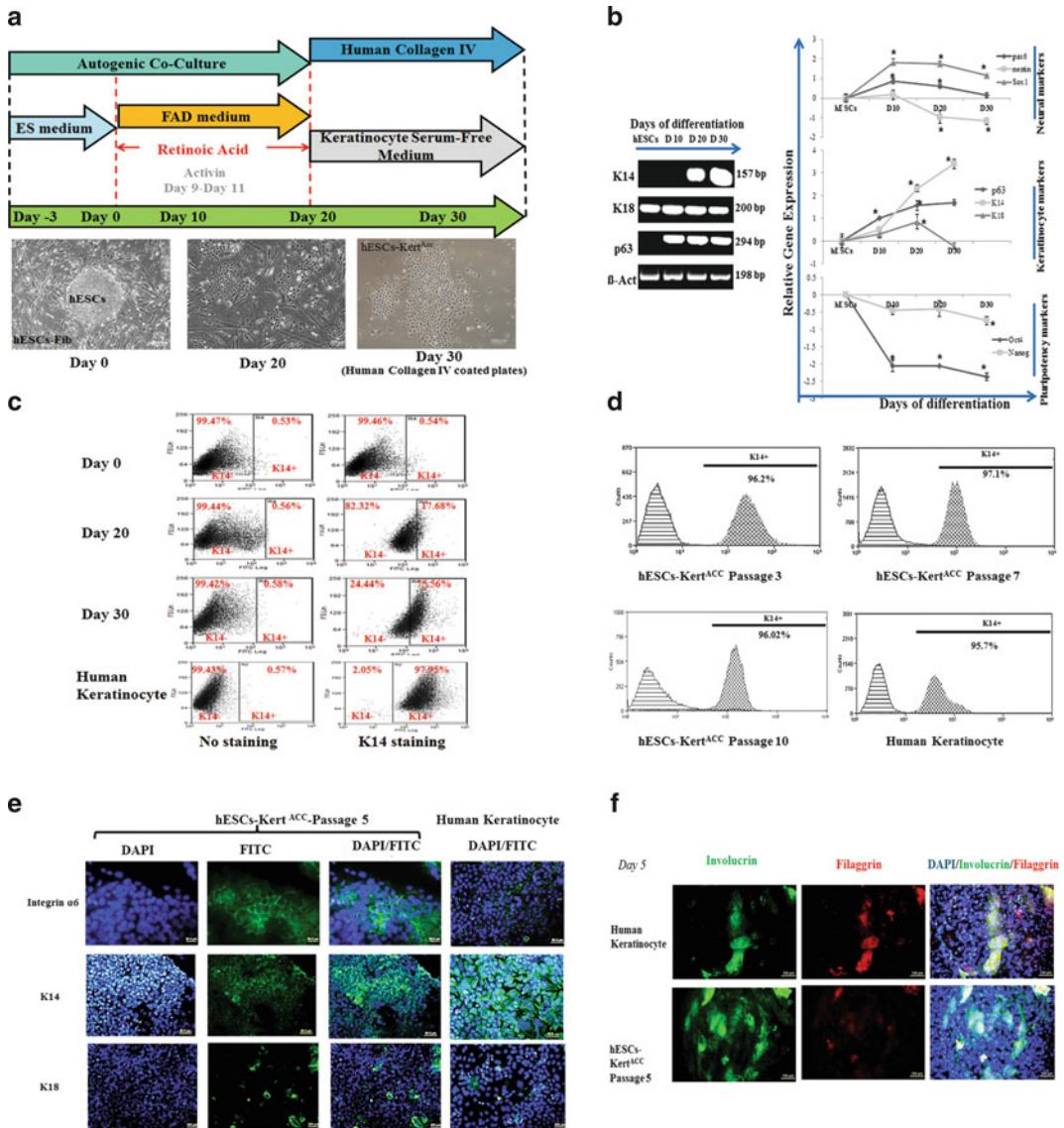


Fig. 3 Differentiation and characterization of hESC-Kert^{ACC} at mRNA and protein levels. **(a)** Schematic diagram showing the supplementation of different growth factors and substrates at different time points during hESC-Kert^{ACC} differentiation. **(b)** Qualitative analysis showing expression kinetics of keratinocyte markers (*left panel*); quantitative analysis showing expression kinetics of keratinocyte, neural, and pluripotency markers at different time points (*right panel*). Error bars = mean \pm SEM ($n = 3$); * = $p < 0.05$, versus "D0" sample. **(c)** Flow cytometric analyses of hESC-Kert^{ACC} showing the percentage of K14⁺ cells at day 0 (undifferentiated hESCs), day 20, and day 30. **(d)** Flow cytometric analyses showing the percentage of K14⁺ cells at different passages of hESC-Kert^{ACC}. **(e)** Immunofluorescence staining of hESC-Kert^{ACC} (passage 5) and HaCaT cell (positive control) for integrin $\alpha 6$ (3H1512), K14 (LL002), and K18 (DC-10) (primary antibody dilution factor, 1:100; secondary antibody dilution factor, 1:100). **(f)** Immunofluorescence staining of hESC-Kert^{ACC} (passage 5) and HaCaT cell (positive control) for involucrin and filaggrin. Abbreviations: β -Act, β -actin; D, day; hESC-Kert^{ACC}, hESC-derived keratinocytes in autogeneic co-culture system. HaCaT is an immortalized human keratinocyte cell line and is used as positive control for the above cell characterization experiments

- (l) Expression level of each target genes was then calculated as $2^{\Delta\Delta Ct}$:

$$\text{Relative gene expression} = 2^{[\Delta Ct_{\text{Gene}} - \Delta Ct_{\beta\text{-actin}}]}$$

- (m) A melting curve was used to verify the PCR products (Table 1).

3.3 Immunofluorescence Staining and Flow Cytometry

hESCs-Kert were also characterized at protein level (Fig. 3c–e).

For immunofluorescence staining

- (a) hESCs-Kert^{ACC} were cultured in a 24-well plate and washed with PBS for 5 min.
- (b) Fixed for 15 min in 4 % paraformaldehyde at room temperature (RT).
- (c) Permeabilized with 0.4 % Triton X-100/PBS for 10 min.
- (d) Blocked with PBS containing 4 % BSA (Sigma) for 1 h at RT.
- (e) Incubated with primary antibody (1:100 dilution, see the list of antibodies in Table 2) overnight at 4 °C.
- (f) Washed twice with washing buffer supplemented with Tween 20 for 5 min (Note 2).
- (g) Incubated with secondary antibody (1:100 dilution, see the list of antibodies in Table 2) for 1 h at RT in the dark.
- (h) Washed twice with washing buffer for 5 min and then mounted with slow fade gold anti-fade reagent containing DAPI (Invitrogen) to localize the nucleus.
- (i) All stained samples were examined under an Olympus IX70 fluorescence microscope.

For flow cytometry

- (j) For quantitative analysis of hESCs-Kert, flow cytometry was performed as previously reported (21).
- (k) hESCs-Kert were scrapped off after collagenase IV treatment. Cells were dissociated into single cells, fixed with fixing solution for 1 h at 4 °C, and permeabilized with permeabilizing solution for 15 min at 37 °C.
- (l) Permeabilization was followed by washing with washing buffer.
- (m) After washing, cell pellet was suspended in 100 µl staining buffer containing primary antibody (1:200 dilution, see the list of antibodies in Table 2).
- (n) The cells were incubated at 4 °C for 2 h.
- (o) After incubation, 1 ml of staining buffer was added and the cell suspension centrifuged ($300 \times g$ for 5 min at 4 °C).

- (p) Supernatant was discarded and the wash repeated for another time.
- (q) Cell pellets were then re-suspended in 100 μ l staining buffer containing secondary antibody (1:100 dilution, see the list of antibodies in Table 2) for 15 min at 4 °C in the dark.
- (r) The cells were washed twice and re-suspended in 1 ml of MACS[®] buffer solution.
- (s) The percentage of cells positively expressing each marker was analyzed by a Dako Cytomation Cyan LX flow cytometry machine.

4 Notes

1. The function of hESC medium was to keep proliferating hESCs in an undifferentiated state. FBS is conventionally used as a nutritive supplementation. However, FBS also contains factors that induce hESC differentiation. Therefore FBS was replaced by defined, serum-free knockout serum (Gibco[®]) as reported previously (20).
2. Tween-20 was used as a nonionic polyoxyethylene surfactant detergent for washing to get quality results.

References

1. Green H, Easley K, Iuchi S et al (2003) Marker succession during the development of keratinocytes from cultured human embryonic stem cells. *Proc Natl Acad Sci U S A* 100:15625–15630
2. Aberdam D (2004) Derivation of keratinocyte progenitor cells and skin formation from embryonic stem cells. *Int J Dev Biol* 48:203–206
3. De Luca M, Pellegrini G, Green H et al (2006) Regeneration of squamous epithelia from stem cells of cultured grafts. *Regen Med* 1:45–57
4. Iuchi S, Dabelsteen S, Easley K et al (2006) Immortalized keratinocyte lines derived from human embryonic stem cells. *Proc Natl Acad Sci U S A* 103:1792–1797
5. Ji L, Allen-Hoffmann BL, de Pablo JJ et al (2006) Generation and differentiation of human embryonic stem cell-derived keratinocyte precursors. *Tissue Eng* 12:665–679
6. Aberdam E, Barak E, Rouleau M et al (2008) A pure population of ectodermal cells derived from human embryonic stem cells. *Stem Cells* 26:440–444
7. Hewitt KJ, Shamis Y, Carlson MW et al (2009) Three-dimensional epithelial tissues generated from human embryonic stem cells. *Tissue Eng Part A* 15:3417–3426
8. Metallo CM, Ji L, de Pablo JJ et al (2008) Retinoic acid and bone morphogenetic protein signaling synergize to efficiently direct epithelial differentiation of human embryonic stem cells. *Stem Cells* 26:372–380
9. Guenou H, Nissan X, Larcher F et al (2009) Human embryonic stem-cell derivatives for full reconstruction of the pluristratified epidermis: a preclinical study. *Lancet* 374:1745–1753
10. Cobo F, Stacey GN, Hunt C et al (2005) Microbiological control in stem cell banks: approaches to standardisation. *Appl Microbiol Biotechnol* 68:456–466
11. Sjögren-Jansson E, Zetterström M, Moya K et al (2005) Large-scale propagation of four undifferentiated human embryonic stem cell

- lines in a feeder-free culture system. *Dev Dyn* 233:1304–1314
12. Skottman H, Hovatta O (2006) Culture conditions for human embryonic stem cells. *Reproduction* 132:691–698
 13. Rajala K, Lindroos B, Hussein SM et al (2010) A defined and xeno-free culture method enabling the establishment of clinical-grade human embryonic, induced pluripotent and adipose stem cells. *PLoS One* 5:e10246
 14. Martin MJ, Muotri A, Gage F et al (2005) Human embryonic stem cells express an immunogenic nonhuman sialic acid. *Nat Med* 11:228–232
 15. Heiskanen A, Satomaa T, Tiitinen S et al (2007) N-glycolylneuraminic acid xenoantigen contamination of human embryonic and mesenchymal stem cells is substantially reversible. *Stem Cells* 25:197–202
 16. Peng Y, Bocker MT, Holm J et al (2012) Human fibroblast matrices bio-assembled under macromolecular crowding support stable propagation of human embryonic stem cells. *J Tissue Eng Regen Med* 6:e74–e86
 17. Mallon BS, Park KY, Chen KG et al (2006) Toward xeno-free culture of human embryonic stem cells. *Int J Biochem Cell Biol* 38:1063–1075
 18. Shalom-Feuerstein R, Lena AM, Zhou H et al (2011) Δ Np63 is an ectodermal gatekeeper of epidermal morphogenesis. *Cell Death Differ* 18:887–896
 19. Metallo CM, Azarin SM, Moses LE et al (2010) Human embryonic stem cell-derived keratinocytes exhibit an epidermal transcription program and undergo epithelial morphogenesis in engineered tissue constructs. *Tissue Eng Part A* 16:213–223
 20. Thomson JA, Itskovitz-Eldor J, Shapiro SS et al (1998) Embryonic stem cell lines derived from human blastocysts. *Science* 282:1145–1147
 21. Fu X, Toh WS, Liu H et al (2011) Establishment of clinically compliant human embryonic stem cells in an autologous feeder-free system. *Tissue Eng Part C Methods* 17:927–937
 22. González S, Aguilera S, Allende C, Urzúa U, Quest AFG, Herrera L et al (2011) Alterations in type I hemidesmosome components suggestive of epigenetic control in the salivary glands of patients with Sjögren's syndrome. *Arthritis Rheum* 63:1106–1115
 23. Sardella A, Gualerzi A, Lodi G, Sforza C, Carrassi A, Donetti E (2012) Morphological evaluation of tongue mucosa in burning mouth syndrome. *Arch Oral Biol* 57:94–101
 24. Liu WF, Zuo HJ, Chai BL, Peng D, Fei YJ, Lin JY et al (2011) Role of tetraspanin CD151- α 3/ α 6 integrin complex: Implication in angiogenesis CD151-integrin complex in angiogenesis. *Int J Biochem Cell Biol* 43:642–650
 25. Jerome-Morais A, Rahn HR, Tibudan SS, Denning MF (2009) Role for protein kinase C- α in keratinocyte growth arrest. *J Invest Dermatol* 129:2365–2375
 26. Gutowska-Owsiak D, Schapp AL, Salimi M, Taylor S, Ogg GS (2011) Interleukin-22 downregulates filaggrin expression and affects expression of profilaggrin processing enzymes. *Br J Dermatol* 165:492–498

Protocol for Serial Cultivation of Epithelial Cells Without Enzymes or Chemical Compounds

Dongxia Ye and Antonio Peramo

Abstract

Deriving keratinocytes from epidermis or oral mucosa is a critical first step in the construction of cell-based tissue engineering and regenerative medicine applications. It would be advantageous to develop a methodology to grow adult somatic cells with maximum plasticity in a rapid fashion and in large numbers with minimal manipulation. With routine methods, keratinocytes are cultured in standard amount of medium and passaged with enzymes, and the confluence of the monolayer induces differentiation and eventual cell death. A protocol to expand keratinocytes in culture by growing keratinocyte in large numbers using a technique in which keratinocytes are released into the overlaying medium, effectively “popping-up” into suspension from the cell monolayer, is described in this chapter. This technique does not require the use of enzymes or chemical compounds for serial cultivation. The cells possess the ability of active cell proliferation at 100 % confluence over 1–2 months’ time. Based on previous characterization reports, these are untransformed, normal keratinocytes that appear to be highly suitable for clinical applications.

Keywords: Keratinocyte, Pop-up, Monolayer/suspension, Serial cultivation, Enzyme

1 Introduction

Keratinocytes derived from epidermis, oral mucosa, and urothelium are used in the construction of cell-based tissue engineering and regenerative medicine applications. Several methods (1–5) are being developed to obtain cells for several clinical applications, including construction of artificial tissues for transplantation, to “correct” specific systemic diseases, and as a source for cell-mediated wound healing therapies. Methods to grow epithelial cells in large number are always of interest for rapid implementation in clinical applications, and these methods can be of particular interest if they minimize cell manipulation or exposure to biological or chemical agents and also circumvent some currently debated, ethical and scientific problems associated with the use of embryonic derived stem cells or induced pluripotent stem cells (6).

In this protocol we describe a technique to expand human epithelial keratinocytes in primary culture to produce large numbers of cells in a combined monolayer/suspension culture, without the use of enzymes for passaging. Preliminary characterization of

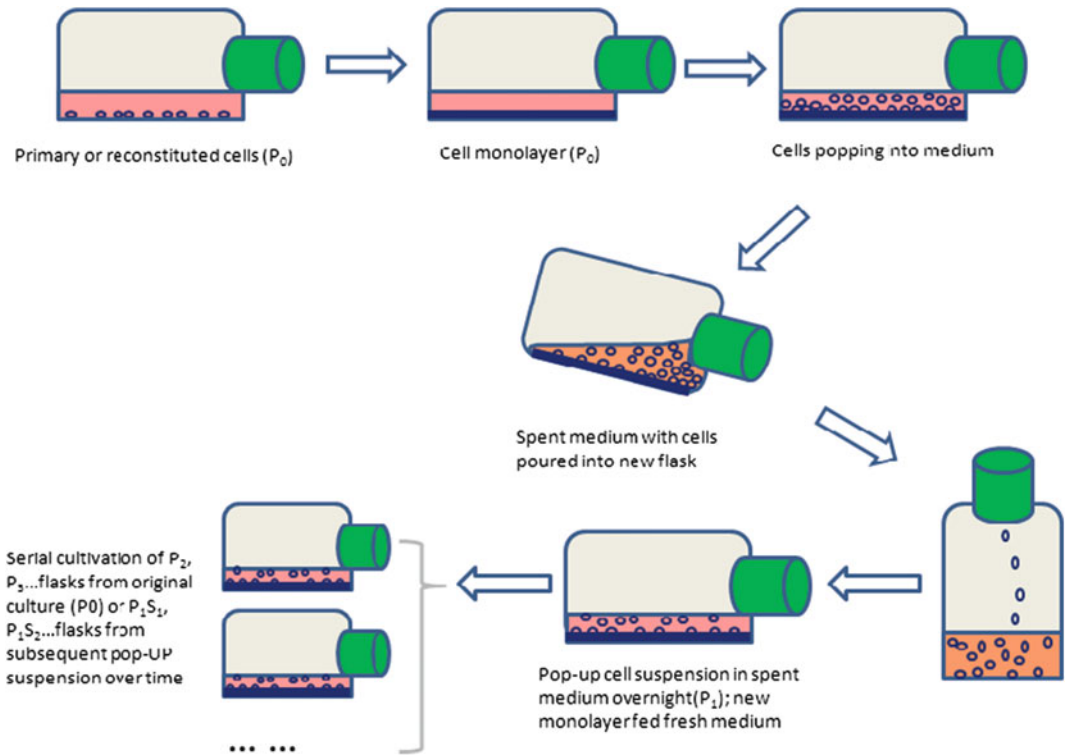


Fig. 1 Protocol of serial culture of pop-up cells in suspension by simple decantation without enzymatic treatment. Primary flask (P₀) will generate P₁, P₂, P₃, etc., and these will in turn generate P₁S₁, P₁S₂, etc. flasks

these cells has been reported previously (7, 8). In this technique, when a monolayer of cells is formed in the culture flasks, the cells in the monolayer continue to proliferate and move into suspension in large numbers. The cells are fed once a day, with 2–3 times the amount of medium (Epilife[®], serum and fatty acid free, low calcium). The cells maintain active cell proliferation at and after confluence so that the progeny cells are pushed or “popped” into the overlying medium. The spent medium (containing the cells in suspension) is then poured into a new flask (Fig. 1), where the cells reattach, forming a new monolayer. When the newly produced flask becomes confluent, the monolayer continues to produce cells in suspension, forming a new monolayer upon transfer to another flask, expanding the cell strain over time.

The novel characteristic of this technique is that the original producing cell monolayer is never trypsinized and is used exclusively to produce cells in suspension in the way described. Combining this technique with the methodologies described recently by Dragunova et al. (9) to obtain primary keratinocytes directly from skin explants would provide a methodology in which enzymatic treatments are completely avoided. This protocol enumerates the

simple steps to expand these epithelial cultures and to identify key aspects of their phenotypic changes, since all cell strains will follow the same pattern of morphological changes over time. As an example of the possible usefulness of the technique, judging simply by the total cell number produced, Duncan et al. (10) reported that the number of cells used in aerosols of keratinocytes to cover wounds in patients was just 5×10^5 to cover a 25 cm^2 area. Following our protocol, this number of cells can be produced in a single day by a single T75 flask with 35 mL of medium.

2 Materials

2.1 Primary Keratinocyte Culture

Cells are grown in Epilife[®] medium supplemented with defined growth factors (EDGS) and 0.06 mM Ca^{2+} (Invitrogen, Carlsbad, CA) and at 37°C , 5 % CO_2 gassing and atmospheric oxygen.

Sterile scalpel, forceps (w/teeth), scissors.

Tissue culture dishes (35, 60, 100, 150, 200 mm).

Serological pipettes (5, 10, 25 mL).

Tissue culture flasks (T-25, T-75, T-150).

Centrifuge tubes (15, 50 mL).

Micropipette tips.

Pasteur pipette.

Nylon net filter (11, 20, 30, $40 \mu\text{m}$) (Millipore).

95 % Ethanol.

Staple, stapler.

DPBS w/o Ca^{2+} , Mg^{2+} .

0.125 % Trypsin solution.

Fetal calf or newborn calf serum (Gibco, Life Technologies).

Trypan Blue (Sigma-Aldrich).

Gentamicin (Gibco, Life Technologies).

Fungizone (Gibco, Life Technologies).

Epilife[®] keratinocyte culture medium (Life Technologies).

Defined growth factors (EDGS) (Life Technologies).

0.06 mM Ca^{2+} (Invitrogen, Carlsbad, CA).

Centrifuge.

Hemocytometer.

Countess[®] Automated Cell Counter (Invitrogen).

Inverted microscope.

2.2 Serial Keratinocyte Cultivation

Serological pipettes (5, 10, 25 mL).
Tissue culture flasks (T-25, T-75, T-150).
Gentamicin (Gibco, Life Technologies).
Fungizone (Gibco, Life Technologies).
Eplife[®] keratinocyte culture medium (Life Technologies).
Defined growth factors (EDGS) (Life Technologies).
0.06 mM Ca²⁺ (Invitrogen, Carlsbad, CA).
Hemocytometer.
Countess[®] Automated Cell Counter (Invitrogen).
Inverted microscope.
Incubator.
CO₂ tank.

3 Methods

Tissue procurement: Either primary strains or reconstituted epithelial cells isolated from human tissues (adult epidermis, urothelium, or neonatal foreskin) or oral mucosa had been used previously (8). We will include here the standard methodology we regularly use, but since this has been described extensively, the particular methodology to obtain the primary or the reconstituted cells is open to the preference of the researchers.

The culture volumes in flasks are 60 mL/T150, 30 mL/T-75, and 15 mL/T-25 flasks, changed every 24 h.

3.1 Primary Keratinocyte Culture

Primary human keratinocytes can be obtained with standard techniques using discarded skin tissues from surgeries, as described next.

1. Seek approval from the Institutional Review Board prior to human tissue procurement. Sign the consent form by all individuals. Skin or oral mucosa sample(s) will be harvested without causing any morbidity.
2. Prepare 0.125 % trypsin by diluting 0.25 % trypsin solution with DPBS w/o Ca²⁺ and Mg²⁺ at 1:1. For primary oral mucosa keratinocyte culture, please refer **Note 1**. Prepare Eplife[®] keratinocyte culture medium supplemented with defined growth factors (EDGS) and 0.06 mM Ca²⁺, complete medium plus 2 % fetal calf or newborn calf serum. Keep them at 4 °C before use. Prepare DPBS w/o Ca²⁺ and Mg²⁺ containing 25 µg/mL gentamycin and 0.375 µg/mL fungizone.
3. Prepare a funnel-shaped nylon net filter (30 and 20 µm mesh size filters) by folding the round-shaped filter twice and then

stapling at the edge of the overlapped portion. Soak several filters in 95 % ethanol overnight for disinfection.

4. Obtain specimen from surgery and place it in a 20 cm tissue culture dish. If the specimen is not going to be used immediately, it can be put on ice or alternatively left at 4 °C and submersed in DPBS.
5. Hold the sample with the forceps with teeth, and scrape the sample with scalpel to remove excess fat and blood residue.
6. Add 50 mL of room-temperature DPBS containing antibiotic-antimycotic, for a specimen of approximately the size of a small hand palm (8 cm × 6 cm) (*see Note 1*).
7. Submerge, rinse, and transfer to refrigerator at 4 °C for 30 min. Repeat two times, and leave in refrigerator until the moment for trypsin addition. If rinsing solution comes out too red, repeat cleaning in order to eliminate blood cells.
8. Take the dish from refrigerator, and eliminate DPBS.
9. Slice full-thickness epithelium into 1/8 in. (2–3 mm) wide strip with scalpels. The thinner the strips the better the trypsinization will be.
10. Add 50 mL of 0.125 % trypsin, and leave the tissue culture dish in the laminar flow hood for 15 h at room temperature.
11. After 15 h, add 5 mL pure fetal calf or newborn calf serum to stop trypsinization.
12. Split and remove the epidermis from dermis with forceps, and shake to release attached cells. Gently scrape dermis to remove attached cells.
13. Take the filters from ethanol and thoroughly rinse in DPBS and complete culture medium.
14. Place funnel-shaped filter over the opening of the 50 mL centrifuge tube.
15. Using a 10 mL pipette, dispense the cell suspension into the strainer.
16. Using the same pipette, rinse the tissue culture dish surface with 10 mL complete medium, and pipette the rinse solution into the same strainer.
17. Repeat the previous step with another 10 mL of complete medium.
18. Secure cap on the 50 mL tube, place in centrifuge, and balance contents.
19. Set the centrifuge, and spin cells (200 × *g*, 5 min, at room temperature) (*see Note 2*).
20. Remove the supernatant above the cell pellet with a Pasteur pipette, and be sure not to disturb the cell pellet.

21. Resuspend pellet in newly made complete medium with 2 % serum (or made previous day).
22. Aspirate a 15 μL cell suspension, mix with 15 μL trypan blue, and load 10 μL of the suspended cells into each of the two chambers of the hemocytometer. Count viable cells with a cell counter (hemocytometer or other), and calculate the total number of cells harvested.
23. Plate cells into T-75 tissue culture flask approximately in a range of 25–40 million cells in 30 mL complete medium with 2 % serum (*see Note 3*).
24. Transfer flasks into incubator with 37 °C, 5 % CO₂ gassing and atmospheric oxygen.

3.2 Initial Creation of Cell Monolayers

1. Keep cultures for at least 24 h in medium with 2 % serum but no more than 30 h.
2. Remove the medium containing 2 % serum with a Pasteur pipette.
3. Feed the cells with complete medium every single day. Volume of medium is 35 mL for T-75 and 15 mL for T-25 from first change.
4. Take a look at the flasks under the inverted microscope every day to examine if cells are growing to form a confluent monolayer (*see Note 4*).

3.3 Reconstituted Keratinocyte Culture

Reconstitute previously frozen keratinocytes using routine methods for thawing and plate them at the desired density using the same culture volumes as in primary cells (*see Note 5*). Medium used in reconstituted keratinocytes is complete medium serum free.

3.4 Serial Cultivation and Passaging

This part is the same for either primary or reconstituted keratinocytes. At confluence, the monolayers (referred always as passage P₀) will continue to proliferate, pushing keratinocytes into the overlying medium. The cells in suspension, named epithelial pop-up keratinocytes, can be passaged using serial cultivation (*see Note 6*).

1. At confluence, take the flasks from the incubator, put them in vertical position, and loosen the cap.
2. Pour the spent medium with the cells in suspension to a new flask (referred as P₁).
3. Secure caps, and gently rock the flask to evenly distribute the cellular suspension.
4. Add same volume of complete medium as before to confluent flask (referred before as P₀).
5. Feed the cells (P₀ and P₁) every day, with medium volumes of 35 mL for a T-75 or 15 mL for a T-25. The cells in new flask (P₁) will form new cultures, as depicted in Fig. 1.

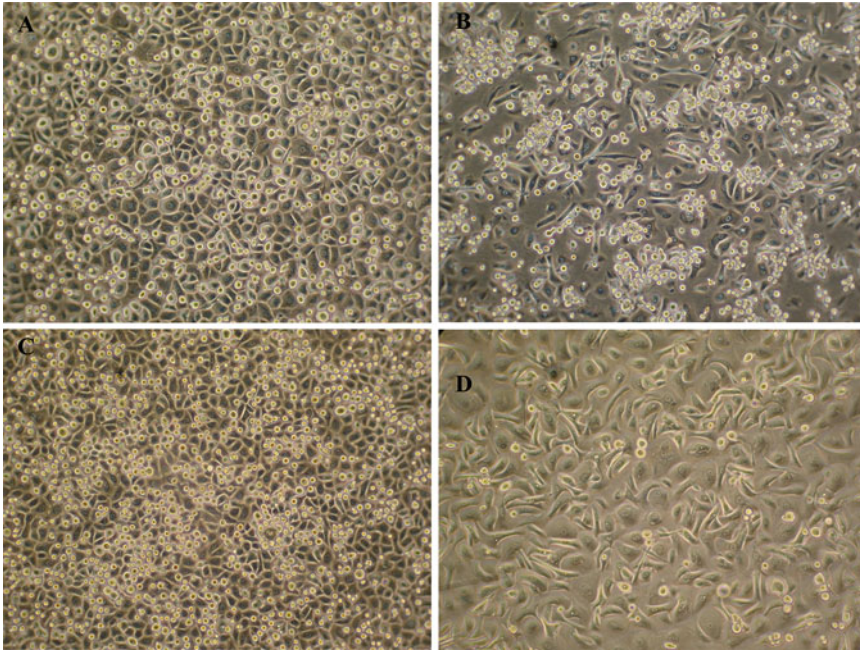


Fig. 2 Example of evolution of the monolayer of polygonal or “cobblestone” keratinocytes over time. (a) and (b) are primary human epidermal cells at 3 and 14 days, respectively; (c) and (d) show reconstituted human breast keratinocytes in a monolayer at 5 and 16 days in culture

6. This process must be repeated every day if serial cultivation is desired, since medium must be changed every day and the culture will again contain new cells in suspension.
7. If the P_1 flask grows into a monolayer, repeat the above mentioned steps and refer to it as P_1S_1 , P_1S_2 , etc. The same can be done for the serial cultivation and labeling for passages from P_0 , P_2 , P_3 , can be achieved.
8. The flask with monolayers should be monitored to determine exhaustion of its capabilities to push cells into suspension (*see Note 7*). Two techniques to evaluate the monolayers, briefly described next, are recommended: (A) morphological evaluation of the cell monolayer and (B) counting the cells in suspension in the medium.
9. (A) Morphological evaluation: From confluence and over a period of 10–15 days, the morphology will change from highly packed small cells with polygonal arrangements to “old” or “senescent” cell morphology where cells become much bigger and elongated and lose cell–cell contact. An example of this process is shown in Fig. 2 (*see also Note 8*). It is helpful to take pictures to check cell morphology.
10. (B) Cell counting evaluation: The purpose is to count the number of cells produced by the monolayer, which are in

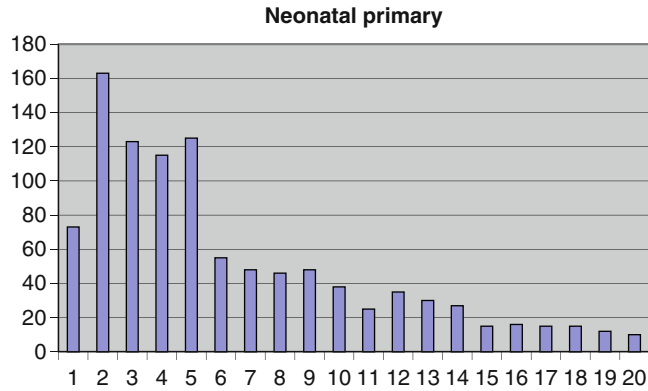


Fig. 3 Number of cells in suspension produced by a culture of neonatal cells over time. The first day of counting represents confluency of the culture. The Y-axis shows the number of cells per mL of spent medium

suspension. After confluence, aspirate a 15 μ L cell suspension from spent medium, mix with 15 μ L trypan blue, and load 10 μ L of the suspended cells into each of the two chambers of the hemocytometer. Count cells, and calculate the total number of cells in spent medium. An example of the number of cells produced in suspension (per day/mL of culture medium, in thousands) is shown in Fig. 3 (*see Note 9*).

4 Notes

1. For primary oral mucosa keratinocyte culture, prepare 0.04 % trypsin solution by mixing 0.25 % trypsin solution with DPBS. Varied tissue culture dishes, such as 100, 150, or 200 mm in diameter, may be required depending on the tissue size obtained.
2. If cell pellet is too loose or there is no cell pellet after centrifugation, spin down again at $290 \times g$ for 5 min.
3. This may need to be adjusted, but because the number of other cell types is unknown, this should give a good plating density. It has been observed that if the total number of cells in the cell suspension is too high, the culture may reach confluence later than with a moderate cell seeding and the pop-up population will be lower. If the cell density of keratinocytes at initial seeding is too low the culture will take much longer to reach confluence. Keratinocytes plated at low density may lack paracrine signals and may not grow well. At least 10–20 % seeding density is recommended.
4. Any break in the protocol will result in reduced cell number and viability of the cells in suspension, lower plating efficiency,

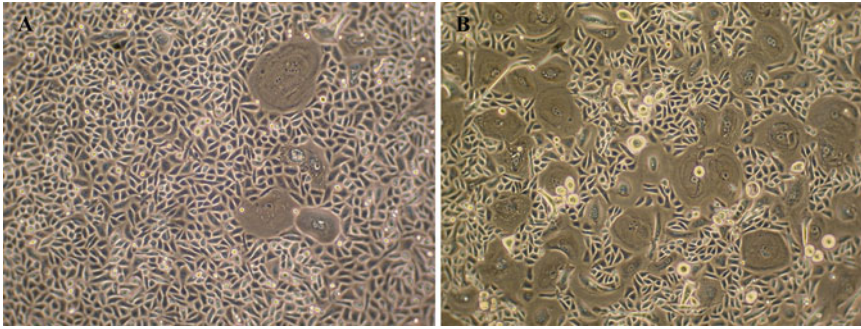


Fig. 4 While giant cells do not prevent keratinocytes to move into suspension, they nonetheless limit the surface area available for growth (a). These cells appear in higher number (b), when the initial cell seeding is low or when using reconstituted cells after freezing, compared to primary cell cultures. They also appear in higher number over time when using serial cultivation, as shown in picture (b)

increased time to confluence, and increased cell size of the cell in the monolayer.

5. A possible observable effect of cryogenic treatment is that serially cultivated flasks will produce fewer cells into suspension. When reconstituted cells are used, the cells are mostly produced into the early days after monolayer confluence, and there may be a substantial decrease in cell production after 4–5 days. In addition, serially cultivated flasks (P_1S_1 , P_1S_2 , etc.) may not reach confluence and may lack production of cells into suspension. In general, this culture technique may be better suited for the initial passages of primary cell culture, i.e., P_0 and P_1 .
6. When the bottom of the flask is covered by a monolayer of cells near confluence (>80 % or 90 %), the cells in the monolayer proliferate by pushing the keratinocytes upward into the overlying medium and into suspension. We recommend to wait 1 or 2 days after this threshold confluence (>80 % or 90 %) to start the serial cultivation.
7. A phenomenon may appear in which giant cells (assumed to be differentiated cells) will be more common in culture, as seen in Fig. 4. These giant cells are less common when the monolayer is formed quickly. If these “big” cells are present at the beginning of the culture, they will occupy a larger area of the surface and then reduce the number of small cells in suspension. To maintain a longer and more successful culture, it is suggested to seed at high density (more than 30 million total viable cells per T75 flask when initiating a primary culture or 7.5×10^5 to 1×10^6 cells when using reconstituted cells). When the original flask stops producing cells into suspension, the monolayer is seen to consist of large, apparently “aged” cells.

8. The cells in suspension in Fig. 2a or c can be used for serial cultivation, but the ones in Fig. 2b or d have poor quality, including lack of attachment when passaged and reduced proliferative capacity. Monitoring the morphology of the monolayer and counting the number of cells in suspension are the two methods to ensure the collection of the cells during the best time window, as described in the protocol.
9. Before reaching complete confluence, the monolayers would already show cells popping into the medium. Broadly (Fig. 3), the number of cells increases, reaches a maximum, and then steadily declines. This helps determine the length of time the culture should be maintained as actively producing cells in suspension. The total number of days for cell counting can be determined by a cutoff number of produced pop-up cells which we suggest is 10,000 cells/mL or less. If the number of cells counted is below this threshold, the culture should be considered finalized.

References

1. Mignone JL, Kreutziger KL, Paige SL et al (2010) Cardiogenesis from human embryonic stem cells. *Circ J* 74:2517–2526
2. Lei P, Andreadis ST (2008) Efficient retroviral gene transfer to epidermal stem cells. *Methods Mol Biol* 433:367–79
3. Hodgkinson CP, Gomez JA, Mirotsoy M et al (2010) Genetic engineering of mesenchymal stem cells and its application in human diseases therapy. *Hum Gene Ther* 21:1513–26
4. Oliveira AA Jr, Hodges HM (2005) Alzheimer's disease and neural transplantation as prospective cell therapy. *Curr Alzheimer Res* 2:79–95
5. Bavister BD, Wolf DP, Brenner CA (2005) Challenges of primate embryonic stem cell research. *Cloning Stem Cells* 7:82–94
6. Lister R, Pelizzola M, Kida YS et al (2011) Hotspots of aberrant epigenomic reprogramming in human induced pluripotent stem cells. *Nature* 471:68–73
7. Marcelo CL, Peramo A, Ambati A et al (2012) Characterization of a unique technique for culturing primary epithelial progenitor/stem-cells. *BMC Dermatol* 12:8
8. Peramo A, Feinberg SE, Marcelo CL et al (2013) Characterization of cultured epithelial cells using a novel technique not requiring enzymatic digestion for subculturing. *Cell Tissue Bank* 14(3):425–435. doi:10.1007/s10561-012-9343-z
9. Dragúňová J, Kabát P, Koller J (2013) Skin explant cultures as a source of keratinocytes for cultivation. *Cell Tissue Bank* 14:317–324
10. Duncan CO, Shelton RM, Navsaria H et al (2005) In vitro transfer of keratinocytes: comparison of transfer from fibrin membrane and delivery by aerosol spray. *J Biomed Mater Res B Appl Biomater* 73:221–228

Growth and Differentiation of HaCaT Keratinocytes

Van G. Wilson

Abstract

HaCaT cells are a spontaneously immortalized, human keratinocyte line that has been widely used for studies of skin biology and differentiation. Under typical culture conditions HaCaT cells have a partially to fully differentiated phenotype due to the high calcium content of both standard media and fetal bovine serum. This chapter describes low-calcium culture conditions for reverting HaCaT cells to the fully basal state followed by subsequent controlled differentiation using calcium induction.

Keywords: HaCaT differentiation, Calcium induction, Basal keratinocytes

1 Introduction

The epidermis has been intensely studied both as a convenient model of tissue differentiation (1, 2) and for its medical importance in wounds (3), oncogenesis (4), congenital and acquired skin dysfunctions (5), and infections (6). As a differentiation model system, human keratinocytes are attractive because primary, immortalized, or transformed cells are all readily available for comparison. Furthermore, keratinocytes are easily induced to differentiate in culture so that state-specific differences can be explored at the biochemical and molecular level (7). One widely utilized human keratinocyte line, known as HaCaTs, is derived from spontaneously immortalized, human keratinocytes (8). While clearly not entirely “normal,” HaCaT cells exhibit basal cell properties and still respond to different inducers of differentiation such as Ca^{2+} (9, 10) and high cell density (11). Furthermore, these cells form a nearly normal epithelial structure when transplanted onto athymic mice (12) or grown in organotypic cultures (13). Lastly, HaCaT cells can be readily infected with adenoviruses (10) or transfected at moderate levels (14, 15) for introduction of transgenes. Given the relatively authentic phenotypes of this line, the extensive published information about its properties, and its consistent growth in culture we believe HaCaT cells to be an excellent model system to conduct analysis of keratinocyte differentiation. This chapter describes the basic methods for growth and maintenance of

HaCaT cells in the basal, undifferentiated phenotype, followed by calcium induction to produce cells exhibiting a differentiated state.

2 Materials

All cell culture components must be kept sterile, so proper aseptic technique should be used and operations should be performed in a Class II Biosafety Cabinet.

2.1 Cell Culture Components

1. 3.0 mM calcium chloride (100× stock): Weigh 333 mg of calcium chloride (Sigma-Aldrich; 99.99 % anhydrous powder) and mix into 1 l of cell culture-grade water. Stir until dissolved, and then filter sterilize directly into a sterile 1,000 ml bottle using the Stericap™ Plus Universal Bottle-Top Filter Device (Millipore; 0.22 µm pore). Store at 4 °C.
2. 280 mM calcium chloride (100× stock): Weigh 31.07 g of calcium chloride (Sigma-Aldrich; 99.99 % anhydrous powder) and mix into 1 l of cell culture-grade water. Stir until dissolved, and then filter sterilize directly into a sterile 1,000 ml bottle using the Stericap™ Plus Universal Bottle-Top Filter Device (Millipore; 0.22 µm pore). Store at 4 °C.
3. Low-calcium fetal bovine serum (FBS): To remove endogenous calcium in the FBS (BenchMark™ Fetal Bovine Serum; Gemini Bio Products) it must be treated with Chelex 100 resin (BioRad; catalog number 142-2832). Distribute 50 ml aliquots of FBS into sterile, 50 ml conical tubes, and add 0.38 g of Chelex to each tube. Incubate tubes for 1 h at 4 °C on a tube rotator and then use immediately for the low-calcium and high-calcium media (see **Note 1**).
4. Low-calcium (0.03 mM) growth medium: To 870 ml of DMEM add 20 ml of 200 mM L-glutamine, 10 ml of 3.0 mM calcium chloride solution, and 100 ml of the low-calcium FBS. Swirl briefly to mix components, and then filter directly into a sterile 1,000 ml bottle using the Stericap™ Plus Universal Bottle-Top Filter Device (Millipore; 0.22 µm pore). This removes the Chelex resin and ensures sterility of the combined solution. Store at 4 °C.
5. High-calcium (2.8 mM) growth medium: To 780 ml of DMEM add 20 ml of 200 mM L-glutamine, 10 ml of 280 mM calcium chloride solution, and 100 ml of the low-calcium FBS. Swirl briefly to mix components, and then filter directly into a sterile 1,000 ml bottle using the Stericap™ Plus Universal Bottle-Top Filter Device (Millipore; 0.22 µm pore). This removes the Chelex resin and ensures sterility of the combined solution. Store at 4 °C.
6. 0.25 % Trypsin, 1 g/l EDTA (Hyclone).

7. Phosphate-Buffered Saline (PBS), pH 7.4 (Life Technologies).
8. DMEM (High Glucose, no Glutamine, no Calcium; Life Technologies).
9. 200 mM L-glutamine (Atlanta Biologicals).

2.2 Phenotype Verification Components

1. 4× SDS sample buffer (100 mM Tris pH 6.8, 20 % glycerol, 8 % SDS, 0.02 % bromophenol blue, and 4 % β-mercaptoethanol): To 60 ml of H₂O add 20 ml of glycerol, 8 g SDS, 4 ml of β-mercaptoethanol, 20 mg of bromophenol blue, and 1.21 g of Trizma base. Stir thoroughly, and adjust pH to 6.8. Bring volume to 100 ml, and store at 4 °C.
2. Immobilon-P membrane (EMD Millipore).
3. BenchMark™ Pre-Stained Protein Ladder (Life Technologies).
4. TTBS (50 mM Tris, pH 7.4, 150 mM NaCl, 0.005 % Tween 20): To 960 ml of H₂O add 6.06 g of Trizma base, 8.77 g NaCl, and 50 μl of Tween 20. Stir thoroughly, and adjust pH to 7.4. Bring volume to 1 l, autoclave, and store at 4 °C.
5. Blocking solution (5 % nonfat dried milk): To 90 ml of TTBS add 5 g of nonfat dried milk powder. Mix thoroughly, and bring final volume to 100 ml with TTBS. Store the blocking solution at 4 °C (see **Note 2**).
6. Anti-Keratin 1 (rabbit polyclonal; Covance PRB-149P).
7. Anti-Involucrin (mouse monoclonal; LabVision MS 126PO).
8. Anti-Alpha Tubulin (mouse monoclonal; Santa Cruz Biotechnology s-5286).
9. Horseradish Peroxidase-conjugated chicken anti-rabbit (Santa Cruz Biotechnology sc-2955).
10. Horseradish Peroxidase-conjugated chicken anti-mouse (Santa Cruz Biotechnology sc-2954).
11. Western Lightning Enhanced Chemiluminescence kit (PerkinElmer).
12. BioMax Light X-ray film (Carestream Kodak).
13. Stripping buffer (62.5 mM Tris-HCl, pH 6.8, 2 % SDS, 100 mM 2-mercaptoethanol): To 90 ml of H₂O add 0.76 g of Trizma base, 2 g of SDS, and 704 μl β-mercaptoethanol. Mix thoroughly, adjust pH to 6.8, and bring final volume to 100 ml. Store at 4 °C.

3 Methods

3.1 Growth and Propagation Under Low-Calcium Conditions

HaCaT cells are commonly maintained in normal DMEM supplemented with 10 % FBS, both of which contain sufficient calcium to induce differentiation. Dedifferentiation to the basal phenotype requires prolonged growth in low-calcium medium.

1. Aspirate medium from a T-75 flask of 80 % confluent HaCaT cells grown in DMEM–10 % FBS. Add 10 ml PBS, and rock gently to rinse cells. Aspirate the PBS, and repeat the rinse with another 10 ml of PBS (see **Note 3**). Aspirate second PBS rinse.
2. Add 1 ml of trypsin, and rock to cover cells thoroughly. Incubate for 15–20 min at 37 °C in a 5 % CO₂ incubator.
3. Add 5 ml of low-calcium growth medium, and pipet medium up and down 5–10 times to dislodge and resuspend cells.
4. Place 1 ml of the cell suspension into a new T-75 flask along with 14 ml of low-calcium growth medium per flask, and discard the remaining cells.
5. Incubate at 37 °C in a 5 % CO₂ incubator.
6. Split cells whenever the cultures reach 75–80 % confluency and keep in low-calcium growth medium (see **Note 4**).

3.2 Induction of Differentiation

Induction can be done to establish parallel cultures of basal versus differentiated HaCaT cells or can be done to examine dynamic changes during the differentiation process which typically takes 5–7 days to complete. To establish permanent differentiated cultures of HaCaT cells simply replace the low-calcium medium with high-calcium medium and maintain the cells in high-calcium medium subsequently (see **Note 5**). Below is the procedure to produce individual plates of HaCaT cells that can be harvested at different times post induction to examine the events occurring during the differentiation process.

1. Aspirate the medium from a T-75 flask of basal HaCaT cells in low-calcium medium at 75–80 % confluency (see **Note 6**).
2. Wash twice with room-temperature PBS, and trypsinize as in steps 1 and 2 in the previous section.
3. After the trypsin incubation, add 12 ml of low-calcium medium and resuspend the cells by pipetting up and down 5–10 times.
4. Add 1 ml of cell suspension to 12 × 60 mm tissue culture plates containing 9 ml of low-calcium medium. Swirl gently to distribute the cells (Fig. 1).
5. Incubate the plates overnight at 37 °C in the 5 % CO₂ incubator to allow reattachment of the cells.
6. The following day aspirate the media, and add 10 ml of high-calcium medium to each plate to initiate differentiation. For zero time samples immediately aspirate the high-calcium medium and harvest the cells for the desired analysis. Place the remaining plates back into the CO₂ incubator.
7. Typically samples are harvested at 24-h intervals to follow changes occurring during differentiation, but any schedule can be developed as needed for the experimental regimen (see **Note 7**).

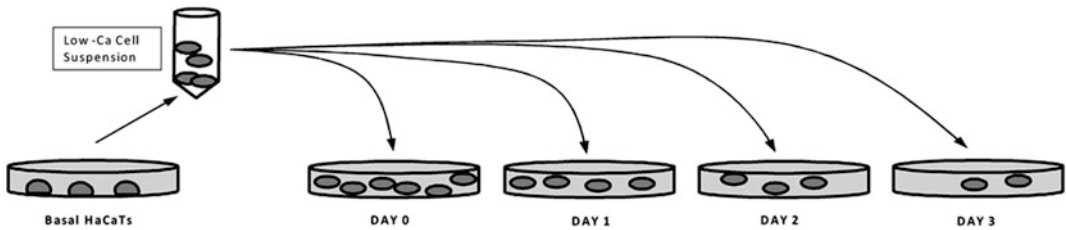


Fig. 1 A diagram of the procedure for preparing individual plates of basal HaCaT cells for differentiation time course studies. Basal cells are all seeded on day 0 into plates containing high-calcium medium to induce differentiation, and cells will be harvested on the indicated day post plating. Decreasing numbers of cells are seeded for plates to be harvested on subsequent days to compensate for continued cell proliferation occurring during the differentiation process

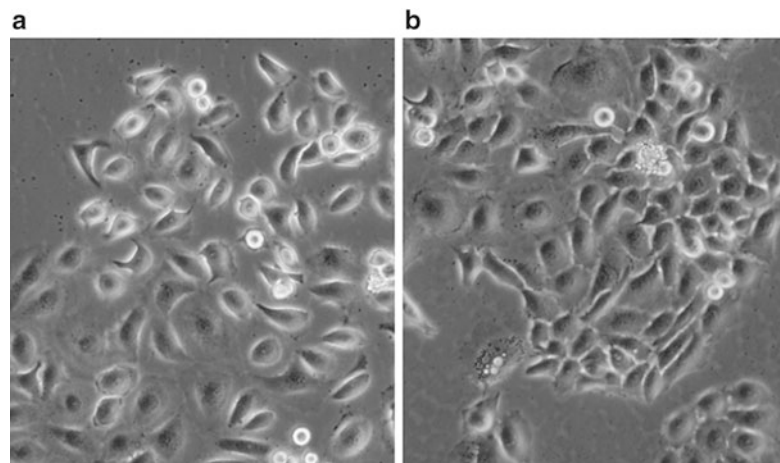


Fig. 2 Phase contrast microscopy of basal, low-calcium maintained (a) and differentiated high-calcium maintained (b) HaCaT cells

3.3 Verification of Basal and Differentiated Phenotypes

Basal HaCaT cells should be spindle shaped and loosely packed (Fig. 2a), while differentiated cells (Fig. 2b) should be more cuboidal with tight packing (10). In addition to morphologic differences, basal and differentiated states should always be confirmed biochemically by immunoblotting for known differentiation markers such as keratin 1 and involucrin. Both of these markers should be absent or only barely detectable in basal HaCaT cells and should start to appear between 48 and 72 h after calcium induction of differentiation (Fig. 3; see **Note 8**). Alpha-tubulin is a housekeeping marker that is present in both basal and differentiated keratinocytes and can be used for normalization of overall protein levels between different samples.

1. Aspirate the medium from a 60 mm plate, add 5 ml of 4 °C PBS, and swirl gently over the cells. Aspirate the PBS, repeat the rinse with another 5 ml of 4 °C PBS, and aspirate thoroughly.

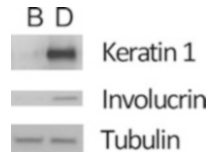


Fig. 3 Immunoblots of basal (*B*) and differentiated (*D*) HaCaT cell extracts showing the expression of keratin 1, involucrin, and tubulin as indicated

2. Add 500 μ l of boiling 4 \times sample buffer. Swirl sample buffer quickly over the plate surface to detach and lyse cells, and then pass the solution ten times through a 27-gauge needle on a 2 ml syringe. Individual samples can be stored at -20°C until all samples for an experiment are prepared.
3. Load 20 μ l of each sample on a standard 10 % SDS-polyacrylamide gel. One lane should be used to run the BenchMarkTM Pre-Stained Protein Ladder (mix 10 μ l of the Ladder with 10 μ l of 4 \times SDS sample, and load all 20 μ l on the gel). After electrophoresis, the gel contents are transferred to a 0.2 μ m Immobilon-P membrane using any standard immunoblot transfer device. Monitor successful migration of the samples by transfer of the BenchMarkTM Pre-Stained Protein Ladder from the gel to the membrane.
4. Block the membrane by incubating in 25 ml of 5 % nonfat dried milk solution (NFDMS) for 30 min with gentle rocking at room temperature.
5. Remove the blocking solution and replace with 25 ml of 5 % NFDMS containing one of the primary antibodies at the appropriate dilution: 1:1,000 for anti-keratin 1; 1:1,000 for anti-involucrin; or 1:15,000 for anti-alpha tubulin. Incubate with primary antibody for 1 h at room temperature with gentle rocking. Alternatively, incubation can be carried out overnight at 4°C if more convenient.
6. Remove the primary antibody solution, and add 10 ml of 5 % NFDMS containing a 1:5,000 dilution of the appropriate horseradish peroxidase-conjugated secondary antibody. Rock the membrane gently for 1 h at room temperature.
7. Remove the secondary antibody solution, add 10 ml of TTBS, and rock for 5 min at room temperature. Remove the TTBS, and repeat with another 10 ml of TTBS. The membrane can be used immediately or stored overnight at 4°C in this buffer with gentle rocking.
8. Prepare the Western Lightning Enhanced Chemiluminescence Reagent working solution by mixing equal volumes of the Enhanced Luminol Reagent with the Oxidizing Reagent. It will take 0.1 ml of working solution for every cm^2 of the membrane.

9. Remove the TTBS, and add the Enhanced Chemiluminescence working solution to the membrane. Incubate for 5 min at room temperature with gentle agitation.
10. Remove the working solution, and place the membrane in a plastic sheet protector.
11. Expose the membrane to BioMax Light X-ray film for 30 s, and then develop the film. The membrane can be re-exposed to the film for shorter or longer exposures as necessary (see **Note 9**).
12. To strip the membrane for reuse with another primary antibody, rinse the membrane four times with 10 ml of TBBS. For each rinse, gently rock in the TBBS for 5 min at room temperature.
13. Incubate the membrane for 30 min at 50 °C in stripping buffer.
14. Rinse the membrane six times with 10 aliquots of TBBS. Each rinse is for 5 min at room temperature.
15. Remove the final rinse, and return to step 4 to block the membrane.
16. Repeat steps 5–11 with a new primary antibody (see **Note 10**).

4 Notes

1. Since the Chelex 100 resin is not sterile, the Chelex-treated FBS may not be sterile and should not be stored. Instead, the Chelex-treated FBS is mixed immediately with the DMEM and then filtered to remove the Chelex particles and sterilize the medium.
2. To avoid microbial growth in the blocking solution it is best to only make enough stock to last a few days.
3. All volumes are given for a T-75 flask but can be adjusted proportionally for smaller tissue culture plates or larger flasks.
4. Dedifferentiation to the basal phenotype requires 3–4 weeks of maintenance in the low-calcium medium. HaCaT cells are also very sensitive to cell density, so they should never be allowed to go beyond 75–80 % confluency in low-calcium medium as they may start to differentiate at higher cell density. Verification of reversion to the basal phenotype should be performed as described in Section 3.3. Once a verified stock of basal HaCaT cells is derived it can be passaged and maintained in low-calcium medium indefinitely. Also note that HaCaT cells are temperature sensitive and temperatures over 37 °C may induce differentiation, so basal cells should be kept at or slightly below this temperature.
5. Unlike differentiated primary keratinocytes which stop dividing, differentiated HaCaT cells retain their proliferative capacity, so their cultures can be split, expanded, and propagated indefinitely in high-calcium medium.

6. One T-75 flask at 75–80 % confluency has enough cells to produce twelve 60 mm plates. Scale up the number of T-75 flasks if more plates are needed.
7. Note that plates harvested at subsequent daily intervals will have increasing number of cells compared to the 0-day sample since cell growth and division continue during differentiation for HaCaT cells. When comparing samples harvested at different days this difference in cell number must be accounted for by normalizing the samples to cell number or total protein. Alternatively, fewer cells can be seeded initially on plates for subsequent time points so that by the day of harvest these plates will have similar cell numbers to the 0 time plate. Since HaCaT cells double at roughly 24-h intervals, the volume of cell suspension to seed for any day of harvest is $X/2^n$ where X is ml of cell suspension plated for day 0 and n is the intended day of harvest (i.e., $n = 1, 2, 3, 4$, etc.).
8. Even in the basal cells there may be slight expression of K1 and/or involucrin, but it should be much less than for the differentiated cells.
9. As an alternative to X-ray film, the chemiluminescence signal can also be detected with any appropriate imaging system, for example the ChemiDoc™ XRS + System by Bio-Rad.
10. In addition to the keratin 1 and involucrin markers specified in this section, numerous other markers for both basal and differentiated states have been described and can be used to assess the differentiation status of HaCaT cultures. Regardless of the markers chosen, it is critical to evaluate a housekeeping marker, such as alpha tubulin, in all experiments to control for differences in total protein quantity between samples.

Acknowledgments

Much of our work with HaCaT cells was supported by NIH grant CA089289. We thank all the previous members of the Wilson lab for their help with development of the HaCaT protocols, particularly Drs. Adeline Deyrieux and Phillip Heaton.

References

1. Gandarillas A (2000) Epidermal differentiation, apoptosis, and senescence: common pathways? *Exp Geront* 35:53–62
2. Ghadially R (2012) 25 years of epidermal stem cell research. *J Invest Dermatol* 132:797–810
3. Lootens L, Brussaers N, Beele H et al (2013) Keratinocytes in the treatment of severe burn injury: an update. *Int Wound J* 10(1):6–12
4. Morris RJ (2004) A perspective on keratinocyte stem cells as targets for skin carcinogenesis. *Differentiation* 72(8):381–386
5. Raj D, Brash DE, Grossman D (2006) Keratinocyte apoptosis in epidermal development and disease. *J Invest Dermatol* 126(2):243–257
6. Schroder JM (2010) The role of keratinocytes in defense against infection. *Curr Opin Infect Dis* 23(2):106–110

7. Bikle DD, Xie Z, Tu CL (2012) Calcium regulation of keratinocyte differentiation. *Exp Rev Endocrin Metab* 7(4):461–472
8. Boukamp P, Petrussevska RT, Breitkreutz D et al (1988) Normal keratinization in a spontaneously immortalized aneuploid human keratinocyte cell line. *J Cell Biol* 106:761–771
9. Seo E-Y, Piao Y-J, Kim J-S et al (2002) Identification of calcium-induced genes in HaCaT keratinocytes by polymerase chain reaction-based subtractive hybridization. *Arch Dermatol Res* 294:411–418
10. Deyrieux AF, Rosas-Acosta G, Ozbun MA et al (2007) Sumoylation dynamics during keratinocyte differentiation. *J Cell Sci* 120:125–136
11. Capone RB, Pai SI, Koch WM et al (2000) Detection and quantitation of human papillomavirus (HPV) DNA in the sera of patients with HPV-associated head and neck squamous cell carcinoma. *Clin Cancer Res* 6(11):4171–4175
12. Breitkreutz D, Schoop VM, Mirancea N et al (1998) Epidermal differentiation and basement membrane normalization in mouse grafts of human keratinocytes—implications for epidermal homeostasis. *Eur J Cell Biol* 75:273–286
13. Schoop VM, Mirancea N, Fusenig NE (1999) Epidermal organization and differentiation of HaCaT keratinocytes in organotypic coculture with human dermal fibroblasts. *J Invest Dermatol* 112:343–353
14. Deyrieux A, Wilson VG (2007) In vitro culture conditions to study keratinocyte differentiation using the HaCaT cell line. *Cytotechnology* 54:77–83
15. Heaton PR, Deyrieux AF, Bian XL et al (2011) HPV E6 proteins target Ubc9, the SUMO conjugating enzyme. *Virus Res* 158:199–208

Transgene Delivery to Cultured Keratinocytes via Replication-Deficient Adenovirus Vectors

Vincent P. Ramirez and Brian J. Aneskievich

Abstract

Transient transgene expression can facilitate investigation of that gene-product function or effect on keratinocyte biology. Several chemical and biologic delivery systems are available, and among them adenoviruses offer particular advantages in efficiency and transgene capacity. Here we describe the advantages of bicistronic adenovirus and inclusion of the polycation hexadimethrine bromide to aid in the detection of positively transduced cells and enhance transduction efficiency.

Keywords: Adenovirus, Transduction, Keratinocyte, Reporter gene, Polycation

1 Introduction

Efficient and easily demonstrable gene delivery to keratinocytes represents a significant challenge to studying those genes' products in a keratinocyte environment as well as their consequences to keratinocyte cell biology. Various coprecipitate, liposome, charged polymer, and viral (DNA and RNA) methodologies have been advanced, each with its advantages and disadvantages. Of these, adenoviruses have garnered particular attention because of their transgene size capacity, infection of dividing and nondividing cells, potential to bridge preclinical to clinical gene delivery, and bicistronic expression cassettes for identification of positively infected cells via expression of easily assayable reporters, e.g., green fluorescent protein (GFP).

Adenovirus (Ad) broad infectivity is mediated by the coxsackie and adenovirus receptor (CAR) (1, 2). Its normal physiological role contributes to tight junction assembly. CAR has widespread but variable expression; its germ-line loss results in embryonic lethality (3). CAR contacting the Ad fiber protein initiates cell–virus interaction. Fiber is one of the three major Ad capsid proteins that along with hexon and penton form the virion's icosahedral shell. Viral penton association with a cell's alpha v partner of an integrin dimer then promotes internalization. This virus–cell association, mediated by the arginine–glycine–aspartic acid (RGD) sequence

within penton protein, mimics that of certain extracellular matrix proteins, the physiologic ligands for integrin receptors (4).

Though all details of viral entry have yet to be identified (5), identification of viral capsid–cell receptor interactions guided recombinant modifications of both Ad vectors and target cells to optimize infectivity (6). For instance, the RGD motif has been added to the fiber-encoding gene generating a CAR-independent vector (7) by emphasizing penton–integrin-mediated infection. Separately, cells have been engineered to over-express CAR (8) to increase Ad adsorption (9). However, further recombinant vector work delays investigations when existing viral constructs are available and selection required for enrichment of CAR-overexpressing cells may not be practical for primary cultures. A more immediately applicable approach to improve infection rates includes the use of delivery-enhancing reagents such as calcium chloride, poly-cations, commercial lipid transfection reagents, and HIV peptides (1, 10, 11) aimed at reducing possible repulsion effects of negatively charged cell surface and viral capsid proteins. Here we describe the use of poly-cationic hexadimethrine bromide (Polybrene®) versus culture medium for convenient, efficient, cost-effective Ad vector delivery relevant to keratinocyte cultures.

2 Materials

2.1 Viral Vectors

Bicistronic adenoviral vector: Expression cassettes typically feature constitutive promoter driving transcription of gene of interest followed by internal ribosome entry site (IRES) such as that derived from encephalomyocarditis virus (EMCV) to allow for mRNA cap-independent translation of downstream reporter protein, e.g., humanized GFP or β -galactosidase.

2.2 Reagents

1. $1\times$ PBS: 4.31 mM Na_2HPO_4 , 1.47 mM KH_2PO_4 , 2.68 mM KCl, 137 mM NaCl. Prepare with pyrogen-free water, aliquot, and autoclave on liquid cycle for 25 min.
2. Hexadimethrine bromide (Polybrene®, PB): 10 mg/mL in sterile water.
3. HaCaT keratinocyte medium, serum supplemented (*see Note 1*): Dulbecco's modified Eagle's medium (high glucose, with L-glutamine, with pyroxidine HCl, without sodium pyruvate, without sodium bicarbonate), Ham's F12 (with L-glutamine, without sodium bicarbonate), prepared with 3.07 g sodium bicarbonate per liter, adjusted to pH 7.1, and filter sterilized (*see Note 2*). Add penicillin and streptomycin (100 U/mL, 100 μg /mL, respectively) and fetal bovine serum (10 % for growth or 2 % for infections).

4. Trypsin: 0.1 % trypsin, 0.1 % glucose, 0.02 % EDTA with 100 U/mL penicillin and 100 µg/mL streptomycin in 1× PBS.
5. β-galactosidase (β-gal) 2-nitrophenyl β-D-galactopyranoside (ONPG) assay solutions lysis buffer: 50 mM Tris, pH 7.8, 150 mM NaCl, 1 % Nonidet P-40. Z-buffer: 60 mM Na₂HPO₄, 40 mM NaH₂PO₄, 10 mM KCl, 1 mM MgSO₄, final solution pH 7.0. Supplement an assay's required volume with β-mercaptoethanol to 50 nM on the day of the assay (2.7 µL per milliliter of buffer). ONPG: 4 mg/mL ONPG dissolved in Z-buffer. Aliquot and store at -20 °C. Stop solution: 1 M Na₂CO₃.
6. 4 % Paraformaldehyde in PBS: Handle carefully following institutional safety standards for compounds such as paraformaldehyde. Wear laboratory gloves and goggles, and prepare the solution in a fume hood. For 100 mL, pre-warm 70 mL H₂O to 60 °C on a heater/stir plate. Slowly add 4 g paraformaldehyde while slowly stirring; the powder will not dissolve completely but should be evenly suspended. Maintain temperature at ~60 °C, and stir for 3 min. Add one or two drops of 2 N NaOH, and stir for another ~2 min. The solution should get fairly clear; if not add more NaOH by individual drops waiting at least 2 min after each drop. Do not let the solution temperature exceed 65 °C. Remove from heater plate, and stir for another 5 min at RT. Add 10 mL of 10× PBS, and continue stirring until the solution has reached RT. Adjust the RT solution to pH 7.2 with a few drops of 1 N HCl. Store at 4 °C for 1 week, or aliquot and store at -20 °C.

3 Methods

3.1 Cell Seeding and Infection

1. For HaCaT cells seed 70,000 cells/cm² in standard growth medium for cultures to be infected the next day (*see Note 3*). Seeding densities of 10,000 cells/cm² for primary keratinocytes in serum-free, low-calcium medium are suitable for infecting 2 days post plating (*see Note 4*). Chamber slides can be seeded in parallel for convenient visualization, fixing, and subsequent immunofluorescent processing for transgene expression detection.
2. Seed replica plates or chambers to trypsinize, and count the day of the infection to determine the number of cells present for MOI calculation.
3. Prepare dilutions of virus stock. Using minimal volumes of the 2 % FBS medium (*see Note 1*), add PB stock to a final concentration of 4 µg/mL (*see Note 5*) and evenly mix into the medium. Virus MOI typically ranges (12) from 20 to 500

infectious units (IU) per cell (*see Note 6*). Volumes 20 % of standard vessel culture volume are sufficient for infection periods of several hours. Alternatively, we have used 50 % of culture maintenance volumes (e.g., 5 mL for a 10 cm diameter plate) for overnight infection periods. PB–Ad–media mixes can be added without additional complex formation incubation (**13**) times as might be used with liposome or other transduction enhancers.

4. Aspirate off growth medium and add virus–media mixtures. Cultures with significantly reduced volumes should be rocked periodically (once every ~30 min) to reduce meniscus effects and maximize contact of viral particles with cells. At the conclusion of the infection period, aspirate off the PB–Ad–medium mixture and replace with growth medium (*see Note 7*).

3.2 Reporter Gene Expression Detection

1. The sensitivity of assays used for transgene (e.g., GFP or β -gal) reporter detection may influence the apparent transduction efficiency. Fluorescence-activated cell sorting for GFP detection may be required to recognize expression from early expression time points or low MOI (<24 h, <20 IU/cell).
2. Individual cell infection can be monitored in live cultures with FITC-compatible objectives for visual detection of GFP. Relative infection rates from different MOI may be assessed from parallel cultures set on chamber slides. Aspirate medium, rinse three times in PBS, and fix cells in a 4 % paraformaldehyde/PBS solution for 15 min at room temperature. Remove fixative, rinse three times in PBS (*see Note 8*), and permeabilize cells for 5 min at room temperature in 0.2 % Triton-X 100. Rinse twice with PBS, and coverslip with a DAPI-containing mounting medium. Relative infection rates can be estimated from the numbers of GFP-positive cells versus nuclei counts from several fields.
3. Overall culture infection can be assayed from reporter genes such as β -gal. Deposit Z buffer into microtiter well; volume is based on 160 μ L minus cell lysate volume. Cell extract volume may be up to 80 μ L although lysates from MOI > 100 IU/cell at 48 h post infection will likely require no more than 10–20 μ g protein. Prepare a spectrophotometer blank with extract buffer and Z-buffer. To each well, including blank, add 40 μ L ONPG, seal with adhesive cover, and shake on vortex mixer at the lowest speed for 5 min at RT. Incubate at 37 °C incubator, and record start time. Check color development in about 5–10 min for MOI > 100 IU/cell. Plates may be read during color development targeting 0.1–1.0 OD at 420 nm. Add 50 μ L of 1 M Na_2CO_3 , and record stop time. Use automix function of plate reader, or shake on vortex mixer at the lowest speed for 1 min. Plates are read at 420 nm. β -gal-specific activity can be calculated as $[(A_{420}/0.0045)/\text{min}]/\text{mg protein}$.

4 Notes

1. Infection can be conducted in medium without added serum or with reduced serum concentrations. Components of “serum-free” medium should be reviewed to assure that preparations with negatively charged polymers (13) added for other culture purposes (nutrients, attachment factors) are not used.
2. For live microscopic observation of GFP signals, either use phenol red-free medium or transfer samples to PBS as phenol red may contribute to background fluorescence.
3. The overall protocol is similar for transgene delivery to cultures of malignant keratinocytes such as derived from squamous cell carcinomas (14) although one can expect lower levels of CAR expression than primary keratinocytes. In the absence of western blot detection of CAR from uncharacterized keratinocyte lines relative to known infection-compatible cells, expression might at least be confirmed by CAR RT-qPCR with primers forward: 5'-CTG TGC TTC GTG CTC CTG TG-3', reverse: 5'-GGT CTT CGG GAC TAA GCG TAA AT-3', and cycling conditions for Fast SYBR green systems of 95 °C, 20 s; 95 °C, 3 s; and 40×, 57 °C, 30 s (anneal and elongate). CAR expression levels, by RT-qPCR or immunoblotting, are generally indicative of Ad degree of infection (15).
4. Protocol steps here are transferable to primary keratinocytes. We typically allow 2 days post switch to high-calcium medium before infection for expression under differentiation-inducing conditions.
5. Increasing final PB concentrations (1–8 µg/mL) can increase transgene expression (11, 16) although this does negatively affect proliferation (17) for both primary KC and HaCaT cells.
6. Infectious units (IU) are equivalent to plaque-forming units. In agreement with prior reports (18), we found frequencies of positively infected cells as well as expression levels of transgenes increase with increasing MOI although not by the same fold as the MOI. For instance, a fivefold MOI increase from 20 to 100 IU/cell led to an approximately eightfold increase in β-gal activity. Transgene expression increases more closely parallel to MOI increases at higher IU/cell such as a twofold β-gal activity increase over a MOI increase of 100–250 IU/cell. Similar differential increases were observed for infection done in plain medium or medium with PB.
7. Some protocols call for PBS rinsing following the infection period. We have not found this necessary although it might be beneficial when using PB concentrations greater than 4 µg/mL.
8. Following this PBS rinse, slides may be kept in additional PBS for several days at 4 °C before permeabilizing and mounting.

Acknowledgments

This work was supported by a USPHS/NIH grant to BJA (AR048660) from NIAMS. VPR received partial summer support from the Edward A. Khairallah Fellowship, the Luckens Family Toxicology Fellowship, and the Richardson-Vicks Summa Fellowship in Pharmaceutical Sciences.

References

1. Khare R, Chen CY, Weaver EA et al (2011) Advances and future challenges in adenoviral vector pharmacology and targeting. *Curr Gene Ther* 11:241–258
2. Coughlan L, Alba R, Parker AL et al (2010) Tropism-modification strategies for targeted gene delivery using adenoviral vectors. *Viruses* 2:2290–2355
3. Dorner AA, Wegmann F, Butz S et al (2005) Coxsackievirus-adenovirus receptor (CAR) is essential for early embryonic cardiac development. *J Cell Sci* 118:3509–3521
4. Li E, Brown SL, Stupack DG et al (2001) Integrin $\alpha(v)\beta 1$ is an adenovirus coreceptor. *J Virol* 75:5405–5409
5. Marvin SA, Wiethoff CM (2012) Emerging roles for ubiquitin in adenovirus cell entry. *Biol Cell* 104:188–198
6. Preuss MA, Glasgow JN, Everts M et al (2008) Enhanced gene delivery to human primary endothelial cells using tropism-modified adenovirus vectors. *Open Gene Ther J* 1:7–11
7. Wu H, Seki T, Dmitriev I et al (2002) Double modification of adenovirus fiber with RGD and polylysine motifs improves coxsackievirus-adenovirus receptor-independent gene transfer efficiency. *Hum Gene Ther* 13:1647–1653
8. Fechner H, Wang X, Wang H et al (2000) Trans-complementation of vector replication versus Coxsackie-adenovirus-receptor overexpression to improve transgene expression in poorly permissive cancer cells. *Gene Ther* 7:1954–1968
9. Orlicky DJ, DeGregori J, Schaack J (2001) Construction of stable coxsackievirus and adenovirus receptor-expressing 3T3-L1 cells. *J Lipid Res* 42:910–915
10. Lehmusvaara S, Rautsi O, Hakkarainen T et al (2006) Utility of cell-permeable peptides for enhancement of virus-mediated gene transfer to human tumor cells. *Biotechniques* 40:573–576
11. Clark PR, Stopeck AT, Brailey JL et al (1999) Polycations and cationic lipids enhance adenovirus transduction and transgene expression in tumor cells. *Cancer Gene Ther* 6:437–446
12. Zhu X, Li Z, Pan W et al (2012) Participation of Gab1 and Gab2 in IL-22-mediated keratinocyte proliferation, migration, and differentiation. *Mol Cell Biochem* 369:255–266
13. Miralles M, Segura MM, Puig M et al (2012) Efficient amplification of chimeric adenovirus 5/40S vectors carrying the short fiber protein of Ad40 in suspension cell cultures. *PLoS One* 7:e42073
14. Li D, Duan L, Freimuth P et al (1999) Variability of adenovirus receptor density influences gene transfer efficiency and therapeutic response in head and neck cancer. *Clin Cancer Res* 5:4175–4181
15. Saito K, Sakaguchi M, Iioka H et al (2013) Oncogene advance online publication, 18 March 2013; doi:[10.1038/onc.2013.66](https://doi.org/10.1038/onc.2013.66)
16. Doebis C, Ritter T, Brandt C et al (2002) Efficient in vitro transduction of epithelial cells and keratinocytes with improved adenoviral gene transfer for the application in skin tissue engineering. *Transpl Immunol* 9:323–329
17. Jacobsen F, Hirsch T, Mittler D et al (2006) Polybrene improves transfection efficacy of recombinant replication-deficient adenovirus in cutaneous cells and burned skin. *J Gene Med* 8:138–146
18. Hirsch T, von Peter S, Dubin G et al (2006) Adenoviral gene delivery to primary human cutaneous cells and burn wounds. *Mol Med* 12:199–207

Analyzing the Global Chromatin Structure of Keratinocytes by MNase-Seq

Jason M. Rizzo and Satrajit Sinha

Abstract

Eukaryotic DNA is wrapped around histone octamers, known as nucleosomes, in an orderly fashion that provides the primary structure of chromatin organization. The compaction of DNA into nucleosomal repeats not only allows the tight packaging of the large eukaryotic genomes into the nucleus, it also dictates the accessibility of genetic information. Thus, in order to understand how nucleosomes can affect the dynamics of DNA–protein interactions, such as those associated with transcriptional regulatory mechanisms, it is important to define nucleosomal positioning and occupancy along genomic DNA. Here we describe a method that relies on the enzymatic activity of micrococcal nuclease (MNase) to determine nucleosomal footprints and boundaries. By pairing this technique with next generation sequencing techniques (i.e., MNase-seq), it is possible to generate a genome-wide detailed map of chromatin architecture.

Keywords: MNase-seq, Keratinocytes, Chromatin, Formaldehyde, Nucleosomes

1 Introduction

Chromatin is organized into a distinct structure to facilitate the compaction of genomic DNA (1). Chromatin structure is highly conserved across eukaryotic species and consists of 147 bp stretches of DNA coiled around histone proteins arranged in octamers known as nucleosomes (Fig. 1). DNA–histone interactions are the first-order of chromatin structure and both the strength and locations of these interactions yield a significant influence on the accessibility and regulation of genetic information *in vivo* (2). MNase is a bacterial endo-exo nuclease that preferentially digests naked DNA and the DNA located in linkers between nucleosomes (3). Characterization of the DNA protected from MNase digestion provides information on average nucleosome positions and occupancies within cell populations and can be paired with genome-wide assays of DNA (4, 5). Indeed, such genome-wide views of chromatin structure have radically expanded our understanding of the principles controlling chromatin structure by revealing important global organizational principles that could not have been possible by single gene studies (Fig. 2).

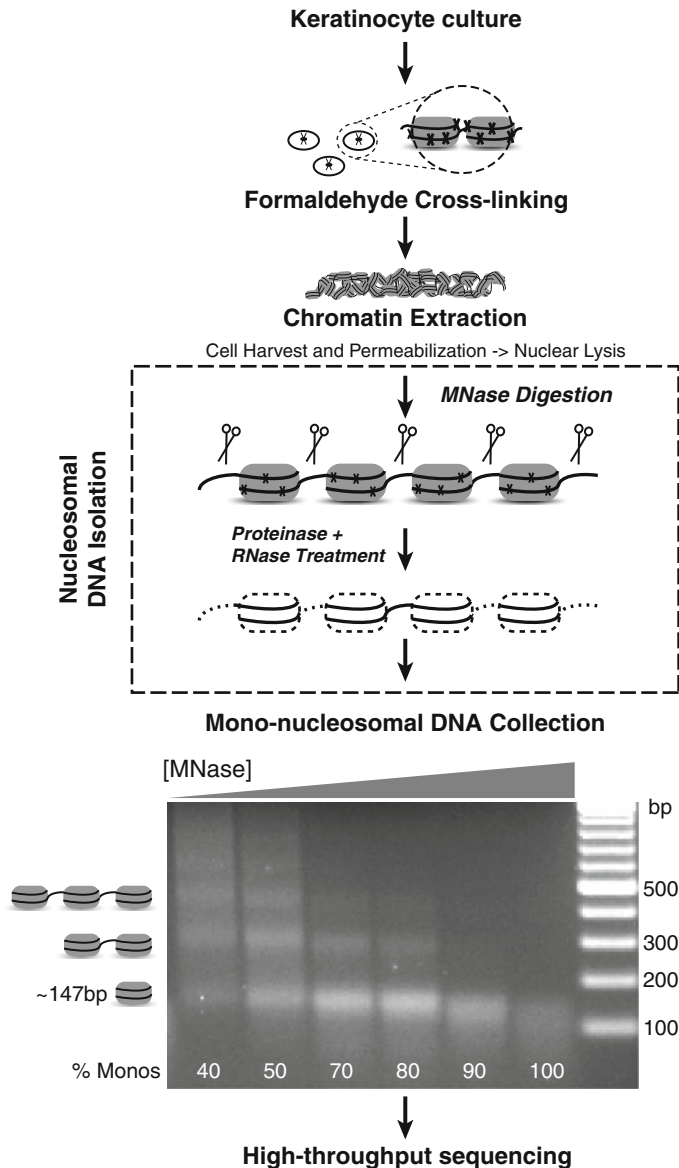


Fig. 1 Schematic of MNase-seq protocol

To determine genome-wide chromatin organization, nucleosomal DNA is first collected by MNase treatment of chromatin extracts and then interrogated using high-throughput DNA sequencing (MNase-seq; Fig. 1). Genome-wide approaches to mapping chromatin structure were first applied to lower organisms such as yeast, but have since been extended to human cells (6, 7). Characterization of nucleosomal (i.e., MNase-protected) genomic DNA populations by MNase-seq methods provides both qualitative and quantitative information on the positioning and occupancies of all nucleosomes for a

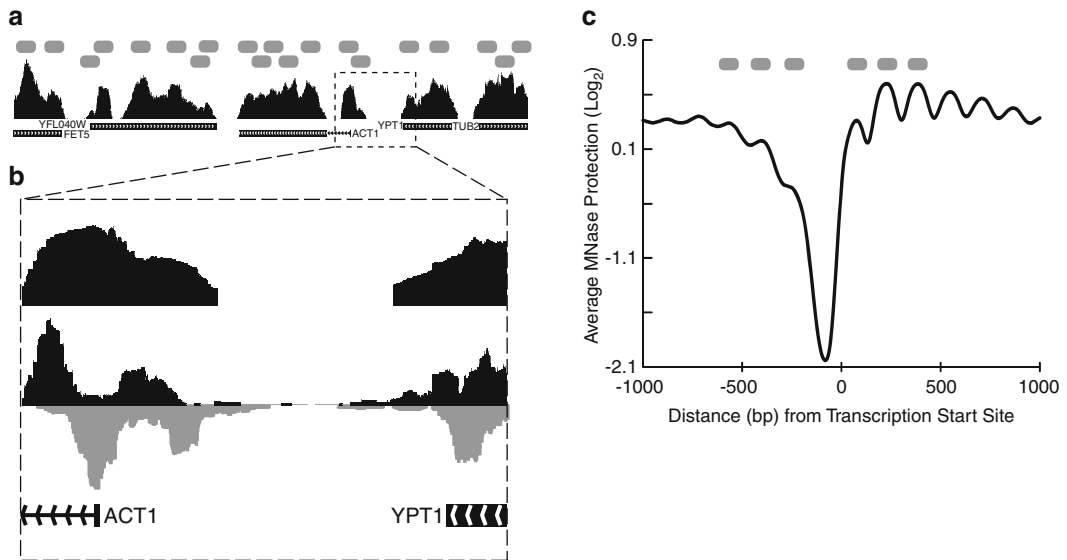


Fig. 2 Example of MNase-seq data output. **(a)** Sample plot of processed MNase-seq signal (i.e., fold-enrichment over genome average of MNase protection) at a well-annotated genomic locus in *S. cerevisiae*. The amplitude of this signal is proportional to nucleosome occupancy on genomic DNA for a given cell population. Similarly, the standard deviation of this signal within a 147 bp window is representative of the positioning of nucleosomes (i.e., low deviation represents strongly conserved positioning). *Gray ovals* represent predicted locations for strongly conserved nucleosome positions based on the illustrated data distribution. **(b)** An example of raw aligned (preprocessed) MNase-seq data. *Bottom panel:* short-end 50–100 bp sequence reads are aligned to the reference genome in a direction-specific manner and totaled (forward in *black*, reverse in *gray*). Short reads represent the ends of sequenced mononucleosomal DNA fragments. *Top panel:* Short-reads are extended to a total length of 120 bp to more accurately reflect nucleosomal DNA protection patterns. Alternatively, a paired-end or longer read-length sequencing reaction provides a similar signal without the need for the aforementioned processing steps. **(c)** An example of the average MNase protection pattern for all genes in *S. cerevisiae*. A conserved promoter chromatin organization exists across all eukaryotic species whereby a well-defined nucleosome depleted region lies upstream of all transcription start sites (TSS) and is flanked by well-positioned nucleosomes directly up and downstream. *Gray ovals* represent predicted locations for strongly conserved nucleosome positions based on the illustrated data distribution

cell population being assayed (Fig. 2). This high-resolution global view of chromatin architecture enables researchers to compare the accessibility of all genomic DNA sequences for targeting by regulatory factors and other DNA-binding proteins. For example, integration of MNase-seq data with genome-wide Transcription Factor (TF) binding data collected using similar ChIP-seq techniques has shown that the majority of TF binding sites that are occupied (bound) *in vivo* are located at genomic regions that are highly sensitive to MNase digestion and thus nucleosome depleted (8). This preference for TFs to bind nucleosome-depleted regions *in vivo* is consistent with the general notion that nucleosomes can regulate transcription by blocking TF binding.

Like ChIP-seq, MNase-seq provides an *in vivo* snapshot of intracellular protein–DNA interactions via heat-reversible fixation with formaldehyde treatment. Unlike ChIP-seq, however, MNase-seq does not rely on an immunoprecipitation (IP) step and thus avoids the potential biases commonly associated with antibody selection and utilization. The indirect relationship between MNase protection and chromatin structure can, however, be strengthened through introduction of IP steps (*see Note 6*) to improve specificity and examine the role of specific histone proteins (e.g., MNase-ChIP-seq) (9). MNase-seq experiments also differ from most ChIP based experiments in that the footprint of histone protection covers the vast majority of genomic sequence—this requires different analytic considerations. Despite these apparent advantages, the use of nuclease protection as a read-out for chromatin structure data is limited by the kinetics of MNase digestion. It is important to note that differences in the extent of MNase digestion alone can confound downstream nucleosome occupancy comparisons between MNase-seq experiments by virtue of a size-selection DNA sampling bias (10).

Undoubtedly, an ability to accurately profile and compare chromatin states between distinct cell populations provides a powerful tool for molecular biologists interested in dissecting gene regulatory mechanisms. Chromatin is a highly dynamic structure, which enables the same genetic sequence to respond in a distinct and physiologically appropriate manner to differing environmental insults. Thus, condition-specific comparisons between distinct chromatin states by MNase-seq can yield significant insights into key genome–environment interactions regulating developmental processes such as keratinocyte differentiation. Thankfully, preparation and analysis of MNase-seq experiments is quick, cost-effective, and relatively straightforward thus affording novice genomics researchers access to this evolving methodology. Several well-curated online databases are available to assist with analysis of the genomic data (11). Moreover, ongoing large-scale genomic data initiatives are collecting data that can be readily integrated with information from MNase-seq to provide a multiscale view of gene regulatory networks (12). Here, we provide a protocol for MNase-seq for keratinocytes grown in culture and outline appropriate experimental design considerations that can be applied for such studies.

2 Materials

2.1 Cross-Linking Keratinocytes

1. 37 % Formaldehyde (Fisher; Cat. no: F79-1).
2. 2.5 M Glycine (Sigma; Cat. no: G8790).
3. 10 × Phosphate buffered saline (PBS) (Invitrogen; Cat. no:14200–075).

4. 95 % ethanol (Aaper; Cat. No:111000190).
5. Dry-ice.

**2.2 Chromatin
Extraction (Mechanical
Lysis of Cell and
Nucleus)**

1. Nuclease Digestion Buffer (DB): 10 mM Tris-HCl, pH 8.0, 2 mM CaCl₂.
1 M Tris-HCl pH 7.5 and 8.0 (Cat. no.: BP1757 & BP1758).
Calcium chloride dehydrate (CaCl₂) (Fisher; Cat. No.: BP510).
2. 1.0–2.5 mm glass beads (Biospec; Cat. No: 11079110).
3. Mini-beadbeater-8 (Biospec Cat. No: 693).
4. 18 G, ½ in. needle.
5. Coomassie Plus (Bradford) Protein Assay (Thermo Scientific; Cat. no.: 1856210).
6. Dry-ice.
7. 95 % ethanol.

**2.3 Micrococcal
Nuclease (MNase)
Digestion**

1. Micrococcal Nuclease (MNase) (Worthington Biochemical Corp; Cat. no: LS004797).
2. MNase Storage Buffer: 10 mM Tris-HCl, pH 7.4, 50 mM NaCl, 1 mM EDTA, 50 % Glycerol.
1 M Tris-HCl pH 7.5 and 8.0 (Cat. no: BP1757 and BP1758).
Sodium Chloride (NaCl) (Fisher; Cat. no: S671).
EDTA (Fisher; Cat. no: BP2927).
Glycerol (Fisher; Cat. no: G31).
3. Stop Solution: 8.6 % SDS, 0.07 M EDTA, pH 8.0.
Sodium Dodecyl Sulfate (SDS) (Fisher; Cat. No: BP166).
EDTA (Fisher; Cat. no: BP2927).

**2.4 Proteinase/
RNase Treatment
and DNA Precipitation**

1. 20 mg/ml Proteinase K solution (Invitrogen; Cat. no: 25530-049).
2. 3 M Sodium acetate, pH 5.2 (Sigma; Cat. no: S-7899).
3. Phenol:chloroform; premixed with isoamyl alcohol (Amresco; Cat. no: 0883).
4. 1× TE Buffer, pH 8.0 (Amresco; Cat. no: E112).
5. 10 mg/ml RNase A (Sigma; Cat. no: R6513).

**2.5 Mononucleosomal DNA
Collection and
High-Throughput
Sequencing**

1. Agarose (Multipurpose) (Fisher; Cat. No.: BP160).
2. 10× DNA Loading Buffer (without Bromphenol Blue): 20 % Ficoll, 0.1 M EDTA, 1 % SDS, 0.25 % Xylene Cyanol.
Ficoll (Acros organics; Cat. No.: AC61186-0050).

EDTA (Fisher; Cat. no.: BP2927).

Xylene Cyanol (Fisher; Cat. No.: O6116).

3. MiniElute DNA purification kit (Qiagen; Cat. No. 28004).

3 Methods

3.1 *Cross-Linking Keratinocytes*

1. Add formaldehyde to a final concentration of 1 % directly to the medium in which keratinocytes are growing ($0.5\text{--}1 \times 10^7$ cells ~ 80 % confluent) and incubate at room temperature for 15 min. Methods to grow keratinocytes have been well described in relevant chapters of this book (*see* **Notes 1** and **2**).
2. Stop the cross-linking reaction by addition of Glycine to the medium to a final concentration of 125 mM (from a 2.5 M stock). Incubate for 5 min at room temperature (quenches the crosslinking reaction).
3. Pellet the cells in 50 ml conical tubes at $250 \times g$ for 5 min at 4°C . Wash pellet twice with 50 ml of $1 \times$ PBS buffer. Vortex and centrifuge at $250 \times g$ for 5 min after each wash and then quick freeze the pellet with either liquid nitrogen or dry-ice and Ethanol. This cross-linked cell pellet can be stored at -80°C until ready for the next step.

3.2 *Chromatin Extraction (Mechanical Lysis of Cell and Nucleus)*

1. Thaw sample on ice and resuspend the pellet with 1 ml of DB buffer and transfer to 1.5 ml tube. Pellet cells at $100 \times g$ for 5 min at 4°C and aspirate all the liquid carefully without disturbing the pellet. It is important to remove all liquid so that the pelleted cells can be weighed accurately. Keep pellets and future lysates on ice.
2. Weigh cells, ensuring that you blank with empty tube.
3. Resuspend pellets weighing less than 0.2 mg with 400 μl of DB buffer. If the cell pellet weighs more than 0.2 mg then split into two (or more) 400 μl samples with less than 0.2 mg of cells. Make sure the cells are completely resuspended before continuing.
4. Transfer suspension to 1.5 ml tubes containing ~ 1 ml of 0.5 mm glass beads.
5. Lyse cells in a mini-beadbeater-8 (Biospec) with four 1 min sessions at the highest setting. Place tubes on ice for 2 min between each session.
6. Recover the extract by punching a small bore hole in the bottom of the tube with a 18 G, $\frac{1}{2}$ in. needle. Spin the liquid through to another tube with a one-pulse-spin ($<500 \times g$) for 30 s. Repeat 2–3 \times to clear lysate from tube.

7. Combine all samples and determine the protein concentration by a Bradford assay (OD595) (*see Note 3*). Ensure consistent yields between chromatin preparations you intend on comparing.
8. Quick-freeze the samples with liquid nitrogen or a (dry-ice + 95 % ethanol) bath. Lysates may be stored frozen at -80°C indefinitely. Samples should be stored in aliquots to limit freeze thawing (typically 5.5 mg per aliquot allows 5 MNase digestions). Even if you plan to continue with digestions on the same day, all samples should still be frozen so that if you need to return to the other aliquots results will be reproducible.

3.3 Micrococcal Nuclease (MNase) Digestion

1. MNase digestions should be performed on 1 mg of total protein in 200 μl DB for 1 h at 37°C .
 - (a) *Initial digest titration*: Three to five test digestions should be setup with a broad range of total units added (e.g., 50, 25, 10, 5, and 1 U total added) for a single sample type. This titration helps to identify the amount of MNase needed to achieve the desired extent of digestion. This result will be specific to each chromatin preparation and MNase stock used (*see Notes 3–5*).
 - (b) *Repeat digest titrations*: For future/additional samples, conduct more focused titrations (3–5 digests) using MNase concentrations both at and surrounding the previous replicate's ideal extent of digestion (as identified in Section 3.5). This ensures collection of multiple samples for comparison and selection of matched mononucleosomal DNA populations.
2. Stop digestion reactions with 29 μl stop solution; make this fresh. Vortex samples upon stop solution addition. For 110 μl add 95 μl 10 % SDS + 15 μl 0.5 M EDTA, pH 8. Final concentration in 229 μl : 1 % SDS and 8.86 mM EDTA (*see Note 6*).

3.4 Proteinase/RNase Treatment and DNA Precipitation

1. Add 2 μl Proteinase K (20 mg/ml) to reverse cross-links. Incubate 30 min at room temperature and then at 65°C for 6 h to overnight.
2. Add 300 μl of Phenol:Chloroform:Isoamyl (PCI) alcohol in each tube. Vortex and spin for 4 min at $15,000 \times g$ at 4°C . Transfer aqueous (top) layer to a new tube. Add additional 100 μl DB buffer to PCI, vortex and spin and transfer aqueous combining with previous samples.
3. Repeat the extraction again with 300 μl of Phenol:Chloroform:Isoamyl alcohol, vortex, spin, and transfer aqueous layer to new tube.
4. Add 30 μl of 3 M Na Acetate (pH 5.2) to the aqueous phase and mix.

5. Ethanol precipitate with 1.3 ml 95 % EtOH, mix. Spin down at 4 °C for 20 min, at $15,000 \times g$ and discard the ethanol. DNA precipitates may be stored in 95 % EtOH at -80 °C indefinitely.
6. Rinse pellet with 70 % ethanol. Spin down for 10 min, at $15,000 \times g$ and decant again out the ethanol. Try to remove as much ethanol as possible to allow easy drying. Be careful not to disturb the pellet.
7. Dry pellet by placing open tube upside down in the hood for 10–20 min. Avoid using a heated vacuum to minimize degradation.
8. Resuspend in 50 μ l TE + 2 μ l RNase (10 mg/ml) and incubate at 37 °C for 30 min.
DNA may be stored at -20 °C for 3–6 months following RNase treatment. Optional: Cleanup sample using a MinElute spin column into 10 μ l (Qiagen). This is the portion of the genomic DNA covered by nucleosomes.

3.5 Mononucleosomal DNA Collection and High-Throughput Sequencing

1. To assess the extent of digestion of your samples, run 5–10 μ l of the elution with $1 \times$ loading buffer (without Bromophenol Blue dye) on a 2 % agarose gel. Select the sample preparation that has a smear at 120–150 bps and is completely digested or, alternatively, digested to the desired extent (*see Notes 7–9*). You may need to perform repeat MNase titration as described in Section 3.3, step 1(b) to ensure that the samples are adequately digested for downstream comparisons and applications.
2. To select matched MNase digestions run all of the chromatin DNA samples you wish to compare (i.e., similar digests) on the same 2 % gel (10 μ l of each sample + 1 μ l $10 \times$ loading buffer/gel lane) to identify matched digests using gel image analysis (*see Note 10*).
3. Column purify matched samples of interest with MinElute spin column (Qiagen) and elute DNA in 10 μ l.
4. Quantify nucleosomal DNA population with picogreen assay and use as input for Illumina's TruSeq DNA PCR-Free Sample Preparation Kit for low-throughput sequencing protocol (*see Notes 11 and 12*).
5. Data analysis: Short sequence reads of ~ 50 –100 bp are output from Illumina's analysis pipeline and aligned to the reference genome of interest (e.g., mm10 for mouse genome). Only reads with two or fewer sequence mismatches are retained. These reads are then extended to a total length of 120 basepair (bp). Overlapping reads are then summed for each bp and then divided by the genome average, and transformed into Log_2 space to calculate relative MNase protection ratios (Fig. 2b).

4 Notes

1. Protocol can be scaled up proportionately as needed.
2. The protocol described here can also be performed with mouse skin epidermis. For this, skin samples are isolated and treated with Dispase II (Roche Catalogue #04942078001) overnight at 4 °C. The epidermis is then separated, washed five times with PBS, and finely chopped. Next, the epidermis is cross-linked with 1 % formaldehyde in PBS at room temperature for 15 min and the subsequent steps for MNase-seq procedures are followed.
3. Alternatively, both chromatin extraction yields and standardized MNase digestions inputs can be calculated based on DNA-based absorption methods such as Hoescht assay or pico-green quantitation assay (13).
4. Additional digests across a broader range of MNase may be necessary to achieve desired extent of digestion. Always store MNase in MNase storage buffer at -80 °C in 10–15 µl aliquots. For consistency/reproducibility thaw each aliquot once only; discard any unused samples. When setting up MNase digests, first mix all thawed aliquots needed together, then prepare a diluted MNase stock for lower concentration digests (e.g., dil stock = 5 µl stock + 45 µl DB; use 5 µl diluted stock for 5U/200 µl reaction;). Never pipette less than 1 µl MNase.
5. “Desired extent of MNase digestion”: Both *in vivo* and *in silico* analysis has shown that differences in extent of MNase digestion between samples can confound downstream comparisons between MNase-seq experiments by virtue of a size-selection DNA sampling bias (10). To control for this bias, we recommend comparing only MNase digestions that are closely matched in their extent of digestion (% of Mononucleosomes). Moreover, we suggest the use of complete-digested chromatin preparations (100 % mononucleosomal DNA) since this provides the most consistent chromatin collection and sampling and an MNase-seq signal closest to true nucleosome occupancy (10). Alternatively, multiple or different (i.e., incomplete) digestion titrations can be collected, but only “matched” samples should be compared for the aforementioned reasons (14). The extent of digestion can be gauged as described in Section 3.5.
6. Specific amino acid residues of each histone protein also undergo an assortment of covalent modifications, including methylation, ubiquitination, and acetylation, which further diversifies the chromatin landscape (12). Therefore, researchers may wish to incorporate an additional IP step to enrich for specific nucleosome populations. Consult ChIP literature for

appropriate IP conditions. Experimental options include histone-specific antibodies, histone-variant antibodies, or TF antibodies to probe for TF–nucleosome interactions (15).

7. Use a DNA loading buffer that does not include Bromophenol Blue dye, which runs around 300 bp and may interfere with downstream image analysis (*see Note 10*).
8. Alternatively, extent of MNase digestion can be assessed using an Agilent Bioanalyzer. The type of assay used will depend on the initial concentration of the samples (e.g., High Sensitivity dsDNA Bioanalyzer assay for low amounts).
9. MNase digestions should reveal a laddering of nucleosomal DNA populations (*see Fig. 1*). Often, compacted higher-order chromatin structures may prove recalcitrant to MNase digestion and produce a smearing on imaging instead of clean laddering. In this situation, an additional sonication step can be added to sample preparation prior to digestion to facilitate decompaction. For this purpose, you can use a Bioruptor sonicator (Diagenode) for 5 min on High using 30 s pulses and 30 s rest.
10. The size distribution of protected nucleosomal DNA populations can be estimated relative to a known standard using gel image analysis software or alternatively using an Agilent Bioanalyzer tracer. Correlations between standardized post-digest size distributions can then be utilized to identify and select matched digestion profiles.
11. Many downstream protocols, such as high-throughput DNA sequencing, are extremely quantity-sensitive. Therefore, final concentrations of prepared mononucleosomal DNA are best determined using ultra-sensitive fluorescent nucleic acid staining techniques (i.e., PicoGreen dye), since this measure has a larger dynamic range and is specific for double-stranded DNA. Use of fluorescent quantification will also ensure that you have sufficient dsDNA for downstream applications (13).
12. Illumina's low-throughput protocol enables multiplexing up to 24 samples, however, MNase-seq experiments require an average coverage of at least $10 \times$. Therefore, we recommend multiplexing conservatively. For mouse samples, for, e.g., one would require a minimum of $\sim 2 \times 10^8$ reads for each experiment (~ 2.7 Gb/genome/147 bp/nucleosomes \times 10 reads/nucleosome).

Acknowledgments

This work is partially supported by grants R21DE021137 and R03HD073891 to SS. We thank Dr. Michael Buck and Dr. Maria Tsompana for their help and advice with the MNase-seq experiments.

References

1. Hayes JJ, Hansen JC (2001) Nucleosomes and the chromatin fiber. *Curr Opin Genet Dev* 11:124–129
2. Venters BJ, Pugh BF (2009) How eukaryotic genes are transcribed. *Crit Rev Biochem Mol Biol* 44:117–141
3. Axel R (1975) Cleavage of DNA in nuclei and chromatin with staphylococcal nuclease. *Biochemistry* 14:2921–2925
4. Jiang C, Pugh BF (2009) Nucleosome positioning and gene regulation: advances through genomics. *Nat Rev Genet* 10:161–172
5. Rizzo JM, Buck MJ (2012) Key principles and clinical applications of “next-generation” DNA sequencing. *Cancer Prev Res (Phila)* 5:887–900
6. Gaffney DJ, McVicker G, Pai AA et al (2012) Controls of nucleosome positioning in the human genome. *PLoS Genet* 8:e1003036
7. Kaplan N, Moore IK, Fondufe-Mittendorf Y et al (2009) The DNA-encoded nucleosome organization of a eukaryotic genome. *Nature* 458:362–366
8. Harbison CT, Gordon DB, Lee TI et al (2004) Transcriptional regulatory code of a eukaryotic genome. *Nature* 431:99–104
9. Wal M, Pugh BF (2012) Genome-wide mapping of nucleosome positions in yeast using high-resolution MNase ChIP-Seq. *Methods Enzymol* 513:233–250
10. Rizzo JM, Bard JE, Buck MJ (2012) Standardized collection of MNase-seq experiments enables unbiased dataset comparisons. *BMC Mol Biol* 13:15
11. Sun H, Qin B, Liu T et al (2013) CistromeFinder for ChIP-seq and DNase-seq data reuse. *Bioinformatics* 29:1352–1354
12. Bernstein BE, Birney E, Dunham I, Green ED, Gunter C, Snyder M (2012) An integrated encyclopedia of DNA elements in the human genome. *Nature* 489:57–74
13. Gallagher SR (2011) Quantitation of DNA and RNA with absorption and fluorescence spectroscopy. *Curr Protoc Neurosci Appendix 1: Appendix 1K*.
14. Cui K, Zhao K (2012) Genome-wide approaches to determining nucleosome occupancy in metazoans using MNase-Seq. *Methods Mol Biol* 833:413–419
15. Egelhofer TA, Minoda A, Klugman S et al (2011) An assessment of histone-modification antibody quality. *Nat Struct Mol Biol* 18:91–93

Analysis and Meta-analysis of Transcriptional Profiling in Human Epidermis

Claudia Mimoso, Ding-Dar Lee, Jiri Zavadil, Marjana Tomic-Canic, and Miroslav Blumenberg

Abstract

Because of its accessibility, skin has been among the first organs analyzed using DNA microarrays; psoriasis, melanomas, carcinomas, chronic wounds, and responses of epidermal keratinocytes in culture have been intensely investigated. Skin has everything: stem cells, differentiation, signaling, inflammation, hereditary diseases, etc. Here we provide step-by-step instructions for bioinformatics analysis of transcriptional profiling of skin. We also present methods for meta-analysis of transcription profiles from multiple contributors, available in public data repositories. Specifically, we describe the use of GCOS and RMAExpress programs for initial normalization and selection of differentially expressed genes and RankProd for meta-analysis of multiple related studies. We also describe DAVID and Lists2Networks programs for annotation of genes, and for statistically relevant identification of over- and underrepresented functional and biological categories in identified gene sets, as well as oPOSSUM for analysis of transcription factor binding sites in the promoter regions of gene sets. This work can serve as a primer for researchers embarking on skinomics, the comprehensive analysis of transcriptional changes in skin.

Keywords: Affymetrix, Annotation, Clustering, Epidermal differentiation, Gene sets, Nonparametric, Ontological categories, Skinomics, Transcriptome

1 Introduction

This contribution is a follow-up on the article titled: “Comprehensive transcriptional profiling of human epidermis, reconstituted epidermal equivalents and cultured keratinocytes, using DNA microarray chips” (1). In the revision we edited and slightly modified several sections, specifically those dealing with the bench-top isolation and handling of RNA from epidermal sources. We deleted several sections dealing with algorithms that were out-of-date and outdone by more advanced approaches. Most important, we include here a novel primer for meta-analysis of data available in public repositories. The past years witnessed a tremendous increase in transcriptional profiling research; most journals nowadays require that such data be made publicly available as a condition for publication. This has provided a treasure trove for meta-analyses, allowing researchers to integrate their own data into the common fund of knowledge and thereby

make new discoveries, define new biological relationships and advance scientific understanding. Thus, the methods described allow for “big data” analyses approaches, which has been one of the major initiatives launched by NIH (<https://commonfund.nih.gov/bd2k/index.aspx>).

The advent of genomics made possible comprehensive and efficient analysis of gene expression. DNA microarrays are an ideal approach for such systematic comparisons because they can simultaneously measure the expression of, potentially, the entire genome (2). DNA microarray is an ordered arrangement of nucleic acid sequences from thousands of different genes arrayed at fixed locations on supports, usually silicon chips or glass microscope slides. DNA chips come in two varieties: printed cDNA and synthetic oligonucleotide. The first, originated by P. Brown at Stanford (3), are often homemade, inexpensive, and two-color, i.e., a treated sample and the control samples can be hybridized and compared on the same chip. They are easy to customize for a specific application. Synthetic oligonucleotide microarrays are commercially available, at a price, but because each gene is probed with multiple oligonucleotides, they tend to be more reliable and require less redundancy. They are one-color, i.e., they probe only one sample per array, but the newer ones contain all the known human genes and are able to identify the splicing variants as well (4). To address the differences in technique, data quality, etc., the microarray community has promulgated a set of guidelines known as “MIAMI” rules (*minimal information about microarrays*), which must be complied with if a manuscript is to be accepted in a growing list of journals.

Bioinformatics is a very fast-moving field and new and improved approaches, types of chips, hardware, software, and data repositories are constantly being developed. To keep up with the field, we find very useful the special “Database issue,” http://nar.oxfordjournals.org/content/vol36/suppl_1/index.dtl published by The Nucleic Acids Research every January. This edition describes the function and role of all molecular biology data repositories, including those that collect microarray data. Another invaluable resource is the growing set of algorithms assembled in Bioconductor <http://www.bioconductor.org/>. Particularly important for the work presented here are the Automated Affymetrix Array Analysis Umbrella Package <http://www.bioconductor.org/packages/release/bioc/html/a4.html> and the RankProd algorithm <http://www.bioconductor.org/packages/release/bioc/html/RankProd.html>. Bioconductor packages are freely available, usually well described and annotated, and we find that the developers of the programs are ready to help with trouble-shooting and hand-holding.

The epidermis presents the most accessible target and consequently skin was among earliest targets of DNA microarray studies (5). The RNA from the skin surface can even be recovered using an

easy, noninvasive procedure named “tape stripping” (6). The large volume of bioinformatics data relevant to skin led to the coinage of the term Skinomics (7). Skinomics DNA microarray studies focused on epidermal differentiation, skin cancers, inflammatory diseases, wound healing, ageing, stem cells, etc. (8). Specific for skin has been a series of studies on the effects of UV light (9–13). Melanomas and basal and squamous cell carcinomas have been intensely investigated using DNA microarrays and so was psoriasis, one of the most common human inflammatory diseases (14, 15). In addition, genomics analyses of chronic, nonhealing wounds, yielded critical information about pathogenesis that are revising clinical approaches to treatment (16–19). The presence of many different cell types in skin, unfortunately, creates difficulties. Potentially very informative, skin samples taken directly from patients differ in proportions of various cell types, sample age and body sites, history of sun exposure, etc. (8).

The transcriptional profiling in skin is rapidly expanding. Unavoidably, some of the recommendations in this manuscript will be outdated even by the time it reaches print. Virtually every analysis tool mentioned is associated with a dedicated team of developers and programmers devoted to making them better, more versatile, and user friendly. Therefore, dear readers, if you see an innovation or a new useful approach, please contact us at Miroslav.Blumenberg@nyumc.org and we will keep an updated running manual of the described procedures. Conversely, if you embark on transcriptional profiling in skin and would like to find out about new developments, or just need some hand-holding, do not hesitate to get in touch.

2 Materials

2.1 Growth and Isolation of Keratinocytes

1. Normal epidermal keratinocytes or skin samples from surgery. Human skin samples are obtained from patients undergoing elective breast reduction surgery, usually within 2–6 h after surgery.
2. Serum-free keratinocyte growth medium supplemented with 0.05 mg/ml bovine pituitary extract, 5 ng/ml epidermal growth factor, and 1 % penicillin/streptomycin (KGM from Gibco-BRL).
3. Trypsin, adjusted to 0.025 % (Gibco-BRL).
4. Trypsin inhibitor, 0.5 mg/ml in PBS (Sigma).
5. Reconstituted Human Epidermis (SkinEthic Laboratory, Nice, France).
6. Dispase (2.4 U/ml, Roche).
7. RNase inhibitor (4 U/ml Roche).
8. RNA*later* (Ambion).

**2.2 Separation
of Epidermal Layers
and Isolation of Basal
Layer Keratinocytes**

1. PBS, phosphate-buffered saline.
2. Solution of 0.05 % trypsin, 0.02 % EDTA (GibcoBRL).
3. Solution of 0.5 mg/ml trypsin inhibitor (Sigma).
4. Cell Strainer tissue filters (Falcon).
5. Magnetic beads, M-450 Rat anti-Mouse-IgG1, prepared as suggested by the manufacturer (Dyna).
6. Antibody 3E1, which binds integrin $\beta 4$ from (GibcoBRL).

**2.3 Isolation of Total
RNA, Preparation
of Labeled Probes,
and Hybridization**

1. Qia shredders and on-column RNAses-free DNase Set (Qiagen).
2. RNeasy kits (Qiagen).
3. Trizol (Invitrogen).
4. RNAlater (Ambion).
5. Affymetrix microarrays.

2.4 URL Sites Listed

1. <http://rmaexpress.bmbolstad.com/>
2. <http://david.abcc.ncifcrf.gov/>
3. <http://rana.stanford.edu/software/>
4. <http://www.tm4.org/>
5. <http://www.pangloss.com/seidel/Protocols/venn.cgi>
6. <http://www.cisreg.ca/cgi-bin/oPOSSUM/opossum/>
7. http://nar.oxfordjournals.org/content/vol36/suppl_1/index.dtl
8. <http://www.bioconductor.org/>
9. <http://www.bioconductor.org/packages/release/bioc/html/a4.html/>
10. <http://www.bioconductor.org/packages/release/bioc/html/RankProd.html>
11. <http://www.skinethic.com/>
12. <http://www.mattek.com/>
13. <http://www.ncbi.nlm.nih.gov/pubmed/>
14. <http://www.ebi.ac.uk/arrayexpress/>
15. <http://amp.pharm.mssm.edu/lachmann/upload/register.php/>
16. <http://www.add-ins.com/>
17. <http://www.affymetrix.com/support/technical/libraryfilesmain.affx/>
18. <http://www.lgtc.nl/MaRe/>
19. <http://www.biomart.org/biomart/martview/39658a1f84f2d1822db6e184a5cc356e>
20. <http://sourceforge.net/projects/arrayexpress/files/>
21. <http://commonfund.nih.gov/bd2k/index.aspx/>

3 Methods

3.1 Provenance and Maintenance of Samples

1. Normal epidermal keratinocytes from human foreskin were initiated using 3T3 feeder layers as described (20, 21) and then frozen in liquid N₂ until used. Once thawed, the keratinocytes are grown without feeder cells in defined serum-free keratinocyte growth medium supplemented with 0.05 mg/ml bovine pituitary extract, 5 ng/ml epidermal growth factor, and 1 % penicillin/streptomycin (KGM from Gibco-BRL) at 37 °C, in 5 % CO₂. The medium is replaced every 2 days (Note 1).
2. The reconstituted human epidermis consists of a three-dimensional multilayered keratinocyte structure grown on air-liquid interface, without any other cell type. These are available from SkinEthic <http://www.skinethic.com/> or MatTek <http://www.mattek.com/> (Note 2). The media for cell culture are usually prepared without antibiotics and antimycotic agents (22, 23).
3. Human skin samples are obtained from patients undergoing elective breast reduction surgery, usually within 2–6 h after surgery (Note 3). The fat layer and most of the dermis are removed using surgical scissors and by gentle scrapping with a scalpel, leaving the epidermis as the predominant cellular structure (~0.2 mm deep). Samples are then cut into strips of approximately 0.5 × 3 cm and stored in RNALater (Ambion) overnight at 4 °C.

3.2 Isolation of β 4+ and β 4- Keratinocytes from Skin

1. Skin, discarded after reduction mammoplasty, as described above, is first washed six times with PBS and excess liquid drained. Using scissors and a scalpel, fat and dermis is removed as much as possible. The tissue is cut into 3 mm wide strips and incubated with dispase (2.4 U/ml, Roche) and RNase inhibitor (4 U/ml Roche) at 4° overnight.
2. Next day, the epidermis is gently separated from the dermis using forceps, and incubated in 0.05 % trypsin, 0.02 % EDTA (GibcoBRL) at 37°. After 10 min, two volumes of 0.5 mg/ml trypsin inhibitor (Sigma) is added and the tissue filtered through Cell Strainer (Falcon). The trypsinization of the tissue is repeated twice more. The cells are collected by centrifugation, examined using trypan-blue, counted and, if appropriate, the isolates combined. This represented the unfractionated, total epidermal cell population.
3. Magnetic beads, M-450 Rat anti-Mouse-IgG1, are prepared as suggested by the manufacturer (Dynal). The cells are incubated with the beads in the following ratio: 100 μ l beads: 10–20 μ g β 4 antibody: 4 × 10⁶ cells (exactly!) in 1 × PBS, 0.1 % BSA, at 4° for 1–2 h. We used M-450 Rat anti-MouseIgG1 beads and

the 3E1 clone $\beta 4$ antibody from GibcoBRL (24). The beads are separated on a magnetic separator for 2–3 min, washed 3–4 times with PBS, collecting and combining the nonadherent, $\beta 4^-$ cells, which represents the suprabasal cell population. The beads bound to the $\beta 4^+$ basal cells are used in RNA isolation without removing the cells from the beads.

3.3 Isolation of Total RNA from Human Epidermis

To obtain RNA of appropriate quality for chip analysis from in vivo epidermis, we have tested several purification methods. After extensive experimentation, we settled on the following approach:

1. First, the epidermal cells are disrupted and the RNA is isolated using Trizol (Gibco).
2. This is followed by the use of Qiashredders to homogenize cell extracts with centrifugation at $1,800 \times g$ for 2 min.
3. DNA is removed with on-column DNase digestion using RNases-free DNase Set (Qiagen). RNeasy kits from Qiagen are used to prepare the RNA according to the manufacturer's protocols (Note 4). If the sample is not immediately processed for RNA isolation, it is cut into 3 mm-wide strips and stored in RNAlater overnight at 4 °C, then at -20 °C. With this procedure, we routinely prepare RNA of high quality (Note 5).
4. From the reconstituted epidermis and cultured keratinocytes, total RNA is isolated using Qiashredders to homogenize cell extracts, and RNeasy kits procedure. The RNA samples are stored in water at -80 °C until hybridization.
5. To ensure good RNA quality, 28S and 18S ribosomal bands are visualized on a nondenaturing agarose gel and OD_{260/280} spectrophotometric ratio of at least 1.8 is ascertained. Five micrograms of total RNA is reverse transcribed, amplified, and labeled as described (25).
6. Approximately 5–8 μg of total RNA is reverse transcribed, amplified, and labeled as described (9, 26). Labeled cRNA is hybridized to the arrays (Affymetrix), which are washed, stained with anti-biotin streptavidin-phycoerythrin-labeled antibody using Affymetrix fluidics station and then washed again according to the Affymetrix protocol.
7. Arrays are scanned using the Agilent GeneArray Scanner system (Hewlett-Packard) and GeneChip 3.0 software to determine the expression of each gene. A representative picture of a hybridized Affymetrix microarray is shown in Fig. 1.

RT-PCR, Northern and Western blot analyses that confirm microarray data will not be described here; any standard molecular biology protocol compilation can be consulted for this purpose.

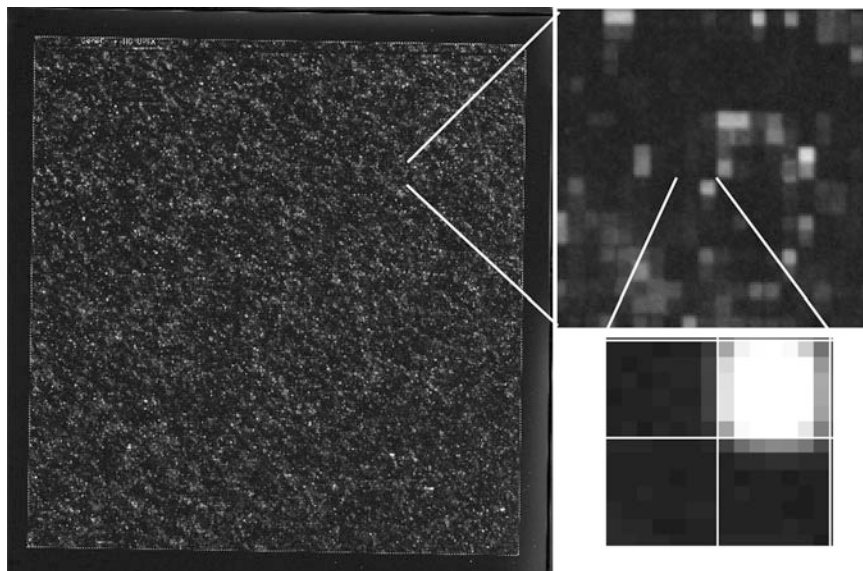


Fig. 1 Affymetrix microarray chip. The *left* side shows the entire chip; on the *right* zoom-in shows details of pairs of perfect match and mismatch hybridization, *top*, and actual pixels, *bottom*. The picture on the *bottom right* shows the grid, *thin white lines* separating the chip features. Note that the rim pixels are discarded and only the 4×5 array of pixels in the middle is averaged to determine the level of hybridization

3.4 Searching for and Finding Relevant Studies in Public Repositories for Meta-analysis

Microarray data usually are deposited into annotated and curated databases. Probably the largest is The National Center for Biotechnology Information (NCBI) Gene Expression Omnibus, GEO (<http://ncbi.nlm.nih.gov/geo>) (27), which contains close to 1,000,000 gene expression profiles and grows by 150 % annually. Sloughing through such an enormous database to find all relevant studies is somewhat difficult and more of an art than science.

The two main data repositories that collect and annotate transcription profiling using microarrays and other high throughput methods (e.g., SAGE and next generation sequencing, NGS), are NIH-GEO, reached at <http://www.ncbi.nlm.nih.gov/pubmed>, and ArrayExpress at <http://www.ebi.ac.uk/arrayexpress/> (Fig. 2). The two resources overlap to a large extent, but there are also significant differences, i.e., microarray studies present in one but not the other collection. This may be partly due in part to different data sets in each database, and partly to differences in search engines and handling of the search terms. While there may be additional datasets in proprietary databases, e.g., classified industry-generated data, or published but not yet submitted, the two repositories are reasonably comprehensive and abundant; we find searching for the additional data is usually frustrating, time-consuming, and unproductive.

ArrayExpress allows specifying human studies only. Those ArrayExpress experiments that are also found in GEO have designations E-GEOD, e.g., E-GEOD-10121. ArrayExpress also allows

a

squamous cell & expression profiling & human - GEO DataSets - NCBI - Windows Internet Explorer

http://www.ncbi.nlm.nih.gov/gds?term=squamous%20cell%20%26%20expression%20profiling%20

File Edit View Favorites Tools Help

NCBI Resources How To My NCBI Sign In

GEO DataSets GEO DataSets squamous cell & expression profiling & human Search

Save search Limits Advanced Help

Display Settings: Summary, 20 per page, Sorted by Default order Send to: All (82) Filter your results: All (82) DataSets (7)

Results: 1 to 20 of 82 << First < Prev Page 1 of 5 Next > Last >>

1: GDS3627 record: Non-small lung cancer subtypes: adenocarcinoma and squamous cell carcinoma [*Homo sapiens*]

Summary: Comparison of two non-small cell lung cancer histological subtypes: adenocarcinomas (AC) and squamous cell carcinomas (SCC). Results provide insight into the molecular differences between AC and SCC.
Parent Platform: GPL570
Reference Series: GSE10245

Type: Expression profiling by array, transformed count
Subsets: 2 disease state sets.
Samples: 58

GSM258553: NSCLC_SCC_22
GSM258555: NSCLC_SCC_25
GSM258556: NSCLC_SCC_30
GSM258557: NSCLC_SCC_37

Note, some arrays are profiling noncoding RNAs

Top Organisms [Tree]
Homo sapiens (73)
Mus musculus (8)
Rattus norvegicus (1)
BK polyomavirus (1)
Simian virus 40 (1)
More...

Find related data
Database: Select
Find items

2: GDS3125 record: Radioresistant tumor response to ionizing radiation: time course [*Homo sapiens*]

Summary: Analysis of nu61 radioresistant tumors 5 and 24 hours following exposure to ionizing radiation. Nu61 tumors derived from the

Start iTunes Inbox - Microsoft... squamous cell... MetaanalysisPri... Microsoft Excel Microsoft PowerP... 2:57 PM

b

Experiments | ArrayExpress Archive | EBI - Windows Internet Explorer

http://www.ebi.ac.uk/arrayexpress/browse.html?keywords=squamous+cell+%26+expression+p

File Edit View Favorites Tools Help

EMBL-EBI Filter first time Find Help / Feedback

Databases Tools Research Training Industry About Us Help

Experiment, citation, sample and factor annotations [clear] Filter on [reset] Display options [reset]

squamous cell & expression profiling & human All species 50 experiments per page

ArrayExpress data only Advanced query syntax All arrays Detailed view

Submitter/reviewer login ArrayExpress Browser Help All assays by molecule by All technologies Query

ID	Title	Assays	Species	Date	Processed	Raw	Atlas
E-GEO-27480	Gene-expression analysis of Oncostatin-M (OSM) signalling in cervical squamous cell carcinomas over-expr...	72	<i>Homo sapiens</i>	2011-09-29			
E-GEO-20189	A gene expression signature from peripheral whole blood for stage 1 lung adenocarcinoma	162	<i>Homo sapiens</i>	2011-09-22			
E-GEO-32115	MRNA array based, miRNA expression profiles of head and neck squamous cell carcinoma patients	4	<i>Homo sapiens</i>	2011-09-14			
E-GEO-31800	DNA copy number and gene expression profiles of resected non-small cell lung cancer tumors	320	<i>Homo sapiens</i>	2011-09-11			
E-GEO-31799	Gene expression profiles of NSCLC tumors	49	<i>Homo sapiens</i>	2011-09-11			
E-GEO-31853	Expression data from oral squamous cell carcinoma (OSCC)-derived cell lines and normal oral keratinocytes	11	<i>Homo sapiens</i>	2011-09-01			
E-GEO-25104	Expression and SNP array data for oral squamous cell carcinoma	201	<i>Homo sapiens</i>	2011-08-31			
E-GEO-25099	Expression data from 57 patients with oral cancer and 22 normal persons	79	<i>Homo sapiens</i>	2011-08-31			
E-GEO-29627	Human lung ADC and SCC comparison study	24	<i>Homo sapiens</i>	2011-08-30			
E-GEO-31552	Expression Data from Human Lung tissue of Patients with Non Small Cell Lung Cancer (NSCLC)	111	<i>Homo sapiens</i>	2011-08-25			
E-GEO-31287	Gene expression from head and neck squamous cell carcinoma (SCCHN) cancer cells before and after figt...	6	<i>Homo sapiens</i>	2011-08-09			
E-TABM-1058	Transcription profiling by array of human carcinomas of unknown primary	20	<i>Homo sapiens</i>	2011-08-04			
E-GEO-31056	A gene signature in histologically normal surgical margins is predictive of oral carcinoma recurrence	96	<i>Homo sapiens</i>	2011-08-02			
E-GEO-28442	Expression of marker genes in the lymph nodes predicts the recurrence of squamous cell vulvar carcinoma.	8	<i>Homo sapiens</i>	2011-07-31			
E-GEO-30979	Gene expression in hypoxic non-small lung cancer	20	<i>Homo sapiens</i>	2011-07-27			
E-GEO-30784	Gene expression profiling of oral squamous cell carcinoma (OSCC)	229	<i>Homo sapiens</i>	2011-07-21			
E-GEO-29817	Membranous Expression of Ectodomain Isoforms of the Epidermal Growth Factor Receptor (EGFR) Predicts ...	151	<i>Homo sapiens</i>	2011-07-18			
E-GEO-20853	Subclassification of lung adenocarcinoma	164	<i>Homo sapiens</i>	2011-07-18			
E-GEO-27556	Novel HLA ligands and Toll epitopes for immunotherapy of lung cancer	10	<i>Homo sapiens</i>	2011-07-01			
E-GEO-18668	Differentiation of NUT midline carcinoma by epigenomic reprogramming	20	<i>Homo sapiens</i>	2011-07-01			
E-GEO-29927	Diagnostic marker for lung cancer through microarray analysis	20	<i>Homo sapiens</i>	2011-06-14			
E-GEO-27501	Quantitative Analysis of Alternative Spliced Variants in HNSCC	15	<i>Homo sapiens</i>	2011-06-10			
E-GEO-26419	Notch signaling in CD64+ cells drives the progression of Human cervical cancers	9	<i>Homo sapiens</i>	2011-06-09			
E-GEO-26418	Microarray analysis of Lin- CD64+ and Lin- CD66- cells isolated from primary Human cervical cancer	5	<i>Homo sapiens</i>	2011-06-09			
E-GEO-21644	FN1 expression is a marker of radioresistance in head and neck squamous cell carcinoma	10	<i>Homo sapiens</i>	2011-06-09			
E-GEO-28835	Large airway epithelial cells from cigarette smokers with and without lung cancer undergoing flexible bronc...	13	<i>Homo sapiens</i>	2011-06-01			
E-GEO-23036	Gene expression signatures and molecular markers predict response to therapy in locally advanced head a...	68	<i>Homo sapiens</i>	2011-05-31			
E-GEO-26177	Functional evidence that Drosophila over-expression in cervical squamous cell carcinoma affects cell phenotyp...	24	<i>Homo sapiens</i>	2011-05-26			
E-GEO-26176	Functional evidence that Drosophila over-expression in cervical squamous cell carcinoma affects cell phenotyp...	6	<i>Homo sapiens</i>	2011-05-25			
E-GEO-26175	Notch signaling in CD64+ cells drives the progression of Human cervical carcinoma affects cell phenotyp...	18	<i>Homo sapiens</i>	2011-05-25			
E-GEO-23767	Expression data from Human squamous cell lung cancer line H&A and highly bone metastatic subline H&A...	7	<i>Homo sapiens</i>	2011-05-19			

Terms of Use EBI Funding Contact EBI © European Bioinformatics Institute 2011. EBI is an Outstation of the European Molecular

Start iTunes Inbox - Microsoft... Experiments | ... MetaanalysisPri... Microsoft Excel Microsoft PowerP... 3:03 PM

Fig. 2 Screen shots of GEO (a) and ArrayExpress sites (b) searches for relevant transcription profiling experiments. The search terms are highlighted in yellow in the ArrayExpress screen

specifying only experiments that do not overlap those in GEO, which have different designations e.g., E-MATB-482; we find this somewhat risky, differences in search protocols may catch some of the GEO experiments not flagged by the GEO search engine, and sorting through redundant GSE- and E-GEOD- experiments is an easy task.

The flagged experiments have to be parsed individually because they include many that are not directly appropriate for the study at hand (e.g., “MicroRNA profiling by array of NCI-60 human cancer cell-lines” or arrays containing only cell lines, arrays dealing with peripheral blood cell samples, and tumor-associated fibroblasts). We also remove studies that do not contain mRNA expression profiling (i.e., those analyzing DNA methylation, SNPs, gene copy number, exon, and miRNA arrays); also left out are studies that use small proprietary microarrays, such as those with less than 10 K genes probed, and, currently, studies using RNA sequencing. Usually, approximately half of the studies use Affymetrix platforms, the remainder use Agilent or, Illumina; less common are Hitachi, Sentrix, GE Healthcare, or proprietary arrays.

We will illustrate the search using three examples, EGFR inhibitors, psoriasis, and retinoic acid.

1. To identify transcriptional studies in which *EGFR inhibitor* was used, two repositories were searched: PubMed GEO and EMBI-EBI ArrayExpress. Several combinations of search terms were used: “EGFR & inhibitor,” “EGFR & (Lapatinib | Gefitinib | Erlotinib | Cetuximab | Panitumumab | Zalutumumab | Nimotuzumab | Matuzumab | AG1478 | inhibitor),” the following terms were not found in GEO DataSets: Panitumumab, Zalutumumab, Matuzumab. We limited the search to human samples, i.e., studies that used human microarrays. Ultimately, in GEO, the search terms “EGFR & inhibit*” flagged 191 items, including 61 series. Setting the limits in the search to “expression profiling by array,” “genome tiling” or “sequencing” yielded 50 sets, while eliminating the SNP, promoter arrays, and ChIP studies. Searching Array Express with “EGFR and Inhibit*” yielded 44 sets; with a few exceptions these had equivalents in the GEO Datasets. The GEO and ArrayExpress searches combined identified 67 different data sets, which were individually screened for comparing directly EGFR inhibitor treated vs. untreated samples. Of the 67 sets 22 compared directly EGFR inhibitor treated with untreated samples; 14 sets compared EGFR inhibitor-resistant vs. sensitive cell lines; in six studies we found both inhibitor-treated vs. untreated comparisons and inhibitor-resistant vs. sensitive cell lines. In several studies multiple cell lines or tissues were treated, these should be analyzed independently, i.e., each cell line analyzed separately. One data set, GSE6128, compared long term

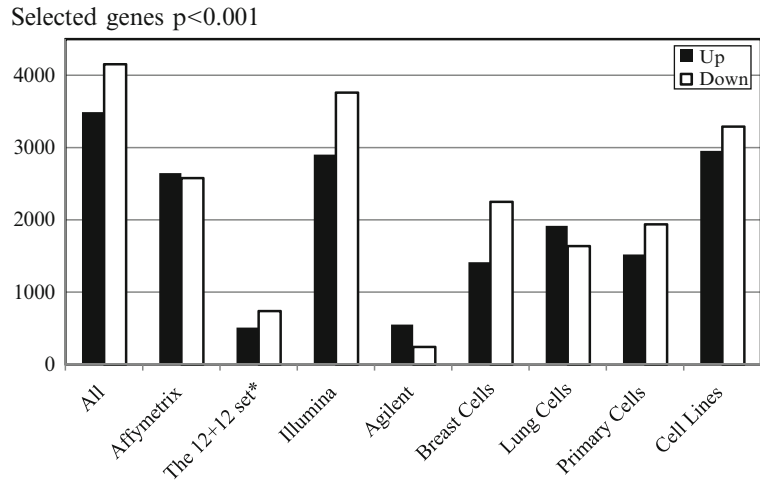


Fig. 3 Numbers of differentially expressed genes provided by RankProd analysis. Studies of EGFR inhibitors are presented. The entire collection (All), was subdivided by the microarray platforms and by types of cell targeted (M.B., in preparation). *Up* stands for induced, *Down* for suppressed genes. The “12 + 12” (*asterisk*) represents the largest single study, containing 12 treated and 12 control samples

(48 h) inhibitor-treated cells with the same cells after removal of the inhibitor, i.e., the inverse of EGFR inhibitor treated vs. untreated samples. Two sets, GSE41860 and GSE17498, used HGU95v2 platform, which has significantly fewer gene targets than other platforms. The majority of datasets used Affymetrix microarray platforms (11 studies), particularly the HG_U133_Plus_2 version (9 studies). Illumina and Agilent microarrays were used in six and three studies, respectively. The larger the number of studies included in the analysis, the longer the list of genes found to be regulated at significant p -value (Fig. 3).

2. In the case of *psoriasis*, through a PubMed GEO Datasets data mining search using terms such as “psoriasis” and “psoriatic” we found a total of 654 hits divided into four categories: Data-Sets (6), Platforms (2), Samples (599) and Series (47). From the 47 series, we found a total of nine experiments that met our criterion, i.e., contained samples from psoriatic lesions and healthy nonlesional controls. For each of the nine experiments, data and study information were collected into an Excel spreadsheet labeling study ID number (accession), number of participants, title, number of chips, file type (CEL, or TXT), platform, description of subjects (psoriasis lesional (PP), psoriasis nonlesional (PN) or healthy volunteers (NN)), the type or form of psoriasis used (only three of the nine studies specified the type of psoriasis used, two plaque psoriasis, one plaque-like psoriasis)

and description of experiment performed. The nine studies comprised seven Affymetrix-based (571 genechips) and two non-Affymetrix (Sentrix and Illumina) based studies (74 genechips) for a total of 645 genechips. Within the Affymetrix-based studies, 263 psoriasis lesional (PP), 198 psoriasis nonlesional, and 110 healthy (NN) genechips for a total of 401 CEL genechips were found.

3. To select microarray studies that compare retinoic acid-treated and untreated cells we used MaRe (<http://www.lgtec.nl/MaRe/>) (28). Focusing only on the human cells, we used as keyword *retinoi**, the asterisk serving to include all suffixes, such as -ds, and -c acid, and *Homo sapiens* as the species. This resulted in 101 different GSE experiments from GEO (<http://www.ncbi.nlm.nih.gov/gds>) and 35 experiments from ArrayExpress (<http://sourceforge.net/projects/arrayexpress/files/>). We manually curated these 136 entries, to remove SAGE results, and small microarrays (those with <5,000 genes), the miRNA microarrays and those that did not use RA as a reagent, but were flagged by the *retinoi** keyword somewhere in the description. This resulted in 22 studies with 329 arrays; of these, 17 studies used Affymetrix microarrays, 3 Agilent, and one each Sentrix and NKI-CMF.

3.5 Downloading Data Files

Different microarray platforms used for transcriptional profiling yield different, characteristic data files, which have to be worked up separately and then harmonized. These files are large and compressed, use proprietary gene IDs and represent expression values in various formats. It is, therefore, not trivial to match data from multiple studies for meta-analysis.

1. For the data deposited in studies using the Affymetrix arrays the simplest approach is to click on the ‘download’ button next to the CEL or TXT field. The downloaded CEL files are first unzipped and then processed using free to download RMAExpress software (<http://rmaexpress.bmbolstad.com/>). RMAExpress is a program that uses the Robust Multichip Average protocol (29) to calculate gene expression summary values for every gene on an Affymetrix genechip and at the same time provide quality control for each microarray. The Chip Description Files, CDFs, for the individual Affymetrix microarray platforms can be downloaded from the Affymetrix site (<http://www.affymetrix.com/support/technical/libraryfilesmain.affx>). First, the corresponding CDF is loaded into RMAExpress, and then the CEL files for all microarrays are imported into RMAExpress. IMPORTANT: only one type of CDF file can be uploaded at a time – RMAExpress can only compare and analyze data from the same microarray platform. RMAExpress results are calculated with following parameters: *background adjustment*,

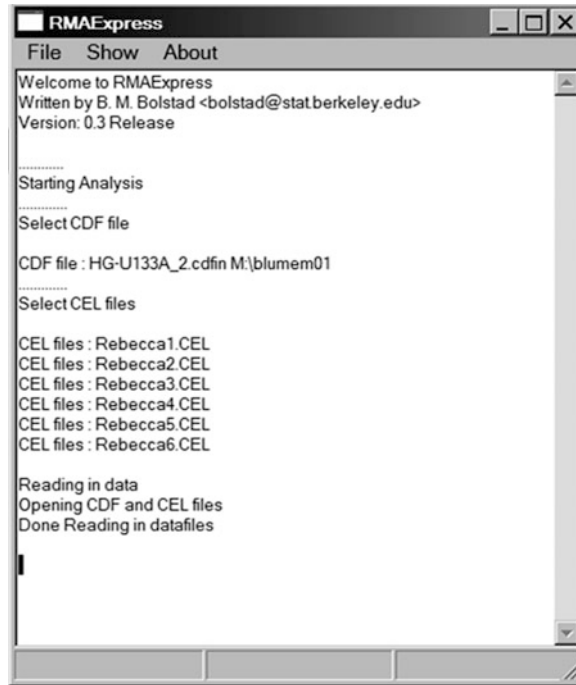


Fig. 4 Screen shot of RMA express

quantile normalization, and *PLM summarization* method. The results are saved as \log_2 transformed TXT files and later converted into Excel spreadsheets.

2. Once you have downloaded and installed RMAExpress and the CDF file, invoke the program (Fig. 4). Click on “File” → “Read unprocessed file.” There comes a dialog box, “Please select your CDF file,” select the data file corresponding to the type of chip you are using, e.g. HG-U133A_2.cdf. Then another dialog box appears, “Please select your CEL file,” select the files you want to analyze. Then you may use the menu bar “File”—“Add new CEL files” to add additional CEL files for the current analysis. After it shows “Done reading in datafiles,” you may select from the “File” menu—“Compute RMA measure.” A dialog box “Select preprocessing steps” appears; for “Background Adjust” chose “Yes,” for Normalization, “Quantile” (sic), and check the box of “Store Residuals.”
3. After it is done, select from the menu bar Show-Residual Images. Now you can check the quality of the chips. For example, chips that are consistently and evenly pink are very good, while a chip that shows blue smudges or a red border probably is not a good chip (Fig. 5).
4. Save the results as text file: “File”—“Write results to file (log scale),” which converts the expression values into their \log_2

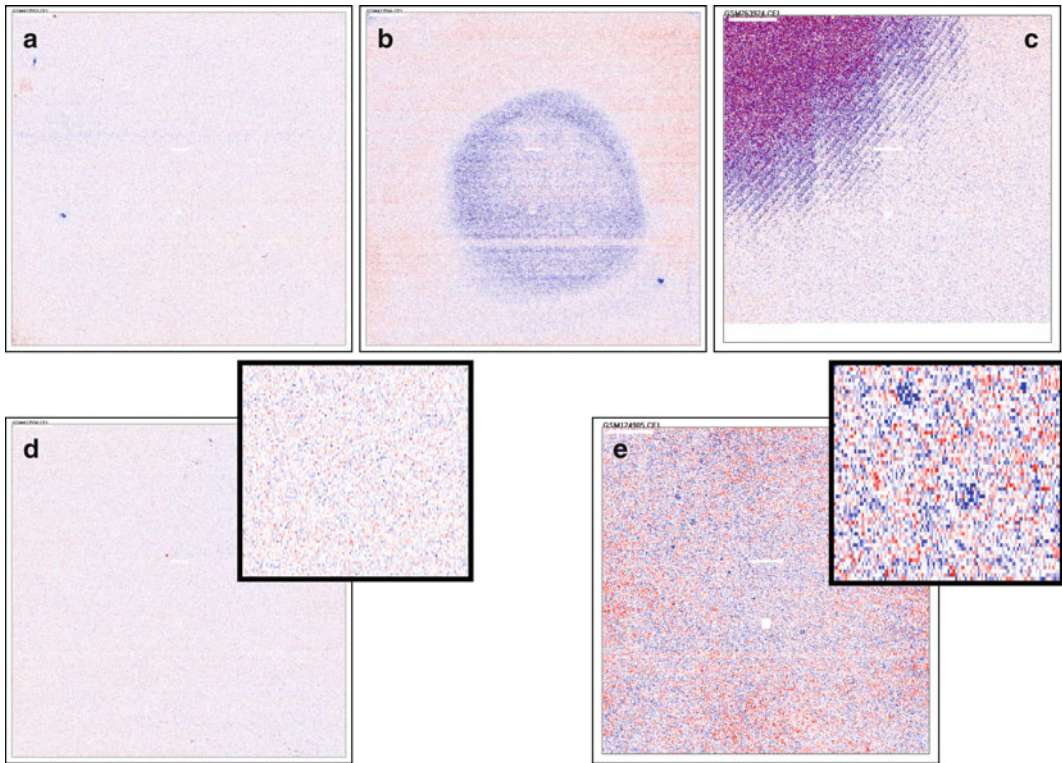


Fig. 5 RMAExpress “residuals.” Two near-perfect microarrays are shown on the *left*. The others show uneven hybridization and a smudge. Note the characteristic coarse-grained appearance of a chip with poor-quality RNA sample

derivative. Also save the results with the “Write results to file (natural scale),” which may be useful for some downstream uses, algorithms that require untransformed expression values. You will later open these with Excel.

5. It is important, at this point, to perform quality control on the microarrays. The quality control graphs can be viewed in the QC Statistic Visualizer. Before viewing diagrams graph, it helps to add IQR limits and Control Limits, and then use RLENUSEMultiPlot (Fig. 6a). NUSE, RLE, and RLENUSET2 diagrams can be saved into their appropriate folders for future reference. We find Normalized Unscaled Standard Error, NUSE, the easiest and most robust quality control measure. Those genechips that have NUSE medians 5 % or more different from other chips are considered “bad” chips and are to be omitted. Then the RMAExpress is rerun with only the “good” chips. An example is provided in Fig. 6b. This procedure provides a measure of relative chip quality derived from the residuals from the RMA model (for details see (29)). In one large representative case, using RMAExpress,

GSE10433aa

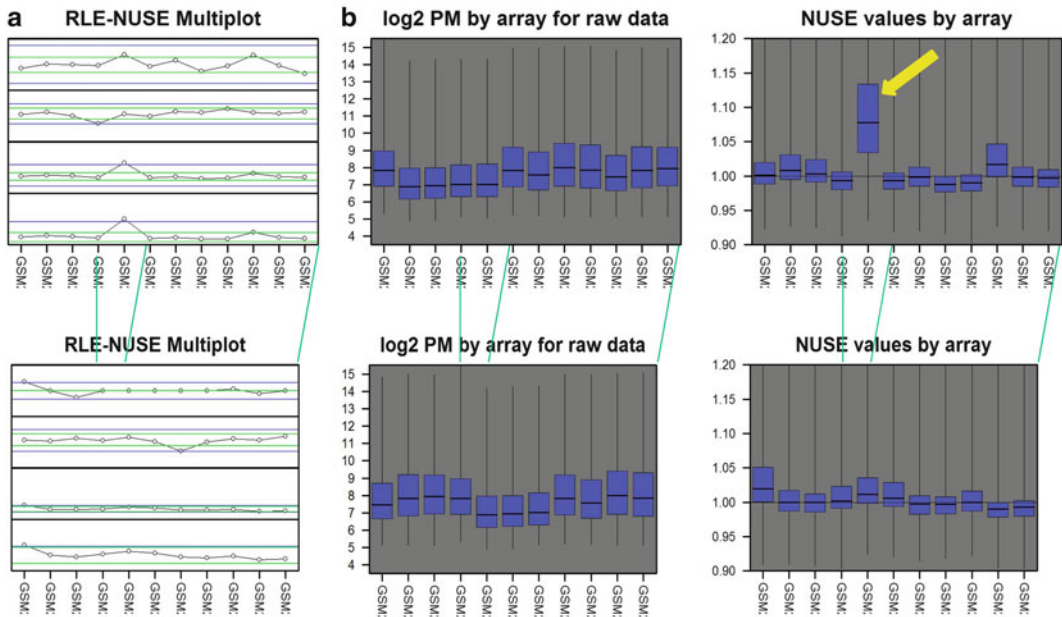


Fig. 6 Quality control features of RMAExpress. (a) Multiplot. (b) RMAExpress NUSE before and after removing a “bad” chip

only a total of 15 out of 645 genechips, 2.3 %, were discarded as “bad” chips.

The “bad” chips usually result from degraded or poor quality RNA input. The residual values for these have a characteristic coarse-grained appearance (Fig. 5c, compare with d). Occasionally, poor and uneven hybridization, a faulty chip or grime in the sample can also cause problems (Fig. 5b, c). Note that a few spots and marks do not disqualify a chip (e.g., Fig. 5a); each gene is probed multiple times, at dispersed sites on a chip and statistical analysis can eliminate a limited number of outlier measurements.

- For studies that use identical platform, e.g., Affymetrix_133_Plus_2, the RMAExpress-derived spreadsheets are combined by sorting each by the Probeset IDs and then using the copy and paste commands in Excel. This creates a large spreadsheet with as many columns as there are samples, and 54,677 rows, i.e., gene probes. Importantly, when combining studies that use identical platform, it is important within each study to group the control and the treated samples (e.g., 12 + 12, see Fig. 3) so that they can be assigned correctly in the subsequent steps. This large combination Excel file should be also saved in the tab-delimited text format for subsequent use in RankProd analysis.

7. In the case of *non-Affymetrix* studies, downloading the uncompressed `_RAW.tar` files often yields several `TXT.gz` files; these also have to be uncompressed (performing uncompressing twice!) to give `.txt` files that excel can import. The simplest way to download `TXT` data files from the PubMed GEO site, <http://www.ncbi.nlm.nih.gov/pubmed>. First click to choose GEO DataSets, and then insert one of the relevant data sets into the search field, e.g., GSE10121. The search yields the GSE10121 data set series, as well as any related series, in this case GSE31056. Next, clicking on the GSE10121 record brings up the details of the data set “Accession display.” Near the bottom of the page one finds “Series Matrix File (s)”; clicking on this opens a new window with the URL, in our case <ftp://ftp.ncbi.nih.gov/pub/geo/DATA/SeriesMatrix/GSE10121/>, which allows downloading the data file [GSE10121_series_matrix.txt.gz](ftp://ftp.ncbi.nih.gov/pub/geo/DATA/SeriesMatrix/GSE10121/GSE10121_series_matrix.txt.gz). This is a 10 MB zipped, compressed file. The simplest way to download another data file is to replace the digits in the URL (e.g., in our case 10121 with 31056, which leads to a 7 MB download). We find it convenient to download all compressed files into a same directory; this allows batch uncompressing of the downloaded files. Uncompressing the `TXT.gz` files yields `.TXT` files, which can be imported into Excel, saved as spreadsheets and then manipulated further. For example, the 10 MB compressed file is uncompressed into a 22 MB `TXT` file. Right-clicking on this file usually gives a menu option “open with”; choosing excel gives a spreadsheet which can be saved as an 18 MB `.xls` file.

For Agilent platform, we download the `txt` files with the data. For example, using GEO DataSet we downloaded the ~130 MB `TXT` file `GSE32333_RAW.tar`. This file was unzipped, extracted into a folder with the same name, which comprised fourteen `*.txt.gz` files; these were unzipped again into 14 separate `*.txt` text files, ~26 MB each. The text files can be opened with Excel and saved as spreadsheets. A simpler and easier alternative is to click on the GSE32333 record then scroll to the bottom and click and download the Series Matrix File. This 1.5 MB file can be unzipped into a 5 MB `txt` file, opened with Excel and saved as a spreadsheet. The spreadsheet needs a little editing, mostly deleting the information at the top, above the expression values. The spreadsheet clearly designates each of the samples as control, treated, etc. However, this spreadsheet does not identify the features on the microarray, except by the internal coding of Agilent (e.g., `GT_44k_23_P100001`). To annotate the features, we return to the original search results, and click on the second record, GPL13252. This record contains the data pertaining to the microarray platform itself. Near the bottom of the next page, which describes the microarray platform, is a box marked

“View full table. . .” Clicking on this box opens a new tab with the details of the microarray. It may take a minute or two for this file to fully load, but then it can be downloaded by clicking on “File,” “Save as. . .” and specifying “Save as type. . . Text File (*.txt).” The saved file can be opened in Excel and saved as a spreadsheet with a same name. To combine the annotations with the data file we use AddIns DataLoader <http://www.add-ins.com/>. Alternatively, both the data and the annotations can be sorted by the Agilent IDs and, after making sure the ID columns are congruent, using copy-and-paste function of Excel.

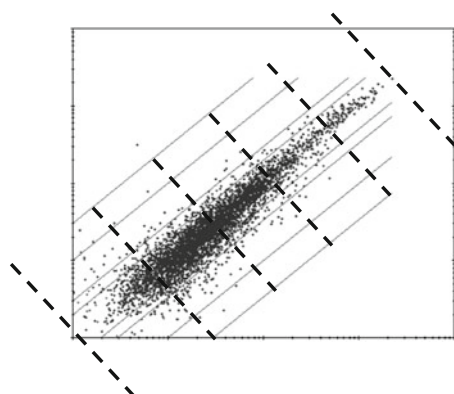
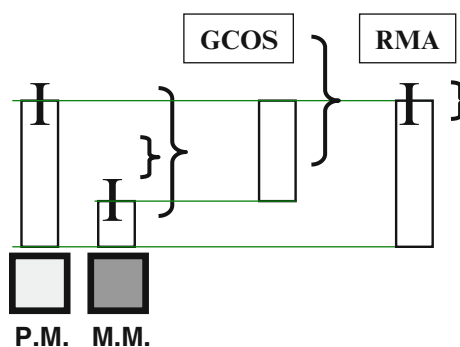
Similar approaches can be used for uncommon and proprietary microarray platforms. For example, GSE6473 series uses GPL3054 platform, which contains 18,861 60-mer oligonucleotides representing 17,260 unique genes (designed by Compugen, San Jose, CA, USA), printed in-house at Microarray Core Facility of the Vrije Universiteit Amsterdam, The Netherlands. Downloading the 1.6 MB GSE6473 Series Matrix file, when uncompressed and saved, yields a 3.9 MB spreadsheet. The annotations of the GPL3054 are in a 6.5 MB file, which, when uncompressed, contains the GeneBank accession and Unigene ID numbers (along with expression data from a number of chips; these should be ignored, only the top ~20,000 rows are relevant for us). The GeneBank and Unigene IDs can be loaded from GPL3054 into GSE6473 spreadsheet using either copy/paste function of excel or, preferably, using the DataLoader AddIn.

3.6 Integrating the Results of GCOS and RMAExpress

Therese two programs different approaches to initial data processing, as illustrated in Fig. 7.

1. Use Excel to open two .txt result tables, the RMAExpress table with log scale, and the GCOS results table. Merge the two files by using copy and paste functions (alternatively, use the DataLoader function of the add-ins suite of programs, <http://www.add-ins.com>, which we find to be inexpensive and very useful). *Make sure the order of the genes of GCOS, RMA, and annotation table are the same before you copy and paste!* This is easily accomplished by sorting the two files by their Affymetrix Ids in the first column. Also copy and paste part of the functional annotation table, e.g. HG-U133A_2_annot, into the above merged table, including at least the columns of gene title, gene symbol, function, and Entrez Gene id. Now you have a table showing results of GCOS, RMAExpress, and functional annotation together. Make sure to save this original version of the data, you may have to return to it if you make a mistake later.
2. First, filter out all those genes that are not expressed in any of your samples. Use the results of GCOS to select those genes marked as “present” (P) at least once in all the experiments analyzed. Select the first row of the table and from the menu bar click on “Data” “Filter” and select “Autofilter.” Now each

M.M. can add higher variability to the data.



RMA uses better normalization and background subtraction methods, but it does not remove the unexpressed genes.

Fig. 7 Differences between the GCOS and RMA approaches. The mismatch, MM, values can add to the data variability, *top*. RMAExpress uses perfect match values only, and normalizes the expression values in quintiles, across all the chips, *bottom*. For reference, see Fig. 1, *right panels*, which show perfect match and mismatch hybridizations

cell in the first row has a downward arrowhead. For *ALL* those columns showing the results of Detection from GCOS (i.e., columns with P, A, or M), click the arrowheads, choose “custom,” then “does not equal to,” then type “p.” Delete all the rows that remain. Now from the menu bar click on “Data” “Filter” and select “Show All”. What remains are only those genes that are present at least once. Sort the spreadsheet again to remove the empty rows. Save as a new file with a new name, e.g. “Present.” Since we have finished using GCOS data at this time, you might want to delete the columns derived from the GCOS file, while retaining the RMA data, to make the table smaller and easier to manipulate. (Alternatively, you may want to keep the “Signal Log Ratio” and “Change” columns, to compare the GCOS and RMA results.)

	A	B	C	D	E	F	G	H
1	Probesets	Control	Chip 1	Chip 2	Chip 3	C - B	D - B	E - B
2	212143_s_at	11.292	11.336	11.288	11.331	0.04	0.00	0.04
3	210095_s_at	7.547	9.900	9.586	9.388	2.35	2.04	1.84
4	210096_at	6.637	5.534	5.591	5.719	-1.10	-1.05	-0.92
5	205363_at	8.380	8.406	8.462	8.417	0.03	0.08	0.04
6	207324_s_at	3.641	4.804	4.480	4.712	1.16	0.84	1.07
7	213240_s_at	8.598	7.017	6.617	6.546	-1.58	-1.98	-2.05

Fig. 8 Spreadsheet of RMAExpress analysis results. The data are already \log_2 transformed; to get fold regulation, the values are simply subtracted

- Next, select those genes that are regulated at least once in all the samples compared. First, subtract the expression level of the control/background chip from the level on the experimental chip to obtain the fold change of expression in experimental compared with the control samples. Insert a new blank column; this will be the fold change column. Find the two columns of RMA expression level (note the data are in \log_2 scale) for both the experimental and the control in the table, say column B and column C (Fig. 8). In the uppermost cell corresponding to the first gene of the blank column, type “=B2-C2”, then enter. You get the difference between the values in B2 and C2 cells. Since it’s in \log_2 scale, “1” represents a twofold upregulation and “-1” a twofold downregulation. You’ll notice there is a small “+” on the right lower corner of that cell. Just hold the mouse and drag all the way down to the last cell corresponding to the last gene of that blank column. In the same way, you can obtain the differences between any two pairs of chips you want to compare. Save this spreadsheet.
- You may use the same method as above to exclude those genes not regulated even once. For example, if you set twofold as the threshold of regulation, from the downward arrowheads of those columns you just obtained, choose “custom,” then choose “is less than” and type “1” in the right box, click “and,” on the lower box, choose “is greater than,” type “-1” in the right box. After you have done so for all the columns of results of subtraction between the experiment and the control, delete all the rows that remain in the table. This will delete all rows where expression levels differences are less than twofold. From the menu use “Data,” “Filter,” “Show All,” re-sort. Save as a new file, which contains all the genes regulated at least once. Sort this table by Gene Symbol, eliminate those redundant, duplicated rows to make all genes with the same gene symbol appear only once in this table. Save this file. Use this file as a basic work-horse table to select those genes you want to analyze with the following programs (Note 6).

3.7 Cross-Referencing and Merging Different Platforms for Meta-analysis

One of the significant stumbling blocks in meta-analysis is the need to merge data from different microarray platforms. The problem stems from different number of genes on different platforms, redundancies in probing genes and incongruity among different ways to identify genes.

Studies using identical platforms are combined by sorting each by the Probeset IDs and then using a copy and paste commands in Excel. It is important when combining, within each study to group the control and the treated samples (e.g., 12 + 12, Fig. 3), so that they can be assigned correctly in the subsequent steps. Certain data sets may use multiple target cell types; for each cell type it is important to compare separately the treated vs. control samples, which results in many individual pair-wise comparisons. Occasionally, the same controls are present twice, when separately compared to multiple treatments (e.g., in GSE17948).

To download a set of cross-referencing ID for various platforms we use BioMart (<http://www.biomart.org/biomart/martview/39658a1f84f2d1822db6e184a5cc356e>). At the “Choose Database” menu we choose “ENSEMBL GENES 68 (SANGER UK)”; at CHOOSE DATASET menu “Homo sapiens genes (the current version).” In the “Filters” we chose “Limit to genes” with our microarray, e.g., “with Affymetrix Microarray hg u133 plus 2 probeset IDs,” or leave it blank. In the “Attributes,” in “GENE” we keep the two marked ENSEMBL ID choices. Expanding the “EXTERNAL,” we mark three external references, always “HGNC symbol” and two more; we found “EntrezGene ID” and “RefSeq mRNA” the most useful. In the field “Microarray probes/probesets” we usually choose our microarray, to ensure that we are retrieving the correct IDs, and another microarray, either Agilent or Illumina, for cross-referencing. Note that this retrieval from BioMart can be done several times, with different choices. Clicking on the “Count” near the top, left, gives the number of genes in the selected data set, out of the total (i.e., the number of genes that passed the filters out of the total number of genes in the database. The resulting spreadsheet can be previewed by clicking on “Results” in this frame. More useful is to choose TSV, the format for the downloaded file. Viewing more than 10 records, say 100, often presents data in some of the columns that originally appear empty. Clicking “Go” with the green check mark starts the download of the file in a .txt format. We do not find it necessary to ask for alert by e-mail, but we give each download a different name to be able to identify them later. Right-clicking on the downloaded files allows them to be opened with Excel and then saved as spreadsheets.

To combine disparate types of microarrays we use AddIns DataLoader (<http://www.add-ins.com/>). For example, we downloaded the Affymetrix GPL570 data file, converted it to excel spreadsheet and then, using DataLoader and using as cross-referencing IDs both

gene symbols (e.g., DDR1) and separately GeneBank accession numbers (e.g., NM_005505), loaded the Illumina IDs from GPL6884, GPL10558 and GPL5104. Next, we used DataLoader to import the data columns from the Illumina subsets. This creates a large spreadsheet of Illumina data, with 48,803 data rows. Finally, we use AddIns to load the data from all Illumina experiments into the large spreadsheet with the Affymetrix columns. Using equivalent steps, *mutatis mutandis*, we combine the Affymetrix/Illumina spreadsheet with the data from the studies using the Agilent platforms. This creates a large spreadsheet of Illumina data with as many columns as there are samples and 50,239 rows of gene features. Within each study we took care to group the control and the treated samples so that we can assign them correctly in the subsequent steps.

3.8 Dealing with Empty Cells and Negative Numbers and Selecting Data Subsets

Where the smaller Affymetrix, the Illumina and the Agilent arrays did not have a value corresponding to the largest Affymetrix microarray IDs (i.e., into empty cells) we simply added 1. Specifically, we used find/replace function of excel to replace all empty data cells with “1,” thus allowing the program to include “empty” cells where some of the platforms are missing some of the genes. Noting that this should not affect the subsequent nonparametric step of analysis, i.e., should not affect the relative ranks of the gene features, we tested this notion with the Affymetrix arrays alone, large plus small, with added 1 s or with just the 22,200 rows present in all arrays and found that the added 1 s did not affect the outcome (M.B. unpublished).

Certain experiments present suppressed values as negative numbers (e.g., GSE38302); we converted these by adding the same large value, 20, to each cell in the set. Note that these alterations do not change the relative ranking of the cells, important for the next step in analysis.

From the large spreadsheet it is easy to cull several subsets, e.g., including all studies that use the same treatment or target cell type. For illustration purposes, in meta-analysis of EGFR inhibitors, we selected the subset of studies using Affymetrix arrays and one matching subset of 12 treated and 12 untreated samples from the same study, GSE11729, the largest such congruent pairing (Fig. 3). It is important to note, however, that the larger the overall number of microarrays analyzed, the larger number of differentially regulated genes will be detected (Fig. 9). This rule of thumb is mitigated to a degree, because studies using the same or related microarray platforms, e.g., the Affymetrix chips, tend to be more congruent.

Save the resulting files. Use this file as a basic work-horse table to select those genes you want to analyze with the following programs (Note 6).

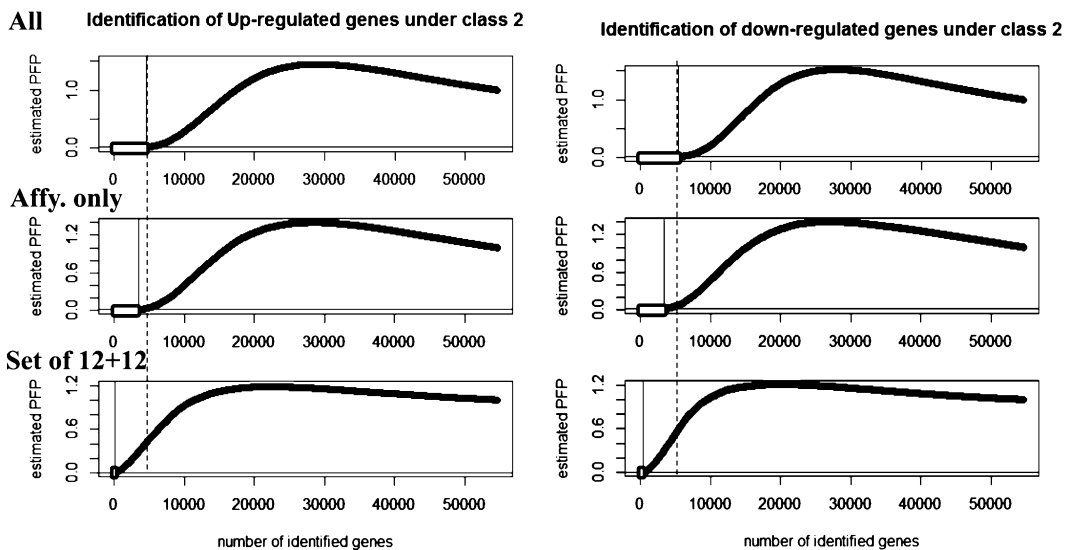


Fig. 9 Graph plotting the results of RankProd analysis. *Open bars* show the number of genes differentially expressed with a p -value better than 10^{-4}

3.9 Selecting Differentially Expressed Genes for Meta-analysis Using RankProd

Because different platforms use different labeling techniques, data acquisition, etc., meta-analysis must use a nonparametric approach to comparing datasets. RankProd is such a nonparametric method for identifying differentially expressed genes, both up- or down-regulated, based on the estimated percentage of false predictions (30). The method combines data sets from different studies in meta-analysis, which increases the number of identified differentially regulated genes. To comply with the requirements of data structure for RankProd, the next step in analysis, it is important to delete all extraneous rows and columns, leaving only column A, containing the Affymetrix feature IDs, and the top row containing the sample IDs. Note: the top row must not have any spaces, periods, etc., which would be interpreted as additional column headings; we found it simplest to number the columns consecutively. The final combined spreadsheet is saved, in addition to in a spreadsheet format, as a tab-delimited text file for use in RankProd (Note 6).

Here we present a simulated RankProd commands list for a hypothetical analysis of three datasets with 12 + 12, 6 + 11 and 24 + 2 microarrays (treated + controls):

```
memory.size(max = FALSE)1
memory.limit(size = 24,000)
library(RankProd)
data(Your_txt_file)
n1 <- 12
n2 <- 12
```

¹ Increases you computer's memory dedicated for this task.

```

n3 <- 6
n4 <- 11
n5 <- 24
n6 <- 2
c1 <- rep(c(0,1,0,1,0,1), c(n1,n2,n3,n4,n5,n6))2
c1
rownames(Your_txt_file) = Your_txt_file[,1]3
Your_txt_file = Your_txt_file[,-1]
origin <- c(rep(1, 24), rep(2, 17), rep(3, 26))4
origin
RP.adv.out <- RPadvance(Your_txt_file, c1, ori-
gin, rand = 100)5
plotRP(RP.adv.out, cutoff = 0.01)6
topGene(RP.adv.out, cutoff = 0.01)
write.table(topGene(RP.adv.out, num.gene = 1,000),
row.names = TRUE, col.names = NA, file = " Your_txt_
file.txt")7.

```

Important note: RankProd will not recognize the quotation marks “and” from word; you must use the generic quotation marks “(!)

The outputs of RankProd analysis do not have gene IDs; these must be imported from the input txt file. Usually we select those induced and suppressed genes that were differentially expressed with a p -value of 10^{-4} or better. These lists are uploaded into DAVID set of programs for further analysis (see the next section).

3.10 Annotation of Gene Lists

The lists of IDs of regulated genes, obtained from GCOS/RMAExpress or from RankProd analyses need to be annotated so that biological meanings can be assigned to them. Importantly, even when the lists of individual genes from different experimenters do not overlap extensively, the overrepresented ontological categories do. For example, if a certain treatment induces proliferation in multiple cell types, the differentially expressed cell cycle genes may vary from cell type to cell type, and even from experiment to experiment in the same cell type. However, the ontological categories “cell_cycle” and “cell_proliferation” will be statistically overrepresented in all gene lists.

1. For annotation we find the DAVID program (*Database for Annotation Visualization and Integrated Discovery*) extremely

² Indicates to the program that chips 1–12; 25–30 and 42–66 belong to class 1, while 13–24, 31–41, and 67–68 belong to class 2 (controls) and that there are six sets of replicate chips.

³ Marks the leftmost column as containing the IDs of the genes.

⁴ Indicates to the program that there are three experiments with 24, 17, and 26 chips respectively.

⁵ Starts the program running (with 100 random permutations to derive p -values).

⁶ Plots a graph of regulated genes as shown in Fig. 9.

⁷ Exports the results of the analysis into a txt file with top 1,000 up- and downregulated genes

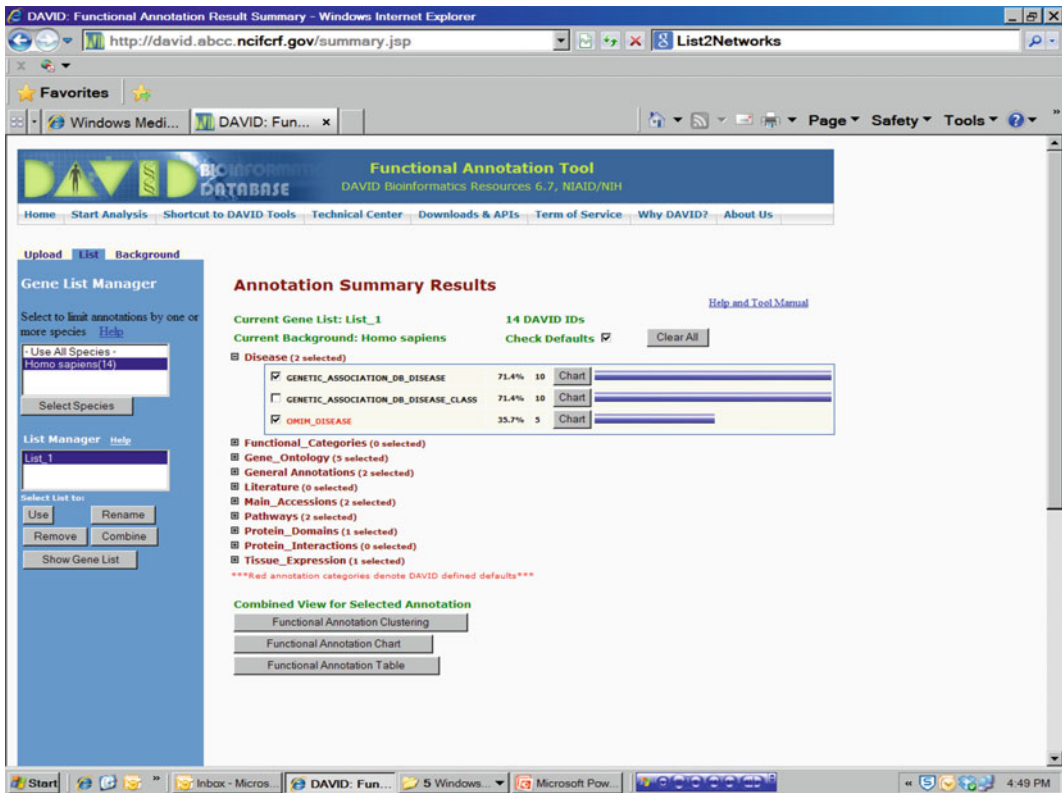


Fig. 10 Screenshot of the DAVID analysis portal. The list of regulated genes, as Affymetrix IDs, can simply be pasted in the field A

useful and convenient (<http://david.abcc.ncifcrf.gov>) (31, 32). Transcription factor binding sites can also be evaluated using DAVID, in a separate analysis. We use lists of Affymetrix IDs of regulated genes and upload them to DAVID (31). DAVID provides “tables” containing functional and ontological details of the genes in the uploaded list, “charts” containing ontological categories, pathways, etc., overrepresented in the gene lists, “clusters” of such ontological categories (which consolidates redundancies and overlaps), transcription factors overrepresented in the promoters of the genes, as well as sub-lists of genes specific for each ontological category.

From the DAVID program URL, <http://david.abcc.ncifcrf.gov/>, (Fig. 10), choose “Start Analysis” in the upper bar. In the left blue box, choose “Upload” and under Enter Gene List field Paste a list of the genes you want to analyze from work-horse Excel file. This is done most conveniently by sorting the spreadsheet by descending fold change values, selecting the Ids from the first column for all values >1 (i.e., twofold upregulated) and pasting directly into the DAVID field. Select Identifier: AFFYMETRIX_3PRIME_IVT_ID; choose List Type: Gene List and click Submit List.

2. After a few seconds appears the “Gene List Manager” in the left blue box. In “Select to limit annotations by one or more species” choose “HOMO SAPIENS” if you want to analyze only human genes (of course, not if you work with murine samples). For “Background,” usually you don’t have to do anything. Now you have “successfully submitted gene list,” Step 1. To Analyze above gene list with one of DAVID tools, choose “Functional Annotation Tool.” Now appears the “Annotation Summary Results” screen.
3. Choosing “Functional Annotation Tool,” we include several categories, such as disease associations, gene ontology categories, pathways, tissue expression, and cytoband and official symbol. We download for each list of genes a “table” containing functional and ontological details of the regulated genes (Fig. 11a), a “chart” containing ontological categories, pathways, etc., overrepresented in the gene lists (Fig. 11b), and a “cluster” of such ontological categories, which identifies and clusters redundancies and overlaps (Fig. 1c). This approach allows us to identify specific functional commonalities in various lists of genes, providing the meta-analysis results. We separately identify the transcription factors with binding sites overrepresented in the promoters of the genes (Fig. 11d); including the transcription factors in the chart analysis tends to overwhelm all other categories.

In the sets of DAVID categories we find the following most useful (Fig. 10):

In “Disease” we select: GENETIC_ASSOCIATION_DB_DISEASE and OMIM_DISEASE (see Fig. 10).

In “Functional_Categories”: none.

In “Gene Ontology”: GOTERM_BP_ALL, GOTERM_CC_ALL and GOTERM_MF_ALL, and somewhat redundant PANTHER_BP_ALL and PANTHER_MF_ALL.

In “General annotations”: CYTOBAND and GENE_SYMBOL.

In “Literature”: none.

In “Main Accessions”: ENTREZ_GENE_ID, and ENSEMBL_GENE_ID.

In “Pathways”: BIOCARTA and KEGG_PATHWAY.

In “Protein Domains: PANTHER_FAMILY.

And in “Tissue Expression”: UP_TISSUE.

4. You should experiment with these, and see which ones are useful to you, which are not. You may want more detailed descriptions, or you may not be interested in chromosomal location, etc. However, it is important to choose a consistent

a

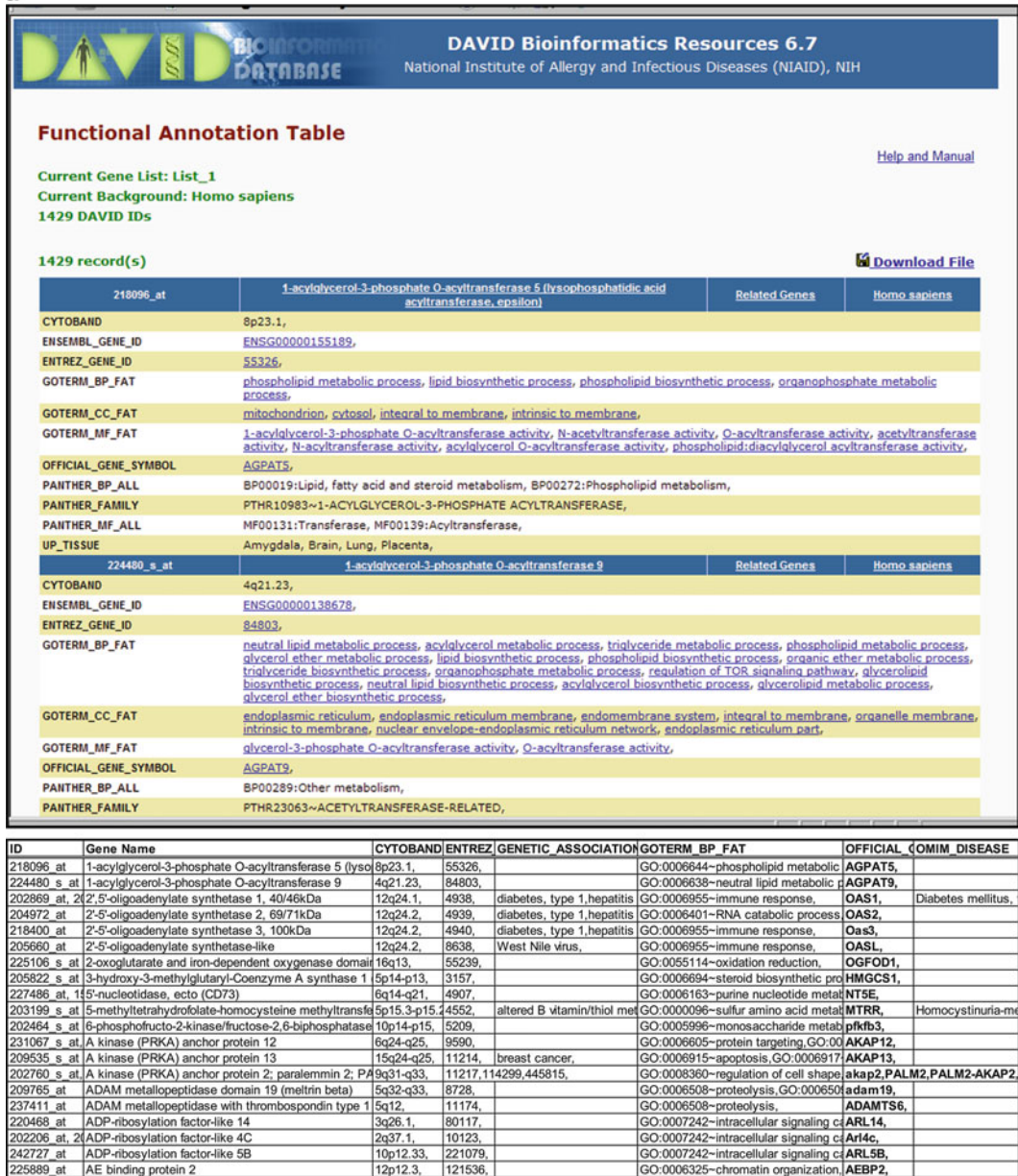


Fig. 11 Outputs from DAVID programs. (a) Table of genes in the submitted list. Note that redundant features from the microarray, i.e., probe sets targeting the same gene, are consolidated. For each gene, the Table compiles all data requested (see Fig. 10). (b) Chart of categories. Numbers of genes in each category are given, as well as the *p*-values for the category being overrepresented in the submitted list of genes. (c) Clusters of categories. Note that largely redundant categories are “clustered” in congruent sets. (d) Transcription factors with sites overrepresented in the promoters of the genes in the list. These are identified by the DAVID Chart program. The figure shows both the DAVID screen shots and the resulting data files as imported into Excel

b

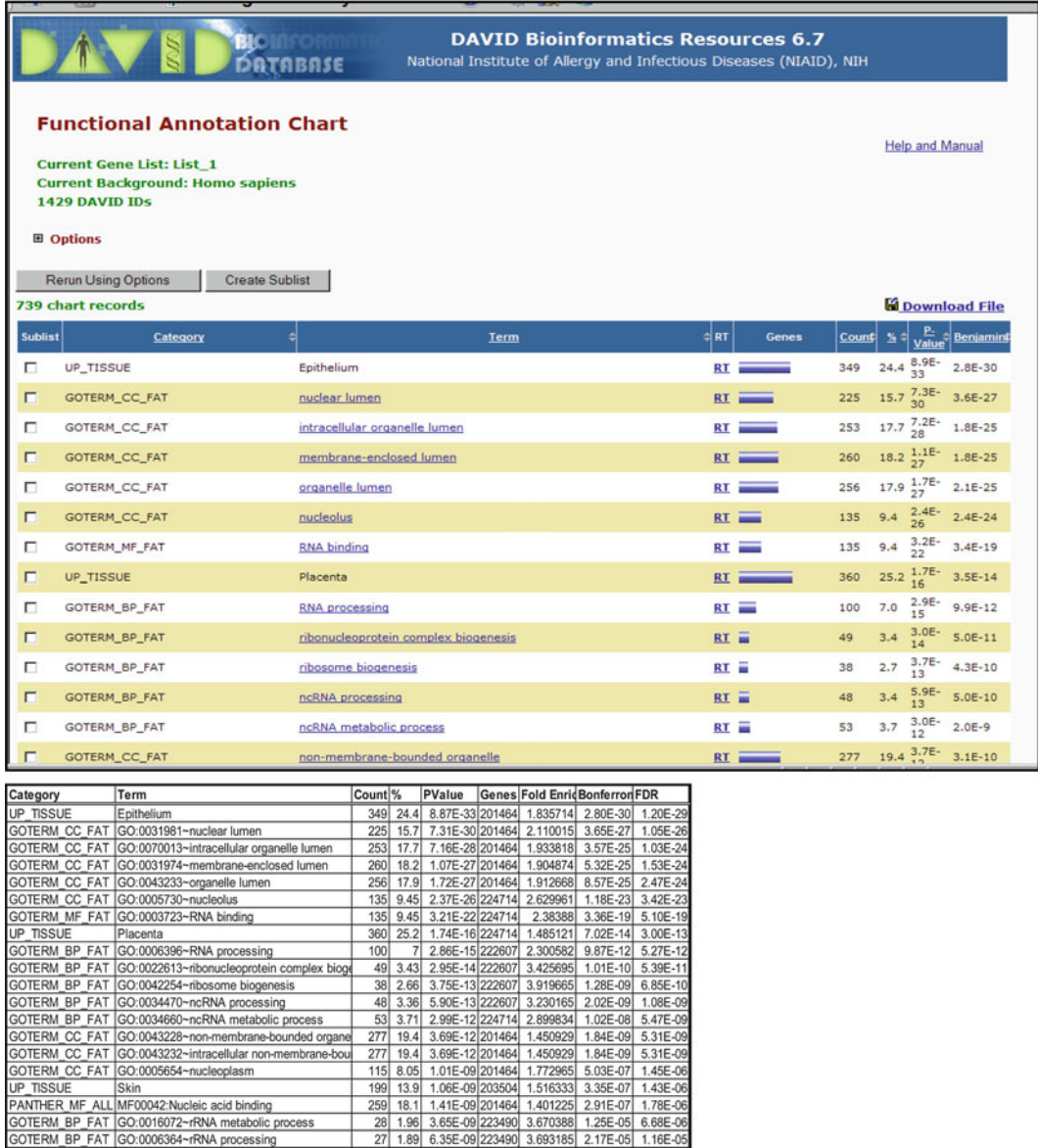



Fig. 11 (continued)

C



DAVID Bioinformatics Resources 6.7

National Institute of Allergy and Infectious Diseases (NIAID), NIH

Functional Annotation Clustering

[Help and Manual](#)

Current Gene List: List_1
Current Background: Homo sapiens
1429 DAVID IDs

Options **Classification Stringency:** Medium

[Download File](#)

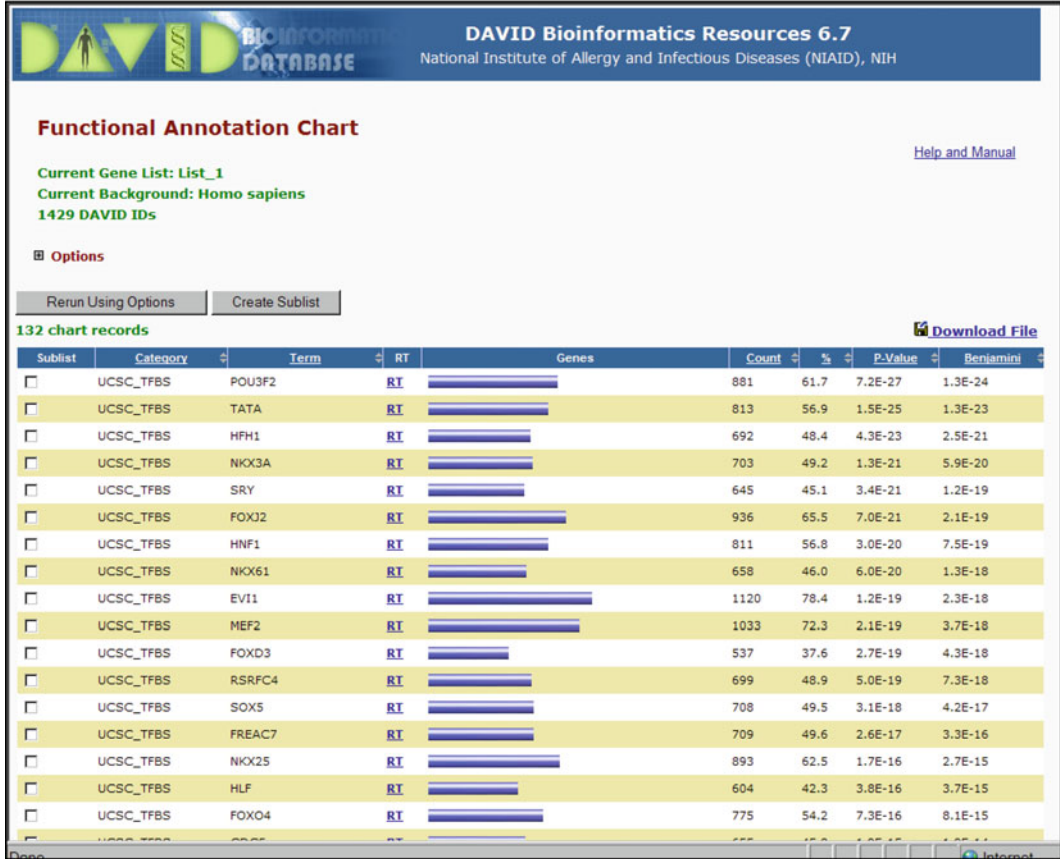
298 Cluster(s)

Annotation Cluster 1	Enrichment Score: 20.94	Count	P-Value	Benjamini
<input type="checkbox"/> GOTERM_CC_FAT	nuclear lumen	RT	225	7.3E-30 3.6E-27
<input type="checkbox"/> GOTERM_CC_FAT	intracellular organelle lumen	RT	253	7.2E-28 1.8E-25
<input type="checkbox"/> GOTERM_CC_FAT	membrane-enclosed lumen	RT	260	1.1E-27 1.8E-25
<input type="checkbox"/> GOTERM_CC_FAT	organelle lumen	RT	256	1.7E-27 2.1E-25
<input type="checkbox"/> GOTERM_CC_FAT	nucleolus	RT	135	2.4E-26 2.4E-24
<input type="checkbox"/> GOTERM_CC_FAT	non-membrane-bounded organelle	RT	277	3.7E-12 3.1E-10
<input type="checkbox"/> GOTERM_CC_FAT	intracellular non-membrane-bounded organelle	RT	277	3.7E-12 3.1E-10
<input type="checkbox"/> GOTERM_CC_FAT	nucleoplasm	RT	115	1.0E-9 7.2E-8
Annotation Cluster 2	Enrichment Score: 11.06	Count	P-Value	Benjamini
<input type="checkbox"/> GOTERM_BP_FAT	ribonucleoprotein complex biogenesis	RT	49	3.0E-14 5.0E-11
<input type="checkbox"/> GOTERM_BP_FAT	ribosome biogenesis	RT	38	3.7E-13 4.3E-10
<input type="checkbox"/> GOTERM_BP_FAT	ncRNA processing	RT	48	5.9E-13 5.0E-10
<input type="checkbox"/> GOTERM_BP_FAT	ncRNA metabolic process	RT	53	3.0E-12 2.0E-9
<input type="checkbox"/> GOTERM_BP_FAT	rRNA metabolic process	RT	28	3.7E-9 2.1E-6
<input type="checkbox"/> GOTERM_BP_FAT	rRNA processing	RT	27	6.3E-9 3.1E-6
Annotation Cluster 3	Enrichment Score: 6.66	Count	P-Value	Benjamini
<input type="checkbox"/> GOTERM_BP_FAT	ncRNA metabolic process	RT	53	3.0E-12 2.0E-9
<input type="checkbox"/> GOTERM_BP_FAT	tRNA metabolic process	RT	24	4.6E-5 6.0E-3

Annotation Cluster 1	Enrichment Score: 20.938255633170126						
Term	Count	%	PValue	Genes	Fold Enrich	Bonferroni	FDR
GO:0031981~nuclear lumen	225	15.7	7.31E-30	201464	2.1100147	3.65E-27	1.05E-26
GO:0070013~intracellular organelle lumen	253	17.7	7.16E-28	201464	1.9338177	3.57E-25	1.03E-24
GO:0031974~membrane-enclosed lumen	260	18.2	1.07E-27	201464	1.9048744	5.32E-25	1.53E-24
GO:0043233~organelle lumen	256	17.9	1.72E-27	201464	1.9126678	8.57E-25	2.47E-24
GO:0005730~nucleolus	135	9.45	2.37E-26	224714	2.629961	1.18E-23	3.42E-23
GO:0043228~non-membrane-bounded organ	277	19.4	3.69E-12	201464	1.4509286	1.84E-09	5.31E-09
GO:0043232~intracellular non-membrane-bo	277	19.4	3.69E-12	201464	1.4509286	1.84E-09	5.31E-09
GO:0005654~nucleoplasm	115	8.05	1.01E-09	201464	1.7729652	5.03E-07	1.45E-06
Annotation Cluster 2	Enrichment Score: 11.05724319679922						
GO:0022613~ribonucleoprotein complex bio	49	3.43	2.95E-14	222607	3.4256951	1.01E-10	5.39E-11
GO:0042254~ribosome biogenesis	38	2.66	3.75E-13	222607	3.9196645	1.28E-09	6.85E-10
GO:0034470~ncRNA processing	48	3.36	5.90E-13	222607	3.2301654	2.02E-09	1.08E-09
GO:0034660~ncRNA metabolic process	53	3.71	2.99E-12	224714	2.8998342	1.02E-08	5.47E-09
GO:0016072~rRNA metabolic process	28	1.96	3.65E-09	223490	3.6703876	1.25E-05	6.68E-06
GO:0006364~rRNA processing	27	1.89	6.35E-09	223490	3.693185	2.17E-05	1.16E-05
Annotation Cluster 3	Enrichment Score: 6.662722684293186						
GO:0034660~ncRNA metabolic process	53	3.71	2.99E-12	224714	2.8998342	1.02E-08	5.47E-09
GO:0006399~tRNA metabolic process	24	1.68	4.59E-05	155722	2.5594955	0.145308	0.083885
GO:0008033~tRNA processing	18	1.26	7.48E-05	219143	2.9804651	0.225542	0.136513
Annotation Cluster 4	Enrichment Score: 5.206855334136483						
GO:0001944~vasculature development	44	3.08	1.17E-06	201464	2.2059928	0.003987	0.002135
GO:0048514~blood vessel morphogenesis	39	2.73	1.39E-06	201464	2.325987	0.004755	0.002548
GO:0001568~blood vessel development	43	3.01	1.53E-06	201464	2.2086531	0.0052	0.002787
GO:0001525~angiogenesis	25	1.75	5.98E-04	201464	2.1257071	0.870776	1.087683
Annotation Cluster 5	Enrichment Score: 5.016895751635733						
GO:0010608~posttranscriptional regulation o	41	2.87	1.83E-07	229841	2.4452684	6.24E-04	3.34E-04
GO:0006417~regulation of translation	27	1.89	2.45E-05	214314	2.4800951	0.080486	0.044837
GO:0032268~regulation of cellular protein m	61	4.27	1.98E-04	201464	1.6194839	0.492451	0.361803

Fig. 11 (continued)

d



Term	Count	%	PValue	Genes	Fold Enrich	Bonferroni	FDR
POU3F2	881	61.7	7.22E-27	201464	1.274312	1.28E-24	8.87E-24
TATA	813	56.9	1.46E-25	233888	1.295086	2.59E-23	1.80E-22
HNF1	692	48.4	4.30E-23	201464	1.332353	7.61E-21	5.28E-20
NKX3A	703	49.2	1.33E-21	233888	1.311379	2.36E-19	1.64E-18
SRY	645	45.1	3.39E-21	233888	1.337108	6.00E-19	4.16E-18
FOXJ2	936	65.5	6.98E-21	233888	1.210109	1.24E-18	8.57E-18
HNF1	811	56.8	2.97E-20	233888	1.251154	5.25E-18	3.65E-17
NKX61	658	46	6.03E-20	233888	1.316003	1.07E-17	7.41E-17
EVI1	1120	78.4	1.19E-19	233888	1.143213	2.10E-17	1.46E-16
MEF2	1033	72.3	2.08E-19	201464	1.168669	3.69E-17	2.56E-16
FOXD3	537	37.6	2.65E-19	233888	1.377936	4.69E-17	3.26E-16
RSRFC4	699	48.9	4.97E-19	233888	1.286265	8.80E-17	6.11E-16
SOX5	708	49.5	3.08E-18	233888	1.273808	5.46E-16	3.78E-15
FREAC7	709	49.6	2.60E-17	233888	1.263387	4.61E-15	3.20E-14
NKX25	893	62.5	1.75E-16	233888	1.194387	3.93E-14	2.78E-13
HLF	604	42.3	3.83E-16	233888	1.301153	5.90E-14	4.11E-13
FOXO4	775	54.2	7.27E-16	201464	1.227499	1.38E-13	9.55E-13
CDC5	655	45.8	1.94E-15	233888	1.269414	3.34E-13	2.32E-12
NKX22	651	45.6	3.11E-15	233888	1.268793	5.50E-13	3.82E-12
E4BP4	635	44.4	6.97E-15	233888	1.271442	1.24E-12	8.59E-12
TBP	533	37.3	1.13E-14	201464	1.318143	2.00E-12	1.39E-11

Fig. 11 (continued)

set of annotations and use the same set in future analyses, which will make all the spreadsheets have a consistent structure.

5. First choose “Functional Annotation Table.” Here come the results. Choose “download file” near the right upper corner and save it as text file. Click once (not twice) the file, use the right button of mouse to choose “open with” and select “Microsoft Office Excel”. In the Excel file, you get many annotation columns; save this file as “Microsoft Office Excel Worksheet” file type. This is a very important file because it contains all the annotations and identifiers for all the genes. Note, however, that it does not have the results of your microarrays: the chip data are not in it. If you want, you can insert them using the DataLoader function of the Add-ins (see above).
6. Return to DAVID and click “Functional Annotation Chart.” Here come the results. Choose “download file” near the right upper corner and save it as text file. As described above, use the right button of mouse to choose “open with” and select “Microsoft Office Excel.” In the Excel file, the ontological categories are sorted by their p -values. In general, the p -values better than 10^{-5} are highly significant! This, however, strongly depends on the number of genes in the list uploaded to DAVID. These ontological categories are statistically overrepresented in the set of genes you submitted. Save this file as “Microsoft Office Excel Worksheet” file type. Back in David, you can click on “Term” to have it described, “RT” for related terms and “Genes” to get the sub-list of those genes that specifically belong to this ontological term. You can play with the options; we sometimes find it useful to restrict the categories to those with four or more genes.

In analyses of regulated genes, one finds many redundant or overly general ontological categories, which has to be parsed in order to detect the specific and important ontological categories regulated in parallel. For example, we find often very general categories, such as “biological process,” “metabolic process” or “cell communication” and redundant categories “nuclear lumen,” “intracellular organelle lumen,” “membrane-enclosed lumen,” “organelle lumen” *et sim.* (Fig. 11b).

7. Return to DAVID and click “Functional Annotation Cluster.” Here come the results. Choose “download file” near the right upper corner and save it as text file. Click the file once, use the right button of mouse to choose “open with” and select “Microsoft Office Excel.” Save as “Microsoft Office Excel Worksheet” file type. Back in DAVID, you can click on “Term” to have it described, “RT” for related terms and the horizontal bar to get the list of genes that belong to this *cluster of ontological terms*. You can play with the options; we did not

find this useful. The important value in this view is “Enrichment Score.” While the significance cut-off depends on the number of genes submitted, for 300–400 genes, scores >4 are very significant.

3.11 Comparing Lists of Regulated Genes: The Lists2Networks Algorithm

Lists2Networks is a web-based system that provides integrated analysis of lists of mammalian genes or proteins. Lists2Networks can analyze networks of protein–protein interactions, as well as compare gene lists with several preexisting gene list libraries, such as signaling, metabolic pathways, kinase-substrate, microRNA targets, and protein–protein interactions. The analyses can be applied simultaneously to multiple gene lists. We find Lists2Networks to be very user friendly and will “remember” your lists so that it can be revisited many times with adding new data.

From DAVID Tables (see Fig. 11a), lists of official symbols of regulated genes can be collected and submitted to the Lists2Networks analysis program <http://amp.pharm.mssm.edu/lachmann/upload/login.php> (33). The program compares lists for mutual overlaps within specific categories, e.g., ontological biological processes, GenMAPP and KEGG pathways, KEA kinase targets, predicted promoter sites, and OMIM disease-associated genes, returning statistical evaluation of the overlaps. This allows us to identify specific functional commonalities in various lists of genes, providing the meta-analysis results and insights. While we usually analyze many different relevant categories, we find “Gene Ontology Biological Process” to be the most informative, probably because it is the best-annotated and most complete. The Lists2Networks analysis provides both a matrix of p -values for overlapping of related gene lists (Fig. 12a), as well as spreadsheets of p -values of individual biological processes, Bonferoni-corrected for multiple comparisons (Fig. 12b). We also use the Lists2Networks program for prediction of transcription factor binding sites in the promoters of regulated genes. For example, we see E2F and NFY binding sites overrepresented in the promoters of genes suppressed by Ephrin B2 in keratinocytes (Fig. 12c) (data from reference (34)). Lists2Networks can also be used to identify the kinases whose target proteins are overrepresented in the products of regulated genes (33). Using the KEA kinase targets analysis, we found the targets of MAPKs overrepresented in the protein products of genes suppressed by Ephrin B2 (Fig. 12d).

3.12 Clustering and Comparison of Lists

There are several additional tools available for comparisons and clustering of lists. Commonly, microarray studies include hierarchical trees of genes, self-organizing maps, and principal component analyses.

1. The data set containing the expression patterns of the regulated genes can also be clustered and visualized using Cluster and

a

	EphB2 1h UP	EphB2 4h UP	EphB2 48h UP	EphB2 24h UP	EphB2 1h DN	EphB2 4h DN	EphB2 48h DN	EphB2 24h DN
EphB2 1h UP	1.00	9.27E-04	1.43E-08	2.07E-03	9.09E-03	3.49E-61	4.96E-28	4.42E-88
EphB2 4h UP	7.93E-04	1.00	3.85E-25	1.43E-135	2.13E-06	5.47E-01	2.87E-01	7.31E-01
EphB2 48h UP	8.41E-09	7.19E-25	1.00	1.36E-44	7.50E-03	8.68E-14	6.48E-01	8.25E-01
EphB2 24h UP	2.09E-03	2.18E-112	1.63E-41	1.00	1.50E-06	2.09E-08	1.09E-01	1.00E+00
EphB2 1h DN	9.43E-03	3.68E-06	8.39E-03	1.72E-06	1.00	4.47E-05	4.58E-21	3.70E-16
EphB2 4h DN	1.53E-57	5.48E-01	6.85E-13	3.21E-08	4.98E-05	1.00	2.89E-24	3.49E-135
EphB2 48h DN	8.34E-27	2.91E-01	6.48E-01	1.11E-01	1.18E-20	3.18E-24	1.00	6.85E-93
EphB2 24h DN	7.09E-73	7.26E-01	8.19E-01	1.00E+00	6.14E-15	3.87E-118	4.89E-83	1.00

b

	EphB2_1h_DN	EphB2_4h_DN	EphB2_48h_DN	EphB2_24h_DN	minimum
organelle organization GO 0006996			1.34E-08		1.34E-08
microtubule based process GO 0007017			1.68E-08		1.68E-08
microtubule cytoskeleton organ GO 0000226			8.44E-08		8.44E-08
spindle organization GO 0007051			1.17E-05		1.17E-05
regulation of cell cycle GO 0051726			1.82E-05		1.82E-05
nuclear mRNA splicing, via spl GO 0000398	8.26E-05				8.26E-05
regulation of mitotic cell cyc GO 0007346			8.97E-05		8.97E-05
RNA splicing, via transterifer GO 0000375	9.19E-05				9.19E-05
mRNA processing GO 0006397	1.62E-04				1.62E-04
cell cycle GO 0007049			1.65E-04	1	1.65E-04
epidermis development GO 0008544		1.24E-03		1	1.86E-04

c

	EphB2 24h DN	EphB2 48h DN	EphB2 4h DN	EphB2 1h DN	EphB2 1h UP	EphB2 24h UP	EphB2 48h UP	EphB2 4h UP	min
NFYC	5.77E-01	4.46E-05	1	2.39E-01	1	1	1	1	4.46E-05
E2F3	8.51E-03	2.25E-03	1	1	1	1	1	1	0.002246
E2F4	8.51E-03	2.25E-03	1	1	1	1	1	1	0.002246
E2F5	8.51E-03	2.25E-03	1	1	1	1	1	1	0.002246
E2F2	8.51E-03	2.25E-03	1	1	1	1	1	1	0.002246
NFYB	1	9.80E-03	1	2.85E-01	1	1	1	1	0.009804
E2F1	2.03E-01	1.47E-02	1	1	1	1	1	1	0.014665
NFYA	1	1.75E-02	1	4.22E-02	1	1	1	1	0.017462
POU3F1	1	7.66E-01	6.66E-02	1	1	1	1	1	0.066635

d

	EphB2_4h_UP	EphB2_48h_UP	EphB2_24h_UP	EphB2_1h_UP	EphB2_1h_DN	EphB2_4h_DN	EphB2_48h_DN	EphB2_24h_DN	min
CDC2	1	1	1	1	6.45E-03	1	1.26E-10	1	1.26E-10
MAPK14	1	1	1	2.50E-01	9.15E-05	1	1.54E-04	2.12E-05	2.12E-05
AURKA	1	1	1	1	1	1	1.30E-04	1	1.30E-04
GSK3A	1	1	1	1	2.73E-04	1	1	1	2.73E-04
CDK2	1	1	1	1.11E-02	9.61E-03	1	1.33E-03	9.66E-02	1.33E-03
SRPK2	1	1	1	1	1.59E-03	1	1	1	1.59E-03
MAPK8	1	1	1	1	2.22E-03	1	1	1	2.22E-03
LIMK1	1	1	1	1	1	1	2.42E-03	1	2.42E-03
AURKB	1	1	1	1	1	1	2.78E-03	1	2.78E-03
PRKCD	1	1	1	1	2.82E-03	1	1	1	2.82E-03
ERBB4	1	1	1	1	1.43E-02	1	1	1	1.43E-02
MAPK9	1	1	1	1	1.91E-02	1	1	1	1.91E-02

Fig. 12 Outputs from Lists2Networks programs. **(a)** Lists2Networks matrix. Comparison of the identical lists is shown in *black* cells. The closely related upregulated and downregulated lists are marked in gray. All data are from (34). **(b)** Bonferoni-corrected gene ontology values for biological functions. The data are sorted by the minimum value in any of the columns. **(c)** Transcription factors with sites overrepresented in the promoters of the genes in the lists. These are as identified by the Lists2Networks program. **(d)** KEA, Kinase substrate proteins overrepresented in the submitted lists

Tree View software available at <http://rana.stanford.edu/software> (35). First, the data are imported into the Cluster and Tree View software in a tab-delimited format. A data set containing the expression patterns of the regulated genes can be clustered based on the similarity of gene expression and based on the similarity between different samples (i.e., clustering genes or clustering chips, respectively). The clusters are observed using the TreeView program (35).

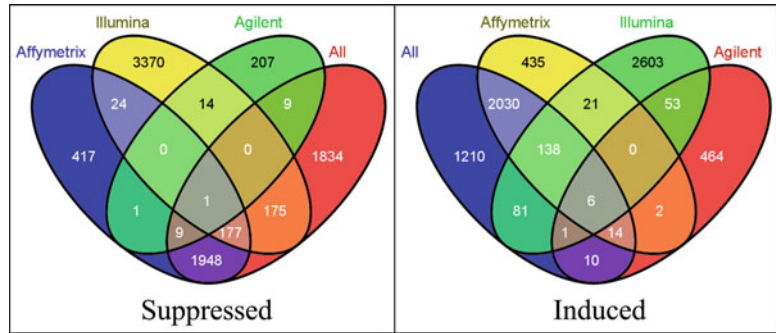


Fig. 13 Venn diagrams. The overlaps among three or four lists of genes can be easily visualized

2. A large set of clustering programs is available from e.g., <http://www.tm4.org/>; these are very easy to implement and apply. They could be useful, in theory. However, in practice, we generally did not find these very informative. They will cluster genes into induced and suppressed, highly induced, early induced or similar. Individual clusters can, then, be analyzed using DAVID or L2L. In studies using many chips with many patient samples, clustering of the samples (as opposed to genes) can be extremely interesting, e.g., pointing out to a specific subset of patients. We had no opportunity to use clustering programs this way.
3. Simple Venn diagrams can also be very useful. They can be obtained from site <http://www.pangloss.com/seidel/Protocols/venn.cgi>. You upload three or four lists of genes, Affymetrix or any other identifying symbol, and it will generate the diagram as well as provide the lists of all intersect and unique genes, as in Fig. 13.

3.13 Promoter Analysis

We find the oPOSSUM set of programs for promoter analysis, <http://www.cisreg.ca/cgi-bin/oPOSSUM/opossum>, very sophisticated, comprehensive, convenient and easy to use (36, 37). For “Human Single Site Analysis,” we prefer to use “Custom Analysis,” button near top right, which allows better-tailored analyses (Fig. 14a).

1. Choose species (human), gene ID type (usually we use Entrez gene, or RefSeq provided by DAVID in the Table download; oPOSSUM does not accept the Affymetrix IDs) and enter a list of co-expressed genes; it is easiest to copy and paste gene IDs. The submitted list will be compared to a list of 15,000 random genes.
2. Select transcription factor binding site matrices; we usually select by taxonomic supergroup, choosing “vertebrate.”

a

b

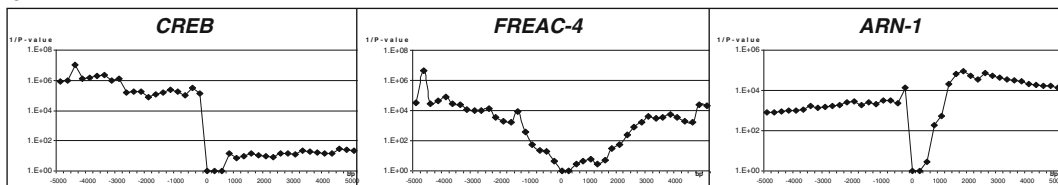


Fig. 14 oPOSSUM analysis. (a) Screenshot of the oPOSSUM analysis result. Remember to click on the custom analysis button, which will give you more options for analysis. (b) Results of an oPOSSUM analysis. The binding sites for different transcription factors can aggregate close upstream from the transcription start site, or be found at significant lengths, upstream or downstream. Data from (37). (c) Results of an oPOSSUM analysis in a spreadsheet form. Additional information can be obtained by clicking on the blue values

3. Select parameters. You can calibrate the following parameters to obtain the optimal statistical p-value. (a) Level of conservation: Top 10, 20 or 30 % of conserved regions; this depends on the % homology between the human and murine promoter sequences that will be analyzed. We use 30 %, the least

C

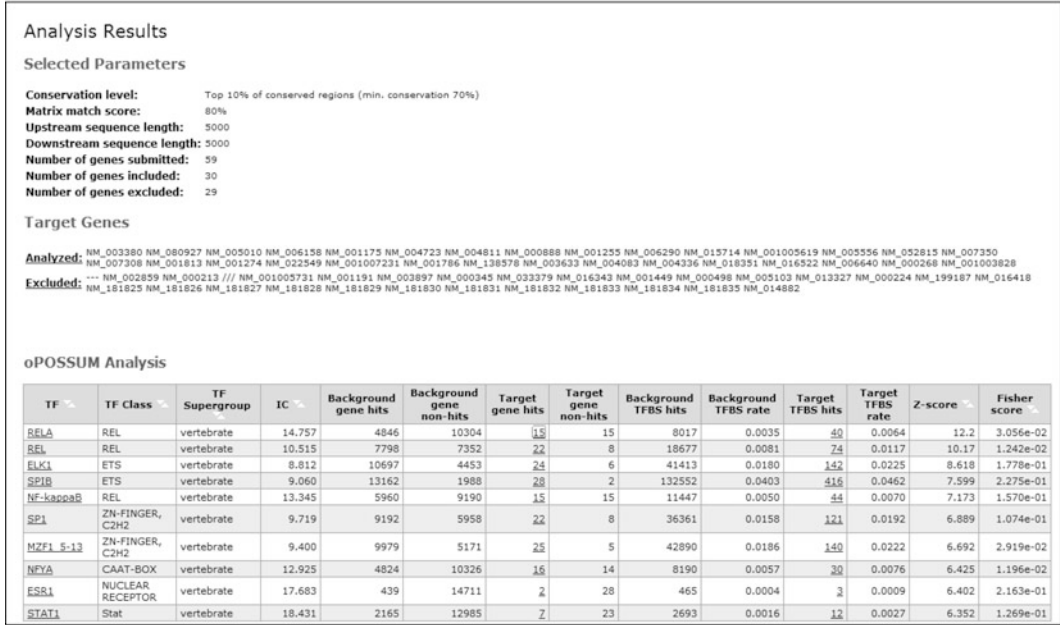


Fig. 11 (continued)

restrictive cut-off. (b) Matrix match threshold: 75, 80 or 85 %; this is the % match between the “optimal” canonical transcription factor binding site and the similar site in the promoter DNA. We use 80 %, which gave us the best *p*-value for the NFkB-dependent genes (see (38)). (c) Amount of upstream/downstream sequences. We usually start with the promoter-proximal sequences, e.g. 250/0 and repeat in 250–500 bp increments (Fig. 14b). Once you have decided the parameters to be used, you have to decide “Number of results to display,” choose “OR only results with Z-score ≥ 10 and Fisher score ≤ 0.001 .” Finally, “sort results by Fisher score.” Then submit.

4. The next screen will mirror the parameters you chose, on top, which is followed by the lists of included and excluded genes. The included ones are those for which human/murine sequences were found and are among the, say, top 30 % of all comparisons; the excluded genes did not make this cut.
5. Below this is the data file (Fig. 14c). The first three columns give the transcription factors, their classes and their information contents, “IC”; This last value is related to the size of the binding site: small IC values, 8–10, are usually for short, 4–5 bp binding sites, which occur very frequently in all sequences; large IC values, >14 , are for larger and rarer sites. “Target gene hits” are different from “Target TFBS hits,” because

some genes have multiple transcription factor binding sites, TFBSs. The most important columns are the “Z-score” and “Fisher score,” which are calculated from the target TFBS hits and the target gene hits, respectively. Fisher score better than 10^{-5} is usually highly significant.

6. The analysis result can be downloaded as text file and then be opened with Excel to edit.

3.14 Conclusion

The methodology described here can be used for transcriptional profiling of human skin cells in culture or in vivo. The methodology allows analysis of Affymetrix and other commercial and proprietary microarrays. Moreover, we describe a method for meta-analysis of multiple datasets from public repositories, their identification, downloading, fusion, and nonparametric identification of differentially expressed genes. The methodology can serve as a paradigm for analysis and meta-analysis of a wide range of skinomics data and can be applied to tissues other than skin.

4 Notes

1. The cells are expanded through three passages for the experiments, trypsinized with 0.025 % trypsin, which was neutralized with 0.5 mg/ml of trypsin inhibitor. We avoid using serum to neutralize the trypsin because serum can promote certain aspects of keratinocyte differentiation. For most of our experiments, we use third-passage keratinocytes 1 day after reaching confluence.
2. The reconstructed epidermis samples are available from the two companies in many formats and sizes. They can be ordered with or without antimicrobials. Furthermore, complex samples, e.g., containing melanocytes, are available. If one wants to follow the process of epidermal differentiation, immature, undifferentiated versions of reconstituted epidermis are also available. Samples from different epithelia, e.g., cornea, oral, and vaginal, are available in addition to the epidermal ones.
3. The advantages of these samples include the relatively homogeneous age group, 20–35 olds, sun-protected area and rather large specimens.
4. Trizol gives good yields and effectively disrupts the epidermis, but the purity of the RNA is inadequate for the subsequent steps; the RNA isolation kit gives adequate purity, but inefficiently disrupts the tissue, which is why the two are used in series.
5. All solutions contain RNase inhibitors. Skin is particularly rich in RNases, necessitating their inhibition.

6. It is important to save spreadsheets often to avoid losing data. More to the point, different algorithms require different formats of the data. Generally tab-delimited text files are used, but the formats of columns and rows within these are usually rigorously prescribed.

References

1. Lee DD, Zavadil J, Tomic-Canic M, Blumenberg M (2010) Comprehensive transcriptional profiling of human epidermis, reconstituted epidermal equivalents, and cultured keratinocytes using DNA microarray chips. *Methods Mol Biol* 585:193–223
2. Quackenbush J, Hegde P, Qi R, Abernathy K, Gay C, Dharap S, Gaspard R, Hughes JE, Snesrud E, Lee N (2003) Genomics. microarrays—guilt by association A concise guide to cDNA microarray analysis. *Science* 302:240–241
3. Schena M, Shalon D, Davis RW, Brown PO (1995) Quantitative monitoring of gene expression patterns with a complementary DNA microarray. *Science* 270:467–470
4. Bingham JL, Carrigan PE, Miller LJ, Srinivasan S (2008) Extent and diversity of human alternative splicing established by complementary database annotation and microarray analysis. *OMICS* 12:83–92
5. Iyer VR, Eisen MB, Ross DT, Schuler G, Moore T, Lee JC, Trent JM, Staudt LM, Hudson J Jr, Boguski MS, Lashkari D, Shalon D, Botstein D, Brown PO (1999) The transcriptional program in the response of human fibroblasts to serum. *Science* 283:83–87
6. Wong R, Tran V, Morhenn V, Hung SP, Andersen B, Ito E, Wesley Hatfield G, Benson NR (2004) Use of RT-PCR and DNA microarrays to characterize RNA recovered by non-invasive tape harvesting of normal and inflamed skin. *J Invest Dermatol* 123:159–167
7. Blumenberg, M. (2005) Skinomics. *J Invest Dermatol* 124, viii-x.
8. Blumenberg M (2012) SKINOMICS: transcriptional profiling in dermatology and skin biology. *Curr Genomics* 13:363–368
9. Li D, Turi TG, Schuck A, Freedberg IM, Khitrov G, Blumenberg M (2001) Rays and arrays: the transcriptional program in the response of human epidermal keratinocytes to UVB illumination. *FASEB J* 15:2533–2535
10. Sesto A, Navarro M, Burslem F, Jorcano JL (2002) Analysis of the ultraviolet B response in primary human keratinocytes using oligonucleotide microarrays. *Proc Natl Acad Sci U S A* 99:2965–2970
11. Murakami T, Fujimoto M, Ohtsuki M, Nakagawa H (2001) Expression profiling of cancer-related genes in human keratinocytes following non-lethal ultraviolet B irradiation. *J Dermatol Sci* 27:121–129
12. Takao J, Ariizumi K, Dougherty II, Cruz PD Jr (2002) Genomic scale analysis of the human keratinocyte response to broad-band ultraviolet-B irradiation. *Photodermatol Photoimmunol Photomed* 18:5–13
13. Howell BG, Wang B, Freed I, Mamelak AJ, Watanabe H, Sauder DN (2004) Microarray analysis of UVB-regulated genes in keratinocytes: downregulation of angiogenesis inhibitor thrombospondin-1. *J Dermatol Sci* 34:185–194
14. Banno T, Gazel A, Blumenberg M (2004) The use of DNA microarrays in dermatology research. *Retinoids* 20:1–4
15. Blumenberg M (2006) DNA microarrays in dermatology and skin biology. *OMICS* 10:243–260
16. Brem H, Stojadinovic O, Diegelmann RF, Entero H, Lee B, Pastar I, Golinko M, Rosenberg H, Tomic-Canic M (2007) Molecular markers in patients with chronic wounds to guide surgical debridement. *Mol Med* 13:30–39
17. Charles CA, Tomic-Canic M, Vincek V, Nassiri M, Stojadinovic O, Eaglstein WH, Kirsner RS (2008) A gene signature of nonhealing venous ulcers: potential diagnostic markers. *J Am Acad Dermatol* 19:19
18. Harsha A, Stojadinovic O, Brem H, Seharafujisawa A, Wewer U, Loomis CA, Blobel CP, Tomic-Canic M (2008) ADAM12: a potential target for the treatment of chronic wounds. *J Mol Med* 86:961–969
19. Stojadinovic O, Pastar I, Vukelic S, Mahoney MG, Brennan D, Krzyzanowska A, Golinko M, Brem H, Tomic-Canic M (2008) Deregulation of keratinocyte differentiation and activation: a hallmark of venous ulcers. *J Cell Mol Med* 28:28

20. Rheinwald JG, Green H (1975) Serial cultivation of strains of human epidermal keratinocytes: the formation of keratinizing colonies from single cells. *Cell* 6:331–344
21. Randolph RK, Simon M (1994) Characterization of retinol metabolism in cultured human epidermal keratinocytes. *J Biol Chem* 268:9198–9205
22. Bernard FX, Pedretti N, Rosdy M, Deguercy A (2002) Comparison of gene expression profiles in human keratinocyte mono-layer cultures, reconstituted epidermis and normal human skin; transcriptional effects of retinoid treatments in reconstituted human epidermis. *Exp Dermatol* 11:59–74
23. Rosdy M, Clauss LC (1990) Terminal epidermal differentiation of human keratinocytes grown in chemically defined medium on inert filter substrates at the air-liquid interface. *J Invest Dermatol* 95:409–414
24. Radoja N, Gazel A, Banno T, Yano S, Blumenberg M (2006) Transcriptional profiling of epidermal differentiation. *Physiol Genomics* 5:5
25. Gazel A, Ramphal P, Rosdy M, De Wever B, Tornier C, Hosein N, Lee B, Tomic-Canic M, Blumenberg M (2003) Transcriptional profiling of epidermal keratinocytes: comparison of genes expressed in skin, cultured keratinocytes, and reconstituted epidermis, using large DNA microarrays. *J Invest Dermatol* 121:1459–1468
26. Mahadevappa M, Warrington JA (1999) A high-density probe array sample preparation method using 10- to 100-fold fewer cells. *Nat Biotechnol* 17:1134–1136
27. Barrett T, Suzek TO, Troup DB, Wilhite SE, Ngau WC, Ledoux P, Rudnev D, Lash AE, Fujibuchi W, Edgar R (2005) NCBI GEO: mining millions of expression profiles—database and tools. *Nucleic Acids Res* 33:D562–D566
28. Ivliev AE, t’Hoen PA, Villerius MP, den Dunnen JT, Brandt BW (2008) Microarray retriever: a web-based tool for searching and large scale retrieval of public microarray data. *Nucleic Acids Res* 36:W327–W331
29. Gautier L, Cope L, Bolstad BM, Irizarry RA (2004) affy—analysis of affymetrix GeneChip data at the probe level. *Bioinformatics* 20:307–315
30. Hong F, Breitling R, McEntee CW, Wittner BS, Nemhauser JL, Chory J (2006) RankProd: a bioconductor package for detecting differentially expressed genes in meta-analysis. *Bioinformatics* 22:2825–2827
31. Dennis G Jr, Sherman BT, Hosack DA, Yang J, Gao W, Lane HC, Lempicki RA (2003) DAVID: database for annotation, visualization, and integrated discovery. *Genome Biol* 4:P3
32. da Huang W, Sherman BT, Lempicki RA (2009) Bioinformatics enrichment tools: paths toward the comprehensive functional analysis of large gene lists. *Nucleic Acids Res* 37:1–13
33. Lachmann A, Ma’ayan A (2010) Lists2Networks: integrated analysis of gene/protein lists. *BMC Bioinforma* 11:87
34. Walsh R, Blumenberg M (2011) EPH-2B, acting as an extracellular ligand, induces differentiation markers in epidermal keratinocytes. *J Cell Physiol* 1:22968
35. Eisen MB, Spellman PT, Brown PO, Botstein D (1998) Cluster analysis and display of genome-wide expression patterns. *Proc Natl Acad Sci U S A* 95:14863–14868
36. Ho Sui SJ, Mortimer JR, Arenillas DJ, Brumm J, Walsh CJ, Kennedy BP, Wasserman WW (2005) oPOSSUM: identification of over-represented transcription factor binding sites in co-expressed genes. *Nucleic Acids Res* 33:3154–3164
37. Gazel A, Nijhawan RI, Walsh R, Blumenberg M (2008) Transcriptional profiling defines the roles of ERK and p38 kinases in epidermal keratinocytes. *J Cell Physiol* 215:292–308
38. Banno T, Gazel A, Blumenberg M (2005) Pathway-specific profiling identifies the NF- κ B-dependent tumor necrosis factor α -regulated genes in Epidermal Keratinocytes. *J Biol Chem* 280:18973–18980

Compound Screening and Transcriptional Profiling in Human Primary Keratinocytes: A Brief Guideline

Raphaela Rid, Harald Hundsberger, and Kamil Önder

Abstract

Cultured human primary keratinocytes constitute suitable targets for in-depth evaluation of the proliferative or differentiative potential of compounds. There is, however, a double-edged and intrinsically inseparable transition from biological activity to cytotoxicity for any agent under investigation. For that reason, we here first of all present an established protocol for the isolation, cultivation, and analysis of primary foreskin-derived keratinocytes. Taking calcitriol as example, we then reveal how a straightforward photometric cell culture assay can be exploited to assess overall cell viability in response to increasing compound doses. With predetermined cellular cytotoxicity at hand, physiologically meaningful (sub-toxic) compound concentrations for subsequent stimulation of cells can be readily selected, and, in doing so, differentially expressed genes with biological significance can be reliably identified.

Keywords: Primary keratinocyte culturing, Compound screening, Cytotoxicity, Calcitriol

1 Introduction

Calcitriol ($1\alpha,25$ -dihydroxyvitamin D_3), naturally acknowledged for its role in maintaining Ca^{++} homeostasis crucial for maintaining bone integrity, constitutes a key modulator of numerous skin cell functions. Calcitriol, as reviewed elsewhere (1–8), for instance affects epidermal differentiation marker expression (4, 9–11), permeability barrier formation (12), apoptotic susceptibility (13, 14), or innate immune defense responsiveness (15, 16). Both importance and breadth of this activity—especially its ascribed antiproliferative and prodifferentiating characteristics—endow it with considerable therapeutic potential, for instance in the management of hyperproliferative skin diseases like psoriasis vulgaris. Hypercalcemia is, however, the most severe restriction of long-term administration of the natural hormone. Irrespective of whether a completely novel compound is extracted as primary hit from a high-content screening library (17) or a synthetic analogue with hopefully improved therapeutic properties is deduced from an already active molecule (18, 19), the early monitoring or rather exclusion of a substance's general cytotoxicity in

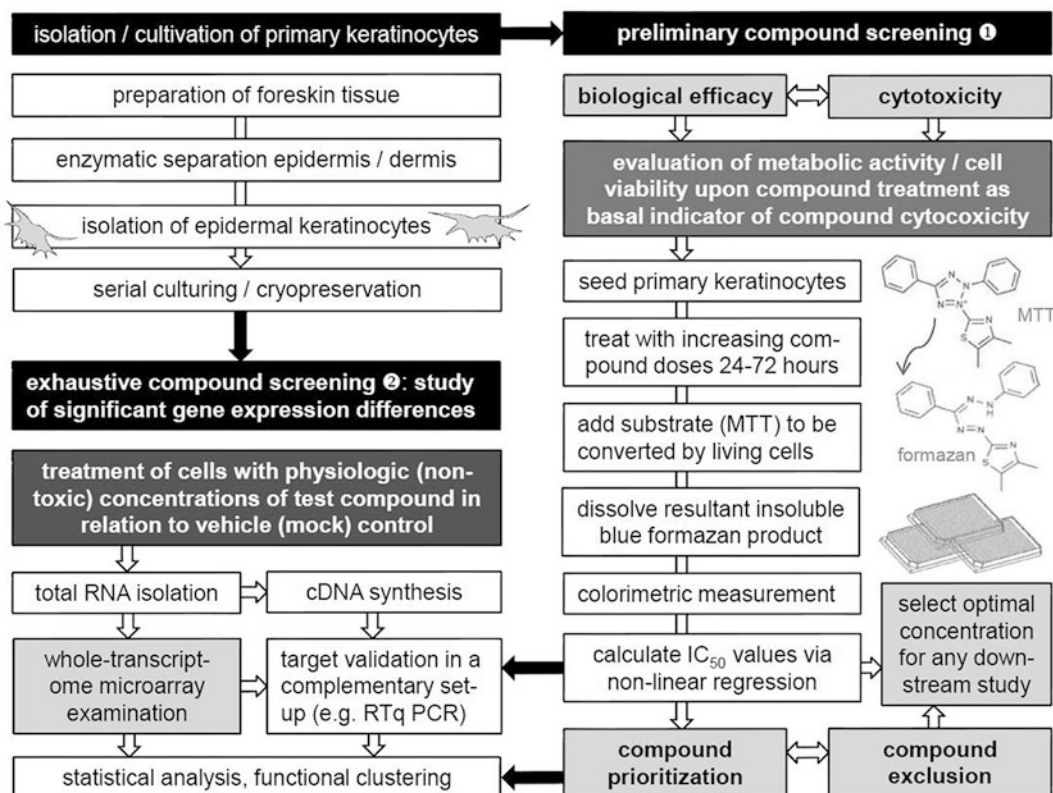


Fig. 1 Workflow of cytotoxicity evaluation and compound screening in keratinocytes. Given the seamless transition from biological activity to cellular toxicity, it is important to assess cell survival in response to compound stimulation. In doing so, physiologically relevant, sub-toxic concentrations for use in differential gene expression profiling can be reliably selected

both cases denotes an essential prerequisite in the drug development and characterization pipeline. At this juncture, we here implement a two-stage compound screening strategy (Fig. 1) that, by combining methods, provides instant information on a test compound's cytotoxicity on human primary keratinocytes and so directly guides downstream analyses. Preliminary step is hereby the evaluation of overall cell survival in the presence of increasing compound doses. In the so-called MTT (3-[4,5-dimethylthiazol-2-yl]2,5-diphenyl tetrazolium bromide) assay performed to this end, respective substrate is taken up by treated cells and—depending on mitochondrial integrity/activity as overall measure of cell viability—reduced to an impermeable and therefore intracellularly accumulating purple formazan product (20, 21). Enforced lysis of cells, finally, causes a liberation of the respective dye which can be quantified via regular colorimetric procedures, making this technique a relatively simple, rapid, sensitive, and inexpensive cell culture test. Nonlinear regression obtained from dose–response curves finally permits to deduce EC_{50} values necessary

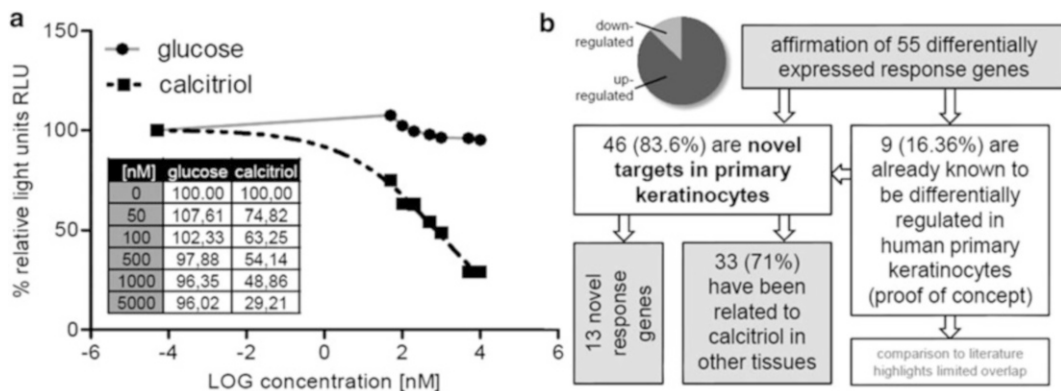


Fig. 2 Identification of novel calcitriol response genes in primary keratinocytes according to our proposed procedure. **(a)** Dose–response curve (MTT assay) showing the effect of increasing calcitriol concentrations in cells after 72-h induction. Data denote % of cell viability. **(b)** Short graphical overview of our recently published novel calcitriol response genes (22)

to select—under applied experimental conditions—physiologically relevant, nontoxic compound concentrations for uncovering, e.g., gene expression differences within respectively stimulated keratinocytes. Such a strategy appears especially useful when dealing with novel compounds for which to date only limited information is available.

One scenario where this strategy has recently been successfully applied was in the unraveling of several novel calcitriol response genes in human skin cells (22). From our initially performed MTT assay (Fig. 2a), we could estimate that 74.83 % of seeded cells were metabolically active (and hence proliferating) at a 50 nM calcitriol concentration after a 72-h exposure, 62.91 % at the 200 nM calcitriol dose, 48.86 % at 1 μ M, and 29.212 % at 5 μ M (half maximal effective concentration EC_{50} : 908.8 nM). In contrast, glucose included as negative control did not show any significant effects. These results seem plausible since calcitriol is known to inhibit cell proliferation in concentration-dependent manner. Reasonable calcitriol concentrations of 1 and 200 nM—values analogously reported in other comparable studies—were subsequently applied for definitive stimulation of primary keratinocytes. Whole-transcriptome microarray examination from total RNA prepared thereof identified 86 probe sets as differentially expressed (67 up- and 19 downregulated genes with fold changes of 1.8 or greater) under 200 nM/16-h calcitriol induction compared to reference conditions (mock control). 55 explicit hits (48 up- and 7 downregulated) selected from the 78 most promising candidates could be independently confirmed and statistically assessed in a subsequent quantitative real-time (RTq) approach—with comparable tendencies (albeit smaller fold changes) and directions (apart from one

exception) to the 1 nM/8-h condition. Resultant hit list of calcitriol response genes within human primary foreskin-derived keratinocytes includes 33 candidates which have previously been related to calcitriol in diverse (tumor-derived) cell lines, 9 (16.36 %) genes (NET1, G0S2, IL1RL1, CD14, KLK6, KLK13, SERPINB1, SEMA3B, DUSP10) previously known as calcitriol-regulated genes in human primary keratinocytes, and 13 nominees (BNC2, CALB2, IGFL3, CYP4F3, FETUB, DHRS9, HCAR3, KRT19, OLFML3, TMEM91, CRABP2, CYP4B1, TMEM63C) which have not previously been identified as being regulated by calcitriol (Fig. 2b) (22). Although some apparent restrictions of the present study have to be taken into account, namely, its absolute in vitro nature and its probably limited representativeness of biological data, it nevertheless underscores the usefulness of our experimental primary keratinocyte screening pipeline.

2 Materials

Most commonly applied chemicals and reagents are, unless otherwise stated, supplied by Sigma-Aldrich Inc. (Taufkirchen, Germany), life technologiesTM (Grand Island, NY, USA), BioRad Laboratories (Hercules, CA, USA), or TPP (Trasadingen, Switzerland). The composition of buffer A (adjust pH to 7.4 with NaOH) is 30 mM HEPES, 10 mM glucose, 3 mM KCl, 130 mM NaCl, 1 mM Na₂HPO₄, and 1x phenol red. Defined SFM medium (GIBCO[®] brand, life technologiesTM) is a ready-to-use serum-free formulation containing L-glutamine, EGF (5 µg/l), bovine pituitary extract (50 mg/l), as well as 0.09 mM CaCl₂. Calcitriol (1α,25-dihydroxyvitamin D₃) is dissolved in 100 % ethanol and stored at -20 °C.

3 Methods

3.1 Cultivation of Human Primary Keratinocytes

1. Uninflamed, sunlight-protected foreskin tissue obtained from healthy individuals in the course of routine surgery is incubated for 2 min in 100 % ethanol to eradicate any bacterial contamination. It is then excessively rinsed with CaCl₂-free Dulbecco's phosphate-buffered saline (PBS), transferred to an uncoated petri dish of 100 mm in diameter, dissected therein (consistently kept moist with some PBS) into small stripes of 3–4 mm width (basically preserving the horizontal orientation) using a pair of forceps and a scalpel, and finally aseptically submerged in 5–6 ml of Dispase solution (2.24 units, GIBCO[®] brand) diluted 1:1 in buffer A at 4 °C for 12–16 h (overnight) (22). This step disaggregates the whitish, semitransparent foreskin epidermis from the underlying dermis (*see Note 1*).

2. Next day, primary keratinocytes are harvested from the slowly peeled off epidermis via incubation for 15 min—interrupted by repeated shaking (every 2–3 min) to assist in cell dissociation—in 2 ml of trypsin–EDTA diluted 1:10 in buffer A at 37 °C (7, 23).
3. Resultant turbid cell suspension is neutralized with an identical volume (2 ml) of 10 % fetal bovine serum (FBS) and centrifuged for 5 min at $200 \times g$ at room temperature. The cell pellet is resuspended in 5 ml defined serum-free, low-calcium, keratinocyte-specific SFM medium and lastly filtered through a 40 μm cell strainer (BD Biosciences, Heidelberg, Germany) into a new Falcon tube. Residual undigested tissue fragments are in doing so entirely removed.
4. Cells in suspension are seeded in uncoated 75 cm^2 flasks pre-filled with 12 ml pre-warmed SFM medium (*see Note 2*) and incubated at 37 °C under a standard 5 % CO_2 atmosphere. Spent medium should optimally be replaced every 2–3 days. For compound screening purpose, cells are cultivated until passage 3 (duration approximately 3 weeks) (24).

3.2 Primary Keratinocyte Splitting, Passaging, and Eventual Cryopreservation

1. Keratinocytes with their typical morphology get decidedly proliferative within about 7 days after seeding single cells. Once a confluence of 70–85 % is reached, the SFM medium is aspirated and cells are carefully rinsed with CaCl_2 -free PBS (10 ml per 75 cm^2 flask).
2. Subsequent trypsinization is performed according to standard procedures. To this end, 2.5–5 ml of trypsin–EDTA diluted 1:10 in buffer A is pipetted directly onto the washed cells and the flask returned to the 37 °C incubator. A check under the light microscope shows that the keratinocytes round up and start to detach—assisted by occasionally tapping the flask—from the bottom surface within 5–10 min.
3. Keratinocytes are instantly neutralized by addition of an identical volume (2.5–5 ml) of 10 % FCS diluted in buffer A and the culture vessel rinsed 2–3 more times to remove as much cells as possible. Resultant suspension is transferred to a sterile 15 ml tube, centrifuged at $200 \times g$ for 5 min at room temperature, the supernatant completely aspirated, and the cell pellet resuspended in 5 ml SFM medium. At this stage, one can either freeze-down cells in 10 % DMSO in liquid nitrogen for long-term storage or alternatively continue with subsequent passages (with a splitting ratio of 1:4–1:8).

3.3 Viability Profiling of Compound-Treated Keratinocytes for Cytotoxicity Assessment: MTT Assay

1. Operatively, 100 μ l of primary keratinocyte suspension in defined serum-free SFM medium is seeded at a density of 2×10^4 cells per well in sterile black (clear-bottomed) polystyrene Corning[®] CellBind[®] 96-well microtiter plates (*see Note 3*). Cell number is calculated from trypsinized samples in a classical Neubauer improved hemocytometer.
2. After a 24-h recovery period, the medium is removed by aspiration and immediately replaced by 100 μ l of SFM supplemented in advance with increasing concentrations of the desired compound under study. Each experiment must also include a vehicle reference plus further internal positive as well as negative controls (*see Note 4*). In the case of calcitriol, a 240 μ M stock solution in 100 % ethanol is for instance prepared; diluted to 0 nM (100 % ethanol only), 50 nM, 100 nM, 200 nM, 500 nM, 1 μ M, 5 μ M, and 10 μ M in culture medium; and administered for 24–72 h. Cells are examined for any apparent morphological abnormalities of the maximal compound dose compared to the unstimulated status under a light microscope.
3. Next, 10 μ l of yellowish MTT solution (prepared as 5 mg/ml stock in PBS, filter-sterilized, aliquoted, and stored at -20 °C) is directly added to the culture medium with a repetitive dispensing pipette. Plates are incubated for further 2 h at 37 °C.
4. Lastly, the medium–MTT mixture is entirely removed, replaced by 100 μ l 100 % dimethyl sulfoxide (DMSO), and placed for 10 min on a microtiter plate minishaker to readily dissolve the formazan crystals through constant agitation. Absorbance is read at 570 nm on a compatible multimode reader (Promega Corporation, Madison, WI, USA). Output values are expressed as percent cell viability compared to vehicle control and EC₅₀ values calculated from resultant dose–response curves via non-linear regression (Graphpad Prism Software Inc., La Jolla, CA, USA). Data are used to determine “safe” doses for subsequent compound screening (*see Note 5*).

3.4 Stimulation of Proliferating Keratinocytes with Decidedly Sub-toxic Compound Doses

1. Proliferating keratinocytes are seeded in 25 cm² flasks (three culture vessels per treatment condition yield three parallel technical replicates) and the next day stimulated with the compound concentration chosen from the MTT assay for 24–48 h. Mock controls (for instance ethanol vehicle in the case of calcitriol studies) are analogously handled (*see Note 6*).

3.5 RNA Isolation from Compound-Treated Primary Keratinocytes

1. Total RNA is extracted from confluent cells with a standard RNA preparation kit (for instance RNeasy Mini Kit, Qiagen GmbH, Hilden, Germany) according to the manufacturer’s instructions, resuspended in nuclease-free water, and

quantified spectrophotometrically (Ultraspec 2000, Amersham Pharmacia, Uppsala, Sweden) at 260 nm (25).

2. Total RNA samples (*see* **Note 7**) can be stored for long term at -80°C for subsequent use in microarray experiments or RTq-PCR assays.

3.6 Whole-Transcriptome Microarray Assessment

1. Biological and/or technical triplicate aliquots of total RNA per treatment condition are forwarded to a commercial supplier for use in probing a high-precision, whole-transcript microarray (Affymetrix, Santa Clara, CA, USA). The entire experimental pipeline from sense target labeling to hybridization, washing, array scanning, and final raw data capture is hereby performed as part of a comprehensive solution leaning on standard protocols, reagents, and instrumentation.
2. Returned raw data are inspected for quality, background-adjusted, quantile-normalized, and statistically analyzed. To this purpose, normalized log₂ intensity values are rank-ordered; fold changes in gene expression calculated; *p*-values—a statistical measure of consistency between paired groups—determined using Student's *t*-test; and differentially expressed genes functionally clustered into biological categories. For this latter purpose, the freely available bioinformatics resource DAVID version 6.7 can, e.g., be applied to thoroughly annotate candidates according to their involvement in diverse cellular processes, pathways, or components by controlled vocabulary GO (gene ontology) assignment (26, 27).

3.7 Confirmatory Quantitative Real-Time PCR

1. RTq-PCR analysis permits identification of induction or repression of differentially regulated genes as relative fold changes in transcript levels. To this end, RefSeq accession IDs of candidate genes are subjected to Batch Entrez (<http://www.ncbi.nlm.nih.gov/sites/batchentrez>) for exposing mRNA sequences. These are forwarded to the WIBR UTR extractor (<http://jura.wi.mit.edu/bioc/tools/utrs>) that excerpts coding regions and pasted into the Primer 3 program (<http://frodo.wi.mit.edu/primer>) to automatically design oligonucleotides (*see* **Note 8**).
2. Meanwhile, total human RNA preparations obtained from primary keratinocytes are digested with DNase I (Deoxyribonuclease kit, Sigma-Aldrich, Taufkirchen, Germany) at room temperature for 20 min. 1.5 μg pure RNA is reverse transcribed into cDNA utilizing an iScriptTM cDNA synthesis kit (BioRad Laboratories, Hercules, CA, USA) according to the supplier's instructions.
3. Resultant cDNA serves as template for subsequent RTq-PCR in plate (array) format using a GoTaq[®] qPCR Master Mix

(Promega Corporation, Madison, WI, USA) and a CFX96™ apparatus (BioRad). All reactions are carried out in a final volume of 25 μ l.

4. Each run profiles the expression of differentially expressed genes in relation to seven unregulated housekeeping transcripts (B2M, HPRT1, RPL13A, GAPDH, ACTB, ANXA1, TUBB). These internal references are important for data normalization, determination of experimental variance, and optimal fold change cutoff estimation (28–30). Also, two built-in intron-specific probes for KRT14 intron 1 and BEST1 intron 2 are used for assessing any contamination with genomic DNA.
5. Product quality is checked by post-PCR melting curve analysis. Fold inductions are calculated according to a mathematical model described by Pfaffl et al. (31) using the formula $2^{-(\Delta\Delta Ct)}$ (where $\Delta\Delta Ct$ is $\Delta Ct_{\text{calcitriol}}$ minus $\Delta Ct_{\text{ethanol}}$, ΔCt designates Ct_{sample} minus $Ct_{\text{housekeeping-pool}}$, and Ct denotes the cycle at which the threshold is crossed).

4 Notes

1. Foreskin samples should, according to our experience, be processed fairly promptly owing to a steady time-dependent reduction of yield and recovery (i.e., poor attachment of cells).
2. Contrary to classical feeder-dependent methodologies as formerly established by Rheinwald and Green (32), we here rather follow a more recent policy (33) using an optimized defined, serum-free formulation to which we principally add neither antibiotics nor antimycotics. Culturing primary keratinocytes herein has the benefit of rapidly removing possibly contaminating cells such as fibroblasts as they do not readily proliferate under respective growth conditions. Importantly, the medium contains only a low (sub-physiological, 0.09 mM) CaCl_2 concentration in order to prevent keratinocyte differentiation. Nevertheless, primary keratinocytes cultivated under described conditions appear more susceptible to (extreme) fluctuations of temperature, pH, and mechanical forces and only undergo a restricted number of passages.
3. Listed cell numbers per well, recovery periods, and induction/equilibration times that altogether may affect metabolic activity and hence tetrazolium dye reduction are the result of our in-house performed optimization procedure for primary keratinocytes, immortalized HaCaT keratinocytes, as well as HepRG hepatocytes (M. Reitsamer, personal communication). Experiments are always performed in technical triplicates each to account for experimental variance. Applying seven different

compound concentrations plus a mock (solvent) control per substance, four different molecules can hence be straightforwardly analyzed per single 96-well microtiter plate.

4. As internal assay controls, we as per definition apply a glucose concentration gradient with apparently no effect on cell viability as well as a Triclosan (prepared as 860 mM stock) and Carbaryl (580 mM stock; both dissolved in DMSO) dilution series—two decidedly cytotoxic agents selected from literature with reproducible EC_{50} values in the middle μ M range. Since excessive DMSO per se has detrimental effects on cell viability, we recommend to prepare 100 \times concentrated stock solutions per individual dose (meaning that transfer of 1 μ l thereof to the 100 μ l culture volume results in the desired compound concentration). Regarding the concentration range of completely novel compounds under study, we usually apply a two-step strategy, analyzing first of all a relatively wide-ranging concentration interval and then refining the definite area of interest.
5. A more precise yet fairly laborious, cost-intensive strategy to in-depth assess cytotoxicity of a compound on molecular level would be to subject cDNA prepared from compound-treated keratinocytes to RTq arrays focusing on different pathways activated in response to toxic drugs. Our primer panel in-house assembled from a literature selection contains gene families involved in apoptosis, necrosis, DNA damage, oxidative stress response, metabolism, etc. Respective setups have not been explicitly applied to calcitriol but for instance used to study potential gene expression differences of therapeutic antibody-treated keratinocytes (in MTT predetermined concentrations) that might eventually be responsible for some of the known adverse side effects.
6. A general rule states to seed cells at 50 % density and start induction when 80 % have been reached. In our experience, this strategy does not always yield reproducible results (M. Reitsamer, personal communication). We therefore rather seed exactly 600,000 cells per small (25 cm²) flask as determined in a Neubauer improved hemocytometer. This guarantees that primary keratinocytes are still in exponential phase at the end of stimulation.
7. RNA preparations are appraised as being suitable for downstream assays only if samples are of sufficient yield (typically in the 100–300 ng/ μ l range), exhibit integer bands corresponding to the 18S and 28S ribosomal RNA subunits as determined by agarose gel electrophoresis in formaldehyde-supplemented 1 \times MOPS running buffer, and simultaneously display no spurious peaks or RNA degradation artifacts on a UV absorption spectrum.

8. This bioinformatics-assisted primer design workflow prevents having to meticulously search coding sequence of assumed targets on a manual one-by-one basis and thereby speeds up downstream research. Also, this fully automated device guarantees high success rate because primers with similar properties (uniform GC content/melting temperature, optimal length, comparable amplicon size) are depicted. By the way, we purchase forward and reverse primer stocks (100 pmol/ μ l) in 96-well format from life technologiesTM, Karlsruhe, Germany. This arrangement offers the advantage that primer mixes can be easily transferred with either plastic pin replicators or a manual pipetting device. Any pipetting errors are hereby minimized.

References

1. Cianferotti L, Cox M, Skorija K, Demay MB (2007) Vitamin D receptor is essential for normal keratinocyte stem cell function. *Proc Natl Acad Sci U S A* 104:9428–9433
2. Svendsen ML, Daneels G, Geysen J, Binderup L, Kragballe K (1997) Proliferation and differentiation of cultured human keratinocytes is modulated by 1,25(OH)2D3 and synthetic vitamin D3 analogues in a cell density-, calcium- and serum-dependent manner. *Pharmacol Toxicol* 80:49–56
3. McLane JA, Katz M, Abdelkader N (1990) Effect of 1,25-dihydroxyvitamin D3 on human keratinocytes grown under different culture conditions. *In Vitro Cell Dev Biol* 26:379–387
4. Bikle DD, Ng D, Oda Y, Hanley K, Feingold K et al (2002) The vitamin D response element of the involucrin gene mediates its regulation by 1,25-dihydroxyvitamin D3. *J Invest Dermatol* 119:1109–1113
5. Lehmann B, Meurer M (2003) Extrarenal sites of calcitriol synthesis: the particular role of the skin. *Recent Results Cancer Res* 164:135–145
6. Reichrath J (2001) Will analogs of 1,25-dihydroxyvitamin D(3) (calcitriol) open a new era in cancer therapy? *Onkologie* 24:128–133
7. Bikle DD, Nemanic MK, Whitney JO, Elias PW (1986) Neonatal human foreskin keratinocytes produce 1,25-dihydroxyvitamin D3. *Biochemistry* 25:1545–1548
8. Bikle DD (2010) Vitamin D: newly discovered actions require reconsideration of physiologic requirements. *Trends Endocrinol Metab* 21:375–384
9. Su MJ, Bikle DD, Mancianti ML, Pillai S (1994) 1,25-Dihydroxyvitamin D3 potentiates the keratinocyte response to calcium. *J Biol Chem* 269:14723–14729
10. Xie Z, Komuves L, Yu QC, Elalieh H, Ng DC et al (2002) Lack of the vitamin D receptor is associated with reduced epidermal differentiation and hair follicle growth. *J Invest Dermatol* 118:11–16
11. Lutzow-Holm C, Heyden A, Huitfeldt HS, Brandtzaeg P, Clausen OP (1995) Topical application of calcitriol alters expression of filaggrin but not keratin K1 in mouse epidermis. *Arch Dermatol Res* 287:480–487
12. Oda Y, Uchida Y, Moradian S, Crumrine D, Elias PM et al (2009) Vitamin D receptor and coactivators SRC2 and 3 regulate epidermis-specific sphingolipid production and permeability barrier formation. *J Invest Dermatol* 129:1367–1378
13. Diker-Cohen T, Koren R, Liberman UA, Ravid A (2003) Vitamin D protects keratinocytes from apoptosis induced by osmotic shock, oxidative stress, and tumor necrosis factor. *Ann N Y Acad Sci* 1010:350–353
14. Lee J, Youn JI (1998) The photoprotective effect of 1,25-dihydroxyvitamin D3 on ultraviolet light B-induced damage in keratinocyte and its mechanism of action. *J Dermatol Sci* 18:11–18
15. Wang TT, Nestel FP, Bourdeau V, Nagai Y, Wang Q et al (2004) Cutting edge: 1, 25-dihydroxyvitamin D3 is a direct inducer of antimicrobial peptide gene expression. *J Immunol* 173:2909–2912
16. Schaubert J, Dorschner RA, Coda AB, Buchau AS, Liu PT et al (2007) Injury enhances TLR2 function and antimicrobial peptide expression through a vitamin D-dependent mechanism. *J Clin Invest* 117:803–811
17. Mayr LM, Bojanic D (2009) Novel trends in high-throughput screening. *Curr Opin Pharmacol* 9:580–588

18. Stein MS, Wark JD (2003) An update on the therapeutic potential of vitamin D analogues. *Expert Opin Investig Drugs* 12:825–840
19. Brown AJ (2001) Therapeutic uses of vitamin D analogues. *Am J Kidney Dis* 38:S3–S19
20. Berridge MV, Herst PM, Tan AS (2005) Tetrazolium dyes as tools in cell biology: new insights into their cellular reduction. *Biotechnol Annu Rev* 11:127–152
21. Mosmann T (1983) Rapid colorimetric assay for cellular growth and survival: application to proliferation and cytotoxicity assays. *J Immunol Methods* 65:55–63
22. Rid R, Wagner M, Maier CJ, Hundtberger H, Hintner H et al (2013) Deciphering the calcitriol-induced transcriptomic response in keratinocytes: presentation of novel target genes. *J Mol Endocrinol* 50:131–149
23. Trost A, Desch P, Wally V, Haim M, Maier RH et al (2010) Aberrant heterodimerization of keratin 16 with keratin 6A in HaCaT keratinocytes results in diminished cellular migration. *Mech Ageing Dev* 131:346–353
24. Aasen T, Izpisua Belmonte JC (2010) Isolation and cultivation of human keratinocytes from skin or plucked hair for the generation of induced pluripotent stem cells. *Nat Protoc* 5:371–382
25. Oender K, Trost A, Lanschuetzer C, Laimer M, Emberger M et al (2008) Cytokeratin-related loss of cellular integrity is not a major driving force of human intrinsic skin aging. *Mech Ageing Dev* 129:563–571
26. da Huang W, Sherman BT, Lempicki RA (2009) Systematic and integrative analysis of large gene lists using DAVID bioinformatics resources. *Nat Protoc* 4:44–57
27. Sherman BT, da Huang W, Tan Q, Guo Y, Bour S et al (2007) DAVID knowledgebase: a gene-centered database integrating heterogeneous gene annotation resources to facilitate high-throughput gene functional analysis. *BMC Bioinforma* 8:426
28. Dallas PB, Gottardo NG, Firth MJ, Beesley AH, Hoffmann K et al (2005) Gene expression levels assessed by oligonucleotide microarray analysis and quantitative real-time RT-PCR—how well do they correlate? *BMC Genomics* 6:59
29. Provenzano M, Mocellin S (2007) Complementary techniques: validation of gene expression data by quantitative real time PCR. *Adv Exp Med Biol* 593:66–73
30. Walker NJ (2001) Real-time and quantitative PCR: applications to mechanism-based toxicology. *J Biochem Mol Toxicol* 15:121–127
31. Pfaffl MW (2001) A new mathematical model for relative quantification in real-time RT-PCR. *Nucleic Acids Res* 29:e45
32. Rheinwald JG, Green H (1975) Serial cultivation of strains of human epidermal keratinocytes: the formation of keratinizing colonies from single cells. *Cell* 6:331–343
33. Tenchini ML, Ranzati C, Malcovati M (1992) Culture techniques for human keratinocytes. *Burns* 18(Suppl 1):S11–S16

Preparation of Primary Cultures of Mouse Epidermal Keratinocytes and the Measurement of Phospholipase D Activity

Lakiea J. Bailey, Vivek Choudhary, Purnima Merai, and Wendy B. Bollag

Abstract

In this chapter information is provided about the outer layer of the skin, the epidermis, and the predominant cells comprising this epithelium, the keratinocytes. The evidence supporting a possible role for the lipid-metabolizing enzyme phospholipase D in regulating keratinocyte differentiation is also discussed. A detailed protocol for the preparation of primary cultures of epidermal keratinocytes from neonatal mice is described, to allow other investigators to obtain data concerning these important cells involved in forming and maintaining the mechanical and water permeability of the skin. Finally, a complete protocol for monitoring phospholipase D activity in intact cells is supplied in the hope that additional research will result in a better understanding of the role of phospholipase D in controlling keratinocyte proliferation and differentiation.

Keywords: Epidermis, Keratinocytes, Mouse, Phosphatidic acid, Phosphatidylalcohol, Phospholipase D, Skin

1 Introduction

1.1 The Epidermis

The body's largest organ, and arguably one of the most important, is the skin. It functions as the foremost barrier against ultraviolet radiation, trauma, and infection and is essential for existence (1). Skin is composed of the epidermal, dermal, and subcutaneous layers. The innermost layer, the subcutis (or subcutaneous fat layer), upon which the epidermis and dermis rest, is composed primarily of adipose and connective tissue. The middle layer, the dermis, is a complex structure comprised of the papillary dermis and the reticular dermis, the primary function of which is to support and maintain the epidermis (1). The epidermis, a stratified squamous epithelium consisting primarily of keratinocytes, holds the distinction of performing the most important function of skin—providing the essential physical and water permeability barrier. This barrier is established and maintained by a careful balance between keratinocyte proliferation and differentiation (2), resulting in a multilayered structure composed of the *stratum*

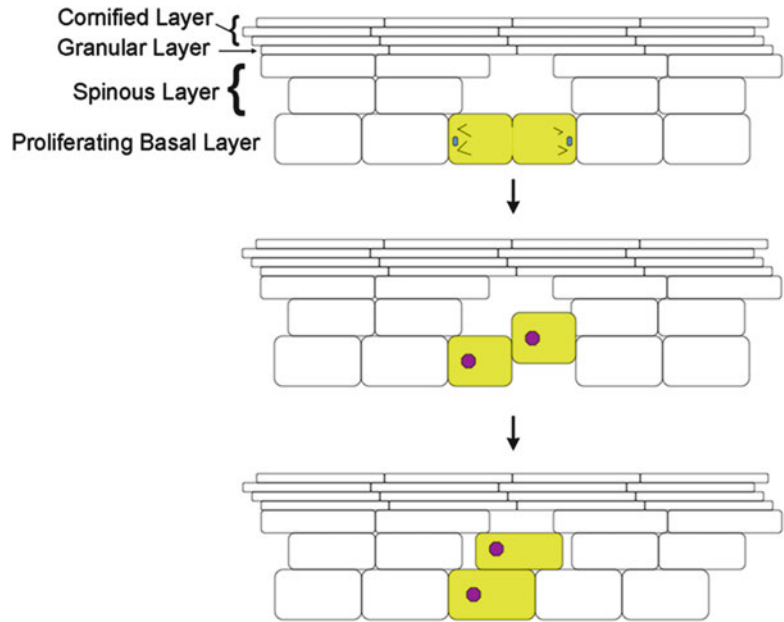


Fig. 1 The epidermis. Shown is a schematic of the epidermis, with the deepest basal layer dividing continuously, as illustrated in the serial panels, to replace cells lost to the environment. One daughter cell remains in the basal layer to continue proliferating while the other moves up into the spinous layer and begins the differentiation process. Differentiation continues in the granular layer, where keratinocytes undergo a programmed cell death to form the cornified layer, from which the cells are eventually sloughed to the surroundings

germinativum or *basale* (basal layer), *stratum spinosum* (spinous layer), *stratum granulosum* (granular layer), and *stratum corneum* (cornified layer).

The deepest layer of the epidermis is the basal layer adjacent to the basement membrane and is composed primarily of epidermal keratinocytes. This single layer of cells possesses the ability to proliferate and continuously replenish the keratinocytes of the epidermis. The early stages of keratinocyte differentiation occur in the layer immediately above this, the spinous layer. The cells in this layer no longer proliferate, exhibiting growth arrest and early markers of differentiation; as the cells migrate up through this layer, they continue to differentiate outward through the granular layer of late stage differentiation and terminating in the outer cornified layer of the epidermis. Keratinocytes within this outermost cornified layer have terminally differentiated and enucleated (3). This distinctly defined multilayered skin is present at birth and is in a constant state of dynamic flux as the keratinocytes proliferate and differentiate outward from the basement membrane to the most superficial layer of squames (Fig. 1). Several human skin diseases, including psoriasis, a common hyperproliferative disorder of the epidermis, and the non-melanoma skin cancers (basal and squamous

cell carcinoma), are characterized by excessive growth and aberrant differentiation of epidermal keratinocytes resulting from dysregulation of this carefully controlled pathway (4). The National Psoriasis Foundation and the American Academy of Dermatology report that approximately 7.5 million Americans and as much as 3 % of the total world population live with psoriasis (5, 6). The American Academy of Dermatology also lists basal and squamous cell carcinomas as the two most common cancers in the world with more than 2 million new diagnoses each year in the United States alone (5). The ultimate goal to decrease human suffering must be first prefaced by a better understanding of the molecular processes regulating keratinocyte proliferation and differentiation under physiological and pathological conditions.

Model systems used for the study of epidermal keratinocytes include, among others, various keratinocyte cell lines, normal human keratinocytes and primary cultures of mouse keratinocytes, as well as three-dimensional culture systems utilizing these cells. Our laboratory has used the primary mouse keratinocyte culture system extensively, accumulating a wealth of data to document and characterize its value. This system offers some advantages over cell lines or human keratinocyte cultures, including high proliferative potential (7), differentiative capacity versus cell lines (which often do not differentiate entirely normally (8–10)), enhanced sensitivity to differentiating agents versus human cultures (11–13), and most importantly, the extension to studies of keratinocytes from transgenic animals and/or in vivo experimentation on an appropriate mouse model (14–18). Nevertheless, we routinely confirm important results in normal human keratinocytes and/or reconstituted human epidermis (e.g., (19, 20)), to verify the translational value of our results. Below we describe the protocol for isolating keratinocytes from neonatal mouse skin or the tail skin of adult mice.

1.2 Phospholipase D1 and Phospholipase D2 in Keratinocyte Differentiation

1.2.1 Phospholipase D

Although the precise mechanisms regulating the induction and regulation of keratinocyte differentiation remain unknown, our laboratory has proposed the idea that phospholipase D isoforms may play an important role in this process. PLD belongs to a superfamily of phospholipases defined by the amino acid motif HXX(X)₄D. This lipolytic enzyme catalyzes the hydrolysis of phospholipids, in particular phosphatidylcholine, to generate lipid molecules that are reported to be involved in keratinocyte signaling (reviewed in (21, 22)). In the presence of water, PLD hydrolyzes phosphatidylcholine to phosphatidic acid (PA) and choline. Lipid phosphate phosphatases, located on the outer surface of the plasma membrane or the luminal surface of internal membranes (23), dephosphorylate PA to yield diacylglycerol (DAG) (24). Thus, the enzymatic action of PLD provides a second mechanism, in addition to phospholipase C, to generate DAG, which can then induce the activation of protein kinase C isoforms involved in

epidermal keratinocyte function (reviewed in (21, 25)). In several systems PLD underlies a portion of sustained DAG production, although DAG generated in this way may differ from phospholipase C-derived DAG due to its different origin (phosphatidylcholine rather than phosphatidylinositol 4,5-bisphosphate or PIP₂) (26), and these separate mechanisms for DAG generation may, in fact, result in activation of different protein kinase C isoforms (reviewed in (21, 25)). In the presence of a primary alcohol PLD also functions to catalyze a transphosphatidylation reaction to generate phosphatidylalcohols. Our laboratory has demonstrated an ability of PLD (in particular PLD2; see below) to use the physiological alcohol glycerol to generate phosphatidylglycerol *in vitro* (27) and has proposed a potential signaling pathway involving PLD2, the water and glycerol channel aquaporin-3, and the lipid messenger phosphatidylglycerol (reviewed in (28)).

To date, two mammalian isoforms of PLD have been identified (PLD1 and PLD2), both of which require phosphatidylcholine as a substrate and PIP₂ as a cofactor. These isoforms share about 50 % amino acid similarity, with the main structural differences occurring at the N- and C-termini, leading to differential expression and activation (29). PLD1 associates primarily with intercellular membranes and is thought to play a role in secretory pathways (30–32). PLD2, on the other hand, localizes at the plasma membrane and is involved with cytoskeletal rearrangements and membrane ruffling (30–32). These isoforms also show somewhat different mechanisms of activation, with PLD1 activated by the small GTPases, RhoA and ADP-ribosylating factor (ARF), and protein kinase C, whereas PLD2 shows constitutive activity, at least under *in vitro* conditions (reviewed in (33, 34)). However, in intact cells PLD2 appears to also be regulated by ARF and protein kinase C (35–39) as well as other interacting proteins (reviewed in (40, 41)).

1.2.2 Phospholipase D in Keratinocytes

Both PLD1 and PLD2 are expressed in keratinocytes (42, 43), and a correlation has been uncovered between sustained PLD activation and the induction of keratinocyte differentiation (44). PLD1 is highly conserved across species (92 % identity, 97 % similarity) and is upregulated in response to 1,25-dihydroxyvitamin D₃ (42). This enhanced PLD1 expression was found to precede the 1,25-dihydroxyvitamin D₃-mediated increase in transglutaminase activity, but not the inhibition of DNA synthesis or induction of the expression of keratin 1 (a marker of early differentiation), suggesting a role for PLD1 in late keratinocyte differentiation (42). Subsequently, the PLD1 promoter was found to possess a vitamin D response element mediating its expression in response to 1,25-dihydroxyvitamin D₃ in the HaCaT human keratinocyte cell line (45). PLD2 has also been linked to keratinocyte differentiation. Bollag and colleagues found that PLD is activated to generate phosphatidylglycerol in response to elevated calcium

concentration-induced stimulation of keratinocyte differentiation (27). This process may be facilitated by the colocalization in membrane microdomains of PLD2 and the water/glycerol channel, aquaporin-3 (27), which is thought to deliver glycerol to PLD2 for use in the transphosphatidylation reaction to generate phosphatidylglycerol (reviewed in (28)). Subsequent studies have shown that manipulation of this PLD2/aquaporin-3 signaling module promotes keratinocyte differentiation (46). Because of the likely role of PLD isoforms in regulating keratinocyte differentiation, it is important to be able to measure the activity of this enzyme in keratinocytes, and we describe appropriate protocols below.

2 Materials

2.1 *Materials for Mouse Keratinocyte Preparation*

Laminar-flow hood or biosafety cabinet to maintain sterility of procedure
 Tissue culture incubator (37 °C with 5 % CO₂)
 Refrigerator and freezer
 Centrifuge
 100 mL beakers (2)
 Dissecting scissors
 Dissecting forceps (2)
 Hemocytometer and cover glass
 100 mm untreated plastic Petri dishes (e.g., Fisherbrand catalog #0875713)
 Ethanol (100 %) diluted to 70 % with distilled water, at 4 °C
 Sterile tissue culture disposable plasticware including 15 and 50 mL conical tubes, 10 mL pipets, filters (0.2 μm), microfuge tubes, storage bottles, tissue culture-treated 6-well plates (e.g., Fisher Scientific catalog 07-200-83) or dishes, etc.
 Hank's buffered saline solution (e.g., Fisher Scientific catalog #MT21021CV)
 Penicillin-streptomycin-antimycotic solution (e.g., Gibco catalog #15240)
 Trypsin (10× or 2.5 %) (e.g., Gibco catalog #15090-046)
 RPMI-1640 containing glutamine and HEPES (e.g., Fisher Scientific catalog #22400-105)
 Fetal bovine serum
 Calcium-free MEMα (Biologos, Inc. catalog #L1028J3)
 Glutamine (100×, Gibco catalog #35050)
 Dialyzed fetal bovine serum (Atlanta Biologicals catalog # S12650)

Insulin-transferrin-selenium with linoleic acid (ITS+; BD Biosciences catalog #354352)
 Epidermal growth factor (EGF; Invitrogen catalog #53003-018; solubilized in deionized water at a concentration of 50 µg/mL EGF)
 CaCl₂ solution (1 M in tissue culture-quality water; filter sterilized)
 Bovine serum albumin (BSA; e.g., Gemini Bio-Products catalog #700-108P; solubilized in MEM α containing 1 % PSA) and bovine pituitary extract (BPE; Invitrogen catalog #13028-014)
 OR serum-free medium (Invitrogen catalog #3701022; the supplements supplied, EGF and BPE, as well as 1 % PSA and 50 µM CaCl₂, should be added as per the manufacturer's instructions)

**2.2 Materials
 for Phospholipase
 D Activity Assay**

Chemical fume hood
 Laminar-flow hood or biosafety cabinet
 Oven (110 °C for heat activation of thin-layer chromatography plates)
 Film developer
 [³H]Oleic acid (Perkin Elmer catalog #NET289001MC) or [¹⁴C] glycerol (Perkin Elmer catalog #NEC441X050UC)
 Ethanol (100 %) or 1-butanol
 SDS
 EDTA
 Chloroform
 Methanol
 Glacial acetic acid
 Ethyl acetate
 Isooctane
 Borosilicate glass test tubes (16 × 100 mm)
 Pasteur pipets and bulbs
 Parafilm
 Glass pipets (25 mL) and graduated cylinders
 Nitrogen manifold for evaporation of organic solvents (e.g., the Evap-O-Rac system, catalog #RZ-01610-35, from Cole Parmer or the evaporation manifold, catalog #VP176, from V&P Scientific)
 20 × 20 cm aluminum-backed, silica gel 60-coated TLC plates with concentrating zone (Merck Millipore, catalog #105582)
 Thin-layer chromatographic tanks (2, for example from Kimble Chase Kontes, catalog # 416180-0000)

Kimble microcapillary pipettes (e.g., 10 μ L, Fisher Scientific, catalog #13-678-18A)

Phosphatidic acid (e.g., Avanti Polar Lipids catalog #840101)

Phosphatidylethanol (e.g., Avanti Polar Lipids catalog #840513) or phosphatidylbutanol (e.g., Avanti Polar Lipids catalog #860203C) or phosphatidylglycerol (e.g., Avanti Polar Lipids catalog #841138)

Iodine crystals (e.g., Sigma catalog #207772)

En³Hance spray (Perkin Elmer catalog # 6NE970C)

Kodak X-OMAT AR X-ray film (VWR catalog #IB1651496)

Film developer

3 Methods

3.1 Primary Mouse Keratinocyte Preparation

We have used the following protocol to prepare primary cultures of mouse keratinocytes from both wild-type outbred neonatal mice and transgenic newborn animals. (Please note that all steps should be performed in a tissue culture hood using aseptic technique.)

3.1.1 Day 1 of the Protocol

1. One- to three-day-old neonatal mice are placed in a 100 mm untreated Petri dish, with a maximum of five per dish, on ice for 5–15 min to precool the skin (in order to maintain keratinocyte viability). At this age the poorly insulated hairless pups are quickly rendered hypothermic and enter a state of torpor. The neonatal mice are then quickly euthanized by decapitation with a sharp dissecting scissors; however, *see* **Note 1**. Also note that data indicate that newborn mice subjected to brief periods of hypothermia exhibit no apparent cognitive impairment in adulthood (47).
2. The decapitated pups are washed with cold 70 % ethanol to kill microorganisms and the Petri dish containing the pups returned to the ice.
3. Two 100 mL beakers are half-filled with 70 % ethanol for skin harvest: one is for sterilizing the forceps and scissors and the other is for rinsing the skin prior to placing the tissue in the trypsin solution (see below).
4. Trypsin (2.5 % or 10 \times) is diluted in Hank's buffered saline solution (HBSS) [1 mL of 10 \times trypsin per 9 mL of HBSS containing 1 % penicillin-streptomycin-antimycotic solution]. This solution (10 mL) is added to each Petri dish (maximum 5 skins/plate).
5. One pup is taken from the dish using sterilized forceps and the legs and tail are removed with scissors; the pup is placed belly

side down on the Petri dish and the skin cut dorsally from the tail to the head. Using two forceps the skin is peeled from each side and the belly of the pup.

6. Using forceps the skin is dipped in the beaker containing 70 % ethanol. As much ethanol as possible is removed by gently shaking or squeezing the skin. The skin is then floated on the HBSS solution with the outer, epidermal side exposed to the air. It should be noted that the dermal side has a darker red color and appears shinier than the epidermis.
7. For each pup/skin the above steps #5 and 6 are repeated, allowing the decapitated neonatal mice to remain on ice until harvest of the skin.
8. The floating skins are incubated overnight in the refrigerator to allow trypsin to diffuse along the dermal–epidermal junction (and *see* **Note 2**).

3.1.2 Day 2 of the Protocol

1. The Petri dish containing the skins is removed from the refrigerator and incubated at 37 °C in a CO₂ incubator for 5–30 min to allow trypsin to act (this time may vary greatly depending on the trypsin and must be determined empirically for each lot of trypsin as in step #3 below).
2. A 100 mL beaker should be half-filled with 70 % ethanol and two pairs of forceps placed into the ethanol to sterilize. The beaker and forceps are placed in the tissue culture hood.
3. In the tissue culture hood the sterilized forceps are used to attempt to separate the epidermis and dermis. The epidermis and dermis should peel apart with reasonable ease; if not, the Petri dish and skins should be returned to the CO₂ incubator for another few minutes and tested again. The exact time of incubation must be determined empirically for each new lot of trypsin.
4. “Air Medium” (10 mL) is added to an untreated Petri dish. Air Medium is composed of 500 mL RPMI-1640 containing glutamine and HEPES, 55 mL fetal bovine serum, and 5.5 mL 100× penicillin-streptomycin-antimycotic; the medium should be filtered and stored at 4 °C.
5. Each skin should be transferred from the HBSS containing trypsin to the Petri dish containing Air Medium, taking care to maintain the proper orientation and layout.
6. The dermis is separated from the epidermis using the forceps, by peeling and reflecting the top epidermal layer as if opening a book. Ideally, the epidermis will remain slightly attached to the dermis to allow easy orientation. The underside of the epidermis should be gently scraped with one forceps while the epidermis is held with the other forceps. The epidermis should not be

scraped excessively as the objective is to release the basal keratinocytes at the dermal–epidermal junction but not the differentiating suprabasal cells in the upper layers. After scraping, the epidermis should be “wrung out” with a twisting motion to express excess cells and liquid. These steps (#5 and 6) should be repeated for all skins.

7. Once all the skins have been separated and basal keratinocytes scraped into the Air Medium, a 10 mL pipet is used to transfer the medium containing the cells into a clean sterile (labeled) 50 mL conical tube. Only 10 mL pipets should be used for transferring and aspirating the cells, as this size better disrupts the cell clumps that may form, particularly following centrifugation.
8. Using a clean 10 mL pipet, the Petri dish is rinsed with an additional 10 mL of Air Medium and this wash is transferred to the conical tube as well (for a total volume of 20 mL of Air Medium containing cells).
9. The conical tube is centrifuged in a refrigerated centrifuge (at 4 °C) for 5 min at approximately $225 \times g$.
10. The conical tube is removed from the centrifuge, and the supernatant aspirated with a clean Pasteur pipet.
11. With a clean 10 mL pipet, 10 mL of Air Medium is added and repeatedly aspirated and expelled to gently resuspend the cell pellet. An additional 10 mL of Air Medium is added to yield a total volume of 20 mL and steps #9 and 10 repeated.
12. After centrifugation and aspiration of the supernatant, 10 mL of Plating Medium is added with a clean 10 mL pipet, and the cell pellet is gently resuspended. Plating Medium is composed of: 1 L calcium-free MEM α , 10 mL 100 \times penicillin-streptomycin-antimycotic (PSA), 10 mL 100 \times glutamine, 20 mL dialyzed fetal bovine serum (dialyzed to remove free calcium), 10 mL insulin-transferrin-selenium with linoleic acid (ITS+), 5 ng/mL (final concentration) epidermal growth factor (100 μ L of 50 μ g/mL EGF), and 25 μ M final concentration calcium (25 μ L of 1 M CaCl₂); the medium is filtered and stored at 4 °C.
13. With a clean 10 mL pipet, an additional 10 mL of Plating Medium is added and the conical tube centrifuged again for 5 min at approximately $225 \times g$. This procedure is repeated and the cells resuspended in Plating Medium to yield a total volume of 20 mL; the cell suspension should be mixed well.
14. To a sterile 1.5 mL Eppendorf tube (*see Note 3*) are added 190 μ L of Plating Medium and 10 μ L of the well-mixed suspension of keratinocytes.

15. The cell suspension is again mixed well and a small aliquot of the cell suspension transferred to a clean hemocytometer in order to count the cells.
16. The keratinocytes are counted, making sure to count only those cells that are perfectly round and demonstrate a high degree of contrast under a phase-contrast microscope. (After counting, the hemocytometer is washed and stored.)
17. Remembering to account for the dilution factor, the cells are plated at a density of 25,000 cells/cm², with rapid distribution of the cells to prevent settling of the cells and an inhomogeneous cell suspension. It should be noted that the counting procedure may need to be adjusted empirically to ensure adequate numbers of cells at the desired confluence. In other words, it must be determined by each individual who prepares the keratinocytes which cells should be counted as viable cells that will plate efficiently.
18. After the cells are plated, they should be distributed evenly throughout the plate by rotating the plates (the cells should not be swirled as the cells will become concentrated in the center) and the plates placed in the CO₂ incubator overnight. (The hood is cleaned with 70 % ethanol.)
19. The next day the medium should be aspirated and replaced with an appropriate growth medium. One such medium is serum-free keratinocyte medium (SFKM). SFKM is composed of:
 - 1,120 mL calcium-free MEM α containing 11.2 mL 100 \times PSA, 11.2 mL 100 \times glutamine, 11.2 mL 50 mg/mL BSA in MEM α with 1 % PSA, 11.2 mL 100 \times ITS+, 25 μ M calcium (28 μ L 1 M CaCl₂), 112 μ L 50 μ g/mL EGF, and 100 mg bovine pituitary extract (BPE). However, we have found that serum-free medium (SFM) from Gibco (the supplements supplied, EGF and BPE, as well as 1 % PSA and 50 μ M CaCl₂, should be added as per the manufacturer's instructions) also supports excellent growth and have recently switched to this medium for the sake of convenience and consistency. The medium should be replaced every other day until the desired cell confluence is achieved.

3.2 Primary Keratinocyte Preparation from the Tail of an Adult Mouse

We have also successfully isolated and cultured keratinocytes from the tail skin of adult mice, an important extension to adult animals and in particular epidermal-specific conditional knockout mouse models.

3.2.1 Day 1 of the Protocol

1. The mouse should first be sacrificed using an appropriate euthanasia method. For tail skin removal, a circular cut should be made using a pair of dissecting scissors at the base of the tail

using minimal pressure so that only the skin is affected (and not underlying tissues). The dorsal side of the tail is then slit downward from the first cut. This second cut should be 1–2 cm long. The skin along the excision is then detached from the underlying tissues with forceps. This skin flap is then held tightly and pulled down to detach the entire skin from the underlying tail structure. The harvested skin should be placed on ice, in a 15 mL conical tube, until processing in a tissue culture hood.

2. In the tissue culture hood the tail skin should be rinsed thoroughly in a 100 mL beaker half-filled with cold 70 % ethanol to sterilize.
3. The tail skin should be cut into four or five smaller pieces using scissors and placed in a Petri dish floating on a trypsin solution (10 mL) prepared from 2.5 % trypsin as described above in the instructions for preparing keratinocytes from neonatal mouse skin. Again, care must be taken to ensure that the inner dermal layer contacts the solution and that the skin is spread to maximize contact with the trypsin solution.
4. The floating tail skins are incubated overnight in the refrigerator to allow trypsin to diffuse along the dermal–epidermal junction; however, *see Note 4*.

3.2.2 Day 2 of the Protocol

1. The Petri dish containing the tail skins is removed from the refrigerator and incubated at 37 °C in a CO₂ incubator for 5–10 min to allow trypsin to act (again, this time may vary greatly depending on the trypsin and should be determined empirically).
2. In the tissue culture hood, and as mentioned in the instructions for preparing keratinocytes from the newborn mouse skin, an attempt should be made to separate the epidermis from the dermal layer using sterilized forceps. The two layers should peel apart with reasonable ease; if not, then the Petri dish with skins should be returned to the incubator for another few minutes and tested again. The exact time of incubation must be determined empirically for each lot of trypsin.
3. Once it is confirmed that the dermis and epidermis are separating with relative ease, the tail skin is transferred to a Petri dish (untreated) containing “Air Medium” (10 mL).
4. The steps (#6 through 19) described above for the preparation of keratinocytes from neonatal mouse skin should then be followed to separate, collect, plate (in Plating Medium), and culture the basal epidermal keratinocytes obtained from the tail skin. On average, one adult tail skin yields a sufficient number of keratinocytes to plate two or three 35 mm dishes (or wells of a 6-well plate). The medium should be replaced after 24 h and

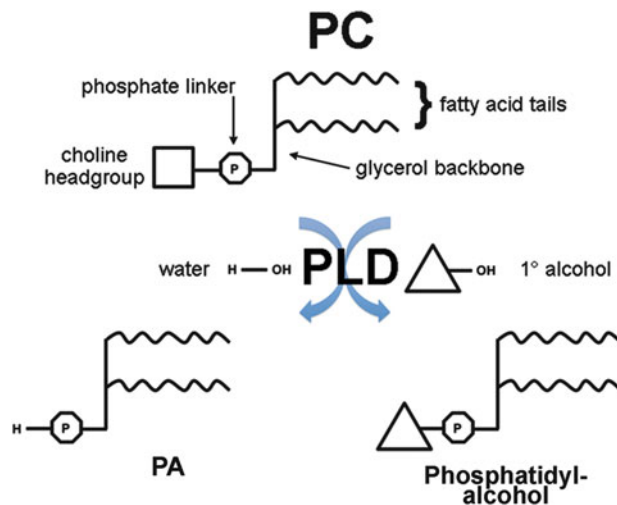


Fig. 2 A schematic showing the reactions catalyzed by phospholipase D. Phosphatidylcholine (PC) is hydrolyzed by phospholipase D (PLD), in the presence of water, to generate phosphatidic acid (PA). However, in the presence of a primary alcohol, such as ethanol, 1-butanol, or glycerol, PLD can catalyze a transphosphatidylation reaction to produce a phosphatidylalcohol as illustrated

every other day with SFKM or SFM until the desired confluence is achieved. It should be noted that these adult keratinocytes will grow more slowly than the keratinocytes isolated from newborn skin.

3.3 Phospholipase D Activity Assay

The activity of PLD results in the production of several molecules, including phosphatidic acid (PA) and choline. However, both of these products can also arise through other metabolic pathways, making it difficult to distinguish whether PLD has been activated. On the other hand, the generation of phosphatidylalcohols by PLD in the presence of a primary alcohol is characteristic of PLD activity and can be used to monitor PLD activity (reviewed in (22, 48)), as schematically illustrated in Fig. 2. Below a protocol for measuring PLD activity is described; it should be noted that the first step should be performed in a tissue culture hood using aseptic technique to prevent microbial contamination of the cultures. Additional tips on using this procedure can be found in reference (48).

3.3.1 Experimental Procedure and Extraction of Phospholipids

1. Near-confluent keratinocytes (~75 % confluent) are incubated for 20–24 h in serum-free medium containing 5 $\mu\text{Ci}/\text{mL}$ [^3H] oleic acid.
2. The medium is aspirated and replaced with medium containing the agents of interest as well as a primary alcohol, such as 0.5 % (by volume) ethanol or 0.3 % (by volume) 1-butanol. The cells are then incubated in a CO_2 incubator at 37 °C for the desired time period (our default time is 30 min).

3. At the end of the treatment period, the medium is aspirated; reactions are terminated and cells solubilized using 0.2 % SDS containing 5 mM EDTA (to complex divalent cations and promote the partitioning of PA into the organic solvent). At this point an aliquot of the SDS lysate can be saved for measurement of protein amounts and normalization of sample values. Cells in SDS are transferred to a clean glass test tube containing ice-cold chloroform, methanol, and glacial acetic acid. The ratio of the solvents should be 4 parts aqueous SDS solution to 5 parts chloroform to 10 parts methanol to 0.4 parts acetic acid (added to promote protonation of PA and thus partitioning of the acidic phospholipid into the organic solvent). For a 35 mm plate or one well of a 6-well plate, we use 0.4 mL SDS containing 5 mM EDTA, 0.5 mL chloroform, 1.0 mL methanol, and 40 μ L acetic acid. At this ratio the solvents should form a single phase with vortexing. (Alternatively, reactions can be terminated using ice-cold methanol and cells scraped from the plate. If methanol is used to terminate the reactions, this methanol replaces the methanol in the tube and instead 5 mM EDTA in deionized water should be added such that the final ratio of aqueous solution/chloroform/methanol/glacial acetic acid should always be 4:5:10:0.4 volume:volume:volume:volume; however, *see Note 5*).
4. After incubation of the single-phase mixture on ice for approximately 60–120 min to allow extraction of phospholipids into the organic solvent, another 5 parts of chloroform (0.5 mL for a 35 mm dish) are added, with vortexing, followed by the addition of 5 parts (0.5 mL) of 0.2 M NaCl and vortexing.
5. At this point the solvents should separate into two phases. The test tubes can be briefly centrifuged to accelerate separation of the phases, although centrifugation is not strictly necessary.
6. The lower chloroform layer containing phospholipids should be collected and transferred to a clean test tube. Care should be taken to ensure that the entire chloroform layer is collected with minimal contamination by the aqueous layer. Our laboratory uses Pasteur pipets and silicone (rather than rubber) Pasteur pipet bulbs, the greater stiffness of which allows greater control of fluid transfer.
7. The organic solvent is then evaporated in a chemical fume hood using an inert gas, such as nitrogen or argon, connected to a manifold to allow evaporation of multiple samples. Our glass manifold was custom manufactured but commercial versions are also available. Samples should remain on ice during the evaporation time to minimize lipid oxidation and/or breakdown.

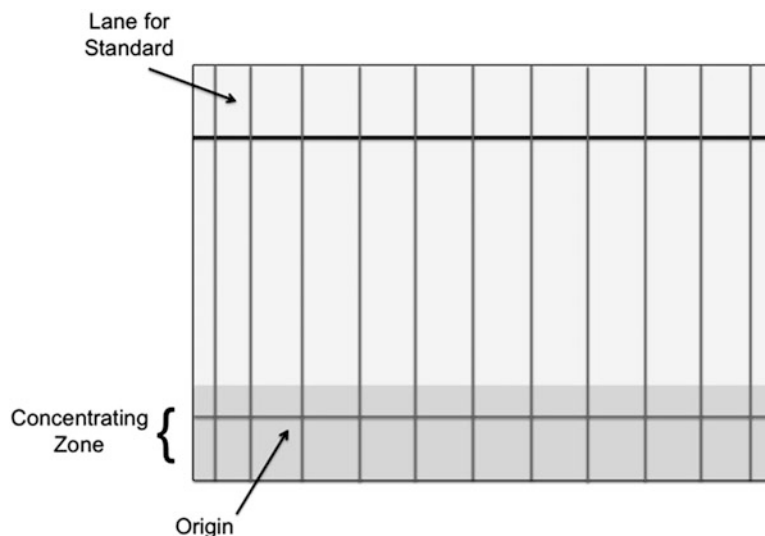


Fig. 3 A thin-layer chromatography plate. A schematic of a TLC plate shows the lanes and origin, which are marked in pencil, and the *scratched line* at the *top* of the plate to prevent continued mobile phase migration. Each lane, other than that for the standard (which is 1 cm wide), is 2 cm wide, the *scratched top line* is 2 cm from the *top* of the plate and the origin is approximately 1.3 cm from the *bottom* of the plate, within the concentrating zone. Alternatively, 12 lanes of 1.5 cm width (along with a 1 cm wide lane for standards) can be marked. In all cases lanes are marked beginning 0.5 mm from the edge of the plate

8. Once the solvent is completely evaporated, the test tubes can be sealed with Parafilm (while still exposed to the inert gas) and stored for up to 3 days at -20°C . Alternatively, they can be separated immediately by thin-layer chromatography (TLC) as described below.
9. All items that contact the samples should be disposed of as radioactive waste or marked as a radioactive hazard.

3.3.2 Thin-Layer Chromatography (TLC) Separation of Lipids

Please note that steps should be performed in a chemical fume hood to minimize exposure of personnel to organic solvents.

1. Prior to thin-layer chromatographic separation of lipids, the TLC plate must first be prepared. Our laboratory uses 20×20 cm aluminum-backed, silica gel 60-coated TLC plates with concentrating zone obtained from Merck Millipore. Lanes (1.5 or 2 cm wide) are marked in pencil as shown in Fig. 3, starting at least 0.5 cm from the edge of the plate (the ends of the plate often do not separate correctly due to aberrant mobile phase migration at these edges). One or more lanes (which can be less than 1.5 cm in width) should be included for separation of authentic standards. A line should also be drawn in pencil approximately 1.3 cm from the bottom of the plate (within the

concentrating zone) to mark the origin. Approximately 2 cm from the top of the plate, a line should be scratched in the silica gel to mark the distance traveled by the mobile phase (see below) and prevent lipids from migrating off the top of the plate. Prior to spotting, the TLC plates must also first be pre-activated by heating to 110 °C for 30 min (to drive off any moisture absorbed by the hygroscopic silica). The plates should be used immediately after pre-activation or stored briefly in a desiccating chamber to maintain activation.

2. Also prior to spotting, the thin-layer chromatographic tank should be readied. The mobile phase for one tank is prepared by combining 104 mL ethyl acetate, 16 mL isooctane, 24 mL glacial acetic acid, and 80 mL deionized water (that is, in a 13:2:3:10 volume:volume:volume:volume ratio) in a glass bottle with a lid. The bottle should be shaken to mix all ingredients; the solution will form two phases (with the aqueous phase on the bottom). After the upper phase has had sufficient time to equilibrate with the water in the lower phase, the upper organic phase only (approximately 100 mL) should be transferred to the TLC chamber using a glass pipet. Use of too great a volume of the mobile phase can result in immediate elution and loss of the lipid samples upon placement of the plate in the TLC chamber; too little volume will lead to poor separation of the sample lipids.
3. For TLC separation of lipids, the samples are then resuspended in a small volume (e.g., 50 μ L) of chloroform/methanol (2:1 volume:volume) containing 20–25 μ g each of phosphatidic acid (PA) and phosphatidylethanol (PEt) standards (which can be obtained from Avanti Polar Lipids). The unlabeled phospholipids are included for proper separation of the labeled lipids; PA and PEt species containing unsaturated fatty acids (e.g., oleic acid) should be used to facilitate visualization using iodine vapor (see below). The samples are then “spotted” at the origin using microcapillary pipets (we use 10 μ L volume microcapillary pipettes) onto the pre-activated TLC plate within a marked lane. Care should be taken to ensure minimal “spreading” of the lipid spot to ensure proper separation of the phospholipids, although use of a concentrating zone assists in minimizing this possibility by concentrating the sample at the junction between the concentrating zone and the separating region of the plate upon migration. In our laboratory we spot two to three samples at a time, a portion at a time, to allow one sample to dry as the second and/or third is spotted. It should be noted that because of variation between the background counts on different TLC plates, each plate should be spotted with appropriate control samples such that treatment groups separated on multiple plates can be compared to a control group from that same plate.

4. Once the entire sample is spotted, the tubes are rinsed with an additional small volume (e.g., 20 μL) of chloroform/methanol (2:1), and this rinse is also spotted onto the TLC plate as above. Authentic PA and PEt standards are also spotted separately, so that the radiolabeled lipids can be identified.
5. Upon spotting of all samples, the TLC plate is placed in the prepared TLC chamber and the mobile phase allowed to migrate until it reaches the line marked at the top of the plate (approximately two to two-and-a-half hours). The TLC plates are then removed and allowed to dry in a chemical fume hood.
6. After the mobile phase has evaporated, the standards and PA and PEt added to the samples can be visualized by exposure of the plates to iodine vapor for approximately 15 min. Iodine stains organic compounds a yellowish brown color; however, the presence of double bonds in a lipid standard enhances staining so that smaller amounts of the lipid can be used. An iodine vapor chamber is created by placing iodine crystals in the bottom of a second (dry) TLC chamber. To prevent contact of the iodine crystals with the TLC plate, the plate should be physically supported above the crystals (we generally place test tubes in the bottom of the chamber). It should be noted that excessive exposure to iodine is a health hazard and this chamber should be set up in a chemical fume hood to minimize exposure.
7. The plate is removed from the iodine chamber and the yellowish brown spots representing the standards and samples are marked lightly in pencil. The iodine is then allowed to evaporate from the plate in the chemical fume hood.
8. To visualize the radioactive PA and PEt spots, plates are then sprayed with En^3Hance , a nonradioactive liquid scintillation fluid in the form of an aerosol spray (and available from Perkin Elmer), and exposed to X-ray film at $-80\text{ }^\circ\text{C}$ for several days. It should be noted that iodine quenches light development by liquid scintillation fluid, so exposure of the plate to iodine should be minimized to prevent excessive staining and allow rapid evaporation and subsequent visualization of the radiolabeled lipids.
9. After the film is developed, and the En^3Hance allowed to evaporate in the fume hood, the radiolabeled spots are marked with pencil using the film (and the previous marked standards) as a guide.
10. The marked PA and PEt spots are then cut from the plate (the aluminum backing is rather easily cut with sharp scissors) and placed in scintillation vials containing scintillation fluid (we use EcoLite from MP Biomedicals, catalog #01882475). The portions of the plate containing the spots should be cut so that the

pieces lie flat in the vial to minimize interference with liquid scintillation spectrometry. In addition, the procedure should be performed over a sheet of weigh paper so that any silica gel that flakes from the aluminum backing can be collected and added to the scintillation vial. All waste should be disposed of as radioactive.

11. The samples are counted and the stimulated values for PA and PEt are expressed relative to the control values.

3.4 Measurement of Phosphatidylglycerol Production

PLD can utilize the physiological primary alcohol, glycerol, in the transphosphatidylation reaction *in vitro* to produce phosphatidylglycerol (PG). Thus, in experiments with PLD2 in the presence of glycerol, phosphatidylglycerol was produced at the expense of PA (or of PEt in the presence of ethanol) (27). In intact keratinocytes radiolabeled PG was also generated from [¹⁴C]glycerol, and [¹⁴C] PG levels were increased when cells were stimulated to differentiate with a moderately elevated extracellular calcium concentration (27). The involvement of PLD in the production of this PG was implied by the ability of ethanol (which competes with glycerol in the transphosphatidylation reaction) to inhibit stimulated PG production but not basal PG levels (27). The ability of PLD to form PG is consistent with the colocalization of PLD2 and the glycerol channel, aquaporin-3 (49). Whether or not other aquaglyceroporins are also functionally associated with a PLD isoform is unknown, but aquaporin-3 is expressed in many epithelia (50), as well as other cell types (e.g., macrophages (51) and other tissues (52)), where it could also presumably interact with PLD2 and generate PG. The production of radiolabeled PG can be measured using a similar protocol to that used for monitoring PLD activity, as described below.

3.4.1 Experimental Procedure and Lipid Extraction

1. Near-confluent keratinocytes (~75 % confluent) are incubated in serum-free medium with the desired agents for the designated time period.
2. [¹⁴C]Glycerol is added to a final concentration of 0.5–1 μCi/mL and the cells incubated for an additional 15–30 min. The medium is then aspirated and the reactions are terminated and cells solubilized using 0.2 % SDS.
3. SDS aqueous lysates are placed in test tubes containing 5 parts chloroform and 10 parts methanol, and the phospholipids are extracted as described above (starting from step #4 of the first part of the protocol above).

3.4.2 Thin-Layer Chromatographic Separation

1. Phospholipids are separated by TLC, also as described above, except that no unlabeled PG is added to the samples and a PG standard, rather than PA and PEt standards, is used.

2. Standards are visualized with iodine vapor and En³Hance, and the PG spot (identified by comigration with the authentic standard) is cut from the plate and quantified by liquid scintillation spectrometry as described above. The stimulated value for PG is expressed relative to the appropriate control value.

3.5 Summary

Keratinocytes are the predominant cells comprising the outer layer of the skin, the epidermis, and are critical for the epidermis to perform its key function as a mechanical and water permeability barrier. Although much is known concerning the processes regulating keratinocyte proliferation and differentiation to form this functional barrier, additional information about these processes under physiological and pathophysiological conditions is required. For this purpose, *in vitro* cultures of mouse keratinocytes, prepared as described above, can be used to investigate the mechanisms underlying keratinocyte growth and maturation. One signaling pathway regulating keratinocyte differentiation appears to be phospholipase D, which metabolizes phosphatidylcholine to yield lipid second messengers, such as phosphatidic acid (which can be dephosphorylated to produce diacylglycerol) and phosphatidylglycerol. Additional data about these lipid signals are needed to delineate the role of phospholipase D in modulating keratinocyte and epidermal function and can be acquired in part using the PLD activity assays and radiolabeled PG production protocols described above.

4 Notes

1. As an alternative to induction of hypothermia on ice and decapitation, anesthesia may be induced by placing the pups in Petri dishes submerged in ice for 2 h. Note that if pups are not decapitated, the yield of keratinocytes is somewhat increased, since the skin of the head of decapitated animals cannot be harvested and represents a relatively large proportion of the skin surface in mice of this age. However, some Institutional Animal Care and Use Committees are uncomfortable with the use of hypothermia to induce anesthesia. Nevertheless, the use of injectable anesthesia is difficult due to the small size of the animals. Since the entire animal is usually placed in a chamber for anesthesia with inhaled anesthetics, these agents are also not appropriate for anesthesia as they may affect the exposed keratinocytes. Using this method of anesthesia, following 2 h on ice the mice in the Petri dish are washed with cold 70 % ethanol and the dish returned to the ice. One pup is then removed from the dish using sterilized forceps and the toe pinched to ensure a proper plane of anesthesia (the pup should not react). The legs and tail are quickly removed with scissors; the pup is placed belly side down on the Petri dish and the skin

cut dorsally from the tail to the head. Using two forceps the skin is peeled from each side of the pup and pulled up over the head (as if removing a sweater) and the animal immediately decapitated. This process is repeated for each pup, allowing the animals to remain on ice until harvesting of the skin.

2. Animal waste should be disposed of appropriately and beakers, scissors, and forceps cleaned with detergent. The instruments are washed thoroughly with water (with a final rinse in distilled or deionized water), wiped dry, and stored.
3. Although most tissue-culture plasticware can be purchased pre-sterilized, microfuge tubes can be sterilized by autoclaving in a closable autoclave-resistant container.
4. As an alternative to incubation overnight, the skin can be placed on sterilized (autoclaved) blotting paper with the dermis contacting the paper, and then the paper with the skin is set in a dish containing trypsin solution. The skin can then be incubated at 37° C for an hour before proceeding with the steps described for Day 2 of the protocol.
5. It should be noted that most plastics are not compatible with organic solvents like chloroform. Indeed, if methanol is used to terminate reactions followed by cell scraping, the plastic plate will demonstrate some damage. However, we have found that for this particular assay, the plastic tips for Gilson Pipetman and repeater pipettes can be used to dispense the organic solvents. It should also be noted that organic solvents should be drawn into the pipet tip and expelled once or twice to allow equilibration of the head space before attempting to transfer the desired volume of solvent, in order to minimize premature expulsion of the solvent and inaccurate volume transfer.

Acknowledgements

W.B.B. is supported by VA Merit Award #CX000590 and a VA Research Career Scientist Award. The contents of this article do not represent the views of the Department of Veterans Affairs or the United States Government.

References

1. Amirlak B, Shahabi L, Javaheri S, Talavera F, Stadelmann WK et al (2011) Skin anatomy. In: Caputy G (ed). www.emedicinemedscapecom/article/1294744-overview
2. Goldsmith L (1991) Physiology, biochemistry and molecular biology of the skin. Oxford University Press, New York
3. Bikle DD, Pillai S (1993) Vitamin D, calcium, and epidermal differentiation. *Endocr Rev* 14:3–19
4. Yuspa S (1998) The pathogenesis of squamous cell cancer: lessons learned from studies of skin carcinogenesis. *J Dermatol Sci* 17:1–7

5. American Academy of Dermatology (2011) *Dermatology A to Z: stats and facts*. American Academy of Dermatology, San Diego, CA. <http://www.aad.org/dermatology-a-to-z>
6. National Psoriasis Foundation (2011) What is known about psoriasis: statistics. <http://www.psoriasis.org/research/science-of-psoriasis/statistics>
7. Bollag WB, Ducote J, Harmon CS (1993) Effects of the selective protein kinase C inhibitor, Ro 31-7549, on the proliferation of cultured mouse epidermal keratinocytes. *J Invest Dermatol* 100:240–246
8. Weissman BE, Aaronson SA (1983) BALB and Kirsten murine sarcoma viruses alter growth and differentiation of EGF-dependent BALB/c mouse epidermal keratinocyte lines. *Cell* 32:599–606
9. Brysk MM, Miller J, Walker GK (1984) Characteristics of a human epidermal squamous carcinoma cell line at different extracellular calcium concentrations. *Exp Cell Res* 150:329–337
10. Boukamp P, Petrussevska RT, Breitkreutz D, Hornung J, Markham A et al (1988) Normal keratinization in a spontaneously immortalized aneuploid human keratinocyte cell line. *J Cell Biol* 106:761–771
11. Bollag WB, Ducote J, Harmon CS (1995) Biphasic effect of 1,25-dihydroxyvitamin D₃ on primary mouse epidermal keratinocyte proliferation. *J Cell Physiol* 163:248–256
12. McLane JA, Katz M, Abdelkader N (1990) Effect of 1,25-dihydroxyvitamin D₃ on human keratinocytes grown under different culture conditions. *In Vitro Cell Dev Biol* 26:379–387
13. Bikle DD, Gee E, Pillai S (1993) Regulation of keratinocyte growth, differentiation, and vitamin D metabolism by analogs of 1,25-dihydroxyvitamin D. *J Invest Dermatol* 101:713–718
14. Strickland JE, Dlugosz AA, Hennings H, Yuspa SH (1993) Inhibition of tumor formation from grafted papilloma cells by treatment of grafts with staurosporine, an inducer of squamous differentiation. *Carcinogenesis* 14:205–209
15. Inohara S, Tateishi H, Takeda Y, Tanaka Y, Sagami S (1988) Effects of protein kinase C activators on mouse skin in vivo. *Arch Dermatol Res* 280:182–184
16. Wojcik SM, Bundman DS, Roop DR (2000) Delayed wound healing in keratin 6a knockout mice. *Mol Cell Biol* 20:5248–5255
17. Mehling A, Loser K, Varga G, Metze D, Luger TA et al (2001) Overexpression of CD40 ligand in murine epidermis results in chronic skin inflammation and systemic autoimmunity. *J Exp Med* 194:615–628
18. Hanakawa Y, Matsuyoshi N, Stanley JR (2002) Expression of desmoglein 1 compensates for genetic loss of desmoglein 3 in keratinocyte adhesion. *J Invest Dermatol* 119:27–31
19. Sougrat R, Morand M, Gondran C, Barre P, Gobin R et al (2002) Functional expression of AQP3 in human skin epidermis and reconstructed epidermis. *J Invest Dermatol* 118:678–685
20. Gherzi R, Sparatore B, Patrone M, Scitutto A, Briata P (1992) Protein kinase C mRNA levels and activity in reconstituted normal human epidermis: relationships to cell differentiation. *Biochem Biophys Res Commun* 184:283–291
21. Bollag WB, Bollag RJ (2001) 1,25-Dihydroxyvitamin D₃, phospholipase D and protein kinase C in keratinocyte differentiation. *Mol Cell Endocrinol* 177:173–182
22. Bollag WB, Zheng X (2005) The role of phospholipase D and keratinocyte biology. In: Robinson JW (ed) *Trends in protein research*. Nova Science Publishers, Inc., New York, pp 79–118
23. Brindley DN, Pilquil C (2009) Lipid phosphate phosphatases and signaling. *J Lipid Res* 50:S225–S230
24. Waggoner DW, Xu J, Singh I, Jasinska R, Zhang Q-X et al (1999) Structural organization of mammalian lipid phosphate phosphatases: implications for signal transduction. *Biochim Biophys Acta* 1439:299–316
25. Bollag WB (2009) Protein kinase Calpha puts the hand cuffs on epidermal keratinocyte proliferation. *J Invest Dermatol* 129:2330–2332
26. Nishizuka Y (1995) Protein kinase C and lipid signaling for sustained cellular responses. *FASEB J* 9:484–496
27. Zheng X, Ray S, Bollag W (2003) Modulation of phospholipase D-mediated phosphatidylglycerol formation by differentiating agents in primary mouse epidermal keratinocytes. *Biochim Biophys Acta* 1643:25–36
28. Qin H, Zheng X, Zhong X, Shetty AK, Elias PM et al (2011) Aquaporin-3 in keratinocytes and skin: Its role and interaction with phospholipase D2. *Arch Biochem Biophys* 508:138–143
29. Gomez-Cambronero J (2011) The exquisite regulation of PLD2 by a wealth of interacting proteins: S6K, Grb2, Sos, WASp and Rac2 (and a surprise discovery: PLD2 is a GEF). *Cell Signal* 23:1885–1895
30. Vitale N, Caumont AS, Chasserot-Gola S, Du G, Wu S, Sciorra VA et al (2001) Phospholipase D1: a key factor for the exocytotic machinery in neuroendocrine cells. *EMBO J* 20:2424–2434

31. Colley W, Sung TC, Roll R, Jenco J, Hammond SM et al (1997) Phospholipase D2, a PLD1-related isoform with novel regulatory properties and discrete subcellular localization that provokes cytoskeletal reorganization. *Curr Opin Cell Biol* 7:191–201
32. Freyberg Z, Sweeney D, Siddhanta A, Bourgoin S, Frohman M et al (2001) Intracellular localization of phospholipase D1 in mammalian cells. *Mol Biol Cell* 12:943–955
33. Su W, Chen Q, Frohman MA (2009) Targeting phospholipase D with small-molecule inhibitors as a potential therapeutic approach for cancer metastasis. *Future Oncol* 5:1477–1486
34. Peng X, Frohman MA (2012) Mammalian phospholipase D physiological and pathological roles. *Acta Physiol (Oxf)* 204:219–226
35. Lopez I, Arnold RS, Lambeth JD (1998) Cloning and initial characterization of a human phospholipase D2 (hPLD2). ADP-ribosylation factor regulates hPLD2. *J Biol Chem* 273:12846–12852
36. Rizzo MA, Shome K, Vasudevan C, Stolz DB, Sung T-C et al (1999) Phospholipase D and its product, phosphatidic acid, mediate agonist-dependent Raf-1 translocation to the plasma membrane and the activation of the mitogen-activated protein kinase pathway. *J Biol Chem* 274:1131–1139
37. Siddiqi AR, Srajer GE, Leslie CC (2000) Regulation of human PLD1 and PLD2 by calcium and protein kinase C. *Biochim Biophys Acta* 1497:103–114
38. Han JM, Kim JH, Lee BD, Lee SD, Kim Y et al (2002) Phosphorylation-dependent regulation of phospholipase D2 by protein kinase C delta in rat pheochromocytoma PC12. *J Biol Chem* 277:8290–8297
39. Park S-K, Provost JJ, Bae CD, Ho W-T, Exton JH (1997) Cloning and characterization of phospholipase D from rat brain. *J Biol Chem* 272:29263–29271
40. Gomez-Cambronero J (2011) The exquisite regulation of PLD2 by a wealth of interacting proteins: S6K, Grb2, Sos, WASp and Rac2 (and a surprise discovery: PLD2 is a GEF). *Cell Signal* 23:1885–1895
41. Frohman MA, Morris AJ (1996) Phospholipid signalling: Rho is only ARF the story. *Curr Biol* 6:945–947
42. Griner RD, Qin F, Jung E, Sue-Ling CK, Crawford KB et al (1999) 1,25-dihydroxyvitamin D3 induces phospholipase D-1 expression in primary mouse epidermal keratinocytes. *J Biol Chem* 274:4663–4670
43. Muller-Wieprecht V, Riebeling C, Alexander C, Scholz F-R, Hoer A et al (1998) Expression and regulation of phospholipase D in the human keratinocyte cell line HaCaT. *FEBS Lett* 425:199–203
44. Jung E, Betancourt-Calle S, Mann-Blakeney R, Griner RD, Bollag W (1999) Sustained phospholipase D activation is associated with keratinocyte differentiation. *Carcinogenesis* 20:569–576
45. Kikuchi R, Sobue S, Murakami M, Ito H, Kimura A et al (2007) Mechanism of vitamin D3-induced transcription of phospholipase D1 in HaCat human keratinocytes. *FEBS Lett* 581:1800–1804
46. Bollag WB, Xie D, Zheng X, Zhong X (2007) A potential role for the phospholipase D2-Aquaporin-3 signaling module in early keratinocyte differentiation: Production of a phosphatidylglycerol signaling lipid. *J Invest Dermatol* 127:2823–2831
47. Janus C, Golde T (2014) The effect of brief neonatal cryoanesthesia on physical development and adult cognitive function in mice. *Behav Brain Res* 259:253–260
48. Bollag WB (1998) Measurement of phospholipase D activity. *Methods Mol Biol* 105:151–160
49. Zheng X, Bollag WB (2003) Aquaporin 3 colocalizes with phospholipase D2 in caveolin-rich membrane microdomains and is regulated by keratinocyte differentiation. *J Invest Dermatol* 121:1487–1495
50. Matsuzaki T, Suzuki T, Koyama H, Tanaka S, Takata K (1999) Water channel protein AQP3 is present in epithelia exposed to the environment of possible water loss. *J Histochem Cytochem* 47:1275–1286
51. Zhu N, Feng X, He C, Gao H, Yang L et al (2011) Defective macrophage function in aquaporin-3 deficiency. *FASEB J* 25:4233–4239
52. Mobasheri A, Wray S, Marples D (2005) Distribution of AQP2 and AQP3 water channels in human tissue microarrays. *J Mol Histol* 36:1–14

Lipid Rafts and Detergent-Resistant Membranes in Epithelial Keratinocytes

Kathleen P. McGuinn and Mý G. Mahoney

Abstract

Our understanding of the plasma membrane has markedly increased since Singer and Nicolson proposed the fluid mosaic model in 1972. While their revolutionary theory of the lipid bilayer remains largely valid, it is now known that lipids and proteins are not randomly dispersed throughout the plasma membrane but instead may be organized within membrane microdomains, commonly referred to as lipid rafts. Lipid rafts are highly dynamic, detergent resistant, and enriched with both cholesterol and glycosphingolipids. The two main types are flotillin-rich planar lipid rafts and caveolin-rich caveolae. It is proposed that flotillin and caveolin proteins regulate cell communication by compartmentalizing and interacting with signal transduction proteins within their respective lipid microdomains. Consequently, membrane rafts play an important role in vital cellular functions including migration, invasion, and signaling; thus, alterations in their microenvironment can initiate signaling pathways that affect cellular function and behavior. Therefore, the identification of lipid rafts and their associated proteins is integral to the study of transmembrane signaling. Here, we review the current standard protocols and biochemical approaches used to isolate and define raft proteins from epithelial cells and tissues. Furthermore, in Section 3 of this chapter, detailed protocols are offered for isolating lipid rafts by subjection to detergent and sucrose density centrifugation, as well as an approach for selectively isolating caveolae. Methods to manipulate rafts with treatments such as methyl- β -cyclodextrin and flotillin III are also described.

Keywords: Lipid raft, Detergent resistant, Membrane microdomain, Caveolae, Caveolin, Methyl- β -cyclodextrin

1 Introduction

In 1972, the fluid mosaic model of the cell membrane was proposed by Singer and Nicolson (1). They hypothesized that lipid and protein molecules are randomly distributed throughout the lipid bilayer; four decades later, a more dynamic model has evolved, revealing organized membrane microdomains, referred to as lipid rafts (2, 3). Lipid rafts contain a high concentration of both cholesterol and glycosphingolipids and are able to float freely within the plasma membrane, thus permitting aggregation and formation of larger, more stable platform domains (4). In addition, protein–protein and lipid–protein interactions, especially by those involving cytoskeletal proteins, increase the stability and regulatory functions of

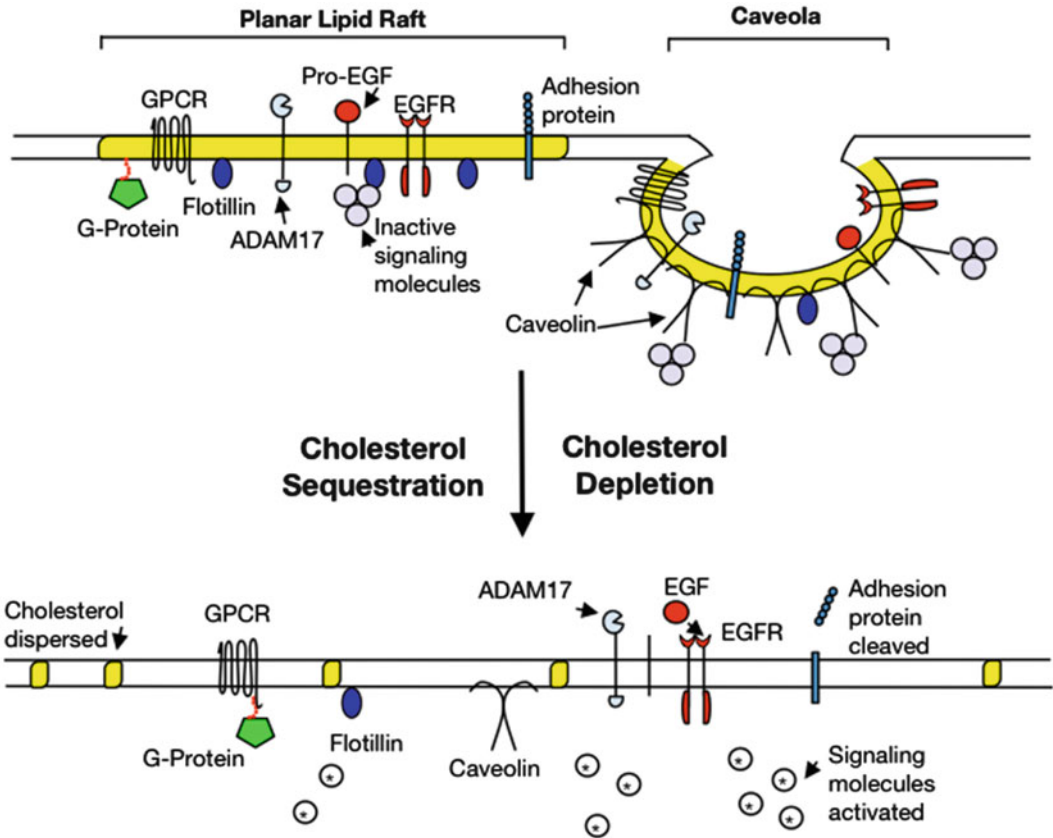


Fig. 1 Planar and caveolae lipid rafts within the plasma membrane. *Yellow*-highlighted regions represent areas of high concentration of cholesterol and sphingolipids. Caveolin proteins, essential to caveolae formation, and flotillin proteins are able to bind and compartmentalize signaling molecules and regulate their activity. Lipid raft disruption by treatment with M β CD, filipin III, or shear stress results in dispersion of cholesterol molecules and leveling of caveolae. Subsequently, several signaling molecules are activated potentiating signal transduction events. Abbreviations: *M β CD* methyl- β -cyclodextrin, *GPCR* G-protein-coupled receptor, *ADAM17* a disintegrin and metalloprotease domain 17 or TACE, *Pro-EGF* pro-epidermal growth factor, *EGFR* epidermal growth factor receptor

membrane rafts (5). There are two types of lipid rafts, planar and caveolae (Fig. 1). Caveolae are distinguishable as flask-shaped invaginations (50–100 nm) of the membrane formed by the integral membrane scaffolding protein, caveolin. In the absence of caveolins, planar lipid rafts are sustained by the integral membrane protein flotillin. Lipid rafts are emerging as key players in many biological functions including protein trafficking, endocytosis, neurotransmission, and cell communication by serving as organization centers for signaling molecules (6, 7).

Discerning the roles of lipid rafts and their constitutive proteins has proven to be a challenging task and is not without controversy with regards to both methods and results. An attractive approach for tackling this endeavor has been to investigate the effects of

disrupting lipid rafts with methyl- β -cyclodextrin (M β CD), a cyclic oligosaccharide that forms soluble complexes with cholesterol and depletes them from the membrane. In keratinocytes, raft disruption results in upregulation of many signal transduction proteins such as IL8, MMPs, EGFR, ERK, Akt, p38 MAPK, and ERK1/2 (8–11). Interestingly, an increase in substrates cleaved by tumor necrosis factor-alpha (TNF- α) converting enzyme (ADAM17 or TACE) occurs with M β CD treatment, leading investigators to postulate that lipid rafts also regulate enzymatic activity by limiting substrate entry into rafts (12). Furthermore, lipid raft disruption by ultraviolet (UV) irradiation results in a decrease in raft cholesterol levels and activation of pro-apoptotic pathways by Fas-receptor protein and ceramide (13). Treatment with sterols, which lessen cholesterol loss, partly decreased this response (14). In summary, results from these studies suggest that lipid rafts are integral to homeostatic cell-to-cell interactions and that their alteration leads to activation of pathways, which affect vital cellular processes.

A point of fact, alterations in lipid rafts have been found to have pathological implications. For instance, an inverse relationship between caveolin expression and severity of the skin disease, psoriasis has been reported (15). Similarly, atopic dermatitis, an inflammatory skin disease, has changes in gene expression that are comparable to those resulting from lipid raft disruption in keratinocytes (9). In cancer, caveolin-1 has been found to have a dual role. Studies in keratinocytes showed that caveolins suppress growth factor signaling pathways (16). This finding is supported by findings in *Cav1* null mice, which lack caveolae, that showed increased epidermal proliferation and susceptibility to premalignant lesions in response to the chemical carcinogen DMBA/TPA (17). Conversely, in anchorage-independent cancer cells, such as melanoma, caveolin expression is associated with increased malignancy and metastasis (18, 19). It is postulated that the association of lipid raft proteins, such as caveolins, with cytoskeletal proteins and their role in cell adhesion processes may partially explain the mechanism for malignant invasion (20). Lipid rafts have been shown to be associated with a number of adhesion junction proteins (Table 1); however, more studies are needed to determine the implications of such interactions. Indeed, the Mahoney lab recently discovered that caveolin-1 associates with desmoglein-2, a desmosomal adhesion protein that modulates mitogenic signaling suspected to be involved in oncogenesis (21).

To date, most of our knowledge of lipid rafts is a result of the hypothesis that the high glycolipoprotein content of the lipid raft renders it insoluble in nonionic detergents; hence, lipid rafts are also known as detergent-resistant membrane domains (22). The method of lipid raft isolation by detergent is controversial in that results may differ depending on the conditions, including temperature, detergent concentration, and type of detergent utilized (23).

Table 1
Adhesion proteins and lipid rafts

Protein	Junction type	Lipid raft association	Reference
Nectin-1	Adherens	No	(45)
Cadherin 13	Adherens	Yes	(46)
Afadin	Adherens	Minimal	(45)
Filamin	Adherens	Yes	(6)
Eplin	Adherens	TBD	
Alpha-catenin	Adherens	Yes	(47)
Beta-catenin	Adherens	Yes	(37, 48, 49)
Plekha7	Adherens	TBD	
Nezha	Adherens	TBD	
E-cadherin	Adherens	Yes	(37, 47)
Claudin 1–5	Tight	Yes	(50)
Claudin 14	Tight	Yes	(51)
Occludin	Tight	Yes	(52)
Jam-1	Tight	No	(53)
Zo-1	Tight	Yes	(54)
Connexin 43, 32, 36, 46	Gap	Yes	(40, 55)
Connexin 26, 50	Gap	No	(55)
Desmoglein 2	Desmosome	Yes	(21, 46, 56)
Desmoglein 3	Desmosome	Yes	(57)
Desmocollin 2	Desmosome	Yes	(58)
Plakoglobin	Desmosome	Yes	(46, 56)
Desmoplakin	Desmosome	Yes	(58)
Actin	Cytoskeletal	Yes	(46)
Integrin, beta 1	Focal adhesion	Yes	(46)

TBD to be determined

Major adhesion junction proteins of epithelial cells and their known association with lipid rafts are listed

Also, biochemical methods are unable to isolate lipid rafts in their innate structure (24). In fact, for some time there was uncertainty regarding the existence of lipid rafts at all, as the nanometric size of lipid rafts is below the diffraction limit of standard confocal laser scanning microscopy, and, thus, rafts were not detectable *in vivo*. Any uncertainty has been disbanded by novel techniques, such as Forster resonance energy transfer, fluorescence polarization

anisotropy, total internal reflection fluorescence microscopy, and single-molecule spectroscopy (25). These techniques have provided confirmation of the existence of cholesterol and sphingolipid microdomains. Furthermore, diffusion of cholesterol-dependent GPI-anchored proteins in the apical plasma membrane has been observed (25, 26). Although promising, these innovative methods still have their own individual challenges, which may affect the intrinsic state of the cell (25).

Similarly, biochemical techniques for lipid raft isolation and proteomic analysis are not without criticism, but they do have the advantage of being well studied. The detergent Triton X-100 (TX-100) at 4 °C is most commonly used for lipid raft purification, but other detergents have been utilized with results perhaps reflecting the nature of the raft domain isolated (27). Other detergents studied include Brij 58, Brij 96, Brij 98, Lubrol WX, CHAPS, and Triton X-114 (28). Notably, Brij 98 may be used at physiologic temperature, 37 °C, thus avoiding any effect temperature may have, as it has been suggested that lipid rafts aggregate upon treatment at 4 °C, therefore not allowing identification of proteins in distinct rafts (27). Ideally, the least amount of detergent that will dissolve the non-raft membrane proteins, such as transferrin receptor, should be used (27). The reproducible solubility of these proteins is the advantage of using TX-100. Inconsistent reports of whether Lubrol WX sufficiently dissolves non-raft membrane proteins have been published, and while Brij 96 and Brij 98 are efficient at solubilizing the non-raft membrane when compared to Lubrol WX, the detergent-resistant, light density fraction still contains non-raft proteins (28). Furthermore, Schuck et al. compared the lipid component of insoluble fractions from various detergents and found that the lipid component of TX-100 contained a lipid ratio comparable to that expected in lipid rafts. Conversely, Lubrol WX and Brij 98 contained a ratio more comparable to the total membrane, suggesting that these detergents are not as accurate in preferentially isolating lipid rafts. On the other hand, TX-100 solubilizes some lipid raft proteins including insulin receptors, which are known to interact with caveolins (29). Manipulation of lipid rafts can be performed biochemically as well. Removal of cholesterol may be achieved with M β CD, and inhibition of cholesterol synthesis may be accomplished with HMG-CoA reductase inhibitors (2). Additionally, rafts may be sequestered with antimicrobial agents such as nystatin A or filipin III (30). Cholera toxin, which targets gangliosides, can be used to stain for lipid rafts (31).

In summary, there is no single, ideal method for isolating lipid rafts, and thus, an integrated approach utilizing biochemical, imaging, and novel techniques needs to be established. As biochemical techniques for lipid raft isolation are currently the most widely used and cost-effective methodology available, this chapter focuses on and provides validated biochemical methods as well as practical notes for the isolation and analysis of lipid rafts.

2 Materials

2.1 Major Equipment

1. SW60 swing bucket rotor (Beckman Coulter, Brea, CA, USA); corresponding ultracentrifuge tubes (Cat# 326819; 5.0 mL thinwall, polyallomer tubes for SW60 rotor; Beckman Coulter).
2. SW41Ti swing bucket rotor (Cat# 333790, Beckman Coulter); corresponding ultracentrifuge tubes (Cat# 331372; 13.2 mL thinwall, polyallomer tubes for SW41 rotor; Beckman Coulter).
3. Ultracentrifuge (Beckman Coulter).

2.2 Reagents

Unless otherwise stated, most reagents are available from Sigma-Aldrich (St. Louis, MO). Dulbecco's modified Eagle's medium (DMEM), fetal bovine serum (FBS), and penicillin–streptomycin (P/S) (Life Technologies, Grand Island, NY); CnT-57 medium and supplements (CELLnTEC, Bern, Switzerland); EpiLife medium supplemented with Human Keratinocyte Growth Supplement (Life Technologies); 5-cholestene-5- β -ol (Steraloids, Newport, RI); Caveolin-1 competing peptide—a fusion of the caveolin-1 scaffolding domain peptide (aa 82-101) with the cell permeable Antennapedia sequence (aa 43-58) (Cat# 219482) and scrambled caveolin-1 negative control peptide (Cat# 219483) (Millipore, La Jolla, CA); Trypan Blue Exclusion Assay (Cat# 15250061, Life Technologies).

2.3 Buffers

1. Phosphate-buffered saline (PBS; Cat# BP665-1; Fisher Scientific, Pittsburgh, PA).
2. TNE buffer: 25 mM Tris–HCl (pH 7.5) (Cat# BP1757-500; Fisher Scientific), 150 mM NaCl, and 5 mM EDTA.
3. Complete cell lysis TNE buffer: 25 mM Tris–HCl (pH 7.5), 150 mM NaCl, 5 mM EDTA, 1 % (v/v) Triton X-100 (TX-100; Cat# BP151-500; Fisher Scientific), 1 mM phenylmethanesulfonylfluoride or phenylmethylsulfonyl fluoride (PMSF; Cat# 93482), complete protease inhibitor cocktail (Cat# 11697-498-001, Roche Diagnostics, Indianapolis, IN), and phosphatase inhibitor cocktail 2 (Cat# P8340).
4. 90, 35, or 5 % (w/v) Sucrose (Cat# 84097) in TNE buffer: Dissolve 90, 35, or 5 g of sucrose with TNE buffer to bring the volume to 100 mL. Warm with stirring until sucrose is dissolved.

2.4 Antibodies

Antibodies to lipid raft proteins include anti-caveolin-1 (Cat# sc-894; Santa Cruz Biotechnology, Santa Cruz, CA); anti-caveolin-2 (Cat# 8522; Cell Signaling Technology, Danvers, MA); anti-caveolin-2 (Cat# ab2912; Abcam, Cambridge, MA); anti-flotillin-1 (Cat# 610820; BD Transduction Labs, Franklin Lakes, NJ); and anti-flotillin-2 (Cat# 610383; BD Transduction Labs).

2.5 Cells

1. HaCaT, a spontaneously immortalized, nontumorigenic cell line derived from human keratinocytes (32, 33).
2. A431, an epidermoid carcinoma cell line (Cat# CRL-1555; ATCC, Bethesda, MD).
3. Alternatively, primary human epidermal keratinocytes can be used and are available from several commercial sources: PHEK (CELLnTEC) and HEK (Life Technologies).

3 Methods

3.1 Cell Culture

HaCaT and A431 cells are maintained in DMEM supplemented with 10 % FBS, 2 mM glutamine, and 1 % P/S (33, 34). PHEK and HEK cultures are grown in complete CnT-57 or EpiLife supplemented with human keratinocyte growth supplement, respectively. All cells are maintained in a humidified incubator with 5 % CO₂ at 37 °C. Cells are plated at a density of approximately 2×10^6 in 100 mm culture dishes to obtain approximately 9×10^6 cells at confluence. If grown in FBS-containing medium, cells are serum-starved from 1 to 24 h prior to experimentation. Cells should be approximately 70–80 % confluent when used.

3.2 Lipid Raft Disruption by Cholesterol Depletion

To disrupt lipid rafts by depleting or sequestering membrane cholesterol, cultured cells in serum-free medium are treated with M β CD (10 mM or 1 %) or filipin III (2 μ g/mL) for 1 h. Alternatively, cells can be treated with 5-cholestene-5- β -ol (5 μ M) for 2 h or simvastatin (5 mg/mL) for 24 h. Repletion is performed by adding cholesterol (5 μ M or 10 μ g/mL) or cholesterol-loaded M β CD (5 μ M or 10 μ g/mL) (35–38). Trypan blue exclusion assay can be used to measure the level of cell death after drug treatment.

3.3 Disruption of Caveolin Association by Scaffolding Domain Peptide

To displace proteins from binding to caveolin-1, treat cells with a cell-permeable caveolin-1 scaffolding domain peptide (3 μ M) for up to 24 h (16). As negative control, treat cells with a scrambled peptide (3 μ M) of the caveolin-1 scaffolding domain.

3.4 Preparation of Lipid Raft Fraction

The following ultracentrifugation method relies on two unique properties of lipid rafts: (1) cold detergent resistance and (2) low buoyant density.

1. Pre-chill all equipment and solutions on ice.
2. Wash cells three times with ice-cold PBS, and scrape cells in 2 mL complete TNE (*see Note 1*) buffer lysis buffer containing 1 % TX-100 (*see Notes 2 and 3*) using a cell scraper (Cat# 08-771-1A; Fisher Scientific) (21, 39).
3. Disrupt cell by passing through a tight-fitting glass Dounce Homogenizer (Cat# NC0253759; Fisher Scientific) 20 times

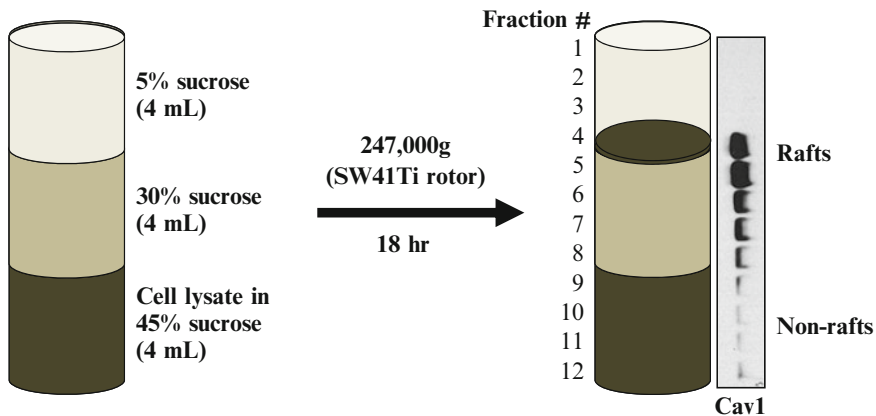


Fig. 2 Schematic diagram showing isolation of lipid rafts by discontinuous sucrose gradient centrifugation. Cell lysate is prepared in a lysis buffer containing 45 % sucrose and transferred to an ultracentrifuge tube. Two, 4 mL each, of 30 and 5 % sucrose are layered over the sample as shown. The gradient is subjected to centrifugation for 18 h at approx. $247,000 \times g$ allowing the buoyant lipid rafts to float to the 30 and 5 % interface. Twelve 1-mL fractions are collected from the top and aliquots prepared for Western blotting showing the presence of caveolin-1 (Cav1) in the light density fractions (#4 and #5) (21)

or by repeated aspiration through a 23-gauge needle (Cat# 305120; BD Biosciences, Waltham, MA) using a 5 mL syringe (Cat# 309646; BD Biosciences) 20 times.

4. Vortex and transfer 2 mL into a 13-mL ultracentrifuge tube. Save the remaining sample for total cell lysate.
5. Add 2 mL of 90 % sucrose in TNE to bring the sucrose concentration to 45 %.
6. Carefully overlay with 4 mL each of 35 and 5 % sucrose in TNE by gently adding the solutions down the side of the tube (1 mL at a time; Fig. 2).
7. Centrifuge the gradients at 38,000–40,000 rpm (maximum force of approximately $273,865 \times g$) for 16–20 h in an SW41Ti rotor at 4 °C (see **Notes 4** and **5**).
8. Collect twelve 1-mL fractions from the top while keeping all samples on ice (Fig. 2).
9. Boil aliquots (10–40 μ L) of each fraction in Laemmli buffer in preparation for SDS-PAGE and immunoblotting. Store the remaining samples at -70 °C.

3.5 Characterization of Lipid Raft-Associated Proteins

1. Western blotting: Equal amount of each fraction (Section 3.4) is resolved over SDS-PAGE (12.5 % acrylamide) and electro-transferred onto a nitrocellulose or a PVDF membrane for immunoblotting as previously described (21) for caveolin-1, caveolin-2, flotillin-1, and flotillin-2 (all antibodies at 1:1,000 dilution).

2. Immunoprecipitation: Combine fractions 4 and 5 (Section 3.4) for immunoprecipitation using anti-caveolin-1 or -caveolin-2 antibodies as previously described (40).

4 Notes

1. Alternative to TNE, the following buffers can also be used:
 - (a) MBS buffer: 25 mM 2-(N-morpholino)ethanesulfonic acid (MES, pH 6.6, Cat# M2933) and 150 mM NaCl.
 - (b) RIPA buffer: PBS, 1 % Nonidet P-40 (Cat# 98379), and 0.5 % sodium deoxycholate (Cat #30970).
2. Alternative to TX-100, other nonionic detergents can be used including Lubrol WX (1 %), CHAPS (1 %), Brij 98 (1 %), or 500 mM sodium carbonate (41, 42). Note that cholesterol resides in both lipid rafts and non-lipid rafts, and this may alter results from membrane extractions in the presence of detergents (43).
3. Acute depletion of membrane cholesterol also disrupts other lipids including PI(4, 5)P₂, and thus not all cellular changes result solely from disruption of lipid rafts (44).
4. Membrane preparations must be subjected to ultracentrifugation immediately and not frozen.
5. If using an SW60 rotor, mix 0.4 mL cell lysate in complete TNE with 1 % TX-100 with 0.4 mL of 90 % sucrose in TNE. Layer with 2.2 mL 30 % sucrose in TNE and then 1.2 mL of 5 % sucrose in TNE. Centrifuge at 49,000 rpm for 18 h, and collect 0.4 mL fractions.

Acknowledgments

We thank Dr. Michael DiPersio (Center for Cell Biology & Cancer Research, Albany Medical College), Dr. Mon-Li Chu, Donna Brennan, and Andrew Overmiller for critically reading the paper and for their insightful discussions. We thank Jordan Wesolowski and Dr. Fabienne Paumet for the protocol using the SW60 rotor. This work was supported by grants from the National Institutes of Health (Mahoney, R01AR056067).

References

1. Singer SJ, Nicolson GL (1972) The fluid mosaic model of the structure of cell membranes. *Science* 175:720–731
2. Simons K, Toomre D (2000) Lipid rafts and signal transduction. *Nat Rev Mol Cell Biol* 1:31–39
3. Suomalainen M (2002) Lipid rafts and assembly of enveloped viruses. *Traffic* 3:705–709
4. Lingwood D, Simons K (2010) Lipid rafts as a membrane-organizing principle. *Science* 327:46–50

5. Head BP, Patel HH, Insel PA (2014) Interaction of membrane/lipid rafts with the cytoskeleton: Impact on signaling and function: membrane/lipid rafts, mediators of cytoskeletal arrangement and cell signaling. *Biochim Biophys Acta* 1838:532–545
6. Head BP, Patel HH, Roth DM, Murray F, Swaney JS, Niesman IR, Farquhar MG, Insel PA (2006) Microtubules and actin microfilaments regulate lipid raft/caveolae localization of adenylyl cyclase signaling components. *J Biol Chem* 281:26391–26399
7. Stuermer CA (2010) The reggie/flotillin connection to growth. *Trends Cell Biol* 20:6–13
8. Giltaire S, Lambert S, Poumay Y (2011) HB-EGF synthesis and release induced by cholesterol depletion of human epidermal keratinocytes is controlled by extracellular atp and involves both p38 and ERK1/2 signaling pathways. *J Cell Physiol* 226:1651–1659
9. Mathay C, Pierre M, Pittelkow MR, Depiereux E, Nikkels AF, Colige A, Poumay Y (2010) Transcriptional profiling after lipid raft disruption in keratinocytes identifies critical mediators of atopic dermatitis pathways. *J Invest Dermatol* 131:46–58
10. Bang B, Gniadecki R, Gajkowska B (2005) Disruption of lipid rafts causes apoptotic cell death in HaCaT keratinocytes. *Exp Dermatol* 14:266–272
11. Gniadecki R (2004) Depletion of membrane cholesterol causes ligand-independent activation of Fas and apoptosis. *Biochem Biophys Res Commun* 320:165–169
12. Tellier E, Canault M, Rebsomen L, Bonardo B, Juhan-Vague I, Nalbone G, Peiretti F (2006) The shedding activity of ADAM17 is sequestered in lipid rafts. *Exp Cell Res* 312:3969–3980
13. Grether-Beck S, Salahshour-Fard M, Timmer A, Brenden H, Felsner I, Walli R, Füllekrug J, Krutmann J (2008) Ceramide and raft signaling are linked with each other in UVA radiation-induced gene expression. *Oncogene* 27:4768–4778
14. Bayer M, Proksch P, Felsner I, Brenden H, Kohne Z, Walli R, Duong TN, Götz C, Krutmann J, Grether-Beck S (2011) Photoprotection against UVA: effective triterpenoids require a lipid raft stabilizing chemical structure. *Exp Dermatol* 20:955–958
15. Ma WY, Zhuang L, Cai DX, Zhong H, Zhao C, Sun Q (2012) Inverse correlation between caveolin-1 expression and clinical severity in psoriasis vulgaris. *J Int Med Res* 40:1745–1751
16. Qin H, Bollag WB (2013) The caveolin-1 scaffolding domain peptide decreases phosphatidylglycerol levels and inhibits calcium-induced differentiation in mouse keratinocytes. *PLoS One* 8:e80946
17. Trimmer C, Sotgia F, Lisanti MP, Capozza F (2013) Cav1 inhibits benign skin tumor development in a two-stage carcinogenesis model by suppressing epidermal proliferation. *Am J Transl Res* 5:80–91
18. Staubach S, Hanisch FG (2011) Lipid rafts: signaling and sorting platforms of cells and their roles in cancer. *Expert Rev Proteomics* 8:263–277
19. Fecchi K, Travaglione S, Spadaro F, Quattrini A, Parolini I, Piccaro G, Raggi C, Fabbri A, Felicetti F, Carè A (2012) Human melanoma cells express FGFR/Src/Rho signaling that entails an adhesion-independent caveolin-1 membrane association. *Int J Cancer* 130:1273–1283
20. Parton RG, del Pozo MA (2013) Caveolae as plasma membrane sensors, protectors and organizers. *Nat Rev Mol Cell Biol* 14:98–112
21. Brennan D, Peltonen S, Dowling A, Medhat W, Green KJ, Wahl JK, Del Galdo F, Mahoney MG (2011) A role for caveolin-1 in desmoglein binding and desmosome dynamics. *Oncogene* 31:1636–1648
22. Simons K, Ikonen E (1997) Functional rafts in cell membranes. *Nature* 387:569–572
23. Babiychuk EB, Draeger A (2006) Biochemical characterization of detergent-resistant membranes: a systematic approach. *Biochem J* 397:407–416
24. Heerklotz H (2002) Triton promotes domain formation in lipid raft mixtures. *Biophys J* 83:2693–2701
25. Simons K, Gerl MJ (2010) Revitalizing membrane rafts: new tools and insights. *Nat Rev Mol Cell Biol* 11:688–699
26. Pinaud F, Michalet X, Iyer G, Margeat E, Moore HP, Weiss S (2009) Dynamic partitioning of a glycosyl-phosphatidylinositol-anchored protein in glycosphingolipid-rich microdomains imaged by single-quantum dot tracking. *Traffic* 10:691–712
27. Chamberlain LH (2004) Detergents as tools for the purification and classification of lipid rafts. *FEBS Lett* 559:1–5
28. Schuck S, Honsho M, Ekroos K, Shevchenko A, Simons K (2003) Resistance of cell membranes to different detergents. *Proc Natl Acad Sci U S A* 100:5795–5800
29. Gustavsson J, Parpal S, Karlsson M, Ramsing C, Thorn H, Borg M, Lindroth M, Peterson

- KH, Magnusson KE, Strålfors P (1999) Localization of the insulin receptor in caveolae of adipocyte plasma membrane. *FASEB J* 13:1961–1971
30. Brown DA (2006) Lipid rafts, detergent-resistant membranes, and raft targeting signals. *Physiology (Bethesda)* 21:430–439
 31. Vind-Kezunovic D, Nielsen CH, Wojewodzka U, Gniadecki R (2008) Line tension at lipid phase boundaries regulates formation of membrane vesicles in living cells. *Biochim Biophys Acta* 1778:2480–2486
 32. Schoop VM, Mirancea N, Fusenig NE (1999) Epidermal organization and differentiation of HaCaT keratinocytes in organotypic coculture with human dermal fibroblasts. *J Invest Dermatol* 112:343–353
 33. Boukamp P, Petrussevska RT, Breitkreutz D, Hornung J, Markham A, Fusenig NE (1988) Normal keratinization in a spontaneously immortalized aneuploid human keratinocyte cell line. *J Cell Biol* 106:761–771
 34. Giard DJ, Aaronson SA, Todaro GJ, Arnstein P, Kersey JH, Dosik H, Parks WP (1973) In vitro cultivation of human tumors: establishment of cell lines derived from a series of solid tumors. *J Natl Cancer Inst* 51:1417–1423
 35. Klein U, Gimpl G, Fahnenholz F (1995) Alteration of the myometrial plasma membrane cholesterol content with beta-cyclodextrin modulates the binding affinity of the oxytocin receptor. *Biochemistry* 34:13784–13793
 36. Powers KA, Szászi K, Khadaroo RG, Tawadros PS, Marshall JC, Kapus A, Rotstein OD (2006) Oxidative stress generated by hemorrhagic shock recruits Toll-like receptor 4 to the plasma membrane in macrophages. *J Exp Med* 203:1951–1961
 37. Roitbak T, Surviladze Z, Tikkanen R, Wandinger-Ness A (2005) A polycystin multi-protein complex constitutes a cholesterol-containing signalling microdomain in human kidney epithelia. *Biochem J* 392:29–38
 38. Moss JI, Garrett TJ, Hansen PJ (2012) Involvement of free cholesterol and high-density lipoprotein in development and resistance of the preimplantation bovine embryo to heat shock. *J Anim Sci* 90:3762–3769
 39. Galbiati F, Volonte D, Brown AM, Weinstein DE, Ben-Ze'ev A, Pestell RG, Lisanti MP (2000) Caveolin-1 expression inhibits Wnt/beta-catenin/Lef-1 signaling by recruiting beta-catenin to caveolae membrane domains. *J Biol Chem* 275:23368–23377
 40. Langlois S, Cowan KN, Shao Q, Cowan BJ, Laird DW (2008) Caveolin-1 and -2 interact with connexin43 and regulate gap junctional intercellular communication in keratinocytes. *Mol Biol Cell* 19:912–928
 41. Pike LJ, Han X, Gross RW (2005) Epidermal growth factor receptors are localized to lipid rafts that contain a balance of inner and outer leaflet lipids: a shotgun lipidomics study. *J Biol Chem* 280:26796–26804
 42. Riddell DR, Christie G, Hussain I, Dingwall C (2001) Compartmentalization of β -secretase (Asp2) into low-buoyant density, noncaveolar lipid rafts. *Curr Biol* 11:1288–1293
 43. Zidovetzki R, Levitan I (2007) Use of cyclodextrins to manipulate plasma membrane cholesterol content: evidence, misconceptions and control strategies. *Biochim Biophys Acta* 1768:1311–1324
 44. Pike LJ, Miller JM (1998) Cholesterol depletion delocalizes phosphatidylinositol bisphosphate and inhibits hormone-stimulated phosphatidylinositol turnover. *J Biol Chem* 273:22298–22304
 45. Bender FC, Whitbeck JC, Ponce de Leon M, Lou H, Eisenberg RJ, Cohen GH (2003) Specific association of glycoprotein B with lipid rafts during herpes simplex virus entry. *J Virol* 77:9542–9552
 46. Blonder J, Terunuma A, Conrads TP, Chan KC, Yee C, Lucas DA, Schaefer CF, Yu LR, Issaq HJ, Veenstra TD, Vogel JC (2004) A proteomic characterization of the plasma membrane of human epidermis by high-throughput mass spectrometry. *J Invest Dermatol* 123:691–699
 47. Seveau S, Bierne H, Giroux S, Prévost MC, Cossart P (2004) Role of lipid rafts in E-cadherin- and HGF-R/Met-mediated entry of *Listeria monocytogenes* into host cells. *J Cell Biol* 166:743–753
 48. Causeret M, Taulet N, Comunale F, Favard C, Gauthier-Rouvière C (2005) N-cadherin association with lipid rafts regulates its dynamic assembly at cell-cell junctions in C2C12 myoblasts. *Mol Biol Cell* 16:2168–2180
 49. Patra SK, Bettuzzi S (2007) Epigenetic DNA-methylation regulation of genes coding for lipid raft-associated components: a role for raft proteins in cell transformation and cancer progression (review). *Oncol Rep* 17:1279–1290
 50. Sugibayashi K, Onuki Y, Takayama K (2009) Displacement of tight junction proteins from detergent-resistant membrane domains by treatment with sodium caprate. *Eur J Pharm Sci* 36:246–253
 51. Lambert D, O'Neill CA, Padfield PJ (2005) Depletion of Caco-2 cell cholesterol disrupts barrier function by altering the detergent

- solubility and distribution of specific tight-junction proteins. *Biochem J* 387:553–560
52. Simons M, Schwarz K, Kriz W, Miettinen A, Reiser J, Mundel P, Holthöfer H (2001) Involvement of lipid rafts in nephrin phosphorylation and organization of the glomerular slit diaphragm. *Am J Pathol* 159:1069–1077
 53. Bruewer M, Hopkins AM, Hobert ME, Nusrat A, Madara JL (2004) RhoA, Rac1, and Cdc42 exert distinct effects on epithelial barrier via selective structural and biochemical modulation of junctional proteins and F-actin. *Am J Physiol Cell Physiol* 287:C327–C335
 54. Bowie RV, Donatello S, Lyes C, Owens MB, Babina IS, Hudson L, Walsh SV, O'Donoghue DP, Amu S, Barry SP, Fallon PG, Hopkins AM (2012) Lipid rafts are disrupted in mildly inflamed intestinal microenvironments without overt disruption of the epithelial barrier. *Am J Physiol Gastrointest Liver Physiol* 302:G781–G793
 55. Schubert AL, Schubert W, Spray DC, Lisanti MP (2002) Connexin family members target to lipid raft domains and interact with caveolin-1. *Biochemistry* 41:5754–5764
 56. Nava P, Laukoetter MG, Hopkins AM, Laur O, Gerner-Smidt K, Green KJ, Parkos CA, Nusrat A (2007) Desmoglein-2: a novel regulator of apoptosis in the intestinal epithelium. *Mol Biol Cell* 18:4565–4578
 57. Delva E, Jennings JM, Calkins CC, Kottke MD, Faundez V, Kowalczyk AP (2008) Pemphigus vulgaris IgG-induced desmoglein-3 endocytosis and desmosomal disassembly are mediated by a clathrin- and dynamin-independent mechanism. *J Biol Chem* 283:18303–18313
 58. Resnik N, Sepcic K, Plemenitas A, Windoffer R, Leube R, Veranic P (2011) Desmosome assembly and cell-cell adhesion are membrane raft-dependent processes. *J Biol Chem* 286:1499–1507

MMP-2, -9 and TIMP-1, -2 Assays in Keratinocyte Cultures

Takashi Kobayashi

Abstract

To determine the status of tissue metabolism in the epidermis, matrix metalloproteinase (MMP)-2 and -9 and tissue inhibitor of metalloproteinases (TIMP)-1 and -2 can be detected using keratinocytes in culture. In addition to Western blotting analysis, gelatin zymography for MMP-2 and -9 and the reverse zymography for TIMP-1 and -2 are useful methods for evaluating such protein expressions both qualitatively and quantitatively, because MMP-2 and MMP-9 are known as gelatinase. Moreover, real-time analysis for zymography can be performed using fluorescein isothiocyanate-labelled gelatin.

Keywords: Gelatinase, MMP-2, MMP-9, TIMP-1, TIMP-2, Keratinocyte, Gelatin, Zymography, Western blotting

1 Introduction

Keratinocytes comprise the majority of epidermal cells. They are located at the interface of the whole body and are considered to play a fundamental role in maintaining the homeostasis of our body. Matrix metalloproteinases (MMPs) and tissue inhibitors of metalloproteinases (TIMPs) are known to play important but contrasting roles in tissue metabolism (1–3). Among them, gelatinases, known as MMP-2 and -9, have been reported to be involved in a variety of pathophysiological conditions in the field of dermatology (3–12). Therefore, methods to detect MMP-2 and -9 and their inhibitors, TIMP-1 and -2, in keratinocytes would be useful tools for understanding the pathophysiology of skin diseases and could also be used to monitor models of diseases, including the quest for new drugs. I describe herein methods of gelatin zymography and reverse zymography which we used together with Western blotting analysis to detect MMP-2 and -9 and TIMP-1 and -2 in conditioned medium from keratinocytes in culture.

By the nature of MMP-2 and MMP-9 as gelatinase (1–3, 13, 14), the gelatin zymography method has been used to detect these enzymes not only qualitatively but also quantitatively (15–20). In contrast, reverse zymography has been developed to identify

TIMP-1 and TIMP-2 (20, 21). These are methods which assess their enzymatic properties together with inhibitory activities. In addition, Western blotting analysis is a useful tool to detect antigenic specificity for each molecule.

2 Materials

All solutions used for gelatin zymography and reverse zymography are made with double-distilled or Milli-Q purified water, except for the destaining solution of 30 % methanol/10 % acetic acid.

2.1 Gelatin Zymography

1. 5 % Gelatin (w/v) (*see Note 1*).
2. Conditioned medium (serum free) from keratinocytes in culture (*see Notes 2 and 3*).
3. Running gel buffer (1×): 1.5 M Tris-HCl, pH 8.8.
4. Stacking gel buffer (1×): 0.5 M Tris-HCl, pH 6.8.
5. 30 % Acrylamide (w/v)–1 % *N*, *N*'-methylene-bis-acrylamide (w/v) in water (*see Note 4*).
6. 10 % Sodium dodecyl sulfate (SDS).
7. *N,N,N',N'*-methylenebisacrylamide (TEMED).
8. 10 % Ammonium persulfate (w/v).
9. Sample loading buffer (5×): 0.25 M Tris-HCl, pH 7.4/25 mM CaCl₂/5 % SDS/0.02 % bromophenol blue/30 % glycerol.
10. Electrophoresis equipment; Minislab apparatus and power supply (*see Note 5*).
11. Electrophoresis electrode buffer: 15 mM Tris/0.192 M glycine/0.1 % SDS (14.35 g glycine, 1.75 g Tris, and 1 g SDS in 1 L of water).
12. 2.5 % Triton X-100 (polyethylene glycol mono-p-isooctylphenyl ether).
13. Enzymatic reaction buffer: 0.05 M Tris-HCl, pH 7.4/20 mM NaCl/5 mM CaCl₂/0.02 % sodium azide.
14. 0.1 % Amido Black 10B.
15. 30 % Methanol/10 % acetic acid.

2.2 Reverse Zymography

All materials from 1. to 15. in Section 2.1 are required.

In addition, human recombinant MMP-9 (Daiichi Fine Chemicals, Toyama, Japan) is required (*see Note 6*).

2.3 Western Blotting Analysis

All materials from 2. to 10. listed for Section 2.1 are required for electrophoresis. Additional materials as described below are also required.

1. Polyvinylidene difluoride (PVDF) membranes.
2. Methanol.
3. Blotting buffer: 0.025 M Tris/0.192 M glycine/20 % methanol (to make this, mix 14.4 g glycine, 3 g Tris, and 200 mL ethanol in 1 L water).
4. Electroblothing apparatus (for example, Trans-Blot Cell and Systems, Bio-Rad, Hercules, CA).
5. Parafilm (American National Can, Menasha, WI).
6. Blocking buffer: 4 % bovine serum albumin (BSA)/0.05 % Tween-20 in phosphate-buffered saline (PBS).
7. Primary antibodies: Monoclonal antibodies raised against MMP-9 or TIMP-1 (purified IgG fraction after protein A Sepharose column, Bio-Rad) (5, 22) or monoclonal anti-TIMP-2 antibody (Daiichi Fine Chemical).
8. Wash buffer: 0.05 % Tween-20 in PBS.
9. Secondary antibody: Horse-radish peroxidase linked anti-mouse Ig antibody (Amersham Biosciences, Little Chalfont Buckinghamshire, UK).
10. Detection reagents and equipment: ECL plus Western blotting detection reagents (Amersham Biosciences) and X-ray film with cassette.

3 Methods

3.1 Gelatin Zymography

The gelatin zymography procedure is made up of three stages: (1) electrophoresis, (2) enzymatic reaction, and (3) staining and destaining of gels.

1. Prepare a running gel, 7.5 % acrylamide–bis-acrylamide gel containing 0.5 % gelatin. Mix 2.5 mL of running gel buffer, 2.5 mL 30 % acrylamide, 2 mL 2.5 % gelatin, 2.7 mL water, 100 μ L 10 % SDS, 10 μ L TEMED, and 190 μ L 10 % ammonium persulfate. Aspirate the mixture, for example, using a 20 mL syringe (*see* Notes 7, 8, and 9). Gently pour the gel between the glass plates. Then, gently overlay acrylamide solution with water and allow it to polymerize.
2. Prepare a stacking gel, 3 % acrylamide–bis-acrylamide gel. Mix 1 mL of stacking gel buffer, 400 μ L 30 % acrylamide, 2.4 mL water, 40 μ L 10 % SDS, 4 μ L TEMED, and 156 μ L 10 % ammonium persulfate. Mix gently and pour over the polymerized running gel after removing the overlaid water, add a suitable comb, and allow to be polymerized.

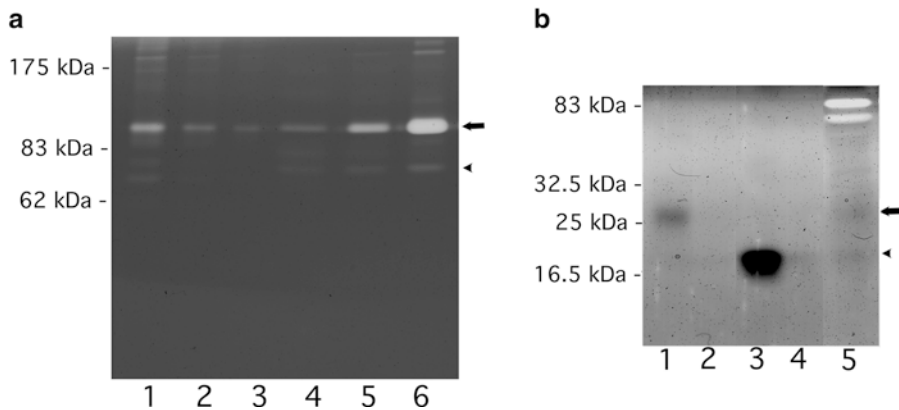


Fig. 1 Gelatin zymography (7.5 % acrylamide gel) (**panel a**) and reverse zymography (12 % acrylamide gel) (**panel b**). (**a**) 1.5 ng (*lane 1*), 500 pg (*lane 2*), or 170 pg (*lane 3*) of human recombinant MMP-9, and aliquots of conditioned culture media of keratinocytes stimulated with high Ca²⁺ concentration (*lane 5*), by the addition of transforming growth factor (TGF)-β 1 (*lane 6*), or without stimulation (*lane 4*). High Ca²⁺-induced MMP-9 secretion selectively, whereas TGF-β 1-stimulated MMP-9 and MMP-2 secretion. The *arrow* and *arrowhead* show the bands of MMP-9 and MMP-2, respectively. (**b**) 13 ng (*lane 1*) or 4.3 ng (*lane 2*) of human recombinant TIMP-1 (Daiichi Fine Chemical), 13 ng (*lane 3*) or 4.3 ng (*lane 4*) of human recombinant TIMP-2 (Daiichi Fine Chemical), or the conditioned medium (*lane 5*) from human keratinocytes in culture. The bands showing gelatinolytic activities of MMP-9 and MMP-2 are also observed. The *arrow* and *arrowhead* show the bands of TIMP-1 and TIMP-2, respectively

3. Dilute the conditioned culture medium from keratinocytes with the sample loading buffer (1/4 volume of the conditioned medium) and mix (*see Note 10*). Do not boil.
4. Run the gel in electrophoresis electrode buffer at 80 V (constant voltage) (*see Note 11*).
5. After running the gel, remove the stacking gel, separate the plates, and mark the gel (i.e., trim a corner, I use the lower right) to maintain the orientation. Incubate the gel in the 2.5 % Triton X-100 for 60 min with shaking (*see Notes 9 and 12*).
6. Transfer the gel into the enzymatic reaction buffer and incubate it at 35 °C (*see Notes 13, 14, and 15*).
7. Stain the gel with 0.1 % Amido Black 10B with shaking (*see Note 16*).
8. Destain the gel with 30 % methanol/10 % acetic acid with shaking (*see Note 17*).
9. Observe the region of gelatin degradation as clear bands against a background of stained gelatin (Figs. 1a and 2a; *see Notes 9, 18, and 19*).

3.2 Reverse Zymography

Reverse zymography is based on the same principle as gelatin zymography and is made up of three stages: (1) electrophoresis, (2) enzymatic reaction, and (3) staining and destaining of gels.

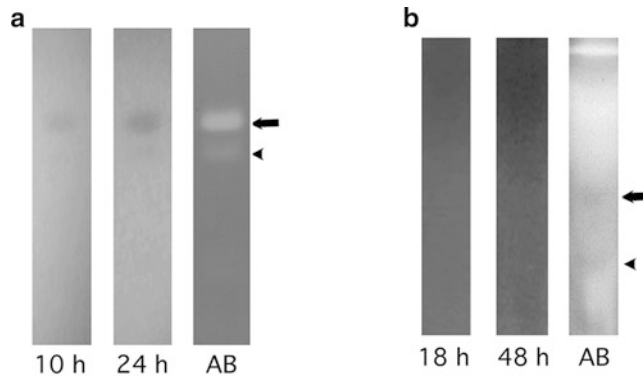


Fig. 2 Real-time zymography (**panel a**) and reverse zymography (**panel b**) analyses. Each conditioned culture medium from keratinocytes was applied in the gel containing FITC-labelled gelatin. In a successive period of time (*lanes* 10 and 24 h in **(a)**, and *lanes* 18 and 48 h in **(b)**) after the incubation in the enzymatic reaction buffer, the gel was set in the ultraviolet transilluminator and observed for each gelatinolytic band (**panel a**) and non-degrading one (**panel b**), respectively, just followed by staining using Amido Black 10B and destaining (*lane* AB) in each panel). The *arrow* and *arrowhead* show the bands of MMP-9 and MMP-2 in **(a)** and those of TIMP-1 and TIMP-2 in **(b)**, respectively

1. Prepare a running gel, 12 % acrylamide–bis-acrylamide gel containing 0.25 % gelatin. Mix 2.5 mL of running gel buffer, 4 mL 30 % acrylamide, 1 mL 2.5 % gelatin, 2.2 mL water, 100 μ L 10 % SDS, 20 μ L 10 μ g/mL human recombinant MMP-9, 10 μ L TEMED, and 170 μ L of 10 % ammonium persulfate (*see* **Notes 7, 8, 9, and 20**). The following steps for electrophoresis are the same as in 2–4 in Section 3.1.
2. After running the gel, incubate it three times in 2.5 % Triton X-100 for 30 min each time with shaking (90 min in total) (*see* **Note 12**).
3. Transfer the gel into the enzymatic reaction buffer and incubate it at 35 °C with shaking (*see* **Note 21**).
4. Stain and destain the gel with 0.1 % Amido Black 10B and with 30 % methanol/10 % acetic acid, respectively (*see* **Notes 16 and 17**).
5. Observe the region of non-degraded bands against a clear background of gelatin degradation (Figs. 1b and 2b; *see* **Notes 9 and 18**).

3.3 Western Blotting Analysis

Western blotting analysis is made up of four stages: (1) electrophoresis, (2) electroblotting, (3) antibody–antigen binding reaction, and (4) detection of signals (*see* **Note 22**).

1. Prepare a 7.5 % acrylamide–bis-acrylamide running gel, which is made using 4.7 mL of water instead of 2 mL of 2.5 % gelatin/2.7 mL water as described above for gelatin zymography to detect MMP-9 or a 15 % acrylamide–bis-acrylamide gel, which is made up of 5 mL 30 % acrylamide and 2.2 mL of water instead

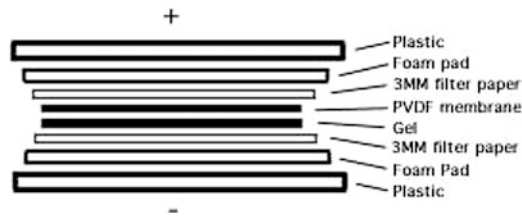


Fig. 3 Schematic representation of the blotting sandwich assembled for Western blotting analysis. + and – indicate cathode and anode, respectively

of 2.5 mL of 30 % acrylamide, 2 mL 2.5 % gelatin, and 2.7 mL water as described in Section 3.1 (*see* **Notes 2, 4, 7, and 8**).

2. Perform electrophoresis as detailed in **steps 2–4** in Section 3.1.
3. Soak a PVDF membrane in methanol for 60 s.
4. Pre-wet the PVDF membrane, filter paper, and foam in blotting buffer at 4 °C.
5. After electrophoresis, carefully assemble the gel and the PVDF membrane as a blotting sandwich in the apparatus, as shown in Fig. 3, with the gel to the anode side (black side in the Bio-Rad apparatus) and the PVDF membrane to the cathode side (clear/white side in the Bio-Rad apparatus) (*see* **Note 23**).
6. Transfer proteins to the PVDF membrane in the transfer apparatus at 80 V for 1 h. Use an ice block to keep cold or transfer at 4 °C. Stir during the transfer.
7. Set the Parafilm attached to the dish.
8. After transfer, cut the membrane to the exact size of the gel and set it (protein side up) on the Parafilm.
9. Soak the membrane in blocking buffer by mounting approximately 1 mL of blocking buffer per 10 cm² membrane using surface tension for 30 min at 4 °C (*see* **Note 24**).
10. Replace the blocking buffer with the first antibody solution (5 µg/mL) diluted in blocking buffer and incubate it overnight at 4 °C (*see* **Note 24**).
11. Wash the membrane with washing buffer for 10 min with shaking, and repeat this three times (four times total).
12. Set the new Parafilm attached to the dish.
13. Soak the membrane in the second antibody solution diluted in washing buffer ($\times 10,000$ for the Amersham second antibody) and incubate it for 3 h at 4 °C (*see* **Note 24**).
14. Wash the membrane with washing buffer for 10 min with shaking, and repeat this three times (four times total).
15. Detect the peroxidase reaction by ECL plus reagent using X-ray film with cassette (Fig. 4).

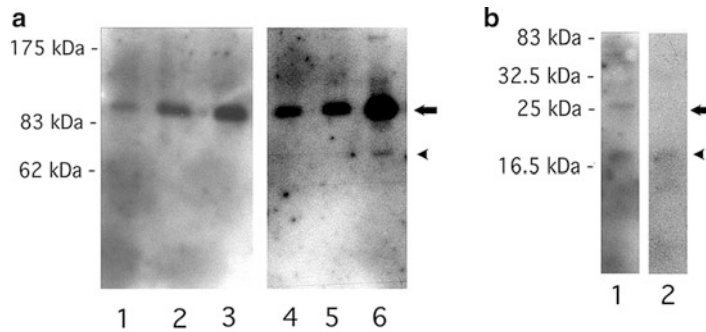


Fig. 4 Western blotting analysis patterns for detecting MMP-9 (7.5 % acrylamide gel) (**panel a**) and TIMP-1 (15 % acrylamide gel) (**panel b**). (**a**) Aliquots of conditioned culture media from keratinocytes stimulated with high Ca^{2+} concentrations (*lanes 2 and 5*), with addition of transforming growth factor (TGF)- β 1 (*lanes 3 and 6*), or without stimulation (*lanes 1 and 4*). Samples were applied and analyzed using monoclonal antibodies raised against human MMP-9, one of which is not cross-reactive to MMP-2 (*lanes 1, 2, and 3*) while the other is cross-reactive to MMP-2 (*lanes 4, 5, and 6*) (22). The MMP-2 band induced by TGF- β 1 was apparently detected by the cross-reactivity. The *arrow* and *arrowhead* show the bands of MMP-9 and MMP-2, respectively. (**b**) Aliquots of the conditioned media were applied and analyzed using two types of monoclonal antibodies, one of which is raised against human TIMP-1 (*lane 1*) (5) and the other is an anti-TIMP-2 antibody (Fuji Fine Chemical) (*lane 2*) without cross-reactivity to TIMP-1. The *arrow* and *arrowhead* show the bands of TIMP-1 and TIMP-2, respectively

4 Notes

1. Gelatin (I use EIA Grade Reagent, Bio-Rad) is hard to dissolve in water at room temperature. It will more easily dissolve in a water bath at approximately 40 °C.
2. It is important to use serum-free medium, because serum itself contains MMP-2 and MMP-9 (23). In the case of HaCat cells or murine keratinocytes, which can be cultured in medium with serum, change them into medium without serum to collect conditioned culture medium for identifying gelatinase from those cells.
3. In my experience, fresh conditioned culture medium is relatively stable at 4 °C for up to 48 h for the assays described above. Please avoid storing it at 4 °C for more than 2 days or at temperatures higher than 4 °C. Frozen samples are often more stable. Repeated freeze and thaw cycles, however, can cause degradation of proteins together with their aggregation.
4. Because the acrylamide monomer is a neurotoxin, handle with care. For example, wear a mask and wear gloves when handling acrylamide powder and its solutions.

5. A running gel of 10 mL and a stacking gel of 4 mL in total are used for two sets of minislabs (8.5 cm × 6 cm and 1 mm thickness).
6. Instead of human recombinant MMP-9, conditioned culture medium from TPA-induced human HT-1080 cells or MMP-9 purified using a gelatin-Sepharose column can be used (20, 24).
7. It is important to aspirate the air from the running gel solution just before pouring it to avoid the formation of bubbles in the polymerized gel, which can cause distortion during electrophoresis. I usually use a 20 mL syringe for 10 mL running gel solution and remove bubbles by closing the opening with Parafilm and applying a negative pressure with the syringe of about 5–10 mL until the air bubbles caused by the low pressure in the syringe disappear.
8. The time required for the gel to polymerize will differ depending on the temperature and will take longer at cold temperature. If the amount of ammonium persulfate is increased, the time required will be shorter. Conversely, reduce the amount of ammonium persulfate to slow down polymerization in a hot environment.
9. Using one part of fluorescein isothiocyanate (FITC)-labelled gelatin in ten parts of the whole gelatin (20), real-time detection of gelatinolytic band and non-gelatinolytic one can be observed in zymography and reverse one, respectively (Fig. 2). For such analyses, the gel container should be in light-shielded condition to avoid decreasing the fluorescence intensity during incubation. Each band in the gel will be detected on the ultraviolet transilluminator (such as UVP Co. M-20, 302 nm) after an appropriate period of incubation. In photographing for such cases, a sharp cut filter to cut off a light under 520 nm (such as Fuji Film Co. SC52) should be used. When each band is detected, the gel could undergo staining and destaining.
10. After diluting the sample with sample buffer, the enzyme will be gradually inactivated by SDS. To avoid this, use of fresh sample after the addition of sample buffer is recommended for gelatin zymography. The addition of dithiothreitol or 2-mercaptoethanol leads to the inactivation of enzymes and should be avoided.
11. High voltage can cause heating of gels, which can inactivate the enzymatic reaction. To avoid this, less than 100 V is desirable. I recommend performing the electrophoresis at 4 °C in an extremely hot environment.
12. To remove the SDS in the gel, incubation in Triton X-100 is important. Please use more than 100 mL of 2.5 % Triton X-100 per gel (approximately 5 mL of running gel) for each wash.

13. The reaction time for conditioned culture medium will differ depending on the concentration of the enzyme. For example, 10–15 μL in 100 μL of conditioned culture medium collected from subconfluent keratinocytes for 24 h in 1 well of a 48-well plate will be enough to observe an MMP-9 band in an overnight reaction.
14. Gelatin zymography is known to be very sensitive, and more enzymatic reaction is expected as the incubation time is longer. However, I have often experienced a limitation in the sensitivity after 5 days of incubation. It is considered that an extremely long incubation time can allow diffusion of enzymes from the gel.
15. The gelatin zymography method is useful not only for detecting metalloproteinases but also sometimes for identifying other species of enzymes such as serine proteases. To do this or to confirm the gelatinolytic activity by MMPs, 10 mM EDTA should be added to the reaction buffer and to the Triton X-100 wash to inhibit the metalloproteinases.
16. Amido Black 10B can be reused several times. The average staining time for the first-time use will be 10 min or so, but it will take longer as the solution is reused. Instead of Amido Black 10B, Coomassie brilliant blue R-250 can also be used.
17. A moderate destaining time will be more than overnight.
18. The gel will shrink in the destaining solution. After destaining, gels can be stored in tap water with 0.02 % sodium azide for several days, and the resolution will be relatively improved after storage in this way. I usually scan the image of each gel using a scanner attached to a personal computer. After scanning, quantitative analysis for the intensity of the band can be performed using NIH image software (16, 18, 19).
19. As the passage of human keratinocytes in culture is repeated several times, MMP-2 secretion into the conditioned medium will decrease (17).
20. The gel containing MMP-9 will be gradually inactivated by SDS. Therefore, electrophoresis should be started within a couple of hours after the gel is ready for use.
21. The reaction time for conditioned culture medium takes much longer in reverse zymography than in the gelatin zymography described above. For example, application of 10–15 μL in a 240 μL sample, which is concentrated by filter (Ultrafree, Millipore, Boston, MA) from 1.2 mL of conditioned culture medium obtained from subconfluent keratinocytes grown for 24 h in 1 well of a 6-well plate, facilitates observation of a TIMP-1 band after 2 days of reaction. In addition, incubation with shaking (60–80 rpm) is important to detect the inhibitory activity of TIMPs against MMP-9.

22. During the whole procedure of Western blotting analysis, wear gloves to avoid contamination with fingerprints. In addition, avoid drying the PVDF membrane during the procedure after soaking in the methanol.
23. To assemble the blotting sandwich, be careful to remove air bubbles between the layers and move as quickly as possible to avoid band diffusion and resolution loss.
24. Moist papers can be used in the area uncovered by Parafilm on the dish with closure of the lid to avoid evaporation during soaking.

Acknowledgment

This work was supported by a Grant-in-Aid for Scientific Research from the Japan Society for the Promotion of Science.

References

1. Birkedal-Hansen H (1995) Proteolytic remodeling of extracellular matrix. *Curr Opin Cell Biol* 7:728–735
2. McCawley LJ, Matrisian LM (2001) Matrix metalloproteinases: they're not just for matrix anymore! *Curr Opin Cell Biol* 13:534–540
3. Kobayashi T (2012) Gelatinases in the skin. In: Oshiro N, Miyagi E (eds) *Matrix metalloproteinases: biology, functions and clinical implications*. Nova, Hauppauge, pp 99–125
4. Stähle-Bäckdahl M, Parks WC (1993) 92-kd gelatinase is actively expressed by eosinophils and stored by neutrophils in squamous cell carcinoma. *Am J Pathol* 142:995–1000
5. Kobayashi T, Onoda N, Takagi T, Hori H, Hattori S, Nagai Y, Tajima S, Nishikawa T (1996) Immunolocalizations of human gelatinase (type IV collagenase, MMP-9) and TIMP (tissue inhibitor of metalloproteinases) in normal epidermis and some epidermal tumors. *Arch Dermatol Res* 288:239–44
6. Fisher GJ, Wang ZQ, Datta SC, Varani J, Kang S, Voorhees JJ (1997) Pathophysiology of premature skin aging induced by ultraviolet light. *N Engl J Med* 337:1419–1428
7. Liu Z, Zhou X, Shapiro SD, Shipley JM, Twinning SS, Diaz LA, Senior RM, Werb Z (2000) The serpin α 1-proteinase inhibitor is a critical substrate for gelatinase B/MMP-9 in vivo. *Cell* 102:647–655
8. Coussens LM, Tinkle CL, Hanahan D, Werb Z (2000) MMP-9 supplied by bone marrow-derived cells contributes to skin carcinogenesis. *Cell* 103:481–490
9. Kobayashi T, Kishimoto J, Ge Y, Jin W, Hudson DL, Ouahes N, Ehama R, Shinkai H, Burgesson RE (2001) A novel mechanism of matrix metalloproteinase-9 gene expression implies a role for keratinization. *EMBO Rep* 2:604–608
10. Mohan R, Chintala SK, Jung JC, Villar WV, McCabe F, Russo LA, Lee Y, McCarthy BE, Wollenberg KR, Jester JV, Wang M, Welgus HG, Shipley JM, Senior RM, Fini ME (2002) Matrix metalloproteinase gelatinase B (MMP-9) coordinates and effects epithelial regeneration. *J Biol Chem* 277:2065–2072
11. Kobayashi T (2011) Suppression of matrix metalloproteinase-9 expression in undifferentiated, non-apoptotic keratinocytes is abrogated by the cleavage of poly(ADP-ribose) polymerase-1. *Apoptosis* 16:1205–1216
12. Kobayashi T, Hayakawa K, Tanaka A, Matsuda H (2013) Increased expression of gelatinase and caspase activities in the skin of NC/Tnd mice, a model for atopic dermatitis. *Dermatitis* 24:254–255
13. Collier IE, Wilhelm SM, Eisen AZ, Marmor BL, Grant GA, Seltzer JL, Kronberger A, He C, Bauer EA, Goldberg GI (1988) H-ras oncogene-transformed human bronchial epithelial cells (TBE-1) secrete a single metalloprotease capable of degrading basement membrane collagen. *J Biol Chem* 263:6579–6587

14. Wilhelm SM, Collier IE, Marmer BL, Eisen AZ, Grant GA, Goldberg GI (1989) SV40-transformed human lung fibroblasts secrete a 92-kDa type IV collagenase which is identical to that secreted by normal human macrophages. *J Biol Chem* 264:17213–17221
15. Salo T, Lyons JG, Rahemtulla F, Birkedal-Hansen H, Larjava H (1991) Transforming growth factor- β 1 up-regulates type IV collagenase expression in cultured human keratinocytes. *J Biol Chem* 266:11436–11441
16. Kleiner DE, Stetler-Stevenson WG (1994) Quantitative zymography: detection of picogram quantities of gelatinases. *Anal Biochem* 218:325–329
17. Kobayashi T, Hattori S, Nagai Y, Sakuraoka K, Nishikawa T (1997) Secretion of different types of gelatinases from cultured human keratinocytes. *J Dermatol* 24:213–216
18. Kobayashi T, Hattori S, Nagai Y, Tajima S, Nishikawa T (1998) Differential regulation of MMP-2 and MMP-9 gelatinases in cultured human keratinocytes. *Dermatology* 197:1–5
19. Kobayashi T, Hattori S, Nagai Y, Tajima S (2000) Differential regulation of the secretions of matrix metalloproteinase-9 and tissue inhibitor of metalloproteinases-1 from human keratinocytes in culture. *IUBMB Life* 50:221–226
20. Hattori S, Fujisaki H, Kiriya T, Yokoyama T, Irie S (2002) Real-time zymography and reverse zymography: a method for detecting activities of matrix metalloproteinases and their inhibitors using FITC-labeled collagen and casein as substrates. *Anal Biochem* 301:27–34
21. Oliver GW, Leferson JD, Stetler-Stevenson WG, Kleiner DE (1997) Quantitative reverse zymography: analysis of picogram amounts of metalloproteinase inhibitors using gelatinase A and B reverse zymograms. *Anal Biochem* 244:161–166
22. Kobayashi T, Hori H, Kanamori T, Hattori S, Takagi T, Watanabe H, Nishikawa T, Nagai Y (1993) Monoclonal antibodies to human polymorphonuclear leukocyte gelatinase (type IV collagenase) are cross-reactive with fibroblast gelatinase. *Biochem Biophys Res Commun* 193:490–496
23. Vartio T, Baumann M (1989) Human gelatinase/type IV procollagenase is a regular plasma component. *FEBS Lett* 25:285–289
24. Kobayashi T, Nishikawa T, Hattori S, Yoshida N, Takagi T, Watanabe H, Hori H, Nagai Y (2001) Systematic separation and purification of elastase, gelatinase (matrix metalloproteinase 9), and collagenase (matrix metalloproteinase 8) from polymorphonuclear leukocytes in dialyzers previously used by patients with renal failure. *Protein Expr Purif* 22:45–51

Reactive Oxygen Species (ROS) Protection via Cysteine Oxidation in the Epidermal Cornified Cell Envelope

Wilbert P. Vermeij and Claude Backendorf

Abstract

The outermost layer of our skin functions as a barrier to protect us from physical, chemical, and biological environmental insults. This protective function is mediated by the epidermal cornified cell envelope (CE) which serves both as a mechanical and permeability barrier. Recently we have discovered that the CE constitutes also a first-line antioxidant shield which relies greatly on cysteine residues in CE precursor proteins. Here we describe methods and protocols to study the cysteine-mediated antioxidant function of the CE at the level of the whole organ (the skin), individual cells (keratinocytes), or isolated proteins (SPRR family).

Keywords: SPRR proteins, Cornified cell envelope (CE), Oxidative stress, ROS regulated function, Cysteine modifications, Redox imaging

1 Introduction

Reactive oxygen species (ROS) are highly reactive molecules that are continuously generated by aerobic metabolism (1). They are one of the major endogenous threats to the integrity and stability of our DNA (2) and are therefore classified as one of the hallmarks of aging (3, 4). Not surprisingly, many age-related diseases appear to be mediated, at least in part, by oxidative stress. For example defects in genes involved in the generation of ROS (mitochondrial complex I), clearance of ROS (SOD1), and clearance of oxidative DNA damage (OGG1) have been associated with Parkinson's disease, amyotrophic lateral sclerosis, and Alzheimer's disease, respectively (5, 6). To counter oxidative stress, several mechanisms exist that can detoxify ROS and repair cellular damage. These include numerous enzymes and low-molecular-weight antioxidants that are expressed in great amount and maintain the highly reducing environment of the cellular cytoplasm (7).

Due to their reactive and transient nature, ROS can be selectively regulated in a spatial and temporal manner. As such, they can act as inter- and intracellular signaling molecules and can mediate processes that include, but are not limited to, cell migration, circadian rhythm, stem cell proliferation, and neurogenesis (1). These signaling

processes are often triggered by oxidative modifications of an amino acid side chain. Because of their unique chemical properties, thiol groups of cysteine residues are ideally suited to convert local changes in ROS levels into global cellular signals via alterations in protein structure, enzymatic activity, or binding characteristics (8–10).

Small proline-rich (SPRR) proteins were recently shown to protect keratinocytes from deleterious ROS levels (11, 12). Together with other cornified envelope precursor proteins, such as loricrin, involucrin, and the late cornified envelope (LCE) proteins, members of the SPRR protein family are cross-linked in the upper layers of the skin by transglutaminases and form a highly insoluble structure termed the cornified cell envelope (CE) (13, 14). The high amount of ROS-accessible cysteine residues in SPRR proteins, either soluble or cross-linked within the CE, adds a protective antioxidant shield to the physical and permeability barrier properties of the skin. As the SPRR proteins are, amongst others, transcriptionally regulated by Nrf2, one of the key players in the antioxidant defense system, adaptation in SPRR protein dosage seems to be central for providing optimal barrier function to diverse external insults (15–17). Also in non-cornifying tissues, cysteine residues of SPRR proteins can be modified by oxidation, allowing regulation in spatial distribution, interaction kinetics, and protein functioning (11, 18). This chapter provides the protocols that have allowed us to study these modifications.

2 Materials

Prepare all solutions using ultrapure MilliQ water (prepared by purifying deionized water to attain a sensitivity of 18 M Ω cm at 25 °C) and analytical grade reagents. Prepare and store all reagents at room temperature (unless indicated otherwise).

2.1 Redox Imaging

1. SuperFrost plus glass slides (Menzel-Glaser, Braunschweig, Germany).
2. Phosphate-buffered saline (PBS) pH 7.0 (see Note 1).
3. *N*-Ethylmaleimide (NEM; Sigma-Aldrich, Saint Louis, MO); dissolve in PBS pH 7.0 to a final concentration of 100 mM; freshly prepare and store shortly at 4 °C (see Note 2).
4. Paraformaldehyde (16 %; Thermo Fisher Scientific, Waltham, MA).
5. Tris(2-carboxyethyl)phosphine hydrochloride (TCEP, 0.5 M, pH 7.0; Sigma-Aldrich).
6. Alexa Fluor 488 Maleimide (Molecular Probes, Life Technologies, Grand Island, NY); store at –20 °C protected from light.
7. Alexa Fluor 555 Maleimide (Molecular Probes, Life Technologies); store at –20 °C protected from light.

8. Reduced thiol labeling solution: 4 % paraformaldehyde, 1 mM NEM, 5 μ M Alexa Fluor 555 Maleimide, in PBS pH 7.0; freshly prepare and temporarily store at 4 °C protected from light.
9. Oxidized thiol labeling solution: 1 mM NEM, 2 μ M Alexa Fluor 488 Maleimide, in PBS pH 7.0; freshly prepare and temporarily store at 4 °C protected from light.
10. VectaShield mounting medium (Vector Laboratories, Inc., Burlingame, CA).

2.2 SPRR Protein Production and Purification

pET16SK-vector containing various SPRR genes can be obtained on request from Dr. C. Backendorf (Leiden University).

1. *E. coli* BL21-CodonPlus(DE3)-RP competent cells (Agilent Technologies, Santa Clara, CA).
2. Chloramphenicol (Cam) stock: 25 mg/ml in 96 % ethanol.
3. Kanamycin (Km) stock: 125 mg/ml in H₂O.
4. IPTG stock 0.5 M in H₂O.
5. Sodium citrate buffer pH 3.6 (=loading buffer for purification): 25 ml 0.5 M Sodium citrate pH 3.6, 1 ml 0.5 M EDTA, 77 mg DTT (has to be added fresh each time), MilliQ water to a total volume of 500 ml.
6. Elution buffer: 1 M NaCl in loading buffer.
7. Liquid nitrogen.
8. Resource S column (GE Healthcare, Pittsburgh, PA).
9. Dialysis membrane, MWCO 6–8,000; boil dialysis membrane in 0.1 mM EDTA for 30 min. Store in 70 % ethanol at 4 °C. Wash carefully with MilliQ water before use.
10. 10 mM Sodium phosphate buffer pH 7.0. To prepare 3 l of 10 mM sodium phosphate buffer pH 7.0 mix 34.62 ml 0.5 M Na₂HPO₄ and 25.38 ml 0.5 M NaH₂PO₄ and fill up with MilliQ.

2.3 Labeling of Oxidation-Sensitive Cysteine Residues

1. H₂O₂ (35 %; Sigma-Aldrich).
2. Rose Bengal (10 mM in H₂O; Sigma-Aldrich). 500-W tungsten halogen lamp.
3. NEM (Sigma-Aldrich) (see Section 2.1 and Note 2).
4. 10 mM Sodium phosphate buffer pH 7.0 (see Section 2.2 and Note 1).
5. Dithiothreitol (DTT; Sigma-Aldrich).
6. Iodoacetamide (Sigma-Aldrich) (see Note 3).

2.4 Tryptic Digestion

1. Trichloroacetic acid (TCA) (Sigma-Aldrich).
2. Acetone (Sigma-Aldrich).

3. 8 M urea, 0.4 M ammonium bicarbonate.
4. DTT (Sigma-Aldrich).
5. Iodoacetamide (Sigma-Aldrich) (see Note 3).
6. Trypsin MS grade (Roche, Mannheim, Germany).

2.5 Redox-Sensitive Protein Interaction Analysis

1. OKF6/TERT-2 immortalized keratinocytes were a kind gift from Dr. Jim Rheinwald (Boston) (19).
2. Keratinocyte-SFM (KSFM; Gibco, Life Technologies, Grand Island, NY) with the following adaptation: Use half the amount of supplied growth factors, and add 0.3 mM CaCl₂ from a 1,000× concentrated stock.
3. PBS (Gibco, Life Technologies) (see Note 4).
4. PBS containing 0.1 mM EDTA (PBS-EDTA).
5. 0.25 % Trypsin solution (Gibco, Life Technologies) in a 1:1 mixture of PBS and PBS-EDTA.
6. PBS containing 10 % Bovine calf serum (BCS; Hyclone, Thermo Fisher Scientific, Waltham, MA).
7. NFB1 buffer: 140 mM Na₂HPO₄/NaH₂PO₄ pH 7.2, 5 mM KCl, 10 mM MgCl₂.
8. Lysis buffer: 50 mM Tris-HCl (pH 7.5), 5 mM EDTA, 250 mM NaCl, 0.1 % Triton X-100, 7 mM CaCl₂ supplemented with 5 mM NaF, 100 mM Na₃VO₄, 20 mM β-glycerophosphate, and 1 protease inhibitor cocktail tablet (Roche, Basel, Switzerland) per 10 mL of buffer, all freshly added before use; store at 4 °C.
9. 0.2 ml Strep-Tactin column (IBA, Göttingen, Germany).
10. Wash buffer: 100 mM Tris-HCl (pH 8.0), 150 mM NaCl, 1 mM EDTA supplemented with 3 mM CaCl₂; store at 4 °C.
11. Redox-elution buffer: 100 mM Tris-HCl (pH 8.0), 150 mM NaCl, 1 mM EDTA supplemented with 3 mM CaCl₂ and 50 mM DTT; prepare fresh and store at 4 °C.
12. Biotin elution buffer: 100 mM Tris-HCl (pH 8.0), 150 mM NaCl, 1 mM EDTA supplemented with 3 mM CaCl₂ and 2 mM biotin; store at 4 °C.

3 Methods

3.1 Redox In Situ Imaging of Skin Specimens

The procedure described here is based on the method first described by Mastroberardino and co-workers (20) and is ideally suited to assess global oxidation states of disulfide bonds (and their variation) in proteins at the level of a whole organ (mouse skin in this case). To obtain more detailed information about specific cysteine residues involved, redox labeling (on purified proteins/structures) should be combined with mass spectrometry, as discussed later in this chapter.

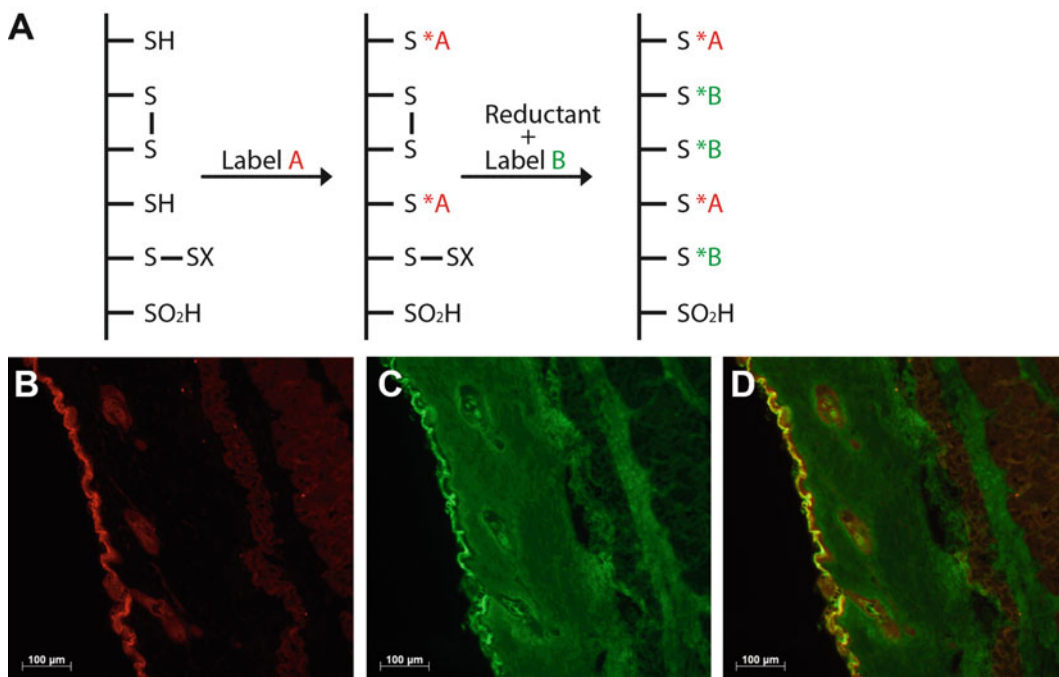


Fig. 1 In situ imaging of the redox state. **(a)** Schematic overview of the cysteine labeling strategy. Cysteine residues in the reduced form are labeled with a first maleimide-conjugated dye (shown in *red*). Subsequently, cysteine residues engaged in disulfide bonds are reduced and labeled with a second maleimide-conjugated dye (shown in *green*). **(b–d)** Representative images of murine skin specimens labeled for reduced **(b)** and oxidized **(c)** cysteine residues. The merge is shown in **(d)**. Cysteine residues in the outer layers of the epidermis, in the fat layer, and in the hair follicles are more in an oxidized state. In the cornified layer high amounts of both reduced and oxidized cysteines are present (shown by the *yellow* overlap)

1. Cut sagittal skin cryosections with a thickness of 10–15 μm , and put each section straight on a Menzel SuperFrost plus glass slide.
2. Fix every slide directly by covering the tissue in freshly prepared “reduced thiol labeling solution” (see Section 2.1) and incubate at room temperature for 30 min. With this step the free thiol groups will be labeled in red.
3. Wash the slides three times for at least 10 min in PBS pH 7.0.
4. Post-fixate for 30 min in 100 mM NEM.
5. Wash three times for 10 min in PBS pH 7.0.
6. Incubate for 20 min in 5 mM TCEP.
7. Wash three times for 5 min in PBS pH 7.0.
8. Incubate for 20 min in “oxidized thiol labeling solution” (see Section 2.1). With this step the thiols previously engaged in disulfide bonds will be labeled in green.
9. Wash three times for 5 min in PBS pH 7.0.
10. The tissue can be blocked in serum and processed further for immunohistochemistry or directly mounted for imaging using VectaShield (see Fig. 1).

3.2 SPRR Protein Production

1. Clone the cDNA sequence of the gene of interest behind the T7 polymerase sequence of a pET16SK-vector and transform to *E. coli* strain BL21-CodonPlus(DE3)-RP (see Note 5).
2. Grow an overnight culture at 30 °C in 50 ml LC medium containing 50 µg/ml kanamycin (Km) and 25 µg/ml chloramphenicol (Cam).
3. Dilute in 2 l LC medium containing 50 µg/ml Km and 25 µg/ml Cam, and mix well.
4. Regularly measure the OD600 of the bacterial culture.
5. Grow the bacteria at 37 °C until an OD600 between 0.4 and 0.55 is reached.
6. Add IPTG to a final concentration of 0.4 mM, and continue growth of the culture for another 3–4 h (see Note 6).
7. Centrifuge the bacteria at 32,000 × *g* for 15 min at 4 °C.
8. Discard the supernatant, and resuspend the pellet in 40 ml sodium citrate buffer pH 3.6.
9. Freeze in liquid nitrogen.
10. Thaw in a water bath of 37 °C, and repeat this procedure another two times.
11. Centrifuge at 3,500 × *g* for 20 min at 4 °C.
12. Ultracentrifuge the supernatant at 92,000 × *g* for 30 min at 4 °C with a Ti60 Beckman rotor.
13. Store the supernatant at –80 °C, in portions of 10 ml, for further purification.

3.3 SPRR Protein Purification

1. Wash a 6 ml Resource S column with 20 ml MilliQ water using an AKTA FPLC station (GE Healthcare Life Sciences) and a flow rate of 2 ml/min.
2. Wash the system with 20 ml ice-cold loading buffer (see Section 2.2).
3. Load 10 ml of the SPRR protein solution on the Resource S column.
4. Wash the system with 20 ml ice-cold loading buffer.
5. Apply a 40 ml salt gradient to a final concentration of 1 M NaCl (see Section 2.2), collect all elution fractions, and store on ice immediately. The purity of the elution fractions can be determined by analyzing aliquots on PAGE.
6. Pool the SPRR protein containing pure fractions and apply to a dialysis membrane.
7. Dialyze overnight at 4 °C in 10 mM sodium phosphate buffer pH 7.0.

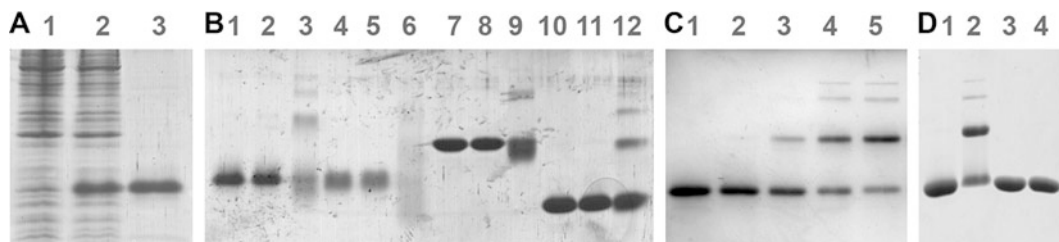


Fig. 2 Multimerization of purified SPRR proteins is mediated via cysteine oxidation. (a) SPRR1B protein production, before (*lane 1*) and 3 h after (*lane 2*) IPTG induction. The subsequently purified fraction is shown in *lane 3*. (b) Multimerization of SPRR1B (*lanes 1–3*), SPRR2A (*lanes 4–6*), SPRR3 (*lanes 7–9*), and SPRR4 (*lanes 10–12*). Equal amount of protein untreated (*lanes 1, 4, 7, and 10*), treated with Rose Bengal without light (*lanes 2, 5, 8, and 11*), and treated with Rose Bengal with white light irradiation to induce oxidation by the generation of singlet oxygen (*lanes 3, 6, 9, and 12*). (c) SPRR4 protein without (1) and with increasing concentration of H₂O₂ (*lane 2*: 2.4 mM, *lane 3*: 4.7 mM, *lane 4*: 9.0 mM, *lane 5*: 17.5 mM). (d) Multimerization of SPRR4 by 20 mM H₂O₂ (*lanes 2 and 4*) is mediated via disulfide bond formation of cysteine residues and cannot be formed after NEM modification (*lanes 3 and 4*). All samples were loaded on gel using sample buffer without β-mercaptoethanol due to the reversible nature of disulfide bonds

8. Determine the protein concentration by diluting and measuring the A230 and A260. The concentration could be calculated with the following formula: $[(187 \times A260) - (81.7 \times A230)] \times \text{dilution}/1,000 = \text{concentration in } \mu\text{g}/\mu\text{l}$ (21).
9. Store SPRR protein samples at -80°C in small vials.

3.4 Labeling of Oxidation-Sensitive Cysteine Residues in Purified Proteins

SPRR proteins are eager to multimerize via the formation of intramolecular disulfide bonds. However, upon oxidation also intermolecular disulfide bonds will be formed. The following technique was used to determine which cysteine residues of SPRR proteins are involved in the formation of intra- and intermolecular disulfide bonds.

1. Apply a gradient of H₂O₂ (ranging from 0 to 100 mM), or any other type of oxidant, to 12 pmol of SPRR protein (see Note 7).
2. Incubate all samples on ice for 10 min during this oxidation step.
3. Singlet oxygen was produced by irradiating 12 pmol of SPRR protein in a 10 mM solution of Rose Bengal for 2 min with a 500-W tungsten halogen lamp.
4. Load the diversely oxidized samples on PAGE, using loading buffer without β-mercaptoethanol, and visualize the different protein bands with Coomassie Brilliant Blue G/R 250 staining (see Note 8 and Fig. 2).

5. Excise the bands of interest from gel, and cut each band separately into small pieces.
6. Incubate the gel pieces for 30 min in 20 mM NEM.
7. Wash three times in 10 mM sodium phosphate buffer pH 7.0.
8. Incubate for 30 min in 45 mM DTT.
9. Wash three times in 10 mM sodium phosphate buffer pH 7.0.
10. Incubate for 20 min in 100 mM iodoacetamide in the dark. In this way, free thiols can be recognized by NEM labeling and cysteine residues originally engaged in disulfide bonds by IAA labeling (see Note 9).
11. Extract the labeled SPRR peptides after in-gel tryptic digestion as described in detail by Shevchenko and co-workers (22), and identify the peptide masses and sequences by Orbitrap tandem mass spectrometry (23). Cysteine modifications of SPRR4 peptides were manually identified in Xcalibur (Thermo Fisher Scientific, Waltham, MA) by using the SPRR4 protein sequence (NCBI accession no. AF335109) and the calculated peptide masses (18).

3.5 Labeling of Oxidation-Sensitive Cysteine Residues in Isolated CEs

CEs can be easily purified from sunburned peeled skin, by boiling the skin pieces in 100 mM Tris-Cl (pH 7.5), 2 % SDS, 1 mM EDTA, and 10 mM DTT in a polypropylene tube (use a 50-fold vol/vol excess of buffer) (see Note 10).

3.5.1 CE Preparation (24)

1. Boil with frequent mixing for 5–10 min until most of the small skin pieces have disappeared and a homogenous suspension of CEs is obtained.
2. Transfer to polystyrene tube (see Note 11).
3. Pellet for 5 min at $3,5000 \times g$ in Sigma centrifuge (10 ml tubes).
4. Wash 2 \times in boiling buffer at RT.
5. Wash 1 \times in PBS. CEs can be stored indefinitely at 4 °C as a damp pellet.

3.5.2 Oxidation-Selective Cysteine Labeling

6. Take up the CEs in PBS, and generate smaller CE fragments by sonication in a Sonics Vibra-Cell VCX 750 sonicator by using a tapered 3 mm microtip for 60 s at a 30 % amplitude.
7. Incubate the CE fragments on ice for 10 min in 10 mM H₂O₂.
8. Centrifuge at maximum speed using an Eppendorf centrifuge, and wash in 10 mM sodium phosphate buffer pH 7.0.
9. Incubate for 30 min in 20 mM NEM.
10. Centrifuge at maximum speed, and wash in 10 mM sodium phosphate buffer pH 7.0.
11. Incubate for 30 min in 45 mM DTT.

12. Centrifuge at maximum speed, and wash in 10 mM sodium phosphate buffer pH 7.0.
13. Incubate for 20 min in 100 mM iodoacetamide in the dark.

By following this approach non-oxidizable cysteine residues will be labeled by NEM, whereas cysteines involved in disulfide bonds can be recognized via IAA labeling.

3.6 In-Solution Tryptic Digestion for MS Analysis

1. Precipitate protein and/or CE samples by addition of TCA to a final concentration of 10 % and incubate at 4 °C for 1 h.
2. Centrifuge for 30 min at maximum speed at 4 °C using an Eppendorf centrifuge.
3. Resuspend the pellet in 200 µl ice-cold 100 % acetone by vortexing.
4. Incubate the sample for 20 min at -20 °C.
5. Centrifuge for 20 min at maximum speed at 4 °C. Remove the supernatant, and repeat steps 3–5 two more times.
6. Dry the pellet at room temperature. This should take approximately 20 min.
7. Resuspend the pellet in 25 µl 8 M urea and 0.4 M ammonium bicarbonate, and confirm the pH by pipetting 1–2 µl sample on pH paper. The pH should be between 7.5 and 8.5.
8. For samples containing none labeled cysteine residues (such as obtained from Section 3.7) add 5 µl of 45 mM DTT and incubate for 30 min at 37 °C. Let the samples cool down to room temperature, add 5 µl of 100 mM iodoacetamide, and incubate for 20 min in the dark.
9. Adjust the total volume to 95 µl with ultrapure MilliQ water.
10. Add a 1:25 enzyme to protein weight-to-weight ratio of trypsin in a volume of 5 µl.
11. Incubate at 37 °C for 16–24 h.
12. Stop the reaction by freezing, StageTip purification (25), or injecting the peptides directly onto the reverse-phase HPLC column of the LTQ-Orbitrap (Thermo Fisher Scientific) tandem mass spectrometer (23). Database searching against all human entries in Swiss-Prot was performed using Mascot (26) (Matrix Science, Boston, MA) (see Note 12).

3.7 In Vivo Detection of Redox-Sensitive Protein Interactions

1. Use the pEXPR-IBA105-vector (IBA, Göttingen, Germany) with the full-length SPRR sequence cloned between the BsaI and HindIII restriction sites of the multiple cloning sequence. In this way a streptavidin-tag is added to the N-terminus of the SPRR protein (18). The plasmids are available on request.

2. Culture immortalized OKF keratinocytes (OKF6/TERT-2) (a kind gift from Dr. Jim Rheinwald (Boston) in defined keratinocyte-SFM (KSFM) at 37 °C, 5 % CO₂ until subconfluency (19).
3. Wash the cells subsequently with 10 ml of PBS and 10 ml of PBS-EDTA. Add 1 ml of trypsin solution for a 100 mm culture dish and incubate at 37 °C for approximately 5–10 min. Check microscopically whether the cells have detached.
4. Inactivate the trypsin by adding at least ten volumes of PBS containing 10 % BCS.
5. Take up 2×10^6 cells in NFB1 buffer, add 5 µg of the above-mentioned plasmid, and mix gently.
6. Transfect the keratinocytes by electroporation using the Nucleofector™ 2b Device (Lonza AG, Cologne, Germany) by using program T-007 (see Notes 13 and 14).
7. Seed the cells in a 100 mm culture dish with 10 ml of KSFM and incubate at 37 °C, 5 % CO₂, for approximately 48 h (see Note 15).
8. Wash the cells twice with cold PBS, completely remove all PBS, and add 0.5 ml lysis buffer for maximally 10^9 cells.
9. Scrape the cells with a rubber police man to one side of the dish and pipet into an Eppendorf tube. Homogenize the samples with a 0.4 mm syringe, and centrifuge the lysate at $3,500 \times g$ for 10 min at 4 °C to pellet the cellular debris. Store on ice until further use.
10. Equilibrate a 0.2 ml Strep-Tactin column with 0.4 ml cold wash buffer. If possible perform the whole purification procedure in a cold room.
11. Load the soluble cell extract (from step 9) onto the column, and wait until all of the cell extract has entered the column.
12. Wash the column five times with 0.2 ml wash buffer.
13. Elute all proteins interacting via or stabilized by disulfide bonds by addition of 0.6 ml redox elution buffer (see Section 2.5). Collect the eluate in several fractions and store on ice.
14. Add 0.6 ml biotin elution buffer to elute all other interaction partners or complexes (either covalently linked or not), collect the eluate in several fractions, and store on ice.
15. Digest proteins as described above (see Section 3.6), and analyze the peptides by mass spectrometry (see Note 16).

The approach allows the identification of proteins that interact with the protein of interest (SPRR in this case) via disulfide bridges (eluted in fraction 1).

4 Notes

1. A correct pH is very important to avoid aspecific reactions.
2. NEM dissolves in water (>100 mM); however, aqueous solutions could be unstable. The rate of hydrolysis depends significantly on the pH.
3. Iodoacetamide can react at low rates with histidine residues.
4. Be careful not to use PBS brands that contain CaCl₂, as calcium can drive terminal differentiation of keratinocytes.
5. For several SPRR and other CE genes such as loricrin and involucrin full-length cDNA sequences were cloned between the EcoRI and NcoI restriction sites of the multiple cloning site of the pET16SK-vector.
6. Save samples before and after IPTG induction to visualize the protein production using PAGE. Protein samples can be prepared by adding 100 µl Laemmli buffer for every 0.5 OD.
7. For the identification of naturally oxidized cysteine residues the oxidation step with H₂O₂ should be omitted.
8. Commassie Brilliant Blue comes in two varieties, G 250 (greenish tint) or R 250 (redish tint). G250 differs chemically from R 250 by the presence of two methyl groups. The R variant is more sensitive for SPRR protein detection.
9. Thiols, oxidized to sulfenic, sulfinic, or sulfonic acid, are not affected by NEM or IAA treatments.
10. Note the reducing character of this buffer (10 mM DTT), which means that CEs will lose all oxidized cysteine residues during the purification procedure and are as such isolated in their native form (as composites of transglutaminase cross-linked proteins and lipids).
11. CEs stick to polypropylene.
12. The following Mascot parameters were used: peptide tolerance 2 ppm, MS/MS tolerance 0.5 Da, variable NEM and IAA modifications (C), variable oxidation (M), two missed cleavages allowed, decoy database option on. The MudPIT scoring algorithm was used with an ion score cutoff of 20, with required bold red only.
13. When more cells are required simply use more cuvettes containing 2×10^6 cells 5 µg of plasmid DNA in NFB1 buffer.
14. Include at least an empty vector control, solely expressing the Strep-tag.
15. Stable cell lines could be generated using neomycin selection.
16. For protein identification on silver-stained PAGE excise bands not present in mock (untransfected) control lysates for analysis.

Acknowledgements

The authors would like to thank all present and former members of the Molecular Cell Signaling group at Molecular Genetics (Leiden Institute of Chemistry), who have contributed to the establishment and testing of the protocols described here, and all current members of the Aging group at Genetics (ErasmusMC, Rotterdam). Bobby Florea (Biosyn, LIC) is acknowledged for his help with the mass spectrometer.

References

- Dickinson BC, Chang CJ (2011) Chemistry and biology of reactive oxygen species in signaling or stress responses. *Nat Chem Biol* 7 (8):504–511. doi:nchembio.607 [pii] 10.1038/nchembio.607
- Hoeijmakers JH (2009) DNA damage, aging, and cancer. *N Engl J Med* 361 (15):1475–1485. doi:361/15/1475 [pii] 10.1056/NEJMra0804615
- Lopez-Otin C, Blasco MA, Partridge L, Serrano M, Kroemer G (2013) The hallmarks of aging. *Cell* 153(6):1194–1217. doi:S0092-8674(13)00645-4 [pii] 10.1016/j.cell.2013.05.039
- Harman D (1956) Aging: a theory based on free radical and radiation chemistry. *J Gerontol* 11(3):298–300
- Finkel T, Holbrook NJ (2000) Oxidants, oxidative stress and the biology of ageing. *Nature* 408(6809):239–247. doi:10.1038/35041687
- Jacob KD, Noren Hooten N, Tadokoro T, Lohani A, Barnes J, Evans MK (2013) Alzheimer's disease-associated polymorphisms in human OGG1 alter catalytic activity and sensitize cells to DNA damage. *Free Radic Biol Med* 63:115–125. doi:S0891-5849(13)00220-7 [pii] 10.1016/j.freeradbiomed.2013.05.010
- Paget MS, Buttner MJ (2003) Thiol-based regulatory switches. *Annu Rev Genet* 37:91–121. doi:10.1146/annurev.genet.37.110801.142538
- Winterbourn CC, Hampton MB (2008) Thiol chemistry and specificity in redox signaling. *Free Radic Biol Med* 45(5):549–561. doi:S0891-5849(08)00280-3 [pii] 10.1016/j.freeradbiomed.2008.05.004
- Winyard PG, Moody CJ, Jacob C (2005) Oxidative activation of antioxidant defence. *Trends Biochem Sci* 30(8):453–461. doi:S0968-0004(05)00180-5 [pii] 10.1016/j.tibs.2005.06.001
- D'Autreaux B, Toledano MB (2007) ROS as signalling molecules: mechanisms that generate specificity in ROS homeostasis. *Nat Rev Mol Cell Biol* 8(10):813–824. doi:nrm2256 [pii] 10.1038/nrm2256
- Vermeij WP, Backendorf C (2010) Skin cornification proteins provide global link between ROS detoxification and cell migration during wound healing. *PLoS One* 5(8):e11957. doi:10.1371/journal.pone.0011957
- Vermeij WP, Alia A, Backendorf C (2011) ROS quenching potential of the epidermal cornified cell envelope. *J Invest Dermatol* 131 (7):1435–1441. doi:jid2010433 [pii] 10.1038/jid.2010.433
- Candi E, Schmidt R, Melino G (2005) The cornified envelope: a model of cell death in the skin. *Nat Rev Mol Cell Biol* 6(4):328–340. doi:nrm1619 [pii] 10.1038/nrm1619
- Kalinin AE, Kajava AV, Steinert PM (2002) Epithelial barrier function: assembly and structural features of the cornified cell envelope. *Bioessays* 24(9):789–800. doi:10.1002/bies.10144
- Schafer M, Farwanah H, Willrodt AH, Huebner AJ, Sandhoff K, Roop D, Hohl D, Bloch W, Werner S (2012) Nrf2 links epidermal barrier function with antioxidant defense. *EMBO Mol Med* 4(5):364–379. doi:10.1002/emmm.201200219
- Huebner AJ, Dai D, Morasso M, Schmidt EE, Schafer M, Werner S, Roop DR (2012) Amniotic fluid activates the nrf2/keap1 pathway to repair an epidermal barrier defect in utero. *Dev Cell* 23(6):1238–1246. doi:S1534-5807(12)00522-9 [pii] 10.1016/j.devcel.2012.11.002
- Cabral A, Voskamp P, Cleton-Jansen AM, South A, Nizetic D, Backendorf C (2001) Structural organization and regulation of the small proline-rich family of cornified envelope precursors suggest a role in adaptive barrier function. *J Biol*

- Chem 276(22):19231–19237. doi:[10.1074/jbc.M100336200](https://doi.org/10.1074/jbc.M100336200) [M100336200](https://doi.org/10.100336200) [pii]
18. Vermeij WP, Florea BI, Isenia S, Alia A, Brouwer J, Backendorf C (2012) Proteomic Identification of in Vivo Interactors Reveals Novel Function of Skin Cornification Proteins. *J Proteome Res.* doi:[10.1021/pr300310b](https://doi.org/10.1021/pr300310b)
 19. Dickson MA, Hahn WC, Ino Y, Ronfard V, Wu JY, Weinberg RA, Louis DN, Li FP, Rheinwald JG (2000) Human keratinocytes that express hTERT and also bypass a p16(INK4a)-enforced mechanism that limits life span become immortal yet retain normal growth and differentiation characteristics. *Mol Cell Biol* 20(4):1436–1447
 20. Mastroberardino PG, Orr AL, Hu X, Na HM, Greenamyre JT (2008) A FRET-based method to study protein thiol oxidation in histological preparations. *Free Radic Biol Med* 45(7):971–981. doi:[S0891-5849\(08\)00364-X](https://doi.org/10.1016/j.freeradbiomed.2008.06.018) [pii] [10.1016/j.freeradbiomed.2008.06.018](https://doi.org/10.1016/j.freeradbiomed.2008.06.018)
 21. Kalb VF Jr, Bernlohr RW (1977) A new spectrophotometric assay for protein in cell extracts. *Anal Biochem* 82(2):362–371
 22. Shevchenko A, Tomas H, Havlis J, Olsen JV, Mann M (2006) In-gel digestion for mass spectrometric characterization of proteins and proteomes. *Nat Protoc* 1(6):2856–2860. doi:[nprot.2006.468](https://doi.org/10.1038/nprot.2006.468) [pii] [10.1038/nprot.2006.468](https://doi.org/10.1038/nprot.2006.468)
 23. Florea BI, Verdoes M, Li N, van der Linden WA, Geurink PP, van den Elst H, Hofmann T, de Ru A, van Veelen PA, Tanaka K, Sasaki K, Murata S, den Dulk H, Brouwer J, Ossendorp FA, Kisselev AF, Overkleeft HS (2010) Activity-based profiling reveals reactivity of the murine thymoproteasome-specific subunit beta5t. *Chem Biol* 17(8):795–801. doi:[S1074-5521\(10\)00257-7](https://doi.org/10.1016/j.chembiol.2010.05.027) [pii] [10.1016/j.chembiol.2010.05.027](https://doi.org/10.1016/j.chembiol.2010.05.027)
 24. Mehrel T, Hohl D, Rothnagel JA, Longley MA, Bundman D, Cheng C, Lichti U, Bisher ME, Steven AC, Steinert PM et al (1990) Identification of a major keratinocyte cell envelope protein, loricrin. *Cell* 61(6):1103–1112. doi:[0092-8674\(90\)90073-N](https://doi.org/10.1016/0092-8674(90)90073-N) [pii]
 25. Rappsilber J, Mann M, Ishihama Y (2007) Protocol for micro-purification, enrichment, pre-fractionation and storage of peptides for proteomics using StageTips. *Nat Protoc* 2(8):1896–1906. doi:[nprot.2007.261](https://doi.org/10.1038/nprot.2007.261) [pii] [10.1038/nprot.2007.261](https://doi.org/10.1038/nprot.2007.261)
 26. Perkins DN, Pappin DJ, Creasy DM, Cottrell JS (1999) Probability-based protein identification by searching sequence databases using mass spectrometry data. *Electrophoresis* 20(18):3551–3567. doi:[10.1002/\(SICI\)1522-2683\(19991201\)20:18<3551::AID-ELPS3551>3.0.CO;2-2](https://doi.org/10.1002/(SICI)1522-2683(19991201)20:18<3551::AID-ELPS3551>3.0.CO;2-2) [pii] [10.1002/\(SICI\)1522-2683\(19991201\)20:18<3551::AID-ELPS3551>3.0.CO;2-2](https://doi.org/10.1002/(SICI)1522-2683(19991201)20:18<3551::AID-ELPS3551>3.0.CO;2-2)

Modified Methods for Growing 3-D Skin Equivalents: An Update

Rebecca Lamb and Carrie A. Ambler

Abstract

Artificial epidermis can be reconstituted *in vitro* by seeding primary epidermal cells (keratinocytes) onto a supportive substrate and then growing the developing skin equivalent at the air–liquid interface. *In vitro* skin models are widely used to study skin biology and for industrial drug and cosmetic testing. Here, we describe updated methods for growing 3-dimensional skin equivalents using de-vitalized, de-epidermalized dermis (DED) substrates including methods for DED substrate preparation, cell seeding, growth conditions, and fixation procedures.

Keywords: Skin, Keratinocyte, Skin equivalent, DED, Epithelial, Differentiation, Stratification, Organ culture

1 Introduction

The ability to differentiate cultured primary cells into artificial tissues or mini-organs has made a tremendous impact in the field of stem cell research (reviewed in ref. 1, 2). Further, tissue-engineered, artificial skins generated from human epidermal keratinocytes are vital tools in industrial and commercial research for product and pharmaceutical testing (3–5). Methods to generate artificial skin equivalents were first described in the early 1980s (6–9), and although refinements have been made over the past three decades, the same basic technique is still in use today—primary epidermal cells are seeded onto a supportive substrate, and then the developing epidermis is grown at the air–liquid interface to promote differentiation and production of barrier proteins and surface lipids (9). The composition of the supporting substrate can vary and can be completely artificial or biologically derived (1). Common substrates include engineered dermal equivalents, often collagen gels embedded with fibroblasts cells, and de-vitalized, de-epidermalized dermis (DED). One advantage in using DEDs is that they retain the extracellular matrix proteins and tissue architecture (undulating rete-ridge patterning) of the vital dermis. Keratinocytes grown on

DEDs differentiate into a fully stratified epidermis with basal, spinous, granular, and cornified cell layers (9, 10).

Classic epidermal keratinocyte growth conditions, first developed in the 1970s by James Rheinwald and Howard Green, require fibroblast feeder support and serum-containing growth media (11). In the past decade in the effort to reduce potential xenobiotic contaminants in cell culture, a range of serum-free, feeder-free growth media have been developed to support growth and clonal expansion of human keratinocytes. Here, we present updated methods for reconstituting skin on DEDs including DED substrate preparation, cell seeding, skin equivalent growth conditions, and preparing the DED for analysis. We find that primary epidermal keratinocytes isolated and propagated in either serum-containing or serum-free media stratify and differentiate into reconstituted skin tissues when seeded on DEDs and grown in the presence of 10 % serum. By 7 days after seeding, keratinocytes grown on DEDs have differentiated into a fully stratified epidermis with basal, spinous, granular, and cornified cell layers as detected by histological and antibody staining. We find that the constituents of the basal medium can vary, but serum is required for cells to stratify in 3-D cultures. Further we found that the epidermis was thicker and organization was improved when serum was heat-inactivated prior to use (10). Reconstituted skins can be maintained for up to 28 days in vitro. We include methods for cryopreservation and tissue fixation suitable for a range of tissue analysis protocols.

2 Materials and Equipment

It is recommended that a lab coat and gloves should be worn at all times while doing these procedures. As primary human cells and tissues will be used, appropriate personal protective equipment must be used and procedures carried out according to laboratory health and safety regulations. Work should be carried out at room temperature, unless otherwise stated.

2.1 General Lab Consumables and Equipment

- Sterile phosphate-buffered saline (PBS) pH 7.2 (1×) endotoxin-free purchased from an outside source. See Note 1.
- 1× PBS: Dilution of a 10× stock. 10× PBS: Weigh 80 g sodium chloride, add 2 g potassium chloride, add 14.4 g sodium phosphate dibasic and 2.4 g potassium phosphate monobasic, make up to 1 l with distilled H₂O. This needs to be autoclaved and then diluted 1 in 10 with sterile water.
- Xylene.
- Graded alcohol series, 100, 95, and 70 % ethanol (diluted with distilled water).

- Distilled H₂O (double distilled).
- Plastic beakers and glass bottles.
- Petri dish (9 cm).
- Cryovial (2 ml).
- Sterile centrifuge tube (50 ml).
- Water bath.
- Microbiological safety cabinet.
- 37 °C incubator with 5 % CO₂.
- Centrifuge, capable of spinning 50 ml centrifuge tubes.

2.2 Method-Specific Consumables and Equipment

2.2.1 DED Preparation

- Human skin. See Note 2.
- 10 % Povidone-iodine solution. See Note 3.
- Sterilized forceps. See Note 4.
- Disposable sterile scalpels.
- Liquid nitrogen.

2.2.2 Primary Epidermal Keratinocyte Propagation

- Human epidermal keratinocytes. See Note 5.
- KGM-Gold media (basal medium supplemented with bovine pituitary extract, human epidermal growth factor, bovine insulin, hydrocortisone, gentamicin, amphotericin-B, epinephrine, and transferrin).
- Alternatively cells can be grown in FAD+ cell culture media: made from three parts Dulbecco's modified Eagle's medium (DMEM) to one part Ham's F12 medium (F12) supplemented with 1.8×10^{-4} M adenine, 100 IU/ml penicillin, 100 µg/ml streptomycin, 10 % fetal bovine serum, 0.5 µg/ml hydrocortisone, 8.47 ng/ml cholera enterotoxin, epidermal 10 ng/ml growth factor, and 5 µg/ml insulin. See Note 6.
- Type 1 rat tail collagen (>95 %). Diluted 1 in 100 in endotoxin-free PBS and then filter sterilized with a 0.2 µm filter.
- T-25 tissue culture flasks.
- Trypsin-EDTA (0.25 %). This is diluted 1 in 3 using endotoxin-free PBS prior to use.
- Hemocytometer.
- Fetal bovine serum. See Note 7.
- Inverted tissue culture microscope with phase contrast.

2.2.3 Skin Reconstitution on DEDs

- 6-well plate and 6-well inserts (pore size 3.0 µM). See Note 8.

2.2.4 Embedding and Sectioning

- 4 % paraformaldehyde (PFA). PFA is a harmful irritant, so this procedure needs to be done in a fume hood. Weigh out 4 g PFA adding 1× sterile PBS to a final volume of 100 ml. pH the mixture to pH7.6. Place the PFA into a 60–65 °C water bath, mixing well every 5 min until the liquid is clear. See Note 9. Aliquot the PFA into falcon tubes and then freeze at –20 °C until use.
- OCT (cryoprotective embedding medium). See Note 10.
- Isopentane.
- Disposable base moulds 24 mm × 24 mm for tissue embedding.
- Tissue embedding/processing cassettes.
- Tissue processor, program: alcohol 1 h × 6, xylene 1 h × 3, wax 1 h 20 min × 3. See Note 11.
- Microtome.
- Microtome blades.
- Charged microscope slides.

2.2.5 Histological Staining

- Harris hematoxylin solution (7 g/l certified hematoxylin).
- Acid alcohol (1 % hydrochloric acid in 70 % EtOH).
- Eosin y solution (0.5 % (w/v) in water).
- DPX mounting solution.
- Cover slips (25 × 50 mm).

3 Methods

3.1 DED Preparation

This procedure should be done in a Category 2 facility in a microbiological safety cabinet.

Before starting the procedure:

- Turn water bath on to 56 °C.
- Place 250 ml of sterile PBS into a 500 ml bottle and pre-warm the PBS to 56 °C.
- Prepare in four 500 ml beakers (volume needs to be sufficient to completely cover the piece of skin).
 - (a) 1 % Povidone-iodine (1:10 dilution of stock solution in sterile water).
 - (b) 70 % Ethanol.
 - (c) PBS.

Begin Procedure:

- If required cut the skin into pieces of approximately 80 cm².

- Place skin in a 9 cm petri dish with the epidermis side down. It is important to remove the fat by gently scraping it away using a disposable scalpel. Alternatively the fat can be cut away by lifting the dermal side of the tissue with forceps and cutting away the fat with sterile tissue scissors.
- The skin is then sterilized by transferring skin through a series of solutions:
 - 1 % Povidone-iodine solution for 30 s.
 - 70 % ethanol for 10 s.
 - 70 % ethanol for 10 s.
 - PBS for 30 s.
- The skin is then placed in the pre-warmed PBS, which is then placed in the 56 °C water bath for 30 min.
- Following incubation the tissue is placed into a new petri dish, dermal side down. Using forceps, peel away the epidermis from the dermis. See Note 12. Discard the epidermis.
- Using sterile disposable scalpels cut the tissue into approximately 1 cm² pieces and then place each piece into a screw top cryovial and freeze in liquid nitrogen.
- The samples need to go through 10× freeze/thaw cycles of liquid nitrogen to room temperature, which do not need to be done in a flow hood. This step ensures that no viable cells remain.

Any excess skin needs to be disposed of according to local regulations pertaining to human tissues.

3.2 Primary Epidermal Keratinocyte Propagation

This procedure should be done in a Category 2 facility using sterile culturing conditions in a microbiological safety cabinet. Here we detail procedures using purchased neonatal human epidermal keratinocytes (NHEKs) grown under serum-free conditions. See Note 13.

- Collagen-coat T25 tissue culture flasks. 3 ml of the diluted collagen is used to collagen coat a T25 flask, see Note 14. When ready to culture the cells, remove the collagen, wash the flask with 4 ml of purchased PBS, remove PBS, and then add 5 ml of KGM-Gold media.
- Pre-warm the KGM-Gold and purchased PBS in a 37 °C water bath.
- Turn on microbiological safety cabinet 15 min prior to using.
- To 9 ml of your KGM-Gold media and add 1 ml (10 %) of FBS to act as a trypsin inhibitor.
- Remove NHEK cells from –150 °C in a liquid nitrogen storage vessel and thaw immediately in a 37 °C water bath.

- When no ice crystals remain, resuspend the cells in the cryovial and add to an appropriate number of pre-prepared T-25 flasks according to the manufacturer's instructions. See Note 15.
- Place the flasks in a 37 °C incubator with 5 % CO₂, changing the media every 2–3 days until the cells are approximately 70–80 % confluent.
- Once 70–80 % confluent, remove the media and wash the cells with 4 ml of endotoxin-free PBS. Next remove PBS and add 1 ml of the diluted trypsin–EDTA, making sure that the trypsin covers the entire bottom of the flask. Put the flask back into the incubator for 1–2 min.
- Gently tap the side of the flask, and check that the cells have detached using an inverted microscope. If not, put the flask back into the incubator for an additional minute. It is important not to expose the cells to the trypsin for too long as it can damage the cells.
- Once the cells are detached, the trypsin solution is inactivated by adding 3 ml of KGM-Gold + 10 % FBS. Pipette this media gently over the bottom of the flask a few times to ensure that the cells have been completely removed.
- Pipette up the media containing the detached cells, place into a sterile centrifuge tube, and centrifuge at $200 \times g$ for 5 min.
- Remove the supernatant, being careful not to disturb the pellet of cells.
- Add 3 ml of KGM-Gold to the cells, and carefully resuspend the cell pellet by pipetting up and down several times. It is important that the cells do not clump together.
- Using a p20 pipette, suck up 20 µl of the resuspended cells. See Note 16.
- Add 10 µl to a hemocytometer. Count cells and calculate the number per ml.
- These cells are now ready to be seeded onto the DED, frozen down (in FBS with 10 % DMSO), or used to maintain the cells in culture. See Note 17.

3.3 Skin Reconstitution on DEDs

1. Defrost a piece of the prepared DED. Using sterile forceps and a scalpel trim the DED so that there is no fat on the bottom and it will sit flat on the insert. Dispose of any excess skin according to local health and safety procedures.
2. Place DED onto a 3.0 µM pore size insert that has been placed inside a well of a 6-well plate (Fig. 1).
3. Using the cells in suspension from Section 3.2, step 12, remove and centrifuge 300,000 cells at $200 \times g$ for 5 min.

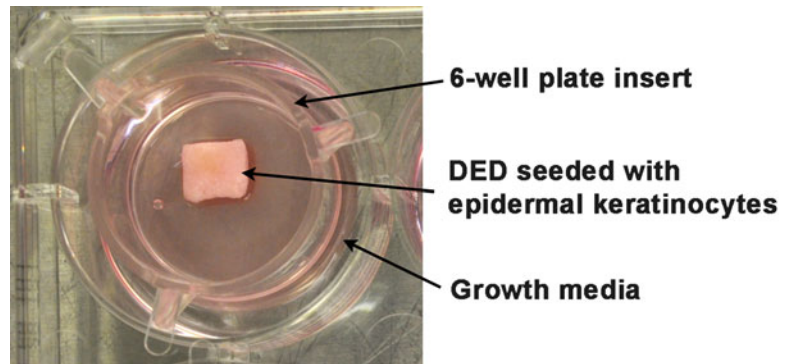


Fig. 1 Photograph of a DED on the tissue culture apparatus. Note DED sits on a 6-well plate insert membrane and culture media is added and removed in the space between the insert and the side of the well

4. Gently remove as much of the supernatant as possible by vacuum suction or using a micro pipette so that approximately 10 μl of media remains covering the cell pellet. Gently loosen and disassociate the cell pellet in the remaining media using a p20 pipette.
5. Pipette the cells and media on top of the DED, in the center. See Note 18.
6. Add 1 ml of FAD+ cell culture media between the insert and the inside wall of the well, and ensure that the media has gone underneath the insert. Be careful not to put media on top of the DED or in the insert.
7. Place the lid on top of the 6-well plate and carefully transfer the plate into a 37 °C incubator with 5 % CO₂.
8. Leave the DED in the incubator for 7–28 days. Change the growth media every 2–3 days.

3.4 Embedding and Sectioning

Once the cells have been growing on the DEDs for 7–28 days, the tissue needs to be fixed for analysis. There are two methods to do this which either result in frozen sections or paraffin-embedded sections. It is possible to cut the DED in half and perform both fixative methods on the same DED (Fig. 2).

3.4.1 Frozen Sections

1. Fill up the well in a disposable base mould with OCT.
2. With sterile forceps, gently pick up the DED and place it into the OCT as shown in the below diagram. It is important that the surface of the DED that the cells have been growing on is at 90° to the base of the mould for sectioning.
3. Pour some isopentane into a beaker and lower beaker into a flask of liquid nitrogen. Care must be taken while handling liquid nitrogen, so ensure that the correct gloves and safety

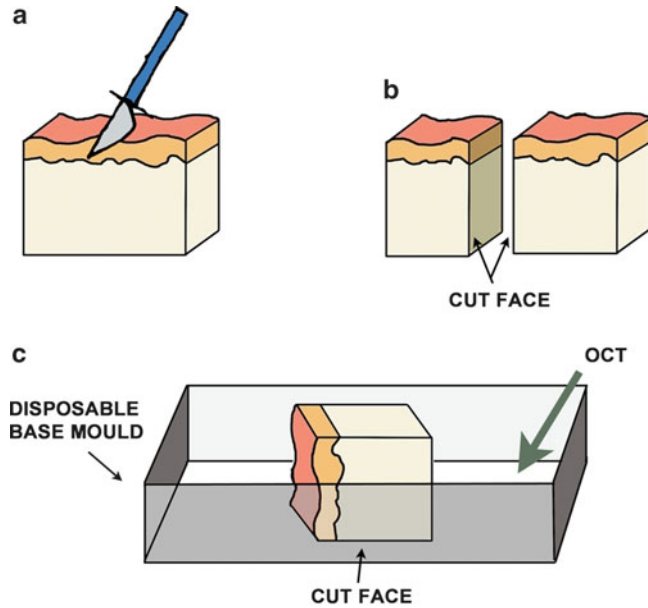


Fig. 2 Preparation of DEDs for tissue analysis. Bisect the DED across the center of the tissue using a disposable scalpel (a) making sure to note which side of the resulting tissues are the cut faces (b). This is important as the epidermis formed on the DED center should be analyzed. DEDs are next fixed in appropriate fixative prior to dehydration and embedding in paraffin wax (not shown) or placed immediately in a disposable base mould and cryoembedded in OCT (c)

goggles are worn. Allow isopentane to reach -150 to -160 °C.

4. Using forceps pick up the base mould and gently place it onto the surface of the isopentane for a few minutes. This will freeze the DED inside the OCT.
5. Once completely frozen the DED can be sectioned on a cryostat or kept in a -80 °C freezer until required.

3.4.2 Paraffin-Embedded Sections

1. Pour 5 ml of 4 % PFA into a glass bottle. See Note 19.
2. Using sterile forceps, pick up the DED and place it into the PFA.
3. Leave overnight at 4 °C. See Note 20.
4. Remove the PFA and wash the DED twice with sterile PBS (30 s each wash) and then place the DED in 5 ml of 70 % ethanol. See Note 21.
5. The DED then needs to go through a series of ethanol and xylene washes to dehydrate the tissue, which can be done using a tissue processor or by hand. See Note 10. Take a tissue embedding cassette, if labeling is required use a pencil. Place the DED into the cassette and close the lid. Place the cassette into a beaker of 70 % ethanol, until ready to start the

processing. This stage needs to be done as quickly as possible to ensure that the DED is only out of ethanol for the minimum amount of time.

6. Once processed, the DED can be taken out of the cassette and placed into a disposable base mould filled with melted paraffin wax, with the DED surface (with a distinctive drier and smoother appearance than the under layer of the DED) 90° to the base of the mould.
7. When the wax has solidified, the embedded DED can be sectioned on a microtome. Collect tissue on charged microscope slides.

3.5 Histological Staining

Once the DED has been sectioned there are a number of protocols that can be used to visualize the new epidermal layer that has formed (Fig. 3).

Hematoxylin and Eosin Staining

For paraffin sections

1. Place the slides in a rack and dewax the sections in a series of washes:
 - Xylene 5 min × 2 (use xylene in a fume hood).
 - 100 % EtOH 3 min × 2.
 - 95 % EtOH 2 min × 2.

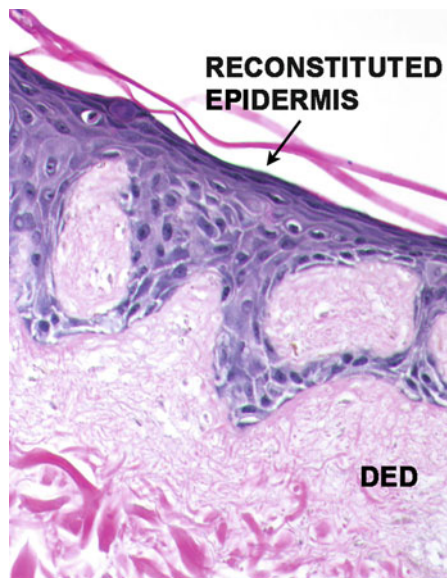


Fig. 3 Histological staining of reconstituted skin. Hematoxylin and eosin-stained section of a DED seeded with keratinocytes and cultured for 7 days. Note well-stratified epidermis with evident cornified material (*pink*) at surface

- 70 % EtOH 2 min × 2.
 - Distilled H₂O 5 min × 2.
2. Cover the slides with Harris Hematoxylin for 10 min.
 3. Leave under a running tap for 1 min.
 4. Differentiate in acid alcohol for 10 s.
 5. Leave under a running tap for 5 min.
 6. Take out of H₂O and cover with eosin for 30s.
 7. Dehydrate the sections by
 - 95 % EtOH 5 min × 2.
 - 100 % EtOH 5 min × 2.
 - Xylene 15 min × 3.
 8. Add a drop of DPX onto the slide and cover with an appropriately sized cover slip.
 9. Cover the slides and leave them to dry overnight.

For cryosections, let the sides come to room temperature (approx 20 min), fix in 4 % PFA for 5 min, rinse in H₂O, and then continue with the above protocol from step 2.

4 Notes

1. For tissue culture it is important to purchase sterile PBS to ensure that it is endotoxin free.
2. Discarded surgical skin is used to make DEDs, which requires informed patient consent and for the handler to be fully compliant with appropriate human tissue legislation. The whole piece of skin can be frozen and kept for several years at -80 °C until required to make DEDs.
3. Videne antiseptic solution can be purchased from Ecolab, which is diluted 1:10 for use. It is a viscous liquid, so it is best to pour these liquids into a measuring container rather than using a pipette.
4. The forceps need to be double wrapped in foil and then autoclaved for 20 min at 121 °C. Only unwrap the foil from the forceps when they are in the safety cabinet.
5. Neonatal or adult human epidermal keratinocytes can be purchased from a number of companies and can be used in this 3-D skin model. Each company will provide information on the best protocol to culture the cells they provide. It is best to use them at a passage number of 5 or less.

6. Our FAD media has a Ca^{++} concentration of 1.4 mM; however, media with lower Ca^{++} levels will support epidermal stratification and differentiation on DEDs (10).
7. Fetal bovine serum can be purchased in 500 ml bottles. It is best to aliquot out this into 50 ml sterile falcon tubes, and these can be frozen and then thawed when required. Heat inactivation of the serum in a 56 °C water bath for 10 min prior to adding to serum-free media has been shown to improve the stratification of the skin on the DED model (10). Sera can be treated with Chelex-100 to remove the Ca^{++} and other divalent ions and then filter sterilized. Final calcium concentration should be adjusted using a sterile calcium chloride solution.
8. Pore size of the insert needs to be large enough to allow efficient media exchange. We use Greiner's 6-well plate and thincerts with 3.0 μM pore size.
9. It is important that this does not take longer than 1 h and that the water bath remains at the correct temperature.
10. We use OCT embedding matrix produced by Raymond Lamb or Tissue-Tek.
11. DEDs can also be processed by hand. Dehydrate samples through a methanol series (25 %, 50 %, 75 %, and 100 % \times 2) for 10 min at each step. Equilibrate samples in 100 % ethanol (2 \times 30 min), then in ethanol:xylene (1:1) (2 \times 30 min), xylene for 30 min, xylene:paraffin wax (1:1) for 30 min at 62 °C, and paraffin wax for 1 h at 62 °C, and then overnight at 62 °C in wax.
12. If the epidermis does not easily pull away, it can be returned back into the pre-warmed PBS. Do not leave it for longer than 1 h in total in PBS.
13. Keratinocytes grown using classic FAD media with feeders are also suitable to use with this skin model.
14. This needs to be left for 2 h at room temperature or can be left for longer to be used when required at 4 °C.
15. The recommended seeding density is 3,500 cells/ cm^2 .
16. It is important to pipette up the cells quickly as the cells will rapidly sink to the bottom of the tube.
17. If continuing to passage the cells seed 150,000 cells into a collagen-coated T-25 in 5 ml of KGM-Gold media.
18. It is best to push down gently with the pipette tip in the center of the DED to create a small well before ejecting the cells.
19. Other tissue fixative reagents could be used instead of PFA.
20. Do not leave for longer than 24 h in the fridge.
21. If possible continue straight to the embedding stage, if not the DED can be left in ethanol at 4 °C for a maximum of 3 days.

References

1. Supp DM, Boyce ST (2005) Engineered skin substitutes: practices and potentials. *Clin Dermatol* 23(4):403–412. doi:[10.1016/j.clindermatol.2004.07.023](https://doi.org/10.1016/j.clindermatol.2004.07.023)
2. Metcalfe AD, Ferguson MW (2007) Tissue engineering of replacement skin: the crossroads of biomaterials, wound healing, embryonic development, stem cells and regeneration. *J R Soc Interface* 4(14):413–437. doi:[10.1098/rsif.2006.0179](https://doi.org/10.1098/rsif.2006.0179)
3. Roguet R, Regnier M, Cohen C, Dossou KG, Rougier A (1994) The use of in vitro reconstituted human skin in dermatotoxicity testing. *Toxicol In Vitro* 8(4):635–639
4. Perkins MA, Osborne R, Johnson GR (1996) Development of an in vitro method for skin corrosion testing. *Fundam Appl Toxicol* 31(1):9–18
5. Robinson MK, Osborne R, Perkins MA (2000) In vitro and human testing strategies for skin irritation. *Ann N Y Acad Sci* 919:192–204
6. Bell E, Ehrlich HP, Buttle DJ, Nakatsuji T (1981) Living tissue formed in vitro and accepted as skin-equivalent tissue of full thickness. *Science* 211(4486):1052–1054
7. Bell E, Ehrlich HP, Sher S, Merrill C, Sarber R, Hull B, Nakatsuji T, Church D, Buttle DJ (1981) Development and use of a living skin equivalent. *Plast Reconstr Surg* 67(3):386–392
8. Bell E, Sher S, Hull B, Merrill C, Rosen S, Chamson A, Asselineau D, Dubertret L, Coulomb B, Lapiere C, Nusgens B, Neveux Y (1983) The reconstitution of living skin. *J Invest Dermatol* 81(1 Suppl):2s–10s
9. Prunieras M, Regnier M, Woodley D (1983) Methods for cultivation of keratinocytes with an air-liquid interface. *J Invest Dermatol* 81(1 Suppl):28s–33s
10. Lamb R, Ambler CA (2013) Keratinocytes propagated in serum-free, feeder-free culture conditions fail to form stratified epidermis in a reconstituted skin model. *PLoS One* 8(1):e52494. doi:[10.1371/journal.pone.0052494](https://doi.org/10.1371/journal.pone.0052494)
11. Rheinwald JG, Green H (1975) Serial cultivation of strains of human epidermal keratinocytes: the formation of keratinizing colonies from single cells. *Cell* 6(3):331–343

A Novel Three-Dimensional Cell Culture Method to Analyze Epidermal Cell Differentiation In Vitro

Yoji Okugawa and Yohei Hirai

Abstract

Studies of the epidermis have been carried out in various models, such as the monolayer culture in vitro model and three-dimensional (3D) skin models, that are spatially organized to display the architectural features seen in human skin. These models have furthered our understanding of epidermal cell biology and provided quite a few lines of evidence on proliferation, cellular metabolism, morphological status, and state of differentiation. In this chapter, we describe a novel method using epithelial cell aggregates embedded in a collagen gel, instead of individual cells, for building cell–cell and cell–matrix interactions. Analyzing cell behaviors during epidermal differentiation would be helpful. Our method would help to analyze a possible regulatory mechanism underlying epidermal differentiation.

Keywords: Keratinocyte differentiation, Cell aggregate, Three-dimensional culture, Anoikis

1 Introduction

Keratinocytes in the basal layer of the epidermis continuously deliver daughter cells upward, producing the stratified multicellular epidermal structure. In skin research, monolayers of both isolated keratinocytes from human skin and established cell lines have been utilized to analyze organ-specific reactions (1). The growth of cells in a monolayer is a useful method to elucidate cell physiology and biology in the epidermis in vitro; however, the cells reveal only limited aspects of the differentiated epidermis and behave differently than they would in the organ as a whole. For example, the processing of caspase-14, which is associated with terminal epidermal differentiation, is not detected in the monolayer culture of human keratinocytes even after 2 days at confluence in high-calcium medium (2). Because of this result, information from epidermal cells cultivated as a monolayer has little relevance in vivo.

To correct this deficit, the first model of 3D skin model that mimics human skin was developed by Bell et al. (3). Numerous subsequent 3D skin models were based on these investigations. The model has a structure in which co-cultures of keratinocytes and fibroblasts are seeded on a collagen gel and display a “tissue-like” epithelial differentiation, morphology, and rates of cell division (4).

Although these models are useful to study the biochemical and morphological properties of human skin, the time required for establishing such 3D organotypic cultures is considerably long.

Here we estimate the 3D cell culture method using epithelial cell aggregates embedded in a collagen gel, which combines the monolayer methods with 3D organotypic methods. Cell aggregates are prebuilt small tissue blocks and have traditionally been used as a powerful tool to understand the principles of cell–cell and cell–matrix interactions (5, 6). One major advantage of the 3D cell culture method is the well-defined stereo architecture, which makes it possible to directly relate structure to function, thereby enabling realistic analyses. The analyses of 3D cell cultures cannot completely replace the analyses of biological mechanisms for relevance *in vivo*. Nevertheless, it is a very convenient method that can rapidly analyze a possible regulatory mechanism underlying epidermal differentiation. The more objective and persuasive conclusions could be achieved by combining the results obtained by this method with those from the conventional methods of analysis.

2 Materials

2.1 Cell Aggregate Preparation

1. HaCaT cells (*see Note 1*) 3 days after seeding at 3.0×10^4 cells/mL on 10 cm² culture dish (BD FALCON).
2. PBS (Sigma-Aldrich).
3. 0.25 % Trypsin (Sigma-Aldrich) in PBS.
4. 1,000 U/mL DNase 1 (Sigma-Aldrich) in sterile water.
5. Ultra low attachment 24-well plate (Corning).
6. Dulbecco's modified Eagle's medium (DMEM)/Ham's F12 (Sigma-Aldrich) supplemented with 10 % fetal calf serum (Hyclone) (DH10).

2.2 Cell Aggregates Embedded in Collagen Gel

1. 5 mg/mL Native collagen bovine dermis (KOKEN).
2. Sodium hydrate (Sigma-Aldrich).
3. Sodium bicarbonate (Sigma-Aldrich).
4. HEPES (Sigma-Aldrich).
5. 48-well culture dish (BD Falcon).
6. Tenfold concentrated DMEM (GIBCO).
7. Edgeless large-bore pipette tips (Watson).

2.3 Analysis

2.3.1 Western Blotting

1. Twofold concentrated sample buffer: 126 mM Tris–HCl (pH 6.8), 20 % glycerol, 4 % SDS, 20 % 2-mercaptoethanol, and 0.005 % BPB in water (*see Note 2*).
2. Electrophoresis gel: 4–15 % polyacrylamide gel (TEFCO).

3. Running buffer: 2.5 mM Tris base, 192 mM glycine, and 0.1 % SDS in water.
4. Transfer buffer: 2.5 mM Tris base, 192 mM glycine, and 10 % methanol in water.
5. Immobilon-P membrane (Millipore).
6. Blocking reagent: For caspase-14 detection, use Blocking One (Nacalai Tesque). For others' detection, use a 5 % skim milk (DIFCO) in PBS.
7. ECL plus Western Blotting Detection System (Amersham Biosciences).

2.3.2 Antibody

1. Anti-involucrin (1:100) (Santa Cruz Biotechnology).
2. Anti-cytokeratin 1 (K1) (1:1,000) (Covance).
3. Anti-cytokeratin 5 (K5) (1:1,000) (Covance).
4. Anti-caspase-3 (1:200) (Stressgen).
5. Anti-caspase-14 (1:500) (Covance).
6. Anti-Dnase1L2 (1:200) (kindly provided by Dr. Eckhert).
7. Anti- β -actin (1:2,000) (Sigma-Aldrich).
8. HRP-linked anti-mouse IgG (1:1,000) (Amersham Biosciences).
9. HRP-linked anti-rabbit IgG (1:1,000) (Amersham Biosciences).
10. Alexa-fluor488 linked anti-rabbit IgG (1:100) (Invitrogen).

2.3.3 Staining of Cell Aggregates

1. Fixing solution: 10 % formalin solution (Wako).
2. Propidium iodide solution: 1 % propidium iodide (Sigma-Aldrich) in water.
3. Mounting solution: VectaShield mounting medium (Vector Laboratories).
4. Embedding solution: 20 % Sucrose (Sigma-Aldrich), 50 % Tissue-Tek OCT compound (Miles Laboratories) and 0.5 % Phenol Red (Sigma-Aldrich) in water.

3 Methods

3.1 Cell Aggregate Preparation

1. Confluent HaCaT cell cultures grown in DH10 are washed twice with PBS and then treated for 10 min with 0.25 % trypsin. The HaCaT cells are trypsinized, and trypsin is inactivated with serum.
2. Depleted cells are centrifuged at $160 \times g$ for 5 min and counted by a hemocytometer.
3. The resulting pellet is treated with 20 μ L of Dnase 1 (1,000 U/mL) to yield a concentration of 1.0×10^7 cells and subsequently incubated for 10 min at 37 °C.

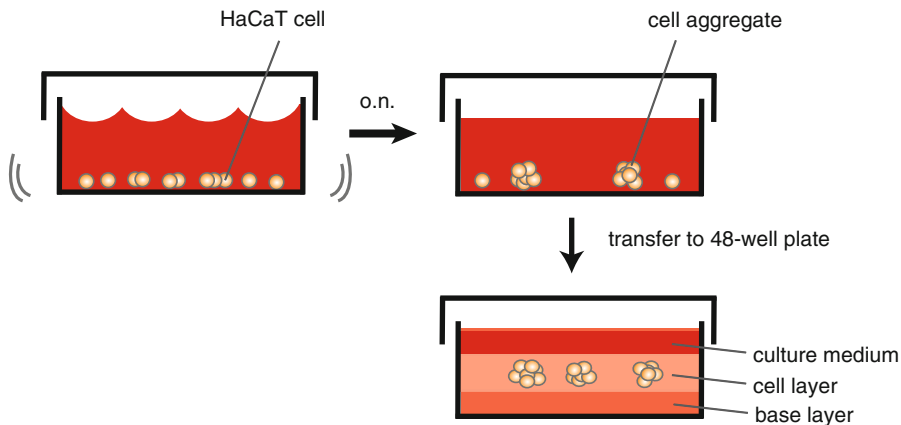


Fig. 1 Experimental procedure. The cell aggregates are formed by rotation culture for 24 h and embedded in collagen gels

4. The cells are resuspended in a fresh medium with the final density being approximately 3.0×10^6 cells/mL. The cells are seeded at 1.0×10^6 cells/well (350 μ L) into a 24-well dish (ultralow attachment surface). Then the cells are incubated on a gyratory shaker at 100 rpm for 24 h at 37 °C.
5. This procedure reproducibly provides smoothly rounded cell aggregates (Fig. 1).

3.2 Cell Aggregates Embedded in Collagen Gel

1. A collagen mixture is achieved by quickly and gently mixing 8 vol. of cold 5 mg/mL native collagen bovine dermis with 1 vol. of tenfold concentrated DMEM and 1 vol. of sterile reconstitution buffer (50 mM NaOH, 260 mM NaHCO₃, and 200 mM HEPES buffer) in a sterile tube kept on ice to prevent immediate gelation.
2. The cold collagen mixture is then dispensed into a 48-well plastic culture dish (0.1 mL/well) and allowed to gel for 30 min at 37 °C (base layer in Fig. 1).
3. The foregoing cell aggregates are placed in a centrifuge tube and are collected by centrifugation at $160 \times g$ for 30 s (*see Note 3*).
4. The cell pellet is resuspended at 2,000–4,000 aggregates/mL of the collagen mixture on ice under cautious stirring and is dispersed into 0.1 mL of the mixture per well on the base layer (cell layer in Fig. 1) (*see Note 4*).
5. For gelation, the culture plate is quickly incubated for 10–30 min at 37 °C in a humidified incubator. Then the collagen gels are gently covered with 0.5 mL of DH10 for 1–5 days (culture medium in Fig. 1).

3.3 Analysis

The DH10 is discarded, and the collagen with the cell aggregates is transferred to a centrifuge tube. The collagen is subsequently dissolved in hot water for a few minutes, and the cell aggregates are collected by gravity flow.

3.3.1 Western Blotting

1. The cell aggregates are dissolved in an equal volume of twofold concentrated sample buffer.
2. Boil the sample at 100 °C for 5 min.
3. Load the sample for electrophoresis: 70–100 V before the bromophenol blue front has moved into the resolving gel and 160–210 V until the bromophenol blue reaches the bottom of the gel.
4. Make the gel for transfer in transfer buffer: 20–40 mA for 90 min.
5. Block the filter with blocking buffer for 1 h at room temperature with gentle agitation on a platform shaker.
6. Discard blocking solution, and immediately incubate membrane with primary antibody for 1 h with gentle agitation on a platform shaker.
7. Discard primary antibody solution, and wash filter three times (5 min each time) with PBS.
8. Immediately incubate the filter with secondary antibody for 1 h with gentle agitation on a platform shaker.
9. Discard secondary antibody solution, and wash with PBS for three times for 5 min each time.
10. Detect the target proteins using the ECL Western Blotting Detection System according to the manual.

3.3.2 Histochemical Analysis

1. Cell aggregates cultured in vitro are embedded into embedding solution, and 10 µm cryostat sections are fixed with ice-cold methanol on a glass slide.
2. The following steps are described above (*see* Section 3.3.1, 5–9).
3. The nuclei are counterstained with propidium iodide.

Epidermal basal cells deprived of extracellular matrix (ECM) association withdraw from the cell cycle and become committed to differentiate to irreversibly undergo terminal differentiation. In HaCaT cell aggregates embedded in collagen gels, the central cell populations that were distal to the collagen matrix launched the differentiation/anoikis program. This program involved enucleation and cell death, leading to the formation of large central lumina within 4 days (Fig. 2). These cell aggregates represent a spectrum of cell differentiation markers. In particular, caspase-14 and DNase1L2, which are specific to epidermal cornification, were up-regulated during this culture period, whereas caspases-3 that

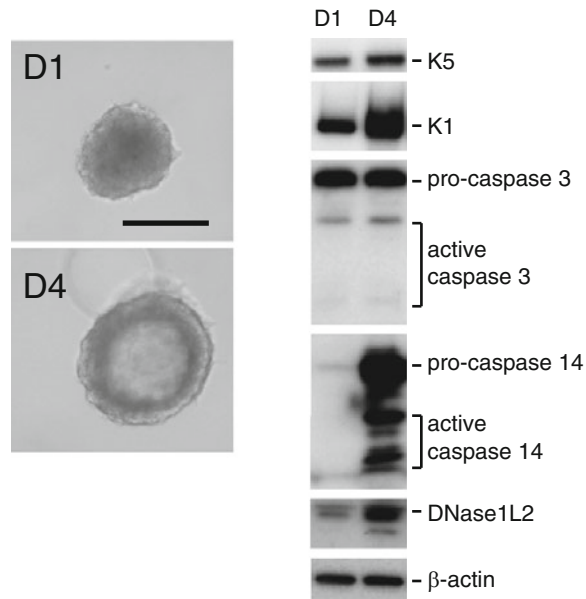


Fig. 2 Morphological appearance of the cell aggregates and induction of several differentiation markers including those for the early stage (keratin5), intermediate stage (keratin1), and the terminal stage (caspase-14, DNase1L2) in the cultured cell aggregates are investigated at days 1 and 4. Bar: 200 μ m

has a central role in classical apoptotic pathways in many cell types but not in keratinocytes remains unchanged (Fig. 2). Caspase-14 but not caspase-3 is processed during keratinocyte cornification (7). These results indicate that normal keratinocyte differentiation/anoikis is exhibited in this culture model.

The keratinocyte requires direct binding to ECM substrates to maintain its undifferentiated states, and deprivation of this interaction triggers the differentiation and cell death program (anoikis) (8). Most of the nascent HaCaT cells, except for the collagen-bound subpopulation, underwent anoikis within a few days, which resulted in the formation of large central space in the aggregates with highly assembled and membrane-proximal cornified envelopes containing involucrin at the apical surfaces of the collagen-bound viable cell layer (Fig. 3).

4 Notes

1. Although normal human epithelial cells are more feasible to use in demanding experimental protocols, such cells still present issues related to variability in different lots. Therefore, we used the human immortalized keratinocyte line HaCaT (9, 10). This particular cell line has been shown to form a complete epidermis when transplanted onto nude mice (11) and produce

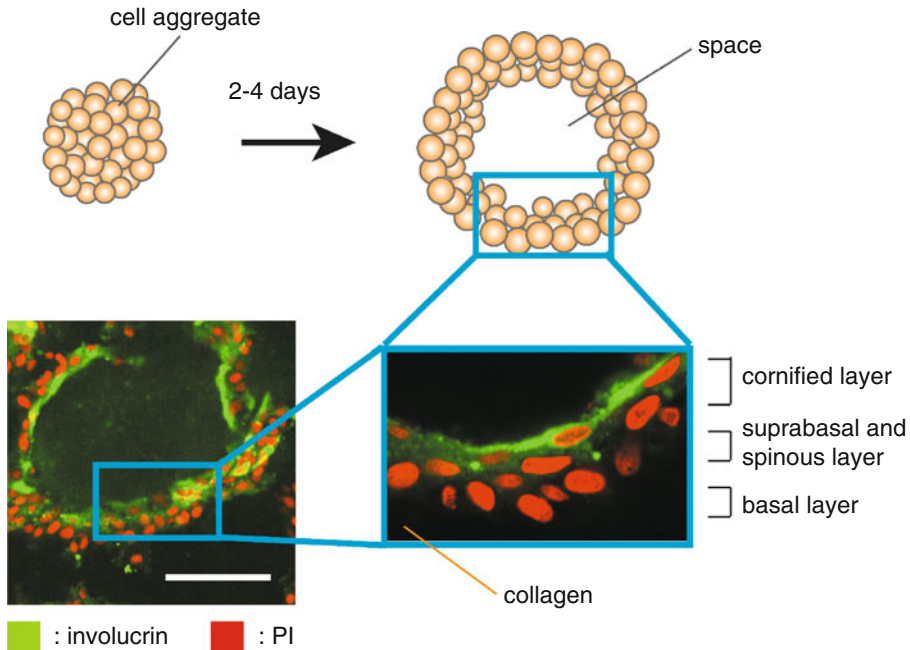


Fig. 3 Immunocytochemical analysis of cell aggregates. The cell clusters display well-developed envelope structures containing involucrin at the membrane proximal region of the apical cell surface. Bar: 100 μ m

well-stratified and normally differentiated epithelium (12–14). HaCaT cells are available from Deutsches Krebsforschungszentrum to only nonprofit organizations for research and teaching purposes.

2. Prior to using the buffer, 2-mercaptoethanol should be added.
3. The size of cell aggregates is dependent on the amount of DH10 and the rotation speed. A large amount of DH10 or a low speed causes large cell aggregates.
4. Edgeless large-bore pipette tips will not damage the cell aggregate when gently pipetting up and down.

References

1. Rheinwald JG, Green H (1975) Serial cultivation of strains of human epidermal keratinocytes: the formation of keratinizing colonies from single cells. *Cell* 6:331–343
2. Sitailo LA, Jerome-Morais A, Denning MF (2009) Mcl-1 functions as major epidermal survival protein required for proper keratinocyte differentiation. *J Invest Dermatol* 129 (6):1351–1360
3. Bell E, Ehrlich HP, And BDJ, Nakatsuji T (1981) Living tissue formed in vitro and accepted as skin-equivalent tissue of full thickness. *Science* 211:1052–1054
4. Lebonvallet N, Jeanmaire C, Danoux L, Sibille P, Pauly G, Misery L (2010) The evolution and use of skin explants: potential and limitations for dermatological research. *Eur J Dermatol* 20 (6):671–684
5. Mueller-Klieser W (1997) Three-dimensional cell cultures: from molecular mechanisms to clinical applications. *Am J Physiol* 273(4 Pt 1): C1109–C1123

6. Lin RZ, Chang HY (2008) Recent advances in three-dimensional multicellular spheroid culture for biomedical research. *Biotechnol J* 3 (9–10):1172–1184
7. Lippens S, Denecker G, Ovaere P, Vandena-beele P, Declercq W (2005) Death penalty for keratinocytes: apoptosis versus cornification. *Cell Death Differ* 12(Suppl 2):1497–1508
8. Frisch SM, Francis H (1994) Disruption of epithelial cell-matrix interactions induces apoptosis. *J Cell Biol* 124:619–626
9. Boukamp P, Petrussevska RT, Breitkreutz D, Hornung J, Markham A, Fusenig NE (1988) Normal keratinization in a spontaneously immortalized aneuploid human keratinocyte cell line. *J Cell Biol* 106:761–771
10. Boukamp P, Stanbridge EJ, Foo DY, Cerutti PA, Fusenig NE (1990) c-Ha-ras oncogene expression in immortalized human keratinocytes (HaCaT) alters growth potential in vivo but lacks correlation with malignancy. *Cancer Res* 50:2840–2847
11. Breitkreutz D, Schoop VM, Mirancea N, Baur M, Stark HJ, Fusenig NE (1998) Epidermal differentiation and basement membrane formation by HaCaT cells in surface transplants. *Eur J Cell Biol* 75:273–286
12. Kehe K, Abend M, Kehe K, Ridi R, Peter RU, van Beuningen D (1999) Tissue engineering with HaCaT cells and a fibroblast cell line. *Arch Dermatol Res* 291:600–605
13. Maas-Szabowski N, Starker A, Fusenig NE (2003) Epidermal tissue regeneration and stromal interaction in HaCaT cells is initiated by TGF- α . *J Cell Sci* 116:2937–2948
14. Schoop VM, Mirancea N, Fusenig NE (1999) Epidermal organization and differentiation of HaCaT keratinocytes in organotypic coculture with human dermal fibroblasts. *J Invest Dermatol* 112:343–353

Reconstruction of Normal and Pathological Human Epidermis on Polycarbonate Filter

Evelyne De Vuyst, Céline Charlier, Séverine Giltaire, Valérie De Glas, Catherine Lambert de Rouvroit, and Yves Poumay

Abstract

This chapter provides methods suitable for the culture of primary human keratinocytes in serum-free culture conditions, starting from very small skin biopsies. It also explains procedures required for reconstruction of a stratified epidermis on polycarbonate filter, starting from keratinocytes cultured in serum-free conditions. Tissues reconstructed according to this method have been proven suitable for characterization of epidermal morphogenesis and for *in vitro* studies of the epidermal barrier. Utilization of the same method for successful isolation of keratinocytes from a patient suffering from Darier's disease and the reconstruction of a pathological epidermis which displays the same histological features as *in vivo* are also presented.

Keywords: Human keratinocytes, Primary culture, Epidermis reconstruction, Darier's disease, Skin biopsy

1 Introduction

Soon after the successful development of cultures of human keratinocytes immersed in liquid medium, limitations in the stages of epidermal differentiation that can be reached under such conditions have led researchers to pursue efforts towards the development of fully differentiated keratinocyte cultures. Already in the early 1980s, the requirement for an exposure of differentiating keratinocytes to the air–liquid interface had been clearly identified in order to produce stratified cultures covered by a fully differentiated cornified layer (1). While those initial methods were using serum-containing medium, together with de-epidermized dermis or equivalent dermis (produced by the contraction of a collagen lattice containing cultured fibroblasts) as biological supports for keratinocytes, the possibility to reconstruct the epidermis only, directly over porous substrates and in chemically defined serum-free medium,

was later demonstrated (2). Availability of standardized, reproducible models of human epidermis paved the way to valuable alternative methods able to replace laboratory animals. From an experimental point of view and in the perspective of cutaneous toxicological studies, such reconstructed human epidermis (RHE) directly anchored to a filter presents the highly valuable advantage that cytokines released by keratinocytes are not trapped into a dermal compartment and can be analyzed in the culture medium, below the porous substrate (3).

In view of their huge potential for basic and applied research, RHE have rapidly become commercially available from several companies. However, for several reasons linked for instance to their relatively elevated price, but also because custom-made design of their environment during tissue reconstruction is frequently required for basic investigations, or simply because the reliability of commercial providers is limited for customers seeking for a guaranteed long-term and stable availability of an epidermal model (4), our laboratory has established a simple protocol for in-house production of RHE (5). For this purpose, we have chosen to rely exclusively on materials available for research worldwide. In addition, this freely available procedure has created conditions for open-source tissue production of RHE (see for instance http://www.tissue-factory.com/en/Skin_Model.html May 31, 2013).

Nowadays, our in-house production of RHE has taken benefit from a few refinements of the method, including the possibility for a decreased cell density at the settings of the culture. A detailed study of tissue morphogenesis has also been performed, illustrating elevated basal cell proliferation during the initial phase of the culture and progressive organization of the differentiating suprabasal layers, as evidenced by immunohistochemical localization of various epidermal differentiation markers (6, 7). In this chapter, the complete and annotated protocol for RHE production is described starting from keratinocyte isolation and growth, in accordance with the procedure for immersed cultures already published in the second edition of this book (8). Moreover, a new procedure which uses very small punch biopsies from human skin as a source of keratinocytes is explained. Finally, the successful utilization of abnormal keratinocytes for epidermal reconstruction is described. Indeed, keratinocytes from a patient with Darier's disease, a genetic condition that results from a defective calcium transporter in the endoplasmic reticulum, were used for in vitro reconstruction of the pathological epidermis. Interestingly, the resulting tissue depicted abnormal features observed in vivo in the epidermis of patients, namely, some loss of adhesion between epidermal cells (acantholysis) and abnormal keratinization (9).

2 Materials

2.1 Primary Culture of Human Epidermal Keratinocytes from a 3 mm Punch Biopsy

1. Medium for culture setting: KBM[®]-2 medium (Clonetics[®] cat. no. CC-3103) is supplemented with SingleQuots[®] KGM-2[®] (Clonetics[®] cat. no. CC-4152) to reach final concentrations of 10 ng/ml human recombinant epidermal growth factor (EGF), 5 µg/ml insulin, 50 µg/ml bovine pituitary extract (BPE), 5×10^{-7} M hydrocortisone, and 5 µg/ml transferrin. For the primary cultures 50 µg/ml gentamycin, 250 ng/ml fungizone, and 2.5 µg/ml ampicillin are added to the medium. When thawing the vials for secondary cultures, these antibiotics are replaced by 50 U/ml of penicillin G and 50 µg/ml of streptomycin.
2. Medium for culture growth: After settings of the cultures, a keratinocyte growth medium is used, based on Epilife[®] medium (Cascade Biologics[™] cat. no. M-EPI-500-CA) and supplemented with antibiotics and HKGS (Cascade Biologics[™] cat. no. S-001-5) in order to reach final concentrations of 0.2 % BPE, 0.2 ng/ml human recombinant EGF, 0.18 µg/ml hydrocortisone, 5 µg/ml insulin, and 5 µg/ml transferrin.
3. Solution A: Washing solution for tissues and cells: 10.0 mM glucose, 3.0 mM KCl, 130.0 mM NaCl, 1.0 mM Na₂H-PO₄·7H₂O (or anhydrous), 0.0033 mM phenol red, 30.0 mM Hepes. Dissolve Hepes in distilled H₂O and adjust pH at 7.4 with 10 M NaOH. Then, dissolve the other compounds and check pH before adjusting the final volume. Solution A is sterilized through a Sterivex[™]-GP 0.22 µm filter (Millipore cat. no. SVGP01015) and stored refrigerated at 4 °C.
4. Dispase II (Roche cat. no. 04942078001): Diluted in solution A to reach a concentration of 10 mg/ml.
5. EDTA (Merck cat. no. 108418): Diluted in solution A to reach a concentration of 1 mM.
6. Trypsin solution used for the initial dissociation of keratinocytes: Trypsin (Sigma cat. no. T-9201) is dissolved at 0.17 % (weight/volume) into ice-cold solution A. The solution is then sterilized through a Millex[™]-GP 0.22 µm filter (Millipore cat. no. SLGP033RB).
7. Trypsin solution used for subculture of keratinocytes: Dissolve 0.01 % ethylenediaminetetraacetic acid (EDTA) into solution A, adjust the pH to 7.4, chill on ice the solution, and then add trypsin (Sigma cat. no. T-9201) to obtain a 0.025 % solution. The solution is then sterilized through a Millex[™]-GP 0.22 µm filter (Millipore cat. no. SLGP033RB).
8. Dialyzed fetal calf serum: Dialysis tubing MWCO-12,000–14,000 Da (Dialysis tubing—Visking Medicell International Ltd) is prepared by boiling in a solution containing

0.1 % EDTA and 0.1 % Na_2CO_3 , followed by two 15-min washes in boiling distilled H_2O . Introduce 100 ml of fetal calf serum (Lonza[®] cat. no. DE14-801F) into the dialysis tubing. Seal the dialysis tubing and stir it at 4 °C into 10 l of phosphate-buffered saline (PBS) solution without calcium (PBS: 0.2 g KCl, 0.2 g KH_2PO_4 , 8 g NaCl, 1.44 g $\text{Na}_2\text{H-PO}_4 \cdot 2\text{H}_2\text{O}$ in 1.0 l of distilled H_2O , pH 7.4). PBS solution is changed four times over a period of 12 h.

9. Blocking solution: Solution A containing 2 % dialyzed fetal calf serum.

2.2 Reconstruction of Epidermis on Polycarbonate Filter

1. Medium for epidermis reconstruction at air–liquid interface: Medium for culture growth but containing 1.5 mM Ca^{2+} and supplemented with 50 $\mu\text{g}/\text{ml}$ vitamin C and 10 ng/ml keratinocyte growth factor (R&D Systems, cat. no. 251KG).
2. Insert: Polycarbonate culture insert with 12 mm diameter and 0.4 μm diameter pore size (Millipore, cat. no. PIPH01250).

2.3 RNA Extraction from Reconstructed Epidermis

1. RNA extraction: To isolate total RNA, RNeasy mini kit (Qiagen cat. no. 74106) and QIAshredder spin columns (Qiagen cat. no. 79656) are used using the spin technology protocol according to the instructions of the manufacturer.

2.4 Protein Extraction from Reconstructed Epidermis

1. Lysis buffer for protein extraction: 0.125 M Tris–HCl pH 6.8, 20 % glycerol, 4 % SDS, 0.2 M DTT.

2.5 Histological Analysis of Reconstructed Epidermis

1. Acetic formalin (4 % formalin and 1 % glacial acetic acid).
2. 100 % methanol.
3. 100 % toluene.
4. Embedding cassettes (Simport).
5. Paraffin embedding station (Shandon Histocentre 2).
6. Microtome (Leica RM2245).
7. Hemalun solution: 1 l of saturated solution of potassium alum containing 3 g standard hematoxylin (Sigma-Aldrich, Fluka) and 20 ml of glacial acetic acid.
8. Erythrosine solution: 1 l of water containing 2 g of erythrosine and ten drops of 35 % formalin solution.

3 Methods

A method for setting up serum-free cultures of keratinocytes from adult human skin samples obtained from excessive tissue removed during abdominoplasty was published in the previous edition of this book (8). The current protocol describes an adaptation of the method to small skin samples with a diameter of 3 mm.

3.1 Primary Culture of Human Epidermal Keratinocytes from Small Skin Samples

1. Collect small skin samples with an area corresponding to 3 mm punch biopsies in Epilife medium supplemented with antibiotics and fungizone and transport on ice to the culture room (*see Note 1*).
2. Transfer the punches into dispase II during 2 h and 30 min at 37 °C to allow separation of the dermis from the epidermis.
3. With a sterile pair of tweezers, separate manually the epidermis from the underlying dermis in an EDTA solution at 4 °C in order to block the activity of dispase.
4. Transfer the epidermal sheet (*see Note 2*) to a well of a 12-well cell culture plate containing 200 µl of 0.17 % trypsin to dissociate the epidermis into single cells.
5. Incubate for 1 h and 30 min at 37 °C.
6. Add 500 µl of cold blocking solution, and dissociate keratinocytes, using a pair of tweezers. Up and downs may also be performed inside a 5 ml pipet (*see Note 3*).
7. Collect the cell suspension and centrifuge at $335 \times g$ during 5 min at 4 °C.
8. Re-suspend the pellet in 1 ml medium for culture setting containing 5 % dialyzed fetal calf serum and transfer into a 12-well cell culture plate.
9. Incubate for 3 days at 37 °C without moving the plate.
10. Change the medium every other day using medium for culture growth for approximately 10 days.
11. Once cells reach about 60–70 % confluence (the culture is then mainly composed of keratinocytes), trypsinize the culture: add 500 µl of trypsin, incubate for 1 min at room temperature, and aspirate the liquid in order to eliminate contaminating cells such as melanocytes and fibroblasts. Add again 500 µl of trypsin and incubate for 10–15 additional minutes at room temperature. When cells are detached from culture plastic substrate (plates can be hit laterally), add 1 ml of cold blocking solution, collect the cell suspension, and centrifuge at $335 \times g$ for 5 min at 4 °C. Re-suspend the pellet into medium for culture growth, and seed the cells into 6-well plates or T25 flasks in order to expand the keratinocyte population. At this stage, a total yield between 25,000 and 50,000 keratinocytes may be expected.

3.2 Reconstruction of Epidermis on Polycarbonate Filter

1. Isolate human keratinocytes from normal adult skin samples from plastic surgery as described previously (8) or from small biopsies as described above. For epidermal reconstruction, third-passage proliferating keratinocytes are used.
2. If keratinocytes are frozen in liquid nitrogen for cryopreservation (8), their proliferation potential must be reactivated by culturing them first in monolayer. Seed approximately 2×10^6 keratinocytes in a 175 cm² culture flask containing 25 ml of medium for culture setting. Incubate cells during 24 h at 37 °C in a humidified atmosphere containing 5 % CO₂. On the next day, renew the culture medium with medium for culture growth in order to remove any trace of DMSO used in the freezing solution of keratinocytes (8) and incubate for 24 h at 37 °C, 5 % CO₂. Then replace medium every other day.
3. When keratinocytes cover approximately 70–80 % of the flask area (*see Note 4*) (usually after 3–4 days of culture), aspirate the culture medium and add 3 ml of trypsin solution. Keep keratinocytes at room temperature during 8–10 min, and then hit the flask laterally to detach the cells from the flask. Then add 12 ml of ice-cold blocking solution, and transfer the cell suspension into a 50 ml centrifugation tube.
4. Centrifuge cells at $335 \times g$ and 4 °C for 5 min.
5. Aspirate the supernatant, and re-suspend keratinocytes from the pellet using 2–3 ml ice-cold medium for culture growth containing 1.5 mM calcium. Keep the cell suspension on ice.
6. Count cells and dilute the suspension with the same medium in order to obtain a minimal cell density of 3×10^5 keratinocytes per ml (*see Note 5*). Keep keratinocyte suspension on ice.
7. Place the polycarbonate culture inserts with a sterile pair of tweezers into a 6-well culture microplate. Add 2.5 ml of medium for culture growth containing 1.5 mM of Ca²⁺ into the wells (*see Note 6*).
8. In the upper chamber of each insert, add 500 µl of keratinocyte suspension (3×10^5 cells/ml) corresponding to 250,000 cells/cm². Incubate culture at 37 °C in a humidified atmosphere containing 5 % CO₂.
9. After 24 h, cells are exposed to the air–liquid interface by careful aspiration of the culture medium in the upper compartment of the insert (*see Note 7*). Replace the medium from the well under the polycarbonate filter by 1.5 ml medium for epidermis reconstruction at air–liquid interface.
10. Renew this medium every other day. After 11 days of culture at the air–liquid interface, the RHE is morphologically fully differentiated (7) (Fig. 1).

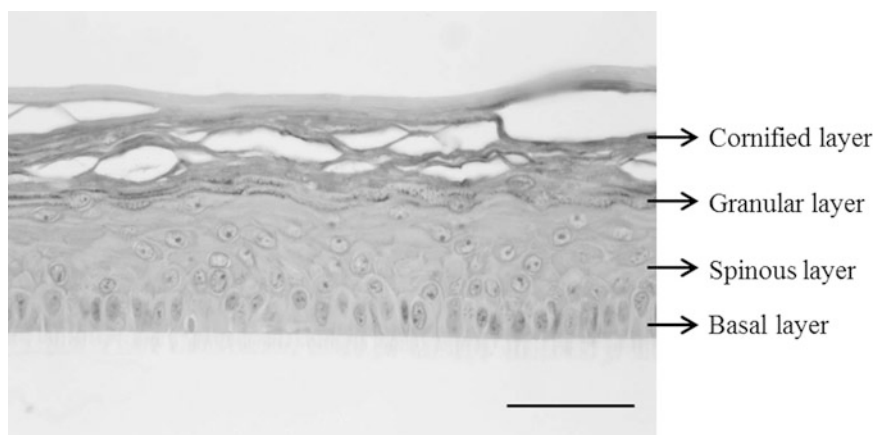


Fig. 1 Histology of reconstructed human epidermis (RHE) at day 11. After 11 days of culture, RHE were fixed in acetic formalin and embedded in paraffin. Then histological sections perpendicular to the surface of RHE were prepared and stained with hematoxylin-erythrosine to allow the morphological analysis of RHE (bar: 50 μm)

3.3 Reconstruction of Epidermis from Pathological Primary Keratinocytes: The Case of Darier's Disease

Primary keratinocytes from a Darier's disease (DD) patient were isolated and used for keratinocyte culture and epidermal reconstruction in accordance with the procedure described above. The pathological biopsy was obtained after informed consent and in accordance with the standards of the relevant ethics committee. DD is a rare dominant genetic skin disorder characterized by warty papules and plaques in seborrheic areas of the skin. Histologically, the pathological epidermis shows acantholysis (loss of intercellular adhesion) and dyskeratotic keratinocytes. After culture as monolayers of keratinocytes from the pathological skin, followed by tissue reconstruction at the air-liquid interface, the Darier RHE showed morphological features strikingly similar to those observed in vivo. This means increased intercellular spaces (acantholysis), abnormal keratinocytes (dyskeratosis) named *corps ronds* or *grains*, and parakeratosis (Fig. 2). In other words, the DD RHE presented defective differentiation, as it can be observed in DD lesions in vivo (9).

3.4 RNA Extraction from Reconstructed Epidermis

1. Total RNA is extracted from the RHE using the RNeasy mini kit and QIAshredder spin column.
2. Dissect using a sharp surgical blade the circumference of the polycarbonate filter covered by the RHE from the bottom of the insert. Then transfer the dissected disc, using a pair of tweezers, into a 12-well culture plate containing 600 μl of RLT buffer (*see Note 8*).
3. After 1 or 2 min, stratum corneum detaches from the epidermis. Remove it with a pair of tweezers and discard (*see Note 9*).
4. For disrupting keratinocytes, gently scratch the epidermis with a micropipette tip in lysis buffer provided by the kit. Homogenize the lysate by pipetting up and down and transfer into a QIAshredder spin column placed in a 2 ml collection tube.

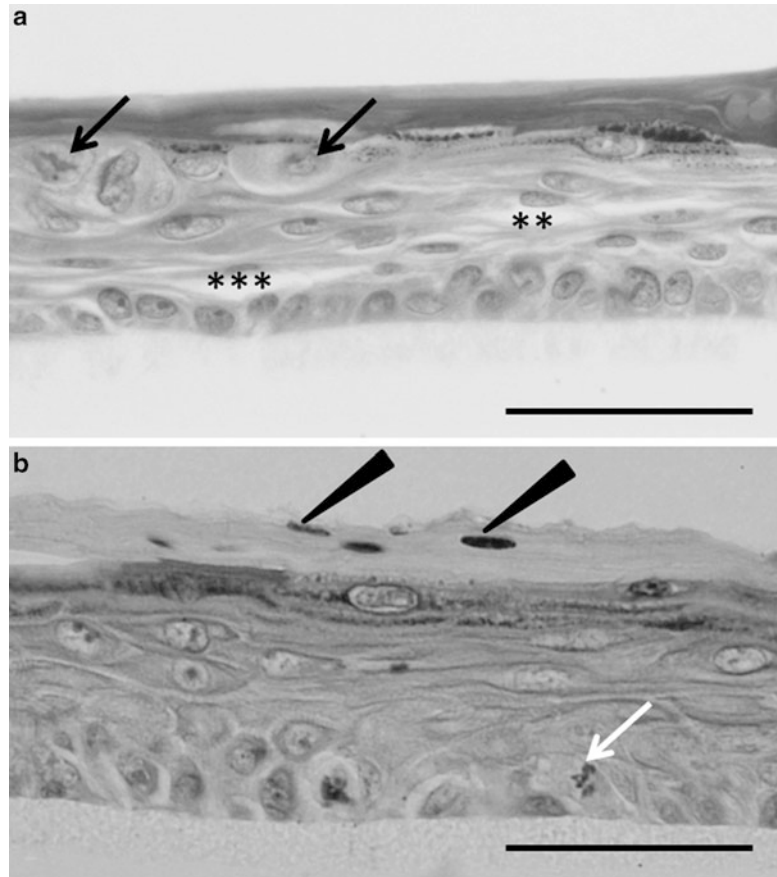


Fig. 2 In vitro reconstruction of epidermis from primary Darier's disease (DD) keratinocytes exhibits similar histopathological features as in DD lesion in vivo. Isolated and amplified DD keratinocytes were seeded on polycarbonate filters and exposed at air-liquid interface in order to obtain DD-RHE. After 11 days of culture, the stratified epidermis exhibits morphological features strikingly similar to those observed in vivo with increased intercellular spaces (acantholysis) (**a**, *asterisks*), abnormal keratinocytes (dyskeratosis) called "*corps ronds*" (**a**, *black arrows*), "*grains*" (**b**, *white arrow*), and parakeratosis (**b**, *black arrowheads*). DD-RHE present a disruption of the differentiation process as observed in DD lesions in vivo (9) (bar: 50 μ m)

5. From this point, follow the instructions of the manufacturer. This procedure allows the recovery of enough RNA from the RHE for RT-qPCR analysis of gene expression.

3.5 Protein Extraction from Reconstructed Human Epidermis

1. Using a sharp surgical blade, dissect the circumference of the filter holding the RHE as described above for RNA, and then transfer the filter and the anchored tissue into 200 μ l of lysis buffer suitable for protein extraction.

2. Boil samples for 5 min at 100 °C. This allows the epidermis to detach from the polycarbonate filter.
3. Scratch the filter with a micropipette tip in order to collect the remaining adherent cell material.
4. Boil the lysate during 2 min.
5. Centrifuge at $9,300 \times g$ during 5 min, in order to pellet the cellular debris not dissolved in lysis buffer, together with the polycarbonate filter.

3.6 Histological Analysis of Reconstructed Epidermis

1. Fix the insert with the RHE in acetic formalin for minimum 24 h at room temperature.
2. Dehydrate in four successive baths of methanol: a quick bath to remove as much water as possible and three other baths for 10 min each.
3. Immerse the insert in toluene, which dissolves the plastic surrounding the polycarbonate filter holding the RHE. The insert is then vigorously stirred in toluene, releasing the disc-shaped RHE (still attached to the filter) (*see Note 10*).
4. Place the sample in an embedding cassette and incubate four times for 10 min in pure toluene.
5. The next step is the inclusion of the sample in paraffin. Soak the sample in a large metal mold containing hot paraffin (60 °C) in order to replace a maximum of toluene impregnated in the sample by liquid paraffin. Then, place the sample in a smaller mold containing hot paraffin and incubate at 60 °C for 1 h or overnight.
6. The disc-shaped RHE can finally be embedded in paraffin. For this step, it is very important to adequately orient the disc in the mold in order to obtain transversal sections of the RHE (*see Note 11*). Transfer the mold to the cooling plate of the embedding station to allow paraffin solidification. When the paraffin is completely solid, remove the block from the mold.
7. For sectioning, trim the sample by cutting 25 μm thick sections, before preparing 6 μm thick sections for histological analysis (*see Note 12*).
8. Separate ribbons of sections into coupons, spread on microscope slides (distilled water is used for spreading), and then let dry for 1 h at 48 °C.
9. Tissue sections are then processed for regular histological staining, using hematoxylin-erythrosine to allow morphological analysis of RHE.

4 Notes

1. Avoid disinfection of the skin surface with iodine antiseptic since it will impede subsequent recovery of cells that exhibit enough proliferation potential.
2. The epidermal surface can be recognized since it is less viscous, thinner, and more transparent than the dermal component.
3. Keep cell suspension on ice as much as possible in order to avoid irreversible cell aggregation.
4. Keratinocytes should be grown up to no more than 80 % confluence as the number of proliferative cells has to be kept at its maximum.
5. 3×10^5 cells/ml is an adequate cell density to prepare RHE. 500 μ l from this suspension seeded into the polycarbonate insert correspond to a culture density of 250,000 cells/cm² in each insert. A lower density of keratinocytes does not allow proper reconstruction of the epidermis since, in this case, the culture medium can overlay the seeded keratinocytes for one or two days after the establishment of an air-liquid interface, impeding the formation of stratum corneum.
6. Place the insert into the well before adding the culture medium. This will avoid the formation of air bubbles between the polycarbonate filter and the bottom of the culture dish.
7. Aspirate delicately the medium above the insert with a micro-pipette, not with a suction pump.
8. Keep 12-well microplates containing the RHE on ice, in order to prevent ribonuclease (RNase) activity.
9. Stratum corneum cannot dissolve and does not get through the QIAshredder spin columns, leading to reduced RNA yields.
10. Do not leave the insert for too long in toluene dissolvent because the plastic melts rather quickly; the 30 ml toluene solution is discarded after the melting of 5–6 inserts to avoid excessive accumulation of melted plastic in the solvent.
11. The disc is immersed vertically to the bottom and in diagonal to the length of the mold filled with hot paraffin. The disc is held in this position (using a pair of tweezers) while laying down the mold on the cooling plate. This particular orientation of the disc ensures transversal histological observation of the RHE after sectioning using a microtome.
12. For a consistent morphological analysis of RHE, the block is generally trimmed to 1,500 μ m, which allows the observation of the RHE along its maximal length.

Acknowledgements

The valuable technical help from Daniel Van Vlaender is gratefully acknowledged. This work was financially supported by FRFC grants 2.4.506.01 and 2.4.522.10F and by FNRS grant 1.5.033.06F to Y.P. E.D.V. and S.G. are supported by a grant from the Région Wallonne.

References

1. Pruniéras M, Régnier M, Woodley D (1983) Methods for cultivation of keratinocytes with an air-liquid interface. *J Invest Dermatol* 81:28s–33s
2. Rosdy M, Clauss LC (1990) Terminal epidermal differentiation of human keratinocytes grown in chemically defined medium on inert filter substrates at the air-liquid interface. *J Invest Dermatol* 95:409–414
3. Coquette A, Berna N, Vandebosch A, Rosdy M, Poumay Y (1999) Differential expression and release of cytokines by an in vitro reconstructed human epidermis following exposure to skin irritant and sensitizing chemicals. *Toxicol In Vitro* 13:867–877
4. Poumay Y, Coquette A (2007) Modelling the human epidermis in vitro: tools for basic and applied research. *Arch Dermatol Res* 298:361–369
5. Poumay Y, Dupont F, Marcoux S, Leclercq-Smekens M, Hérin M, Coquette A (2004) A simple reconstructed human epidermis: preparation of the culture model and utilization in in vitro studies. *Arch Dermatol Res* 296:203–211
6. Frankart A, Coquette A, Schroeder K-R, Poumay Y (2012) Studies of cell signalling in a reconstructed human epidermis exposed to sensitizers: IL-8 synthesis and release depends on EGFR activation. *Arch Dermatol Res* 304:289–303
7. Frankart A, Malaisse J, De Vuyst E, Minner F, Lambert de Rouvroit C, Poumay Y (2012) Epidermal morphogenesis during progressive in vitro 3D reconstruction at the air-liquid interface. *Exp Dermatol* 21:871–875
8. Minner F, Herphelin F, Poumay Y (2010) Study of epidermal differentiation in human keratinocytes cultured in autocrine conditions. *Methods Mol Biol* 585:71–82
9. Lambert de Rouvroit C, Charlier C, Lederer D, De Glas V, De Vuyst E, Dargent J-L, Grammatico P, Binni F, Rousseau C, Hennecker J-L, Nikkels AF, Poumay Y (2013) In vitro reconstruction of epidermis from primary Darier's disease keratinocytes replicates the histopathological phenotype. *J Dermatol Sci* 71:138–140

Methods for the Preparation of an Autologous Serum-Free Cultured Epidermis and for Autografting Applications

John J. Wille, Jeremy J. Burdge, and Jong Y. Park

Abstract

Cell culture techniques for producing a three-dimensional autologous epidermal autograft (cultured epidermal autograft) suitable for tissue grafting and wound healing procedures are described. This chapter commences with surgical biopsy of patient's skin tissue, further reduction of skin tissues to keratinocyte cells by enzymatic treatment, and recovery of viable adult keratinocytes in a new balanced buffered salt media supportive of the growth of clonally enriched isolated basal keratinocytes. Culture techniques required for the formation of a hole-free monolayer of undifferentiated basal keratinocytes without the use of an organotypic matrix substrate are accomplished with a specially designed nutrient basal media (HECK 109) that is a chemically defined and subsequent culture in this serum-free culture media supplemented with hormones and two human recombinant protein growth factors (EGF and IGF-1). Further culture techniques and media manipulations, including brief exposure to β -TGF to induce reversible G₁-phase growth arrest, are followed by para-synchronous induction of a multilayered stratification and keratinizing epidermal differentiation, yielding a living three-dimensional epidermis formed entirely in cell culture. Protocols are listed for its enzymatic removal, floatation, and transfer for shipment to the clinic ready for surgical grafting to the self-same patient's debrided chronic leg ulcers. Recent clinical trial results have demonstrated the utility and efficacy of these grafts in forming durably healed chronic wounds.

Keywords: Autografts, Beta-TGF, Chemically defined, Clonal competence, Chronic wounds, Epidermal keratinocytes, EGF, HECK 109, IGF-1, Nutrient basal medium, Proliferative potential, Serum-free media

1 Introduction

The introduction of biological dressings to wound care arena has had a dramatic impact on outcome, on the efficacy of wound healing, and on the design and choice of the best clinical pathways for treatment of burns and other hard-to-heal wounds (1–5). The term biological dressings refers to the field of biomedical research and practice that focuses on the use of cell culture-derived tissue constructs to replace, restore, and regenerate tissue loss due to damaged or diseased tissue cells. The first successful regenerative medicine application was biological dressings for dermatological applications (6). Initially, for ease of obtaining disposed of neonatal

foreskins, allogeneic epidermal cells were pooled from many different human sources (7, 8) to form cell bank stocks. However, the downside use of allogeneic epidermal keratinocytes led to many serious safety and health concerns including immunological rejection and the possibility of disease transmission from unscreened pathogenic bacteria and viruses. To prevent such consequences, costly screening and quality control tracking systems were required reducing the commercial potential of such products. Moreover, allogeneic epidermal keratinocytes transplanted to host wounds are only of transient benefit and are not permanently integrated into the host's healed tissue (9). In reality, they have only marginally advanced the rate of healing or shortened the time of wound closure of burns and recalcitrant wounds (10). Similarly, tissue-engineered skin substitutes composed of an underlying artificial dermis composed of collagen and other biomaterials and overlain by a cultured epidermal component constructed from allogeneic keratinocytes have failed to capture a major share of the wound dressing market due to cost, safety concerns, and poor results of clinical outcome research (11). In addition, a recent study (12) employing the innovative technique of cell therapy in which spray-applied allogeneic keratinocytes were applied to chronic leg ulcers has also shown little promise in advancing the rate or the time to complete wound closure over and above compression therapy, the standard of care (13).

Here, we describe the techniques and methods used to construct an autologous biological dressing composed entirely of autologous epidermal keratinocytes, isolated and cultured from normal skin of patients suffering from recalcitrant venous stasis ulcer of long duration. These methods differ substantially from both previous biological dressings composed of allogeneic epidermal keratinocyte and other biological dressings composed of autologous epidermal keratinocytes. The latter did, indeed, show clinical improvements vis-à-vis their allogeneic counterparts but still retained safety concerns involved in the use of xenobiotic materials in the preparation and in the finished cultured epidermal autografts (CEAs) (14, 15), in particular, the use of serum-containing culture medium to grow keratinocytes, the use of organotypic matrices as cell substrates, xenobiotics such as cholera toxins, and irradiated mouse feeder layer cells (16). These practices became unnecessary once serum could be eliminated and replaced by a chemically defined nutrient basal media which set the stage for determining the minimal hormonal and growth factor requirements needed to grow mass cultures and even single-cell clones of human keratinocytes (17, 18). These developments underlie the present ability to produce large quantities ($>2 \text{ m}^2$) of CEAs sufficient to cover the entire human body from a small skin sample (approx. $2\text{--}3 \text{ cm}^2$). These developments are embodied in the techniques described herein.

2 Materials

2.1 Source of Chemicals

All used biochemicals for preparation of HECK 109 medium including glucose can be obtained from Sigma-Aldrich Chemical Company. All inorganic chemicals can be obtained from Mallinckrodt Analytical Reagents except sodium bicarbonate which can be purchased from Matheson, Coleman & Bell Analytical Reagent. Trypsin, soybean trypsin inhibitor, and dispase enzymes and growth factors: EGF (human recombinant epidermal growth factor), IGF-1 (human recombinant insulin-like growth factor-1), and beta-TGF (transforming growth factor) were also from Sigma-Aldrich Company (St. Louis, MO).

2.2 Adult Skin Samples

Adult skin samples were obtained from biopsies performed at the Grant Hospital of Columbus, Ohio, under the supervision of Dr. Jeremy Burdge.

3 Methods

3.1 Preparation of HECK 109 Serum-Free Medium

The preparation of HECK 109 serum-free medium is the subject of a patent issued to the author (J.J.W.) (**Note 1 (19)**).

1. Medium nomenclature and labeling

- (a) *Basal medium*—HECK 109 with either 30 μM Ca^{2+} or 100 μM Ca^{2+} when made up and refrigerated is good for 2 weeks (**Note 2**).
- (b) *Standard medium*—HECK 109 (std) is standard with nonprotein factors added. These are ethanolamine, phosphoethanolamine, and hydrocortisone (**Note 3**).
- (c) *Complete medium*—HECK 109 (com) is HECK 109 that has the complete requirements for keratinocyte growth. It is standard medium with EGF and IGF-1 (the protein growth factors) added to it. It should be used within 2 days (**Note 4**).

2. All stock solutions are prepared with purified water using triple-distilled water with an ion conductivity meter measurement less than 2–5 $\text{m}\Omega$. Prepare all stock solutions in 1 L volumetric flasks.

3. Prepare the following ten different amino acid stock solutions [at final medium concentrations] as follows:

- (a) Stock 1: Arginine·HCl [210.7 mg/L]; *histidine* [16.77 mg/L]; *isoleucine allo-free* [1.97 mg/L]; leucine [65.6 mg/L]; lysine·HCl [18.27 mg/L]; *methionine* [4.48 mg/L]; *phenylalanine* [4.96 mg/L]; threonine [11.91 mg/L]; *tryptophane* [3.06 mg/L]; *tyrosine*

- [2.72 mg/L]; valine [35.13 mg/L]; choline [13.96 mg/L]; serine [63.06 mg/L] (**Notes 5 and 6**).
- (b) Stock 2: Biotin [0.0146 mg/L]; Ca pantothenate [0.258 mg/L]; niacinamide [0.03663 mg/L]; pyridoxine HCl [0.06171 mg/L]; thiamine·HCl [0.3373 mg/L]; KCl [111.83 mg/L] (**Note 7**).
- (c) Stock 3: Folic acid [0.79 mg/L]; Na₂HPO₄·7H₂O [536 mg/L] (**Note 8**).
- (d) Stocks 4a, 4b, and 4c (individually prepared): (4a) FeSO₄·7H₂O [1.390 mg/L]; (4b) MgCl₂·6H₂O [122.0 mg/L]; (4c) CaCl₂·2H₂O [4.311 mg/L] (**Note 9**).
- (e) Stock 5: Phenol red [1.242 mg/L]. Make a 1,000× stock solution and store at room temperature in tightly stoppered bottle.
- (f) Stocks 6a, 6b, and 6c: Stock (individually prepared): (6a) Glutamine [877.2 mg/L]; (6b) sodium pyruvate [55 mg/L]; riboflavin [0.03764]. All three stocks should be stored frozen at -20 °C (**Note 10**).
- (g) Stock 7: Cysteine·HCl·H₂O [42.02 mg/L]. Make up as a 100× sterile stock solution (**Note 11**).
- (h) Stock 8: Asparagine [15.01 mg/L]; proline [35.53 mg/L]; putrescine [0.1611 mg/L]; vitamin B₁₂ [0.407 mg/L]. Make up a 100× sterile stock solution and store at 4 °C for 2 months or frozen at -20 °C for longer periods.
- (i) Stock 9: Alanine [8.91 mg/L]; aspartic acid [3.99 mg/L]; glutamic acid [14.71]; glycine [7.51 mg/L] (**Note 12**).
- (j) Stock 10: Inositol [18.02 mg/L]; lipoic acid [0.2063 mg/L]; thymidine [0.7266 mg/L]; CuSO₄·5H₂O [0.00249] (**Note 13**). Store stock 10 at 4 °C for up to 2 months or frozen as a 100× solution at -20 °C for longer periods.
- (k) Stock 11 is a trace element stock solution. First, prepare eight separate concentrated stock solutions; these are then further diluted in by adding a fixed volume (*x*/mL) of each to make up a final of 1.0 L in H₂O as follows: selenic acid [0.02497 mg/L {1.0 mL}]; manganese sulfate [0.3869 mg/L {0.1 mL}]; sodium silicate [14.21 mg/L {50.0 mL}]; ammonium molybdate [0.1236 mg/L {0.1 mL}]; ammonium vanadate [0.05850 mg/L {0.50 mL}]; nickel chloride [0.01189 mg/L {0.05 mL}]; tin chloride [0.01128 mg/L {0.50 mL}]; zinc sulfate [14.38 mg/L {50.0 mL}] (**Note 14**).

- (1) Solids (all components added directly to the final basal medium): Glucose [1,080.96 mg/L]; sodium chloride [6.20 g/L]; sodium acetate [500 mg/L]; *N*-[2-OH-ethyl]piperazine-*N'*-[2-ethanesulfonic acid (Hepes) buffer [4.77 g/L]; sodium bicarbonate [1,176 mg/L].
4. Preparation of final HECK 109 basal medium
Laboratory batches of HECK 109 are generally prepared in 1 L lots by adding the necessary stocks and solids to triple-distilled water (**Note 15**).
5. Prepare final medium additions
The following procedures are for the preparation of 1 L of basal medium. Add {*x* mL} of each to 800 mL of triple-distilled H₂O: stock 1 {10 mL}; stock 2 {10 mL}; stock 3 {20 mL}; stock 6 {1 mL}; stock 6a {60 mL}; stock 6b {10 mL}; stock 6c {10 mL}; stock 7 {10 mL}; stock 8 {10 mL}; stock 9 {10 mL}; stock 10 {10 mL}; glucose {1.081 g}; sodium chloride {6.20 g}; sodium acetate {0.5 g}; Hepes (4.77 g).
6. Adjust to pH 7.4 with 4.0 N NaOH and then add sodium bicarbonate {1.176 g} and triple-distilled water to a final 989 mL (**Note 16**). The medium minus stocks (4a, 4b, and 4c) is then sterile filtered through a 0.22 μm pore size filter and stored frozen at -20 °C in volumes of 200–500 mL for convenient single experiments.
7. When the medium is ready to use add each of the following to 100 mL of final medium: 0.1 mL of Stock 4a (1,000×) to make a final concentration of 3×10^{-5} M; 0.1 mL of Stock 4b (1,000×) to make a final concentration of 6×10^{-4} M; 0.52 mL of 4× (200×) to make a final concentration of 5×10^{-6} M; and 1.04 mL of stock 11 (trace elements) to make a final concentration of 5×10^{-7} M. This completes the preparation of basal HECK 109 medium.
8. To prepare HECK 109 standard medium add the following supplements to 1.0 L of basal medium: 1.0 mL of ethanolamine (1,000×) to make a final concentration of 1×10^{-4} M; 1.0 mL of phosphoethanolamine (1,000×) to make a final concentration of 1×10^{-4} M; 1.0 mL of hydrocortisone (1,000×) to make a final concentration of 5×10^{-7} M.
9. To prepare HECK 109 complete medium add the following proteinaceous growth factors: EGF (10 μg/mL stock), 0.1–100 mL of standard medium, and 0.1 mL of IGF-1 (5 μg/mL stock solution) to 100 mL of standard medium (**Note 17**).
10. The complete formula of HECK 109 basal medium is presented in Table 1 (**Note 18**).

Table 1
Composition of basal nutrient medium HECK-109 concentration in final medium

	Component	mg/L	mol/L
Stock 1	Arginine·HCl	421.4	2.00×10^{-3}
	Histidine·HCl·H ₂ O	33.6	1.60×10^{-4}
	Isoleucine allo-free	3.9	3.00×10^{-5}
	Leucine	31.2	1.00×10^{-3}
	Lysine·HCl	36.6	2.00×10^{-4}
	Methionine	9.0	6.00×10^{-5}
	Phenylalanine	10.0	6.00×10^{-5}
	Threonine	23.8	2.00×10^{-4}
	Tryptophane	6.0	3.00×10^{-5}
	Tyrosine	5.4	3.00×10^{-5}
	Valine	70.2	6.00×10^{-4}
	Choline	28.0	2.00×10^{-4}
	Serine	126.1	1.20×10^{-3}
	Stock 2	Biotin	0.0146
Calcium pantothenate		0.285	1.00×10^{-6}
Niacinamide		0.0333	3.00×10^{-7}
Pyridoxal·HCl		0.06171	3.00×10^{-7}
Thiamine·HCl		0.3373	1.00×10^{-6}
Potassium chloride		111.83	1.50×10^{-3}
Stock 3	Folic acid	0.79	1.80×10^{-6}
	Na ₂ HPO ₄ ·7H ₂ O	536.2	2.00×10^{-3}
Stock 4a	Calcium chloride·2H ₂ O	14.7	1.00×10^{-4}
4b	Magnesium chloride·6H ₂ O	122.0	6.00×10^{-4}
4c	Ferrous sulfate·7H ₂ O	1.30	5.00×10^{-6}
Stock 5	Phenol red	1.242	3.30×10^{-6}
Stock 6a	Glutamine	877.2	6.00×10^{-3}
6b	Sodium pyruvate	55.0	5.00×10^{-4}
6c	Riboflavin	0.03764	1.00×10^{-7}
Stock 7	Cysteine·HCl	37.6	2.40×10^{-4}
Stock 8	Asparagine	15.01	1.00×10^{-4}
	Proline	34.53	3.00×10^{-4}
	Putrescine	0.1611	1.00×10^{-6}
	Vitamin B12	0.407	3.00×10^{-7}
Stock 9	Alanine	8.91	1.00×10^{-4}
	Aspartic acid	3.99	3.00×10^{-5}
	Glutamic acid	4.71	1.00×10^{-4}
	Glycine	7.51	1.00×10^{-4}
Stock 10	Inositol	18.02	1.00×10^{-4}
	Lipoic acid	0.2063	1.00×10^{-6}
	Thymidine	0.7266	3.00×10^{-6}

(continued)

Table 1
(continued)

	Component	mg/L	mol/L
Stock 11	Copper sulfate·5H ₂ O	0.00025	1.00×10^{-9}
	Selenic acid	0.00387	3.00×10^{-8}
	Magnesium sulfate·5H ₂ O	0.00024	1.00×10^{-9}
	Sodium silicate·9H ₂ O	0.1421	5.00×10^{-7}
	Ammonium molybdate·4H ₂ O	0.00124	1.00×10^{-9}
	Ammonium vanadate	0.00059	5.00×10^{-9}
	Nickel chloride·6H ₂ O	0.00012	5.00×10^{-10}
	Stannous chloride·2H ₂ O	0.000113	5.00×10^{-10}
	Zinc chloride·7H ₂ O	0.1438	5.00×10^{-7}

3.2 Preparation of Primary Basal Epidermal Keratinocyte Cultures

1. Prepare CCS solution, a balanced salt solution, according to the following formula: glucose, 10 mM; KCl, 3 mM; NaCl, 130 mM; Na₂HPO₄·7H₂O, 1 mM; phenol red, 0.0033 mM; and Hepes, 20 mM. This formula is the subject of a patent issued to the author (J.J.W.) (**Note 19**) (**20**).
2. Steps in isolation of basal cells and primary cultures
Skin obtained from biopsies or autopsies is first cleaned of adhering subdermal fat, and the dermis is reduced to less than 3 mm² in thickness using a dermatome. The skin sample is then typically cut into 8–12 small pieces (usually 0.5 cm²). These pieces are floated on top of a sterile CCS, a balanced salt solution, containing a trypsin and an antibiotics solution (100 U of both penicillin/streptomycin).
3. A modified split-dermis technique is employed to enzymatically digest the floating skin pieces by adding 0.17 % trypsin (3×, cryst) and 100 U/mL of both penicillin and streptomycin. After 14–16 h of digestion at 4° C the dermis is separated for the epidermis, by inverting the skin sample and placing the cornified layer side of the epidermis onto a clean sterile polystyrene surface. The living epidermis spontaneously detaches, and the dermis is removed with sterile forceps, rinsed with cold CCS and (**Note 20**) keratinocytes are collected into 15 mL conical centrifuge tube on ice. The histology of human skin samples subject to trypsin digestion is shown in Fig. 1.
4. Primary cultures are initiated into HECK 109 complete medium supplemented with the above antibiotics, which are removed 2–3 days later when the proliferating cell cultures are refed fresh complete medium. The initial seeding density for initiating the primary culture is 5×10^4 basal cells per 75 cm² tissue culture flask. Generally, two such flasks are routinely set up from an initial yield of $1-2 \times 10^6$ cells isolated from a 1–2 cm² piece of skin.

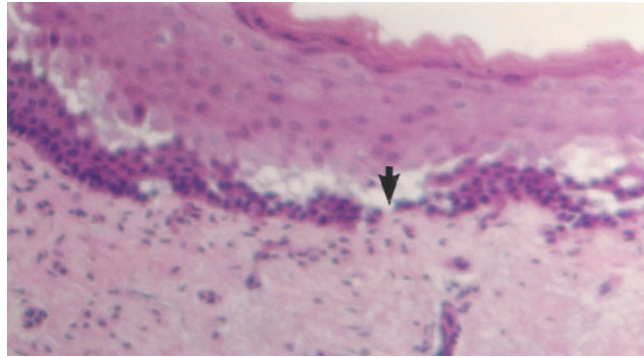


Fig. 1 Photomicrograph of human skin 14–16 h after trypsin digestion. The skin is cleaved along a fracture line (*arrow*), which separates some of the basal cells with the dermis but frees other basal cells lying between the dermis and the fracture line just above the basal cell layer

3.3 Freezing Keratinocyte Cells from Primary Culture

Often it is necessary to establish and maintain a cell bank of patients' frozen cells. Thus, any cells that do not need to be cultured for grafts may be stored in liquid nitrogen.

1. A cell suspension at $2\text{--}4 \times 10^6/\text{mL}$ in complete HECK 109 is diluted with an equal volume of freezing medium (FM) composed of 60 % complete HECK 109 medium, 20 % dialyzed fetal bovine serum (dFBS), and 20 % dimethylsulfoxide (DMSO). The final concentrations are then as follows:
Cells ($1\text{--}2 \times 10^6/\text{mL}$) in 80 % complete HECK 109 medium, 10 % dFBS, and 10 % DMSO.
2. 1 mL of cell suspension in FM is aliquoted into cryotubes and allowed to stand upright in a styrofoam box and frozen at -80°C freezer overnight or longer before transferring to a liquid nitrogen tank.
3. Thawing cells from liquid nitrogen storage
Thaw cells rapidly by hand twirling in a 37°C water bath. Transfer the cell suspension to a 15 mL conical centrifuge tube with approximately 10 mL of cold CCS solution. Centrifuge for 5 min at $140 \times g$ in a cold centrifuge. Aspirate the supernatant with a sterile glass pipette and rubber bulb, and bring the cell pellet up in 10 mL of complete HECK 109 medium and plate into fibronectin ($2\text{--}20 \mu\text{g}/\text{mL}$)-coated flasks.

3.4 Preparation of Secondary Serially Passaged Cultures

1. Secondary cultures initiated from primary cultures are routinely passaged by enzymatic dissociation of cells. The serial passage technique is not standard. It involves the use of ice-cold trypsin (0.025 %) and 0.01 % ethylenediaminetetraacetic acid (EDTA) dissolved in CCS solution to release cells from their plastic substrate (**Note 21**). Before the cells have been harvested by low-speed centrifugation ($50 \times g$) add 2 mL of

soybean trypsin inhibitor (1 mg/mL in CCS solution). Bring the cell pellet up in complete HECK 109 medium at a reasonable concentration (e.g., 2 to 4×10^6 /mL), which works well if there are enough cells so that some may be frozen down. The secondary cultures are seeded in fibronectin-coated flasks (2 μ g/mL) at a cell density of 5×10^3 /cm², but lower seeding densities are possible. By this method, the percent attachment of epidermal cells is typically 50–60 % of the input cells. The colony forming efficiency (CFE) routinely ranges between 0.1 and 0.5 % of the input cells as measured by taking 20 μ L aliquot for counting in a hemocytometer using an ocular micrometer to count living cells (**Note 22**).

3.5 Formation of an Anatomically Complete Autologous Cultured Epidermis (A-CEA)

The formation of a histologically complete A-CEA is a multi-step process. The process is the subject of several patents issued to the author (**Notes 1 and 19**). It can be simplified into four major steps as follows:

1. The formation of a hole-free monolayer of second-passage basal keratinocyte stem cells is accomplished by feeding each of several T-75 cm² culture flasks with complete HECK 109 (FS) a low-calcium medium containing EGF(1–25 ng/mL) and IGF1 (0.3–30 ng/mL) every other day until a confluent monolayer is formed.
2. To achieve reversible inhibition of keratinocyte proliferation HECK 109 FS is replaced with HECK 109 (DM, differentiation medium) containing high calcium (2 mM), beta-TGF (10 ng/mL) is added for 30 min, and beta-TGF is removed by two successive washes with pre-warmed (37° C) CCS solution.
3. To induce a multilayered and keratinizing differentiation re-feed the above cultures by adding HECK 109 high-calcium medium minus EGF but containing IGF-1 (0.3–3.3 ng/mL) until stratification occurs with 2–4 days.
4. To induce multilayered uppermost layer of the epidermis (stratum corneum) replace the above medium with HECK 109 basal medium containing linoleic acid (1–15 μ g/mL) and hydrocortisone (10^{-7} M).
5. To release the cultured epidermis from the plastic substrate, the living CEA is first rinsed several times with pre-warmed (37° C) CCS solution, and then a sufficient volume (4 mL per 75 cm² flask) of type IV collagenase (dispase, 0.4 % solution, 2 mg/mL) is gently added to the surface of the CEA. Sheets detach between 30 and 45 min. Once CEA spontaneously lifts off and floats to the surface, it is then gently washed with several rinses of pre-warmed (37° C) CCS solution. Using sterile forceps, it is picked up and dragged out the flask (the top of the flask has been aseptically removed) with the help of

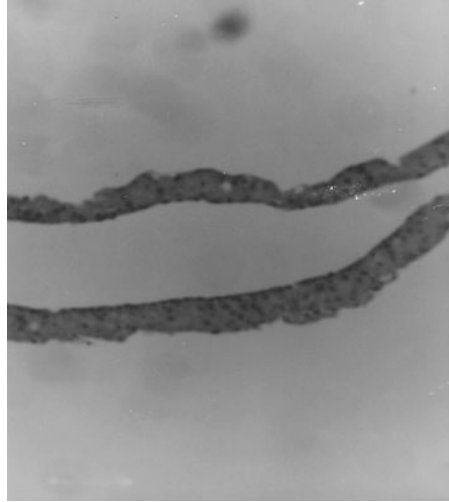


Fig. 2 A photomicrograph of two pieces of sectioned and H&E-stained multilayered epidermis formed in serum-free culture

sterile glass rods and transferred basal layer side up onto Vaseline gauze for transport and application to a debrided wound.

6. One sheet of the A-CEA is fixed in 3.7 % formalin in phosphate-buffered saline (PBS), digital photographs are taken, and the images are stored on a compact disc. Pieces of a third epidermal sheet are flash frozen in OTC medium for sectioning with a cryotome and stained for histology (**Note 23**).
7. The A-CEA epidermal sheet on Vaseline gauze is kept overnight in refrigerator with a small volume of basal HECK 109 medium as per transport.
8. Typically the entire process of forming a cultured CEA takes 2–3 weeks. A photomicrograph of two pieces of sectioned and H&E-stained multilayered epidermis formed in serum-free culture is shown in Fig. 2.

3.6 Preclinical Performance Characteristics of Human Keratinocytes Cultured in HECK 109 Serum-Free Medium

The superiority of the serum-free culture methodology was explored through investigations on the clonal growth capacity of undifferentiated basal keratinocyte cultures established by the above procedures using clonal growth assay method (18).

1. Evidence of the undifferentiated state of proliferating cultures of basal keratinocytes was studied by plating cells at low density ($1 \times 10^3/\text{cm}^2$) and after 2 days of culture in complete HECK 109 serum-free medium. The cells were fixed and stained with Mallory's trichrome stain, which stains basal epidermal cells a blue color (18).

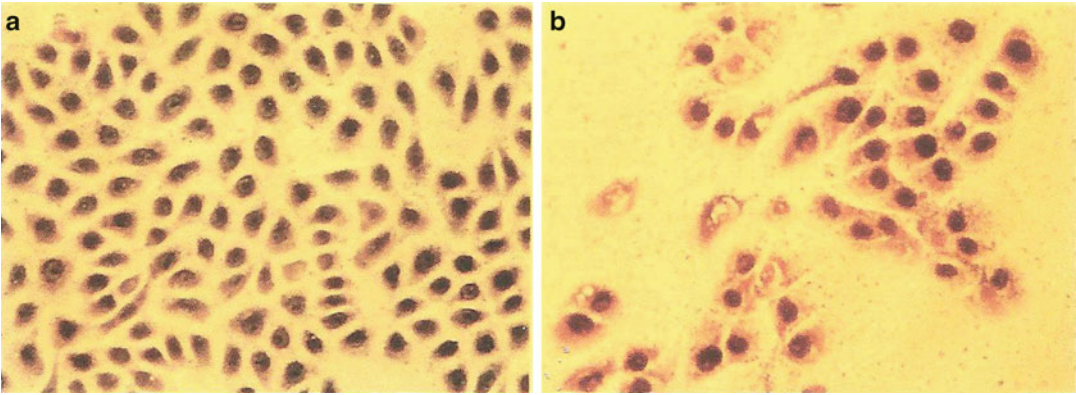


Fig. 3 (a) Microphotograph of Mallory's trichrome-stained culture of rapidly dividing epidermal keratinocytes grown in serum-free complete HECK 109 medium. (b) Photomicrograph of an autoradiograph of a rapidly dividing epidermal keratinocyte. *Note:* The true color of cells in autoradiograph is distorted due to interfering thickness of the emulsion

Figure 3a is a photomicrograph showing that indeed all the proliferating keratinocytes stained a blue color. Further, the technique of autoradiography was employed to detect whether all of the cell nuclei had completed S-phase DNA synthesis in a 24-h pulse-labeling period with radiolabeled tritiated thymidine. Figure 3b is a photomicrograph demonstrating that virtually 100 % of Mallory's trichrome-stained blue-colored cells had dense silver grains over their nuclei, indicating that the entire keratinocyte population consisted of rapidly dividing basal undifferentiated keratinocyte cells. This result is also supported by cell counts of rapidly dividing cultures that demonstrate a linear doubling of cell population every 24 h (18).

2. Clonal growth studies

A series of clonal growth experiments were carried out according to the methods previously reported (18). Such experiments can definitively determine the clonal growth capacity of individual single-celled clones to form a colony when keratinocytes propagated in serum-free complete HECK 109 medium. The results of one such experiment are displayed in Table 2. It compares the clonal growth of a strain of adult epidermal keratinocytes (AH B1) versus a strain of neonatal foreskin keratinocytes (NF 201). The data indicate that 70 % of cells randomly selected from a secondary three serially passaged culture retain the ability for colonies, compared with 48 % for adult keratinocyte cultures selected at random from a three-time serially passaged culture propagated in complete HECK 109 serum-free medium. Both adult and neonatal clonal capacities are sufficient to allow good production of cultured CEAs.

Table 2
Comparison of the proliferative potential of individual adult (AHB1) and neonatal (NF201) keratinocyte basal cells

Prior culture condition ^{a,b}				
Clone no.	Passage no.	Density (10 ⁴ /cm ²)	Average GT (h)	% Proliferative clones (N)
AH B1	3	0.4	48	48 (109)
NF 201	3	7.5	24	70 (106)

^aGT is defined as the average population doubling time (in hours) of the culture

^bN is the number of single-cell clones tested

3.7 Methods for Preparing A-CEA for Grafting to Chronic Venous Stasis Leg Ulcers

These procedures have been successfully conducted in a prospective randomized double-blind clinical trial and the result published (5).

1. Biopsy procedures

A biopsy can only be taken after patient passes the screening, after they have signed an informed consent, and after they have been randomized, and passes all inclusion and exclusion criteria and all laboratory tests are satisfactory as per the protocol (Note 22).

Full-thickness (inguinal fold) skin biopsies of approximately 2–3 in. in length and (under) 1 in. width were surgically excised under sterile conditions using (an injection of 1 % xylocaine with 1:200,000 epinephrine as) local anesthesia. The skin specimen was deposited directly into sterile 50 mL disposable centrifuge tube containing sterile normal saline solution and transferred to the epidermal tissue production laboratory for recovery of epidermal keratinocytes and production of cultured epidermal tissue as described above (see Sections 3.2, 3.4, and 3.5). The donor site incision was closed in standard fashion with deep dermal absorbable sutures and steri strips. All donor sites healed in 10 days with no complications.

2. Post-production procedures

After the patient epidermal tissue is formed in culture it is transferred by shipment overnight delivery labeled Medical Supplies. Upon receipt at the hospital clinic, it is carefully unwrapped and the graft is trimmed to fit with small overlap in the area of the patient's debrided wound. The graft is inserted epidermal basal layer side down into the wound and covered with an additional layer of adaptic petroleum gauze and PBS-soaked sterile gauze.

3. Application of A-CEA to chronic wounds

For application to chronic venous stasis leg ulcer, the technique of high-compression bandaging is instituted to keep the graft in contact with the wound and to apply sufficient pressure to

attain a therapeutic benefit from both the graft and the sustained compression.

4. A prospective, randomized, double-blind clinical trial was undertaken at the Grant Hospital and the Columbus, Ohio, Wound Care Center under the supervision of Dr. J.J. Burdge and the approval of the Grant Hospital IRB committee.
5. The clinical performance of the A-CEA in combination with compression therapy was determined in a 12-week trial as reported (5).
6. There were no adverse effects of the grafting procedure, and the efficacy of healed (closed) wounds was dramatically improved over results using allogeneic cultured graft prepared by culture in serum-containing medium (5).

4 Notes

1. U.S. Patent: 5,686,307 (11/11/97) issued to J.J. Wille discloses the composition of HECK 109 serum-free media for preparing a CEA graft.
2. It can be used after this time if fresh glutamine and pyruvate are added. When a batch is made up one 500 mL bottle is usually made 30 μM Ca^{2+} and given a yellow-colored label.
3. It will keep as long as the basal media is good; i.e., if basal is 2 weeks old, glutamine and pyruvate are added. When a batch is made up, one 500 mL bottle is usually made 30 μM Ca^{2+} and given a red-colored label.
4. When a batch is made up, one 500 mL bottle is usually made 100 μM Ca^{2+} and given a blue-colored label.
5. The six underlined amino acids are made up as an independent stock solution at 6 \times their stated concentration in sterile purified water and added to stock 1 at a final concentration of 2 \times , when the cell culture reaches 1×10^4 cell/cm², to allow a monolayer culture to reach confluence without attaining sub-confluent saturation density inhibition.
6. Gentle heating with stirring is helpful in dissolving the components of stock 1. When a 100 \times stock 1 solution is made it is stored at 4° C for up to 2 months or frozen at -20° C for longer periods.
7. Stock 2 is stored at 4° C for up to 2 months or frozen as a 100 \times stock at -20° C for longer periods.
8. Stock 3 is stored at 4° C for up to 2 months, or a 50 \times stock solution is frozen at -20° C for longer periods.

9. Make up a 200× stock solution of 4a, a 1,000× stock solution of 4B, and a 1,000× stock solution of 4c. For 4a, dissolve solid in 2.5 mL of 4 M HCl. Dilute to 100 mL with H₂O. Discard solution if precipitate or orange color occurs. Store sterile by filtering at room temperature; keeps indefinitely.
10. Stock 6c (riboflavin) must be protected from light.
11. Stock 7 should be prepared fresh for each basal medium preparation.
12. Stock 9 is made up as 100× solution as follows: Aspartic acid and glutamic acid are added to slightly less than the final volume of water. One mL/L of phenol red indicator solution is added, and 1.0 N NaOH is added with stirring just rapidly enough to keep the solution neutral as the acids dissolve. When no solids remain a stable orange-colored solution is achieved, then alanine and glycine are dissolved in the solution, and the rest of the water is added to make up the final volume.
13. Stock 10 is prepared as follows: Lipic acid is dissolved in a few drops of 1.0 N NaOH, then diluted, and added to stock solution. The other 32 components dissolve readily when added to the final solution.
14. Stock 11 is stored sterile at room temperature indefinitely. It should be kept slightly acidic to prevent precipitation of any metal hydroxides by adding 1/100× dilution of a 1 N HCl to the final 1.0 L volume.
15. Stocks 4a, 4b, and 4c are only added to the final medium just before it is to be used.
16. Check the osmolarity. It should be between 280 and 320 mOsmol.
17. Add ethanolamine, phosphoethanolamine, and hydrocortisone to HECK 109 basal medium and filter thru 0.22 μm pore size filter; then add individually sterile filtered EGF and IGF-1 directly to this to prevent them from sticking to or clogging the filter.
18. U.S Patent No.: 5,292,644 (3/8/94 issued to J.J. Wille). It is primarily a methods patent. It claims a method for the formation of a histologically complete skin substitute that is recovered from the culture by treatment with a protease comprising the steps of (a) feeding basal keratinocyte stem cells a medium (HECK 109FS) of low calcium, EGF (1–25 ng/mL) and IGF1 (0.3–30 ng/mL); (b) replacing the above medium with HECK109 (FS)—a high calcium plus beta-TGF (3–30 ng/mL); and (c) replacing the above with HECK 109 basal medium containing linoleic acid (1–15 μg/mL) and hydrocortisone (10⁻⁷ M).

19. U.S. Patent No.: 5,795,781 issued to J.J. Wille claims the composition of a balanced salt solution for keratinocytes isolating, as a holding medium for transferring keratinocytes between serial passages, and rinsing growing culture of proliferating keratinocyte cells.
20. Flow cytometric analysis conducted by the author (J.J.W.) showed that these loosely associated basal cells are larger than the basal cells that remain associated with the dermis, i.e., above the trypsin fraction line (see Fig. 1). In addition, clonal growth experiment carried out by the author (J.J.W.) established that they also have a greater colony-forming ability than the dermis-associated basal cells.
21. Watch under phase-contrast microscope as cells start to round up. After 5 min aspirate most of the trypsin-EDTA (along with any fibroblasts that have floated off).
22. The procedures for calculating CFE of the basal cells recovered from the epidermis and used to initiate a primary culture are to set up duplicate primary cultures at 5,000 cells/cm² as described above, and then using a standard hemocytometer cell counting chamber count the number of cells which attach and which later form a colony of at least eight or more cells 3 days after seeding the primary culture. By this method, the percent attachment of epidermal cells is typically 50–60 % of the input cells.
23. All biopsies were performed at the Grant Hospital in Columbus, Ohio, by Dr. J.J. Burdge, a plastic surgeon using sterile procedures.

Acknowledgments

I wish to acknowledge the excellent technical assistance provided by Ms. Nelle Swanson (deceased) and Professor (Dr.) M.R. Pittelkow, both of the Mayo Medical School in Rochester, MN.

References

1. Leigh IM, Purkis PE (1986) Culture grafted leg ulcers. *Clin Exp Dermatol* 11:650–652
2. Phillips TJ (1998) New skin for old: developments in biological. *Arch Dermatol* 134:344–349
3. Ehrenreich M, Ruszczak Z (2006) Update on tissue engineered biological dressings. *Tissue Eng* 12:1–18
4. Limova M (2010) Advanced wound coverings: bioengineered skin and dermal substitutes. *Surg Clin North Am* 90(6):1237–1255
5. Wille JJ, Burdge JJ, Pittelkow MR (2011) Rapid healing of chronic venous stasis leg ulcers treated by application of a novel serum-free cultured autologous epidermis. *Wound Repair Regen* 19(4):464–474
6. Dieckmann C, Renner R, Milkova L, Simon J (2010) Regenerative medicine in dermatology: biomaterials, tissue engineering, stem cells, gene transfer and beyond. *Exp Dermatol* 19(8):697–706

7. Falanga V, Sabolinski M (1999) A bilayered living skin construct (APLIGRAF) accelerates complete closure of hard-to-heal venous ulcers. *Wound Repair Regen* 7:201–207
8. Zauilyanov L, Kirsner RS (2007) A review of a bi-layered living cell treatment (Apligraf) in the treatment of venous leg ulcers and diabetic foot ulcers. *Clin Interv Aging* 2:93–98
9. Philips TJ, Manzoor J, Rojas A, Isaacs C, Carson P, Sabolinski M et al (2002) The longevity of a bilayered skin substitute after application to venous ulcers. *Arch Dermatol* 138:1079–1081
10. Blok CS, Vink L, de Boer EM, van Montfrans C, van den Hoogenband HM, Mooij MC et al (2013) Autologous skin substitute for hard-to-heal ulcers: retrospective analysis of safety, applicability, and efficacy in an outpatient and hospitalized setting. *Wound Repair Regen* 21:667–676
11. Chaby G, Senet P, Ganry O, Caudron A, Thiullier D et al (2013) Prognostic factors associated with healing of venous leg ulcers: a multicenter, prospective, cohort study. *Br J Dermatol* 169(5):1106–1113
12. Kirsner RS, Marston W, Snyder RJ, Lee TD, Cargill DI, Slade HB (2012) Spray-applied cell therapy with human allogeneic fibroblasts and keratinocytes for the treatment of chronic venous leg ulcers: a phase 2, multicentre, double-blind, randomized, placebo-controlled trial. *Lancet* 380(9846):977–985
13. Marston W (2011) Mixed arterial and venous ulcers. *Wounds* 23(12):351–356
14. Hefton JM, Caldwell D, Biozes DG, Balin AK, Carter DM (1986) Grafting of skin ulcers with cultured autologous epidermal cells. *J Am Acad Dermatol* 14:339–405
15. Limova M, Mauro T (1995) Treatment of leg ulcers with cultured epithelial autografts: treatment protocol and five years experience. *Wounds* 7:170–180
16. U.S. Patent No. 4,304,866 (1981) Transplantable sheets of living keratinous tissue
17. Boyce S, Ham R (1983) Calcium regulation of differentiation of normal human epidermal cells in a chemically and serum-free defined medium. *J Invest Dermatol* 81:33–40
18. Wille JJ, Pittelkow MR, Scott RE (1984) Integrated control of growth and differentiation of normal human prokeratinocytes in serum-free medium: clonal analysis, growth kinetics, and cell cycle studies. *J Cell Physiol* 121:31–44
19. U.S. Patent No. 5,686,307 (11/11/97) Serum-free medium for use in the formation of a histologically-complete living human skin substitute
20. U.S. Patent No. 5,795,781 (8/18/1998) Cell competency solution for use in the formation of a histologically-complete living human skin substitute

Human Keratinocyte Cultures in the Investigation of Early Steps of Human Papillomavirus Infection

Laura M. Griffin, Louis Cicchini, Tao Xu, and Dohun Pyeon

Abstract

Human papillomaviruses (HPVs) are non-enveloped DNA viruses that are highly tropic for mucosal and cutaneous epithelia. The HPV life cycle is tightly linked to epithelial cell differentiation, where HPVs only infect the basal proliferating keratinocytes, and progeny virus assembly and release only occurs in differentiated upper-layer keratinocytes. Therefore, human keratinocyte monolayer cultures provide a useful model to study the early stages of HPV infection. However, previous reports have shown some conflicting results of virus–host interactions during HPV entry, which may be partly attributable to the different cell culture models used to examine these steps of HPV infection. Thus, there is a need to have a standardized in vitro model system to study virus–host interactions during HPV entry. Here, we describe the three most widely accepted keratinocyte models for studying HPV infection: primary human foreskin keratinocytes, normal immortalized keratinocytes, and transformed HaCaT keratinocytes. We also describe methods to genetically manipulate these cells, enabling the study of candidate host genes that may be important during HPV infection. Lastly, we outline simple and robust methods to assay HPV infectivity, which can be used to determine whether knockdown or overexpression of a particular gene affects HPV entry.

Keywords: Keratinocyte, HFK, NIKS, HaCaT, Lentivirus, Transduction, Transfection, Puromycin, Papillomavirus, HPV

1 Introduction

Human papillomaviruses (HPVs) are causally associated with multiple human cancers, including 99 % of cervical, 50 % of other anogenital, and upwards of 25 % of head and neck cancers (1–5). These important human pathogens are notably small, roughly 55 nm in diameter with only an 8 kb double-stranded circular DNA genome encoding usually 8–9 genes. They are non-enveloped, with only two capsid proteins: the major capsid protein L1 and the minor capsid protein L2 (6). HPVs have very strict species and tissue tropism; they productively infect only mucosal and cutaneous epithelia, and their life cycle is tightly linked to epithelial cell differentiation (7, 8). Papillomaviruses must first bind to the basement membrane of the epithelium in order

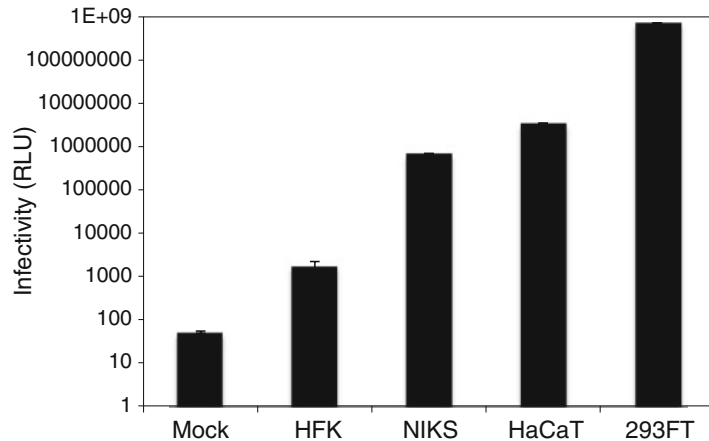


Fig. 1 HPV16-LucF infectivity is limited in primary keratinocytes. The indicated cell lines were inoculated with 10,000 vge/cell of HPV16-LucF and incubated for 48 h. HPV16 infectivity and cell viability were measured by Bright-Glo Luciferase Assay System (Promega) and CellTiter-Glo Luminescent Cell Viability Assay (Promega), respectively. Infectivity data normalized to cell viability are shown as average relative luminescence units (RLU) from quadruplicate samples. The data shown here are from one representative of three independent experiments

to interact with the basal proliferating keratinocytes they infect (9, 10). These viruses cannot infect differentiated keratinocytes, as cell cycle progression is required for HPV infection (11). This feature of the papillomavirus life cycle long prohibited the production of viruses in a laboratory setting, thus thwarting the study of virus–host interactions during HPV entry. In recent years, methods to produce papillomaviruses independent of epithelial cell differentiation have been developed, allowing progress to be made in the investigation of the early steps of HPV infection (12, 13).

Although our knowledge of HPV entry mechanisms has been greatly advanced since the development of robust HPV production methods, several publications show conflicting data regarding the mechanism of HPV internalization and endocytic trafficking in host cells (14–18). These discrepancies could be at least partly attributable to the different cell culture models used in these studies. For example, experiments conducted in non-keratinocyte 293 and COS-7 cells demonstrated a clathrin-dependent mode of HPV entry (14, 16), which contradicts with data obtained from HeLa and HaCaT cells, showing a clathrin-independent mechanism of HPV entry (18–20). We observed striking differences in HPV16 infectivity among different keratinocytes (Fig. 1) and found that host autophagy inhibits HPV16 infection in epithelial cells but not in fibroblasts (data not shown) (21). This highlights the importance of using physiologically relevant cell culture models to study virus–host interactions during HPV entry.

Protocols on how to culture the most widely accepted, physiologically relevant keratinocyte models for HPV infection studies are detailed in Sections 2.1 and 3.1. Primary human foreskin keratinocytes (HFKs) are considered the most relevant native host cells for HPV infection. Ironically, these cells are extremely difficult to infect with HPV (21–23), indicating that they may have more robust host mechanisms to interfere with HPV entry relative to immortalized and transformed keratinocytes (Fig. 1) (21). Indeed, we found that HFKs have higher levels of basal autophagy, recently recognized as a host defense pathway which inhibits HPV16 infection (21). Furthermore, HFKs may have altered heparan-sulfate proteoglycan (HSPG) modifications, which prevent HSPG-facilitated furin cleavage of L2, a prerequisite for infectious entry of papillomaviruses (22). One method reported to overcome the challenges of infecting HFKs is to include exogenous furin in the inoculum, or to pretreat the virus prep with furin, in order to facilitate the required furin cleavage of L2 and enhance infectious entry (22). HFKs do not require feeder cells, and growth medium is commercially available; however, these cells should not be cultured for longer than 4 weeks, as significant morphological changes occur followed by growth arrest by 6 weeks.

Normal immortalized keratinocytes (NIKS) from skin is a spontaneously immortalized near-diploid cell line showing normal growth and differentiation. Thus, NIKS are still considered physiologically relevant yet are much more permissive to HPV infection compared to HFKs (Fig. 1, ~400-fold increase in infectivity) (21, 23, 24). In addition, as immortalized cells, establishment of genetically modified stable cell lines is feasible with NIKS. NIKS are rather cumbersome to culture, compared to HFK or HaCaT, as they require feeder cells and various growth supplements, many of which should be freshly prepared to support healthy growth without spontaneous differentiation. The HaCaT keratinocytes, currently the most widely used in HPV research, are the most convenient and cost-effective cells to culture. While HaCaTs might still be very useful for many initial experiments, data obtained from these cells should be corroborated with normal keratinocytes, such as NIKS or HFK, in several occasions.

To determine whether a particular gene of interest is important during HPV infection, methods to manipulate specific gene expression using RNAi and overexpression are outlined in Sections 2.2 and 3.2. Lentiviral vectors are routinely used to deliver plasmids encoding shRNAs or ORFs into keratinocytes including normal keratinocytes HFK and NIKS. In addition to lentiviral transduction, transfection of keratinocytes using recently introduced reagents such as TransIT 2020 and X-tremeGENE HP has proven effective with reasonable transfection efficiencies (~50 %) (data not shown). Establishment of specific keratinocyte lines is possible by

antibiotic resistance selection and is necessary when a pathway of interest is affected by lentivirus infection or transfection. For example, when studying an innate immune response such as autophagy, we found that lentivirus transduction alone can induce this pathway and confound results (data not shown).

HPV pseudovirions containing luciferase or fluorescent protein genes offer convenient and quantifiable methods to determine relative HPV infectivity. This is instrumental in determining whether a particular gene has a role in the early steps of HPV infection. We routinely use two different types of luciferase reporters, firefly luciferase (FL) and renilla luciferase (RL), and green fluorescent protein (GFP) to produce HPV16 reporter pseudovirions. The pseudovirion *hvp16*-LucF, developed by Chris Buck (25), expresses both FL and GFP in infected cells at high levels and thus is useful when monitoring infection in HFKs, which exhibit very low levels of infection. We developed *hvp16*-phRL pseudovirions containing RL only and HPV16RL containing RL inserted into the HPV16 genome. This offers the advantage of comparing luciferase reporter virions containing HPV genomes (HPV16RL) to those containing only the reporter gene (*hvp16*-phRL). These HPV pseudovirions and chimeric virions are useful when studying viral DNA interactions with host keratinocytes during entry.

2 Materials

2.1 Keratinocyte Culture

2.1.1 Primary Human Foreskin Keratinocytes

1. Human Epidermal Keratinocytes, neonatal (HEKn, aka “HFK”) (Invitrogen Cat. # C-001-5C) (*see Note 1*).
2. EpiLife medium supplemented with human keratinocyte growth supplement (HKGS):

HKGS (Gibco/Invitrogen Cat. # S-001-5)	5 mL
EpiLife with 60 μ M Calcium (Gibco/Invitrogen Cat. # MEP1500CA)	500 mL

3. 0.02 % EDTA/PBS:

0.5 M EDTA	526 μ L
1 \times PBS (MediaTech/Fisher Cat. # MT-20-031-CV)	500 mL

4. 0.05 % trypsin/EDTA (HyClone/Fisher Cat. # SH30236.01).
5. DMEM containing 10 % newborn calf serum (NCS):

DMEM w/high glucose (HyClone/Fisher Cat. # SH30022.FS)	500 mL
NCS (HyClone/Fisher Cat. # SH30401.01)	50 mL

2.1.2 *Normal
Immortalized Keratinocytes
from Skin*

The materials listed below have been adapted from the NIKS culture protocol published by Paul Lambert (26).

1. DMEM containing 10 % NCS (Section 2.1.1, step 5).
2. 1× PBS without calcium and magnesium (MediaTech/Fisher Cat. # MT-20-031-CV).
3. 0.25 % trypsin/EDTA (HyClone/Fisher Cat. # SH30042.01).
4. 50× Mitomycin C: *Wear gloves!*
 - (a) Use a syringe needle to add 2 mL HEPES-buffered Earle's salts (HBES) (Section 2.1.2, step 6) to a 2 mg vial of Mitomycin C (Sigma Cat. # M4287-2MG).
 - (b) Transfer to conical tube, and bring to 10 mL with HBES.
 - (c) Filter sterilize, and store 1 mL aliquots at -20°C .
5. E-Complete medium:

DMEM w/high glucose (HyClone/Fisher Cat. # SH30022.FS)	375 mL
Ham's nutrient mixture F-12 (HyClone/Fisher Cat. # SH30026.01)	125 mL
Fetal bovine serum (FBS) (MediaTech/Fisher Cat. # MT-35-011-CV)	12.5 mL
100× Hydrocortisone	5 mL
100× Cholera toxin	5 mL
100× Adenine	5 mL
100× Epidermal growth factor (EGF)	5 mL
100× Insulin (made fresh)	5 mL

6. HBES:

Earle's salts	100 mL
1 M HEPES, pH 7.3 (Amresco Cat. # J848)	25 mL
Sterile H ₂ O	To 1 L total volume

7. Earle's salts:

NaCl	128 g
KCl	8 g
NaHCO ₃	74 g
NaH ₂ PO ₄ · H ₂ O	2.5 g
MgSO ₄ · 7H ₂ O	4 g
Fe(NO ₃) ₃ · 9H ₂ O	0.002 g
Phenol red	0.1 g
Sterile H ₂ O	To 2 L total volume
*Filter sterilize, and store at RT	

8. 100× Hydrocortisone:

- (a) Make 5 mg/mL hydrocortisone stock solution: Add 5 mL cold 100 % ethanol to 25 mg vial hydrocortisone (Calbiochem/EMDMillipore Cat. # 3867). Store at -20°C for future use.
- (b) Add 0.8 mL of 5 mg/mL hydrocortisone stock to 100 mL HBES containing 5 % FBS (95 mL HBES + 5 mL FBS).
- (c) Filter sterilize, and store 10 mL aliquots at -20°C .

9. 100× Cholera toxin:

- (a) Make 10 μM cholera toxin stock solution: Use syringe needle to add 1.2 mL sterile water to a 1 mg vial cholera toxin (Sigma Cat # C8052-1MG). Store at 4°C for future use.
- (b) Make 100× cholera toxin from 10 μM stock: Add 100 μL of 10 μM cholera toxin stock to 100 mL HBES containing 0.1 % BSA (dissolve 0.1 g BSA into 100 mL HBES by shaking vigorously).
- (c) Filter sterilize, and store 50 mL aliquots at 4°C .

10. 100× Adenine:

- (a) Dissolve 242 mg adenine (Sigma Cat. # A9795) in 100 mL 0.05 M HCl by stirring for 1 h.
- (b) Filter sterilize, and store 10 mL aliquots at -20°C .

11. 100× EGF:

- (a) Add 20 mL sterile water to a 200 μg vial human recombinant EGF (R&D Systems, Cat. # 236-EG-200).
- (b) Transfer to conical tube, and add 180 mL HBES containing 0.1 % BSA (dissolve 0.1 g BSA into 100 mL HBES by shaking vigorously).
- (c) Filter-sterilize, and store 10 mL aliquots at -20°C .

12. 100× Insulin: *Prepare immediately before use and never freeze!*
 - (a) Dissolve 12.5 mg insulin (Calbiochem/EMD Millipore Cat. # 407709-50MG) in 25 mL 0.005 M HCl.
 - (b) Add 2–3 mL FBS to a filter and vacuum it through the filter, discarding the flow-through.
 - (c) Filter sterilize insulin using the above FBS-blocked filter.

2.1.3 HaCaT Keratinocytes

1. E-medium containing 5 % FBS:

DMEM w/high glucose (HyClone/Fisher Cat. # SH30022.FS)	375 mL
Ham's Nutrient Mixture F-12 (HyClone/Fisher Cat. # SH30026.01)	125 mL
FBS (MediaTech/Fisher Cat. # MT-35-011-CV)	25 mL

2. 1× PBS without calcium and magnesium (MediaTech/Fisher Cat. # MT-20-031-CV).
3. 0.02 % EDTA/PBS (Section 2.1.1, *step 3*).
4. 0.25 % trypsin/EDTA (HyClone/Fisher Cat. # SH30042.01).

2.2 Gene Knockdown and Overexpression in Keratinocytes

2.2.1 Production of Lentiviruses for Transducing Keratinocytes

1. DMEM containing 10 % FBS:

DMEM w/high glucose (HyClone/Fisher Cat. # SH30022.FS)	500 mL
FBS (MediaTech/Fisher Cat. # MT-35-011-CV)	50 mL

2. Opti-MEM Reduced Serum Medium (Gibco/Invitrogen Cat. # 31985070).
3. Lentivirus packaging plasmids:
 - (a) pMDG.2 (VSV-G) (Addgene Plasmid # 12259).
 - (b) pCMV-deltaR8.2 (Addgene Plasmid # 12263).
 - (c) Proviral plasmid of choice.
4. Polyethylenimine (PEI).
 - (a) Dissolve Linear PEI (Polysciences Cat. # 23966–2) in H₂O heated to 80 °C to yield 1 mg/mL solution.
 - (b) Allow solution to cool to RT.
 - (c) Adjust pH to 7.0 with 5 M HCl.
 - (d) Filter sterilize, and store at –80 °C. Can also be stored at 4 °C for up to 4 months.
5. 0.45 µm PVDF syringe filters, 13 mm diameter (Fisherbrand Cat. # 09-720-4).

6. Hank's Buffered Saline Solution (HBSS, MediaTech/Fisher Cat. # MT-21-023-CV).
7. Bovine Serum Albumin (BSA, Amresco Cat. # 0332).
8. Ultra-Clear Thinwall ultracentrifuge tubes for SW41Ti rotor, 13.2 mL, 14 × 89 mm (Beckman Coulter Cat. # 344059).
9. 20 % sucrose/HBSS: Dissolve 20 g sucrose into 100 mL 1× HBSS and filter sterilize.

2.2.2 Transduction of Keratinocytes

1. Lentiviruses: as prepared in Section 2.2.1.
2. Keratinocytes and keratinocyte culture medium (Section 2.1).

2.2.3 Transfection of Keratinocytes

1. Keratinocytes and keratinocyte growth medium (Section 2.1).
2. Opti-MEM Reduced Serum Medium (Gibco/Invitrogen Cat. # 31985070).
3. X-tremeGENE HP DNA Transfection Reagent (Roche Cat. # 06366244001): for transfection of HFK and NIKS.
4. *TransIT*[®]-2020 Transfection Reagent (Mirus Bio Cat. # MIR 5404): for transfection of HaCaT.
5. DNA to be transfected: prepared as desired.

2.2.4 Selection of Puromycin-Resistant Cells

1. Keratinocytes transduced or transfected with puromycin-resistance gene.
2. 10 mg/mL puromycin: Add 10 mL sterile water to 100 mg viral puromycin dihydrochloride (MP Biomedicals Cat. # 210055280). Store aliquots at −20 °C. Vortex well upon thawing.

2.3 Human Papillomavirus Infectivity Assay

2.3.1 Luciferase Reporter Assay: *hvp16-LucF*, *hvp16-phRL*, HPV16RL, or Other Luciferase-Containing HPV

1. *hvp16-LucF*, *hvp16-phRL*, HPV16RL, or other luciferase-containing HPV: prepared as described (12, 27, 28) (*see Note 2*).
2. Bright-Glo[™] Luciferase Assay System (Promega Cat. # E2620).
3. Renilla-Glo[®] Luciferase Assay System (Promega Cat. # E2720).
4. CellTiter-Glo[®] Luminescent Cell Viability Assay (Promega Cat. # G7572).
5. DMEM (HyClone/Fisher Cat. # SH30022.FS).
6. Opaque 96-well plates (Life Science Products/VWR Cat. # 89093-598).
7. GloMax[®]-Multi + Detection System with Instinct Software (Promega), or other comparable luminometer.

2.3.2 Fluorescence Microscopy: *hvp16-LucF*, *hvp16-EGFP*, HPV16GFP, or Other Fluorescent Protein Gene-Containing HPV

1. *hvp16-LucF*, *hvp16-EGFP*, and HPV16GFP.
2. Fluorescence microscope.
3. Flow cytometer.
4. Optional: SYTOX[®] Dead Cell Stain (Invitrogen).

2.3.3 *Reverse Transcription-Quantitative PCR (RT-qPCR): HPV Containing Full-Length Genome*

1. HPV containing full-length genome, prepared as described (12, 13, 27).
2. RNeasy mini kit (Qiagen Cat. # 74106).
3. RNase-free DNase set (Qiagen Cat. # 79254).
4. Oligo d(T)_{12–18} Primer (Invitrogen Cat. # 18418012).
5. SuperScript II Reverse Transcriptase (Life Sciences Cat. # 18064–014).
6. Primers for amplification of HPV genes: For HPV16 W12 genome, primers to amplify early genes have been published (11).
7. Hard-Shell® Thin-Wall 96-Well Skirted Plates (Bio-Rad Cat. # HSP-9901) or comparable 96-well plates for qPCR.
8. Bio-rad CFX Connect™ Real-Time PCR Detection System (Bio-Rad Cat. # 185–5200) or comparable qPCR machine.
9. FastStart Universal SYBR Green Master Mix (Rox) (Roche Applied Science Cat. # 04913850001).

3 Methods

3.1 Keratinocyte Culture

3.1.1 Primary Human Foreskin Keratinocytes

Maintain HFKs in EpiLife medium supplemented with HKGS at 37 °C/5 % CO₂. Change medium every other day when cells are sparse and every day as cells approach 50 % confluency. Passage cells when they reach 80 % confluency. Follow the protocol below to passage HFKs (*see Note 3*).

1. Briefly wash cells once with 0.02 % EDTA/PBS. Incubate in 0.05 % trypsin/EDTA for 6 min at 37 °C/5 % CO₂.
2. Rock and tap the dish to dislodge the cells, and then add DMEM containing 10 % NCS to neutralize the trypsin (*see Note 4*). Pipet up and down to obtain a single-cell suspension.
3. Pellet the cells by centrifugation in swinging bucket rotor at 200 × *g* for 5 min.
4. Resuspend cell pellet in EpiLife medium containing HKGS, and plate as desired. If HFK cells are seeded at a density of 1 × 10⁴ cells/cm² they reach confluency in 3–4 days (*see Note 5*).

3.1.2 Normal Immortalized Keratinocytes from Skin

The NIKS culture protocol described below is modified from the previously described protocol for epithelial cell culture (26). Maintain NIKS in E-complete medium and co-culture with growth-arrested 3T3 mouse fibroblasts (aka “feeder” cells) (*see Note 6*) at 37 °C/5 % CO₂. Note that preparation of 3T3s for

NIKS co-culture requires at least 2–4 h. Change the medium on NIKS every 24–48 h (*see Note 7*). Confluency is a critical issue for NIKS. NIKS should be passaged prior to reaching 80 % confluency (as soon as colonies begin touching one another) or when cells in the middle of the colonies appear unhealthy (large, flat, “fried egg” phenotype). Furthermore, NIKS do not proliferate well when too sparse, so never plate below 10 % confluency. The following protocol details maintenance and preparation of 3T3 cells for use as feeders in NIKS cultures as well as NIKS passaging.

1. **Maintain 3T3 cultures for future use in NIKS co-cultures.** 3T3s are maintained in DMEM containing 10 % NCS at 37 °C/5 % CO₂. Frequent medium changes are not necessary for these cells. Passage cells prior to reaching 100 % confluency. To passage 3T3 cells:
 - (a) Wash once with 1× PBS. Incubate in 0.25 % trypsin for 2 min at 37 °C/5 % CO₂.
 - (b) Add DMEM containing 10 % NCS to neutralize trypsin and dilute as desired. If cells are split 1:8 from a confluent dish, they typically reach 90 % confluency in 2 days (*see Note 8*).
2. **Prepare 3T3 feeder cells for NIKS co-culture.** The desired confluency of 3T3 feeder cells in NIKS co-cultures is ~25 %; thus, one confluent dish of 3T3 cells will yield four dishes of feeder cells for NIKS co-cultures. The following is written for one 10 cm dish of 3T3s.
 - (a) Dilute 100 µL of 50× mitomycin C into 5 mL DMEM containing 10 % NCS. Aspirate medium from a 10 cm dish of 3T3s, and add the diluted mitomycin C.
 - (b) Incubate for 2–4 h at 37 °C/5 % CO₂.
 - (c) Wash cells twice with 10 mL 1× PBS. Incubate in 0.25 % trypsin for 2 min at 37 °C/5 % CO₂ (*see Note 9*).
 - (d) Add either DMEM containing 10 % NCS or E-complete to neutralize trypsin. If 3T3 feeders will be added to NIKS culture immediately, then suspend cells in E-complete, otherwise suspend cells in DMEM containing 10 % NCS. 3T3 feeders can be maintained up to 24 h after mitomycin C treatment and before adding to NIKS culture if kept in DMEM containing 10 % NCS.
3. **Remove 3T3 feeder cells from NIKS cultures to be passaged.** As NIKS are far more adherent to tissue culture plastic than mitomycin C-treated 3T3s, the feeders can easily be removed without dislodging NIKS, as follows.

- (a) Wash NIKS/feeder co-culture once with 0.02 % EDTA/PBS. Incubate in 0.05 % trypsin/EDTA for 60 s in 37 °C/5 % CO₂ incubator (*see Note 10*).
 - (b) Rock and tap the dish thoroughly to dislodge the feeders. Check under the microscope to observe that all feeders are lifted and NIKS are still adhered. NIKS should appear rounded but stay adhered to the dish.
 - (c) Remove dislodged feeders by washing twice with 1× PBS.
4. Incubate NIKS in 0.25 % trypsin for 8 min at 37 °C/5 % CO₂.
 5. Rock and tap the dish to dislodge NIKS.
 6. Add E-complete to neutralize the trypsin and pipet up and down thoroughly to obtain a single-cell suspension.
 7. Dilute NIKS as desired, and plate onto new dishes containing feeders, or add feeders to NIKS in suspension and plate together (*see Note 11*).

3.1.3 HaCaT Keratinocytes

Maintain HaCaTs in E-medium containing 5 % FBS at 37 °C/5 % CO₂. Change medium every 2 days, and split cells when they reach 80 % confluency. Passage HaCaTs as follows:

1. Wash HaCaTs once with 1× PBS. Incubate in 0.02 % EDTA/PBS for 15 min at 37 °C/5 % CO₂.
2. Aspirate 0.02 % EDTA/PBS and incubate in 0.25 % trypsin/EDTA for 6 min at 37 °C.
3. Rock and tap the dish to dislodge HaCaTs.
4. Add E-medium containing 5 % FBS to neutralize trypsin. Pipet up and down to collect cells in single-cell suspension.
5. Dilute cells as desired. If cells are split 1:8 they will reach confluency in 2–3 days.

3.2 Gene Knockdown and Overexpression in Keratinocytes

3.2.1 Production of Lentiviruses for Transducing Keratinocytes

As keratinocytes have historically been difficult to transfect without cytotoxicity, lentiviral transduction is commonly used to deliver DNA constructs for shRNA knockdown or ORF overexpression. This protocol utilizes PEI as a transfection reagent to deliver lentivirus-packaging plasmids into 293FT cells. This protocol is written for transfection of one 10 cm dish. Scale as necessary.

1. **Maintain 293FT cells for future use.** 293FT cells are maintained in DMEM containing 10 % FBS at 37 °C/5 % CO₂ (*see Note 12*) and should be passaged prior to reaching 90 % confluency (*see Note 13*). Frequent medium changes are not necessary for these cells. Care should be taken not to disturb the cell monolayer, as 293FTs are only weakly adherent and

will become dislodged easily by physical force (i.e., pipetting).
To passage 293FTs:

- (a) Wash cells once with $1 \times$ PBS. Incubate in 0.25 % trypsin/EDTA for 5 min at $37^\circ\text{C}/5\% \text{CO}_2$.
 - (b) Rock and tap the dish to dislodge cells.
 - (c) Add DMEM containing 10 % FBS to neutralize trypsin, and pipet up and down to obtain a single-cell suspension.
 - (d) Dilute cells as desired. If a confluent dish is split 1:12 they typically reach 90 % confluency in 2 days.
2. One day prior to transfection, plate 4.5×10^6 293FT cells per 10 cm dish (to be 60–80 % confluent the next day) in DMEM containing 10 % FBS.
 3. Transfect 293FT cells:
 - (a) Dilute DNA into 1 mL Opti-MEM and mix well:
 - 5.3 μg pMDG.2 (VSV-G).
 - 8 μg pCMV-deltaR8.2.
 - 10.7 μg proviral plasmid (*see Note 14*).
 - (b) Dilute 72 μL of 1 $\mu\text{g}/\mu\text{L}$ PEI into 1 mL Opti-MEM and mix well.
 - (c) Combine diluted DNA and diluted PEI, and immediately vortex for 5 s.
 - (d) Incubate at RT for 15 min.
 - (e) Add transfection mixture to 10 mL DMEM containing 10 % FBS and mix by pipetting.
 - (f) Aspirate medium from 293FT cells and add the above diluted transfection mixture.
 - (g) Incubate at $37^\circ\text{C}/5\% \text{CO}_2$ overnight.
 4. At 4–18 h post transfection, replace transfection medium with fresh Opti-MEM (cells should not be incubated in transfection mixture for longer than 18 h) (*see Note 15*).
 5. Harvest lentivirus at 48–72 h post transfection:
 - (a) Harvest cells and lentivirus-containing medium by pipetting up and down (no need to trypsinize) (*see Note 16*).
 - (b) Pellet cell debris by centrifugation at $3,200 \times g$ for 5 min.
 - (c) Collect supernatant and pass through 0.45 μm PVDF syringe filter to remove the remaining cell debris.
 - (d) Store 1 mL aliquots at -80°C or (optional) concentrate/purify lentiviruses (*see Note 17*). Lentiviruses should not be frozen and thawed more than three times.

6. If desired, lentiviruses can be concentrated as follows (*see Note 18*):
- (a) Add 5 mL of filtered lentivirus supernatant to SW41Ti ultracentrifuge tube.
 - (b) Underlay 2 mL of 20 % sucrose/HBSS using 2 mL pipet, being careful not to mix layers.
 - (c) Add the remaining lentivirus supernatant to top, being careful not to disturb the interface.
 - (d) Balance tubes with HBSS.
 - (e) Ultracentrifuge at $65,000 \times g$ for 2 h at 4 °C.
 - (f) Pour off supernatant into waste beaker containing 10 % bleach, and let tubes sit upside down over a kimwipe for 5 min. Remove excess liquid from the side of tube with kimwipe or by aspiration.
 - (g) Resuspend pellet with the desired volume of HBSS containing 1 % BSA (usually 50× concentration – 200 μL for one 10 cm dish) by pipetting up and down vigorously (avoid frothing!). Vortex at low speed for 30 min at 4 °C to fully resuspend the virus pellet.
 - (h) Transfer to 1.5 mL tube, vortex, and centrifuge at max speed for 30 s.
 - (i) Transfer supernatant to new tube, and store aliquots at –80 °C.

3.2.2 Transduction of Keratinocytes

HFK and NIKS cells transduce with relatively high efficiency; however, HaCaT cells exhibit low transduction efficiency. This protocol is written for HFK and NIKS only.

1. One day prior to transduction, plate keratinocytes at a density of 1×10^4 cells/cm².
2. Thaw lentivirus on ice (*see Note 19*) and dilute as desired into appropriate culture medium (*see Note 20*).
3. Add diluted lentivirus to keratinocytes and incubate overnight at 37 °C/5 % CO₂.
4. Change medium the next day (*see Note 21*).
5. Assay cells at 48–72 h post transduction.

3.2.3 Transfection of Keratinocytes

We found that keratinocytes can be transfected with reasonable efficiencies with the following reagents (~50 %, data not shown). Follow the manufacturer's instructions. The optimal ratios of transfection reagent to DNA are listed below; however, further optimization may be necessary.

HFK and NIKS:	X-tremeGENE HP DNA Transfection Reagent (Roche) Optimal transfection reagent-to-DNA ratio: 2:1
HaCaT:	<i>TransIT</i> [®] -2020 Transfection Reagent (Mirus Bio) Optimal transfection reagent-to-DNA ratio: 3:1

3.2.4 Selection of Puromycin-Resistant Cells

We routinely use puromycin resistance selection to generate stable keratinocyte lines. The following outlines our procedure for puromycin resistance selection.

1. Add puromycin-containing growth medium to cells at 48 h post transduction or transfection (above). Optimal puromycin concentrations:
 - (a) HFK: 1.0 µg/mL.
 - (b) NIKS: 1.5 µg/mL.
 - (c) HaCaT: 2.5 µg/mL.
2. Culture cells according to the standard protocol (Section 3.1), replenishing puromycin-containing medium every other day. Puromycin will kill non-transduced/transfected cells in 2–3 days.
3. To generate stable cell lines, continue selection process for 1–2 weeks post transduction or 2–3 weeks post transfection.

3.3 Human Papillomavirus Infectivity Assays

3.3.1 Luciferase Reporter Assay: *hpv16-LucF*, *hvp16-phRL*, *HPV16RL*, or Other Luciferase-Containing HPV

1. One day before infection, plate 4×10^3 keratinocytes/well of a 96-well plate (*see Note 22*). Plate in quadruplicate for each sample for statistical analysis.
2. Next day, inoculate keratinocytes with 1,000–10,000 vge/cell (MOI 2–20) *hvp16-LucF*, *hvp16-phRL*, *HPV16RL*, or other luciferase-containing HPV.
3. At 48 h post infection, perform luciferase assay and cell viability assay to determine relative infectivity and viability, respectively (*see Note 23*):
 - (a) Thaw and equilibrate Bright-Glo[™] (FL assay) or Renilla-Glo[™] (RL assay) and CellTiter-Glo[®] (viability assay) reagents at RT.
 - (b) Make master mixes: Combine Bright-Glo[™] or Renilla-Glo[™] and CellTiter-Glo[®] reagents with an equal volume of DMEM at RT.
 - (c) Aspirate culture medium from wells, and add 50–60 µL of desired master mix per well.
 - (d) Incubate at RT for 2–3 min for Bright-Glo[™] or 10 min for Renilla-Glo[™] and CellTiter-Glo[®].
 - (e) Transfer to opaque 96-well plate, being cautious to avoid introducing bubbles.

- (f) Read luminescence with GloMax[®]-Multi + Detection System or comparable luminometer.
- (g) Normalize luciferase activity to cell viability.

3.3.2 Fluorescence

Microscopy: *hvp16-LucF*,
hvp16-EGFP, *HPV16GFP*, or
Other Fluorescent Protein
Gene-Containing HPV

1. One day before infection, plate 1×10^4 keratinocytes/cm² onto 24-well or 12-well plate.
2. Next day, inoculate keratinocytes with 1,000–10,000 vge/cell (MOI 2–20) *hvp16-LucF*, *hvp16-EGFP*, *HPV16GFP*, or other fluorescent protein gene-containing HPV.
3. Check expression of fluorescent protein in infected cells using fluorescence microscope.
4. At 48 h post infection, determine the percentage of cells infected by flow cytometric quantification of fluorescent protein expression. Dead cells can be excluded by staining with SYTOX[®] Dead Cell Stain, according to the manufacturer's instructions.

3.3.3 Reverse

Transcription-Quantitative
PCR (RT-qPCR): HPV
Containing Full-Length
Genome

1. One day before infection, plate 1×10^5 keratinocytes/well of a 6-well plate.
2. Next day, inoculate keratinocytes with 1,000–10,000 vge/cell (MOI 2–20) HPV containing full-length genome.
3. At 48 h post infection, extract total RNA from keratinocytes using RNeasy mini kit and RNase-free DNase set, according to the manufacturer's instructions for on-column DNase treatment.
4. Reverse transcribe total RNA to generate first-strand complementary DNA (cDNA) using oligo d(T)_{12–18} primers:
 - (a) Set up oligo d(T) priming reaction:

RNA sample (≤ 25 μ g)	10 μ L
100 μ M oligo d(T) primer	1 μ L

(b) Incubate at 70 °C for 10 min, and then cool to 4 °C.

(c) Set up cDNA synthesis reaction:

Priming reaction mix	11 μ L
5 \times First-strand reaction buffer	4 μ L
0.1 M DTT	2 μ L
10 mM dNTP mix	1 μ L
Superscript II reverse transcriptase	1 μ L
Nuclease-free H ₂ O	1 μ L

- (d) Incubate at 42 °C for 1 h, and then cool to 4 °C.
 (e) Store at –20 °C for future use.
5. Set up RT-qPCR reaction mixture. Primer sequences for HPV16 early genes are published (11).

forward primer	0.5 μM
reverse primer	0.5 μM
cDNA template	50 ng
FastStart Universal SYBR Green Master (Rox)	10 μL
Nuclease-free H ₂ O to 20 μL total volume	

6. Perform qPCR using the following temperature protocol:

95 °C for 10 min	
95 °C for 15 s	Repeat 40×
59 °C for 1 min*	Repeat 40×
*Include plate read during this step	

4 Notes

- Invitrogen also sells HEKp, which are HEK_n pooled from multiple donors. This protocol will work with either HEK_n or HEKp. It also works well with HFK cells purchased from Lonza (NHEK-Neo, Lonza Cat. # 192906). Among the keratinocyte medium we tested, HFK cultures appear most healthy when cultured in EpiLife medium containing HKGS (data not shown).
- hpv16*-phRL and HPV16RL virions are packaged in 293FT cells as previously described (13). *hpv16*-phRL pseudovirions contain the phRL-SV40 plasmid (Promega), and HPV16RL virions contain a chimeric HPV DNA, generated by insertion of the hRL reporter gene from phRL-SV40 (Promega) into the L2 and 5' L1 genes of the HPV16 W12 genome (28). For more information regarding these constructs, contact Dohun Pyeon at dohun.pyeon@ucdenver.edu.
- Alternatively, HFKs can be cultured following the NIKS culture protocol (see Section 3.1.2). This method of culturing HFKs has been reported to extend their lifetime to more than twice the number of passages compared with culturing in EpiLife medium supplemented with HKGS (29). Importantly, we found that HPV16-*LucF* infectivity of HFKs is dramatically enhanced when they are cultured according to the NIKS protocol (data not shown). We do not currently know why HPV16

infectivity is enhanced, but we speculate that the serum in the E-complete medium may have growth factors and HSPGs which aid in the entry of HPV16 into keratinocytes (Ozbun, MA, personal communication).

4. Any serum-containing medium can be used here to neutralize trypsin, as the cells will be pelleted and resuspended in EpiLife. EpiLife medium supplemented with HKGS will not effectively neutralize trypsin.
5. Each lot of HFKs varies slightly in doubling time, as each lot is obtained from a different donor or a set of multiple donors. Therefore, seeding density for each batch may need optimization.
6. If desired, NIKS cells can be cultured without feeders in reduced-calcium E-complete medium (Paul Lambert, personal communication). We found that even under reduced-calcium environment, a large percentage of NIKS appeared to differentiate within 24 h, as their morphology changed from cuboidal to elongated, and these elongated cells did not appear to divide. For this reason, if an experiment requires the absence of feeders, we limit the feeder-free culture period to 2–3 h.
7. 3T3 feeders in the NIKS co-culture will additionally utilize a significant amount of nutrients from the medium, so frequent medium changes are necessary regardless of NIKS confluency.
8. Because feeders are needed so often, we maintain at least (2) or (3) 10 cm dishes of 3T3s of varying confluency. From a confluent dish, we recommend routinely splitting at a ratio of 1:8, 1:4, and 1:2.
9. If NIKS will be added directly to this dish of feeders, trypsinization is not necessary.
10. Alternatively, feeders can be removed by pipetting up and down after incubation with 0.02 % EDTA/PBS for 1–2 min at RT. Harsh pipetting necessary to thoroughly dislodge feeders sometimes results in physical damage to adhered NIKS; thus, we prefer to remove feeders with trypsin to avoid harsh pipetting.
11. Upon addition to NIKS culture, 3T3 feeders should be replenished every 2 days to maintain NIKS in a healthy, proliferating state. If NIKS cells appear stressed, as in their morphology is flattened and larger morphology, and a clear nuclear membrane and stress granules (“fried egg”), replacing the feeders in fresh E-complete often recovers these cells.
12. 293FT cells can be cultured in DMEM containing 10 % NCS rather than FBS. Though the cells appear to proliferate very well in NCS-containing medium, we find that culturing them in FBS-containing medium increases transfection efficiency.

13. 293FT cells easily transform further in over-confluent conditions. We find that when 293FT cells are kept in an over-confluent state, they become less adherent.
14. Optional: Add 1 µg lentiviral GFP expression plasmid (such as TurboGFP) to visualize transduced cells and calculate transduction efficiency.
15. We obtain significantly higher titers of lentivirus when packaging is carried out in Opti-MEM reduced-serum medium instead of DMEM containing 10 % FBS. We speculate that even though FBS in the medium increases transfection efficiency (*see Note 12*), it later has an inhibitory effect on virus packaging. 293FT cells cultured in Opti-MEM will display significant cytotoxicity; however, production of infectious lentivirus is enhanced.
16. Biohazard warning: Lentiviruses are HIV-derivative viruses and they must be handled in a BSL2+ environment. You must contact your institution's Bio-Safety office to receive permission and specific instructions on how to handle these viruses. We use 10 % bleach to sterilize work areas, followed by water and 70 % ethanol to avoid corrosion of stainless steel surfaces.
17. Lentiviruses can be stored at 4 °C for up to 3 days without significant loss of titer.
18. Further purification/concentration of lentiviruses by ultracentrifugation is recommended if they will be used to transduce HFKs, as HFKs do not tolerate Opti-MEM very well. Note that ultracentrifugation of lentiviruses results in a significant loss of overall titer.
19. Rapid thawing and multiple freeze–thaw cycles will result in significant loss of virus titer.
20. Typically, lentiviruses are diluted 1:10 into culture medium. However, if it is suspected that the titer is lower than normal, lentiviruses can be diluted 1:1 with culture medium. If lentivirus was concentrated, adjust volume according to concentration factor.
21. If desired, lentiviruses can be removed 4 h after inoculation, as most lentiviruses will have adsorbed to the cells within a few hours. We have not observed any significant loss in transduction efficiency by replacing infection medium after 4 h.
22. Keratinocytes may be cultured in sterile, opaque 96-well plates if desired; however, it may be preferable to culture cells in clear 96-well plates in order to visualize the cell condition throughout the experiment. In this case, the lysate can simply be transferred to an opaque 96-well plate immediately prior to measuring luminescence.

23. The CellTiter-Glo[®] cell viability assay usually shows very high signal ($>10^7$ RLU for 96-well plate), which can leak into neighboring wells of the Bright-Glo[™] infectivity assay, thereby skewing the infectivity data. This can be avoided by performing the Bright-Glo[™] assay prior to the CellTiter-Glo[®] assay or by separating the two assays by several wells or on separate plates.

Acknowledgments

We thank Paul Lambert and Denis Lee for technical assistance regarding NIKS cell culture and for providing NIKS and HaCaT keratinocytes as well as the 293FT packaging cells. We acknowledge John Schiller for providing pLucF and p16Shell plasmids and Jerry Schaack for providing pMDG.2 and useful suggestions for lentivirus production and purification. We also thank Paul Lambert, Zhaohui Qian, and members of the Pyeon laboratory for useful support and suggestions.

References

- zur Hausen H (1996) Papillomavirus infections—a major cause of human cancers. *Biochim Biophys Acta* 1288:F55–F78
- Gillison ML, Shah KV (2001) Human papillomavirus-associated head and neck squamous cell carcinoma: mounting evidence for an etiologic role for human papillomavirus in a subset of head and neck cancers. *Curr Opin Oncol* 13:183–188
- zur Hausen H (1999) Viruses in human cancers. *Eur J Cancer* 35:1174–1181
- Burd EM (2003) Human papillomavirus and cervical cancer. *Clin Microbiol Rev* 16:1–17
- Gillison ML, Lowy DR (2004) A causal role for human papillomavirus in head and neck cancer. *Lancet* 363:1488–1489
- Modis Y, Trus BL, Harrison SC (2002) Atomic model of the papillomavirus capsid. *EMBO J* 21:4754–4762
- zur Hausen H (2002) Papillomaviruses and cancer: from basic studies to clinical application, *Nature reviews*. *Cancer* 2:342–350
- Stubenrauch F, Laimins LA (1999) Human papillomavirus life cycle: active and latent phases. *Semin Cancer Biol* 9:379–386
- Joyce JG, Tung JS, Przysiecki CT et al (1999) The L1 major capsid protein of human papillomavirus type 11 recombinant virus-like particles interacts with heparin and cell-surface glycosaminoglycans on human keratinocytes. *J Biol Chem* 274:5810–5822
- Giroglou T, Florin L, Schafer F et al (2001) Human papillomavirus infection requires cell surface heparan sulfate. *J Virol* 75:1565–1570
- Pyeon D, Pearce SM, Lank SM et al (2009) Establishment of human papillomavirus infection requires cell cycle progression. *PLoS Pathog* 5:e1000318
- Buck CB, Pastrana DV, Lowy DR et al (2004) Efficient intracellular assembly of papillomaviral vectors. *J Virol* 78:751–757
- Pyeon D, Lambert PF, Ahlquist P (2005) Production of infectious human papillomavirus independently of viral replication and epithelial cell differentiation. *Proc Natl Acad Sci U S A* 102:9311–9316
- Bousarghin L, Touzé A, Sizaret P-Y et al (2003) Human papillomavirus types 16, 31, and 58 use different endocytosis pathways to enter cells. *J Virol* 77:3846–3850
- Day PM, Lowy DR, Schiller JT (2003) Papillomaviruses infect cells via a clathrin-dependent pathway. *Virology* 307:1–11
- Abban CY, Bradbury NA, Meneses PI (2008) HPV16 and BPV1 infection can be blocked by the dynamin inhibitor dynasore. *Am J Ther* 15:304–311
- Laniosz V, Dabydeen SA, Havens MA et al (2009) Human papillomavirus type 16 infection of human keratinocytes requires clathrin and caveolin-1 and is brefeldin a sensitive. *J Virol* 83:8221–8232

18. Schelhaas M, Shah B, Holzer M et al (2012) Entry of human papillomavirus type 16 by actin-dependent, clathrin- and lipid raft-independent endocytosis. *PLoS Pathog* 8:e1002657
19. Spoden G, Freitag K, Husmann M et al (2008) Clathrin- and caveolin-independent entry of human papillomavirus type 16—involve ment of tetraspanin-enriched microdomains (TEMs). *PLoS ONE* 3:e3313
20. Spoden G, Kühling L, Cordes N et al (2013) Human papillomavirus types 16, 18, and 31 share similar endocytic requirements for entry. *J Virol* 87:7765–7773
21. Griffin LM, Cicchini L, Pyeon D (2013) Human papillomavirus infection is inhibited by host autophagy in primary human keratinocytes. *Virology* 437:12–19
22. Day PM, Lowy DR, Schiller JT (2008) Heparan sulfate-independent cell binding and infection with furin-precleaved papillomavirus capsids. *J Virol* 82:12565–12568
23. Ozbun MA (2002) Human papillomavirus type 31b infection of human keratinocytes and the onset of early transcription. *J Virol* 76:11291–11300
24. Allen-Hoffmann BL, Schlosser SJ, Ivarie CA et al (2000) Normal growth and differentiation in a spontaneously immortalized near-diploid human keratinocyte cell line, NIKS. *J Invest Dermatol* 114:444–455
25. Johnson KM, Kines RC, Roberts JN et al (2009) Role of heparan sulfate in attachment to and infection of the murine female genital tract by human papillomavirus. *J Virol* 83:2067–2074
26. Lambert PF, Ozbun MA, Collins A et al (2005) Using an immortalized cell line to study the HPV life cycle in organotypic “raft” cultures. *Methods Mol Med* 119:141–155
27. Buck CB, Thompson CD, Pang Y-YS et al (2005) Maturation of papillomavirus capsids. *J Virol* 79:2839–2846
28. Xu T, Griffin LM, Guo K et al. APOBEC3A functions as a restriction factor of Human Papillomavirus. (Manuscript submitted)
29. Fu B, Quintero J, Baker CC (2003) Keratinocyte growth conditions modulate telomerase expression, senescence, and immortalization by human papillomavirus type 16 E6 and E7 oncogenes. *Cancer Res* 63:7815–7824

Preparation and Delivery of 4-Hydroxy-Tamoxifen for Clonal and Polyclonal Labeling of Cells of the Surface Ectoderm, Skin, and Hair Follicle

Christine Chevalier, Jean-François Nicolas, and Anne-Cécile Petit

Abstract

To study the cell behavior during morphogenesis of mouse surface ectoderm, skin, and hair follicles, we (1–3) have developed a new method to temporally induce clones that is based on a tamoxifen-dependent Cre recombinase. The classical protocol consisting in dissolving 4-hydroxy-tamoxifen or tamoxifen in corn oil to perform intraperitoneal (ip) injections (4) is not optimal to control the pharmacokinetic parameters of the induction as it leads to experimental variability in terms of timing and level of induction. We have developed a new protocol that consists in solubilizing 4-OHT or tamoxifen in an aqueous solvent using Cremophor® EL (5). This allows for intravenous (iv) and intraperitoneal injections.

Keywords: 4-OHT, Tamoxifen, Cre/lox system, Cremophor® EL, Intravenous, Clonal analysis

1 Introduction

The Cre/loxP method allows for the genetic tagging of one or several cells in a temporally inducible manner in order to perform lineage analysis in mouse embryos and adults (6). This method is based on the modification of a conditional reporter gene (7, 8) by an inducible Cre recombinase. The fusion of the Cre recombinase with a mutated ligand-binding domain (9) of the human oestrogen receptor (ER) results in a tamoxifen-dependent Cre recombinase (CreER^{T2}) that can be activated by 4-OHT or tamoxifen, but not by oestradiol (10). In the absence of its ligand, the CreER^{T2} fusion protein is largely inactive. The binding of 4-OHT induces its activation and the modification of the conditional reporter gene by the recombinase. As a result, the labeled cells and their descendants carry the modified reporter gene and form clones that can be identified by X-gal staining (11) or immunofluorescence mT/mG (12).

The current and most widely used protocol to inject 4-OHT or tamoxifen into mice consists in an ip injection of the chosen product dissolved in corn oil. This solvent was used because of the hydrophobic nature of these products. However, it is not optimal to control the pharmacokinetic parameters of the induction (such

as plasma concentration, time to reach peak plasma concentration, elimination half-life). This is because a significant amount of the inducer may be trapped by adipose tissue present in the intraperitoneal cavity of the mouse. These events lead to experimental variability in terms of timing and level of induction. We have developed a new protocol that permits 4-OHT or tamoxifen to be solubilized in Cremophor[®] EL, a solvent with amphiphilic properties that allow it to bind hydrophobic molecules and to solubilize them in aqueous solvents. We have extensively tested the injection of 4-OHT in Cremophor[®] EL. This solution is painless for the mice and does not exhibit toxicity on embryos and adults. With this protocol, the variability in the induction parameters is minimized: the uptake of 4-OHT into the bloodstream is immediate, and the inducer cannot be trapped by adipose tissue. Its onset of action is probably short, and the duration of the induction depends primarily on the half-life of the molecule. The volume that can be injected intravenously without perturbing blood pressure and heart functioning corresponds approximately to 10 % of the total blood volume of the mouse, i.e., 180 μ L. If needed, ip injection can be performed with 4-OHT dissolved in Cremophor[®] EL.

2 Materials

1. Vortex.
2. Water bath set at 60 °C.
3. 1 mL syringe with needle (BD Plastipak[™], ref: 30015).
4. MYJECTOR U-100 INSULIN 0.3 mL syringe (Terumo, ref: BS30M2913).
5. 1 and 2 mL microcentrifuge tubes.
6. Latex gloves.
7. 4-Hydroxytamoxifen (Sigma, ref: H-7904).
8. Ethanol 100 %.
9. Cremophor[®] EL (Sigma, ref: C5135).
10. 1 \times PBS.
11. Aluminum foil.

3 Methods

3.1 Preparation of 4-OHT Stock Solution

1. In 2 mL microcentrifuge tubes, dissolve the 4-OHT powder (see Note 1) in 100 % ethanol at a 20 mg/mL concentration for injection of low doses of 4-OHT (see Note 2) and at a 40 mg/mL concentration for injection of high doses of

4-OHT (see Notes 3 and 4). As the 4-OHT is light sensitive, keep the tube wrapped in aluminum foil.

2. Vortex for approximately 10 min at maximum speed.
3. Incubate the suspension at 60 °C for 10 min.
4. Vortex again until complete dissolution (see Note 5).
5. Dilute 1:1 the 4-OHT/ethanol solution with Cremophor[®] EL (see Note 6) to obtain a 10 mg/mL concentration for injection of low doses of 4-OHT or a 20 mg/mL concentration for injection of high doses of 4-OHT.
6. Vortex and store the stock solution aliquots of 100 µL at -20 °C.

3.2 Preparation of the 4-OHT Injection Solution (Extemporaneously)

1. Thaw rapidly an aliquot at 37 °C of the 4-OHT/ethanol/Cremophor[®] EL stock solution.
2. Dilute this solution in PBS 1× to the desired concentration for injection. See Table 1a (desired concentration from 2 to 0.25 µg/g) for injection of low doses and Table 2a for injection of high doses of 4-OHT (from 66 to 16.6 µg/g) in 1 mL microcentrifuge tube (see Note 7).
3. Vortex.
4. Keep in the dark at room temperature until used.

3.3 iv or ip Injection of the 4-OHT/Ethanol/Cremophor[®] EL/PBS 1× Solution

1. Weigh the mouse.
2. Whatever the desired dose of 4-OHT (µg/g of mouse, see Tables 1a and 2b) the volume to be injected with respect to the mouse weight remains the same and is indicated in Table 1b (low doses) or Table 2b (high doses).

For example: For injecting a mouse which weighs 28 g at a dose of 66.6 µg/g of mouse, thaw an aliquot of the stock solution at 20 mg/mL. The volume to be injected will be 187 µL of a solution at 10 mg/mL. The solution is very viscous, so it is necessary to prepare a 250 µL volume. Add 125 µL PBS 1× to 125 µL of stock solution 20 mg/mL.

3. Load the syringe without the needle with the required volume, using the MYJECTOR U-100 INSULIN 0.3 mL syringe for iv injections and the 1 mL syringe for ip injections.

Table 1a
Preparation of the 4-OHT solution for low-dose injection (clonal or oligo clonal)

Desired dose of 4-OHT to inject (µg/g mouse)	0.25	0.5	1	2
Concentration of 4-OHT in the stock solution (mg/mL)	10	10	10	10
Concentration of 4-OHT in the injection solution (mg/mL)	0.05	0.1	0.2	0.4

Table 1b
Volume to be injected according to the mouse weight

Mouse weight (g)	Injection volume (μL)
24	120
24.5	122.5
25	125
25.5	127.5
26	130
26.5	132.5
27	135
27.5	137.5
28	140
28.5	142.5
29	145
29.5	147.5
30	150
30.5	152.5
31	155
31.5	157.5
32	160
32.5	162.5
33	165
33.5	167.5
34	170
34.5	172.5
35	175

Table 2a
Preparation of the 4-OHT solution for high-dose injection

Desired dose of 4-OHT to inject ($\mu\text{g/g}$ mouse)	16.6	33.3	66.7
Concentration of 4-OHT in the stock solution (mg/mL)	20	20	20
Concentration of 4-OHT in the injection solution (mg/mL)	2.5	5	10

Table 2b
Volume to be injected according to the mouse weight

Mouse weight (g)	Injection volume (μL)
20	133
21	140
22	147
23	153
24	160
25	167
26	173
27	180
28	187
29	193
30	200
31	207
32	214
33	220
34	227
35	234
36	240
37	247
38	254
39	260
40	267

4. For iv injections (Fig. 1): We use a tunnel device (model no. 02 1025 DI 2001-75, Pascal Dardenne and Jean-Jacques Deschamps, Institut Pasteur Paris) to position and immobilize the mouse, leaving the tail accessible for accurate injection in the tail vein.
5. For ip injections (Fig. 2): Hold the mouse in your left hand (ventral side facing you) if you inject with the right hand. Make sure to grab enough skin so that it cannot turn its head and bite you. Hold the tail by twisting it around your little finger. Locate the injection at the lower part of the belly region.

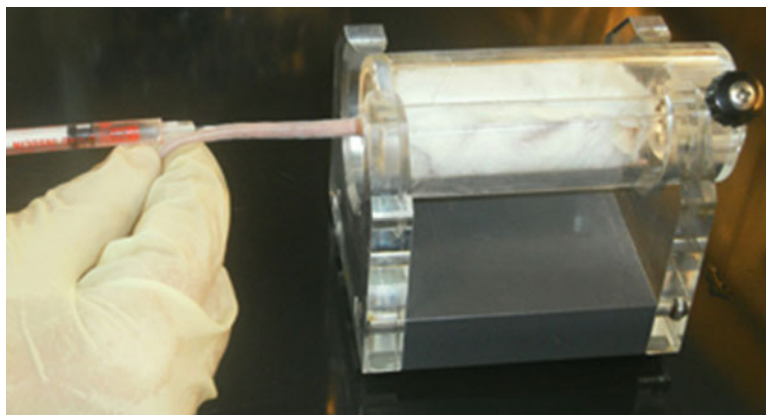


Fig. 1 The essential step is illustrated for iv injection



Fig. 2 The essential step is illustrated for ip injection

4 Notes

1. Precautions for use of 4-OHT powder: No inhalation, no skin contact, do not swallow the powder, and wear protective gloves.
2. The 20 mg/mL concentration is particularly suitable for iv injection for low doses (0.25–2 $\mu\text{g/g}$ mouse) when clonal labeling is required.
3. The 40 mg/mL concentration is adapted for ip injection for high doses (16–66 $\mu\text{g/g}$ mouse) for other purposes than clonal labeling.
4. The choice of the concentration to use depends mainly on the CreER^T inducer line. In our hands clonal labeling is obtained

from 0.25 µg/g mouse for highly efficient CreER inducer lines to 2 µg/g mouse or more for the less efficient ones. Similarly strong induction varies from 16 to 66 µg/g depending on the inducer line.

5. If after step 2, 4-OHT is not completely dissolved, then steps 3 and 4 are absolutely required. Make sure to vortex at step 4 until complete dissolution.
6. The Cremophor® EL is a clear light yellow viscous liquid; draw slowly, and wear protective gloves.
7. For other doses than those indicated in Tables 1a and 2a, calculate the dilution factor in accordance.

Acknowledgements

We thank Yves L. Janin for his suggestion to solubilize 4-OHT in Cremophor® EL and Pascal Dardenne for technical assistance. This work was in part supported by the Institut Pasteur and a grant from Agence National de la Recherche (ANR-10-BLAN-12 1801 to J.-F.N.).

References

1. Legué E, Nicolas J-F (2005) Hair follicle renewal: organization of stem cells in the matrix and the role of stereotyped lineages and behaviors. *Development* 132 (18):4143–4154. doi:10.1242/dev.01975
2. Zhang YV, Cheong J, Ciapurin N, Mcdermitt DJ, Tumbar T (2009) Distinct self-renewal and differentiation phases in the niche of infrequently dividing hair follicle stem cells—supp data. *Cell Stem Cell* 5(3):267–278. doi:10.1016/j.stem.2009.06.004
3. Blanpain C, Fuchs E (2009) Epidermal homeostasis: a balancing act of stem cells in the skin. *Nat Rev Mol Cell Biol* 10 (3):207–217. doi:10.1038/nrm2636
4. Metzger D, Clifford J, Chiba H, Chambon P (1995) Conditional site-specific recombination in mammalian cells using a ligand-dependent chimeric Cre recombinase. *Proc Natl Acad Sci U S A* 92(15):6991–6995
5. Petit A-C, Nicolas J-F (2009) Large-scale clonal analysis reveals unexpected complexity in surface ectoderm morphogenesis. *PLoS ONE* 4(2): e4353. doi:10.1371/journal.pone.0004353
6. Sauer B, Henderson N (1988) Site-specific DNA recombination in mammalian cells by the Cre recombinase of bacteriophage P1. *Proc Natl Acad Sci U S A* 85(14):5166–5170
7. Soriano P (1999) Generalized lacZ expression with the ROSA26 Cre reporter strain. *Nat Genet* 21(1):70–71. doi:10.1038/5007
8. Muzumdar MD, Tasic B, Miyamichi K, Li L, Luo L (2007) A global double-fluorescent Cre reporter mouse. *Genesis* 45(9):593–605. doi:10.1002/dvg.20335
9. Indra AK, Warot X, Brocard J, Bornert JM, Xiao JH, Chambon P, Metzger D (1999) Temporally-controlled site-specific mutagenesis in the basal layer of the epidermis: comparison of the recombinase activity of the tamoxifen-inducible Cre-ER(T) and Cre-ER (T2) recombinases. *Nucleic Acids Res* 27 (22):4324–4327, doi:gkc656 [pii]
10. Vooijs M, Jonkers J, Berns A (2001) A highly efficient ligand-regulated Cre recombinase mouse line shows that LoxP recombination is position dependent. *EMBO J* 2(4):292–297
11. Bonnerot C, Nicolas J-F (1993) Clonal analysis in the intact mouse embryo by intragenic homologous recombination. *C R Acad Sci U S A* 316:1207–1217
12. Sequeira I, Nicolas JF (2012) Redefining the structure of the hair follicle by 3D clonal analysis. *Development* 139(20):3741–3751. doi:10.1242/dev.081091

Microdissection and Visualization of Individual Hair Follicles for Lineage Tracing Studies

Inês Sequeira, Emilie Legué, Suzanne Capgras,
and Jean-François Nicolas

Abstract

In vivo lineage tracing is a valuable technique to study cellular behavior. Our lab developed a lineage tracing method, based on the Cre/lox system, to genetically induce clonal labelling of cells and follow their progeny. Here we describe a protocol for temporally controlled clonal labelling and for microdissection of individual mouse hair follicles. We further present staining and visualization techniques used in our lab to analyze clones issued from genetically induced labelling.

Keywords: Hair follicle, Lineage tracing, Clonal analysis, Cre/lox system, Microdissection, GFP, LacZ, 3D imaging

1 Introduction

Understanding the organization of cells into organs is the starting point for analysis of their cellular homeostasis behavior and development. The hair follicle (HF) provides a model with which to elucidate these processes (1, 2). The HF renews periodically during the life of the animal through neomorphogenesis (3, 4). During HF renewal HFs undergo cycles of resting growth and regression (5–7).

In vivo lineage tracing is a powerful technique to understand the cell behavior in HF development growth stem cell renewal and wounding, and it is the only available technique for long-term studies of cell lineage. Uncovering of how a cell is derived from another cell is critical for understanding the dynamics of tissue growth and maintenance.

Our lab developed a method of clonal analysis for lineage tracing studies in the HF based on the Cre–LoxP system (8), consisting of the genetically induced labelling of cells and the following of their progeny. To temporally control the Cre-recombinase activity, an inducible Cre has been generated whereby Cre is fused to a mutated estrogen receptor (CreER^T or CreER^{T2}) (9). CreER^T transgenic mice (*Cre-inducer line*) are crossed to a

Cre-reporter line, which ubiquitously expresses the reporter gene interrupted by a LoxP site-flanked stop sequence (10). Single-cell labelling can be initiated in mice at any age by injecting low doses of tamoxifen or 4-hydroxytamoxifen (4-OHT). The hormone injection activates the reporter gene in the cells expressing Cre-recombinase by binding to the ER domain of the fusion protein, resulting in the translocation of CreER into the nucleus, where Cre recognizes the loxP site and excises the stop sequence. The recombination results in the expression of the reporter gene, which is transmitted permanently to their progeny when cells divide. Therefore, the labelling is permanent allowing long-term studies.

Although lineage tracing using Cre–LoxP system is a precise approach, it is also subject to some technical and biological limitations. It requires extensive knowledge about the ubiquitous expression of the reporter mouse strain as well as of the Cre line. When using non-ubiquitous mouse Cre lines, the Cre expression should be highly cell type specific and should not be leaky. In the Cre-inducible system, the recombination activity of the Cre should be dependent on the presence of its inducer (9, 11). However, from our lab's experience with different inducible mouse lines, spontaneous activation of the fusion protein CreER can occur in the absence of the tamoxifen or 4-OHT. This potentially spontaneous activation should be carefully characterized for each combination of CreER line and reporter line and taken into account in clonal analysis studies.

Here we present a protocol for microdissection of individual HF s used in clonal lineage tracing studies. We describe approaches to induce clonal labelling with a temporally controlled method—by manipulating the HF cycle—to detect and analyze HF clones, both with LacZ and fluorescent reporter lines.

2 Materials

2.1 *Anaesthesia Solution*

All biopsies and depilations were performed under mouse anaesthesia. We anaesthetize the mouse by intraperitoneal injection of ketamine and xylazine. Depending on local guidelines, different types of anaesthesia may be used, such as avertin administration or by isoflurane inhalation. For 2 mL anaesthetic solution of ketamine and xylazine, mix 0.5 mL of Imalgene 1000 (ketamine 100 mg/mL, Merial) with 0.25 mL of Rompun Injection Solution 2 % (xylazine hydrochloride, Bayer) and bring up to 2 mL final volume with PBS 1×. Use a dose of 0.1 mL per 25 g body weight.

2.2 *Preparation of X-Gal Reaction Solution*

The concentrations of stock solutions are indicated in parentheses. The volumes indicated are for a final volume of 50 mL.

100 µL MgCl₂ (2 M).

2 mL FerrI (potassium ferricyanide, 0.2 M).

2 mL FerrO (potassium ferrocyanide, 0.2 M).

1 mL X-Gal substrate (5-bromo, 3-chloro, indoyl[®]-D-galactoside, 40 mg/mL in DMSO).

The X-Gal reaction solution can be stored at 4 °C in the dark for approximately one week.

2.3 Tools and Equipment

Cold wax strips (Veet).

Insulin syringe with needles.

Surgical instruments: Scissors and blunt forceps (sterilized prior to surgery).

Sutures (absorbable Vicryl JV390, with curved needle attached, 4/0–1.5–75 cm, Ethicon—Johnson & Johnson).

Warm plate for mouse cage.

4-OHT (Sigma-Aldrich).

Cremophor[®] EL (Sigma-Aldrich).

Autoclaved corn oil.

Ethanol 70 %.

Ethanol 100 %.

12-well plates.

96-well plates.

Petri dishes.

Plastic transfer pipettes.

PBS 1×.

PBS-azide 0.05 %.

PFA 4 % in PBS.

30 °C incubator.

Nutator.

Dissection instruments: Forceps (Dumont#5, Fine Science Tools), microscalpels (Stab Knife Straight 10316–14, Fine Science Tools) and scalpel blades.

Stereoscopic dissecting microscope with light source.

Glass coverslips.

Glass slides (precleaned, 25 × 75 × 1 mm).

Mounting medium (SlowFade from Invitrogen or Vectashield cat# H-1000 from Vector Laboratories).

Scotch tape.

Nail polish.

Upright brightfield microscope (for whole-mount LacZ clones) (e.g., Leica DM4000).

Confocal or multiphoton microscope (for whole-mount fluorescent clones) (e.g., Zeiss LSM 700 or 710).

2.4 Mouse Models

For lineage tracing studies, there are a variety of *Cre-inducer lines* that confer widespread expression of Cre-recombinase in all HF cells such as the following:

- (a) CMV CreER^T provided by Daniel Metzger (9, 12) that carries a Cre-recombinase fused to the modified oestrogen receptor ER^T and under the transcriptional control of the enhancer/promoter region of the human cytomegalovirus gene (CMV). The CMV promoter confers wide expression, including the skin and its derivatives.
- (b) Rosa26^{CreERT2} line (from Lars Grotewold and Austin Smith, Wellcome Trust Centre for Stem Cell Research, University of Cambridge, UK) was obtained by introducing the CreER^{T2} gene (13) by homologous recombination into the ROSA26 locus. The ROSA26 promoter confers ubiquitous expression of the Cre-recombinase.
- (c) Other Cre lines that express Cre-recombinase only in a subset of HF cells are also used, such as Lgr5^{CreERT2} (14), Lgr6^{CreERT2} (15), and KI4^{CreERT2} (16).

These inducer lines are crossed to the reporter mouse lines. The most commonly used *Cre-reporter line* is the Rosa26 lacZ line that carries the *lacZ* gene inserted at the ubiquitously expressed ROSA26 locus (10). *lacZ* expression is dependent on Cre-mediated excision of a transcriptional “stop” sequence. Recently, several fluorescent reporter lines have been used that allow confocal three-dimensional imaging and unambiguous resolution of the cellular structure of the HF, such as the following:

- (a) CAG-CAT-EGFP (17) and ROSA26EYFP (18) that express green and yellow fluorescent proteins, respectively, in the recombined cells.
- (b) Rosa26^{mT/mG} reporter mouse that is a double-fluorescent Cre reporter mouse that expresses membrane-targeted tomato protein (tdTomato) prior to Cre-mediated excision and membrane-targeted green fluorescent protein (eGFP) after excision (19), providing an outline of cell morphology.
- (c) A recently developed multicolor Cre-reporter Rosa26-CAG-Confetti does not express any fluorescence prior to Cre-recombinase induction, but after it stochastically places one of the four fluorescent proteins into position directly downstream of the CAG promoter; recombined cells alternatively express

nuclear localized, membrane-targeted or cytoplasmic fluorescent proteins (20, 21).

Detection of the marked cells can be achieved by a variety of methods, depending on the reporter line used. The reporter gene can encode for an enzyme (β -galactosidase or alkaline phosphatase) and be detected by an enzymatic reaction, or encode for a fluorescent protein (GFP, YFP, or combination of several fluorescent proteins) and be detected by using a fluorescent microscope (Note 1).

3 Methods

3.1 Synchronization of HF Cycles

The anagen phase in the dorsal skin is induced by depilating the back of the anaesthetized mice with cold wax (Fig. 1a). Depilation was performed on 7- to 8-week-old mice whose back skin HFs are in telogen. Depilation of telogen HFs mimics exogen and induces synchronously the initiation of anagen in all depilated HFs (7). To have different stages in HF cycle at the induction time in the same animal, different zones may be delineated in the back of the mice and depilated at different time-points prior to induction (22).

1. Weigh the animal (drug amounts to be administered during the experiment are based on body mass).

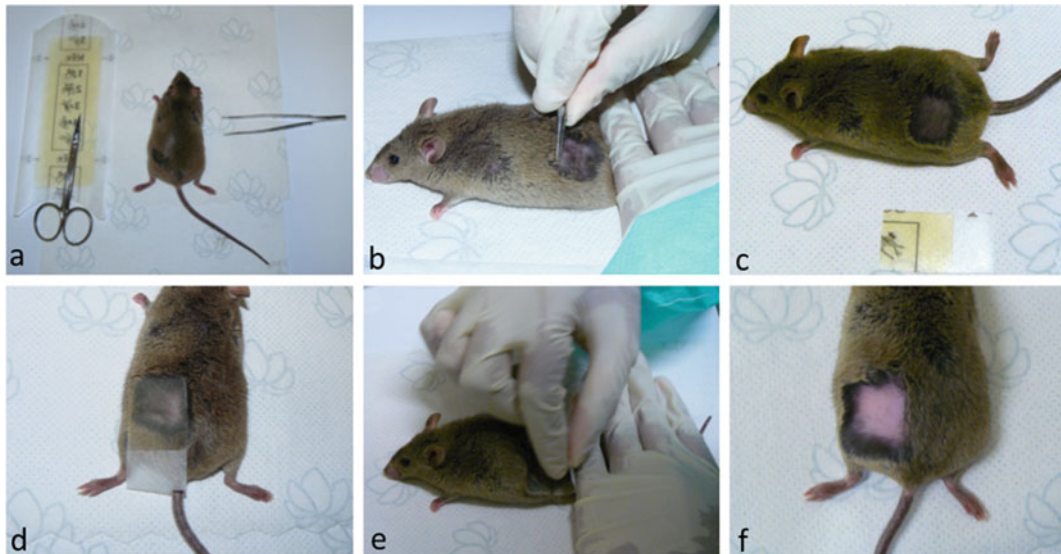


Fig. 1 Depilation of an anaesthetized mouse. (a) Depilate the back of an anaesthetized mouse with cold wax. (b) With one hand, stretch the skin from the back of the mouse, and with forceps pull the hairs in the opposite direction. (c) Use smaller pieces of wax strips the size of the depilated zone. (d) Place one wax strip onto the skin in the direction of hair growth, leaving a wax-free border on the strip. (e) Hold the posterior part of the mouse with one hand and quickly remove the wax strip. (f) The depilated zone should be pink with no traces of injury

2. Inject anaesthetic solution intraperitoneally (Rompun and Imalgene solution, 0.1 mL per 25 g body weight).
3. Remove the hair from the animal's back first using forceps. Make sure that the forceps do not pinch the skin. Gently stretch the skin from the back of the mouse (Fig. 1b), and pull the hairs in the opposite direction.
4. After most of the hair is removed, use cold wax strips. Depilation with cold wax ensures effective hair removal: they are easy to apply, adhere well, and avoid skin irritation usually produced by hot wax patches. Cut small pieces of wax strips, the size of the zone to be depilated (Fig. 1c), leaving a wax-free border on the strip. Warm the wax slightly to body temperature by rubbing a double-wax strip between your fingers for 20 s. The wax strips should be at body temperature.
5. Make sure that the skin is dry and free of irritation. Gently peel the strips apart and place one of the wax strips onto the skin in the direction of hair growth (Fig. 1d). Smooth the strip gently downwards with your fingers to make sure that it is properly adhered.
6. Hold the back skin in the posterior part of the body with one hand, and remove the wax strip with a quick gesture, pulling against the direction of hair growth (Fig. 1e). Make sure to pull the strip parallel to the skin. Repeat if necessary. Since the mouse hairs are long and dense, do not reuse the same strip.
7. The skin should be light pink, clean and without traces of injury or red dots (Fig. 1f). If some traces of wax remain on the skin, they can be removed with the back of a used strip.

3.2 In Vivo Activation of Cre-Recombinase for Clonal Analysis: Treatment with 4-OHT

3.2.1 Preparation of the 4-OHT Solution with Corn Oil

1. Due to the hydrophobic nature of 4-OHT, 4-OHT solution is prepared in a hydrophobic solvent and injected intraperitoneally. 4-OHT is first suspended at a concentration of 100 mg/mL in 100 % ethanol.
2. Dilute in autoclaved corn oil to 10 mg/mL.
3. Sonicate by pulses for 30 min. Sonication helps to break up and dissolve the crystals.
4. Aliquot and store at -20°C , protected from light.
5. Before injection, working stocks are made by diluting the main stock solution in $1\times$ PBS to the desired concentration and vortexing. Keep the working stocks at room temperature.

3.2.2 Preparation of the 4-OHT Solution with CremophorEL

For very low 4-OHT concentrations, a novel protocol is used (Petit and Nicolas 2009). This solution is suitable for intravenous and intraperitoneal injections.

1. Dilute 4-OHT to 20 mg/mL in 100 % ethanol.

2. Then dilute in *Cremophor EL* (Sigma) to 10 mg/mL and again in 1× PBS to 3 mg/mL, and store at −20 °C.
3. Mix by vortexing and keep aliquots of the stock solution at −20 °C, protected from light.
4. Before injection, dilute the suspension to the desired concentration in 1× PBS and keep at room temperature.

(See Chapter “Preparation and delivery of 4-hydroxy-tamoxifen for clonal and polyclonal labelling of cells of the surface ectoderm, skin and hair follicle,” Chevalier et al. for further details)

3.2.3 Injection of the 4-OHT Solution

1. Weigh the animal (drug amounts to be administered are based on body mass).
2. Vortex the 4-OHT solution before injection.
3. Inject intraperitoneally the 4-OHT solution at the desired concentration. Use large needles for 4-OHT solution in corn oil (because it is viscous) and insulin syringes with small needle for 4-OHT solution with CremophorEL (since they are more precise).
4. On the day of the injection, a skin control biopsy can be sampled to verify the stage of the HF at the moment of induction (6).

3.3 Sample Biopsies and Fixation

1. The mouse is anaesthetized by intraperitoneal injection of anaesthetic solution (Rompun and Imalgene solution, 0.1 mL for 25 g mouse weight).
2. Begin surgery only after the animal is nonresponsive. Surgical level of anaesthesia is checked by the absence of paw withdrawal reflexes after toe pinching.
3. Clean the biopsy area with liberal amounts of ethanol 70 % or skin disinfectant (Fig. 2a). Remove the excess of solution with a tissue.
4. Grab a pinch of skin is grabbed and slightly pull up using blunted forceps, and a small incision is performed using the scissors (Fig. 2b). Hold one of the incision with the blunted forceps and enlarge the incision as desired by cutting the skin with the scissors (Fig. 2c). An elliptical sample of full-thickness skin of less than 10 mm × 6 mm is removed (Fig. 2d).
5. Suture the edges of the resulting wound using absorbable Vicryl (Ethicon—Johnson & Johnson) (Fig. 2e, f).
6. Immediately after surgery, place the mouse in a warmed cage for recovery. Once the mouse has recovered full locomotion, transfer it to a clean cage. Mice that have undergone surgery are placed in individual cages to avoid reopening of the wound

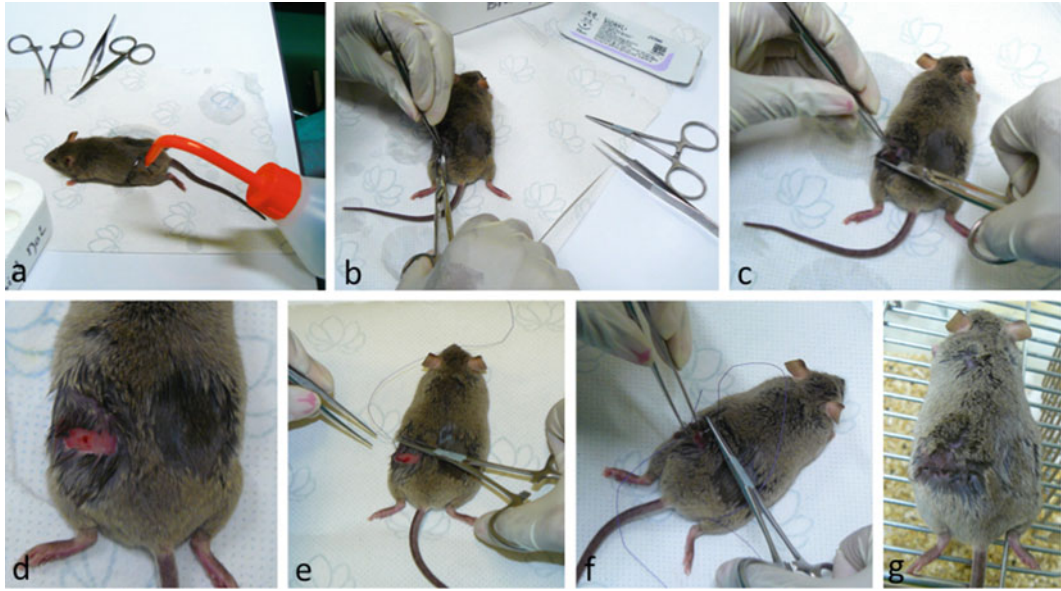


Fig. 2 Biopsy of skin sample. (a) Clean the biopsy area with ethanol 70 % or skin disinfectant. (b) Grab a pinch of skin and pull it up to make a small incision. (c, d) Cut a skin biopsy with scissors. (e, f) Join the skin edges and suture the wound with absorbable suture with needle (Vycril). (g) Place the mouse in a separate warmed cage for recovery

(Fig. 2g). If mice show signs of distress or pain after surgery, administer buprenorphine.

7. The biopsy is placed in cold PBS 1× immediately after sampling in a 12-well plate kept on ice. The PBS is aspirated using plastic transfer pipettes and replaced by cold PFA 4 %. Biopsies are fixed in PFA 4 % for 20 min on a nutator at 4 °C and then rinsed three times for 5 min at 4 °C in PBS before processing.

3.4 Detection of the Reporter Gene: X-Gal Staining

3.4.1 Preparation of the Biopsy

1. To prepare a fixed skin biopsy for X-Gal staining, transfer it to a Petri dish.
2. Remove the layer of muscles and subcutaneous fat using forceps under a stereoscopic microscope. At one edge of the biopsy, the epidermis is grabbed with one pair of forceps and the muscle and subcutaneous fat layer with another pair of forceps. The epidermis, including the HFs, is then pulled apart from the muscle and fat layer. If the muscle and fat layer do not come off in one piece, they are carefully removed to expose the HFs using the fine forceps without damaging the HFs.
3. Transfer the epidermis with exposed HFs to a 12-well plate.

3.4.2 X-Gal Staining

1. The prepared biopsies are in a 12-well plate in cold PBS.

2. Aspirate the PBS using a plastic transfer pipette and replace by X-Gal reaction solution.
3. For whole-mount lacZ staining of skin biopsies, incubate at 30 °C for 48 h (Note 3).
4. After staining, rinse the biopsies three times in PBS and preserved in PBS-azide 0.05 % at 4 °C to avoid contamination.

3.5 Detection of the Reporter Gene: Fluorescent Protein

Biopsies from fluorescent reporter mice require special care, in particular by protecting from light. HF fluorescent clones (after dissection) can be directly observed at the confocal microscope or we can perform fluorescence immunostaining in whole-mount HFs (22).

1. Fix the biopsies with PFA 4 % for 20 min on a nutator at 4 °C. If it is to be followed by antibody staining, an o.n. fixation with 0.5 % PFA at 4 °C on a nutator can be used instead.
2. After fixation, the biopsies are rinsed three times for 5 min at 4 °C in PBS and preserved in PBS-azide 0.05 % at 4 °C, protected from light (Note 4).

3.6 Microdissection of Individual HFs

Traditionally microdissection is the most reliable method for isolating intact HFs. It is essential to have a good dissecting microscope and sharp watchmaker's forceps.

1. Transfer the biopsy into a Petri dish in a drop of PBS.
2. A small piece is cut using the scalpel blade, and the rest of the biopsy is placed back into the 12-well plate at 4 °C, protected from light. The Petri dish is placed under a stereo-dissecting microscope (bright light source for lacZ or UV light and filters for fluorescent samples).
3. Using fine forceps (Dumont#5) and microscalpel, individual HFs are carefully dissected from the epidermis. Small groups can be dissected out first, and then the dissection is refined to obtain single HF. Use one pair of forceps to hold the piece of biopsy at the bottom of the dish, and another pair of forceps for dissection by delicate pulling of the epidermis between the HFs. A microscalpel can be used to cut the fat and the epidermis around the HF.

Special attention needs to be given to the upper part of the HF attached to the epidermis. The identification of the sebaceous glands can help to locate the region of the bulge.

4. Each dissected HF is transferred using the fine forceps in a well plate in PBS-azide 0.05 % for preservation or in PBS for posterior immunostaining. Each HF can also be directly mounted on a microscope slide for observation.

3.7 Observation of LacZ Clones with Brightfield Microscope

After screening the positive HF clones under a dissecting microscope, whole-mount HF can be examined for β -galactosidase-positive cells at 40 \times magnification. Each HF is analyzed and photographed, and a digital library of the clones is produced.

1. Place the dissected HF in a drop of PBS on a glass slide using fine forceps. The HF is gently pushed to the bottom of the drop near the glass.
2. The coverslip is positioned gently above the HF without creating bubbles. The amount of PBS must be sufficient such that the coverslip is slightly floating and does not squash the HF.
3. The coverslipped slide is then examined under a brightfield upright microscope. The HF can be gently turned by slightly moving the coverslip to better visualize the labelled cells within the three-dimensional structure of the HF. For long periods of observation, PBS must be added to ensure that the coverslip is always floating and the HF does not dry out.
4. Images can be acquired using a brightfield microscope with digital camera.
5. Once observation is complete, the coverslip is floated off the slide by adding PBS and gently removed using forceps. The HF is transferred back to the 96-well plate in PBS-azide 0.05 %.

3.8 Observation of LacZ Clones with Confocal Microscope

On average, a back skin HF is 2 mm long and 50–200 μ m wide. Imaging is usually performed with a confocal microscope, but larger HFs may need a multiphoton microscope to ensure the imaging of the whole HF thickness.

1. To prepare the microscope slides, apply scotch tape (sticky side down) onto the slide to create a small pool. This will act as a wall to contain a tiny liquid pool for one HF and will prevent the HF from being flattened between the slide and coverslip after the evaporation of the PBS, and it will keep the HF three-dimensional morphology.
2. Place the HF in a drop of PBS in the pool using fine forceps, and gently push the HF to the bottom of the drop, near the glass in the middle of the pool (avoid the HF touching the scotch tape).
3. Position the coverslip without any air bubble inside the pool.
4. Apply a layer of nail polish on the edges of the coverslip to seal it. This will prevent from drying and will keep the sample still while manipulating the microscope objective. The slides can be kept at 4 °C until they are imaged.
5. Choose the objective, and apply the immersion fluid. Under transmitted light, focus on the region of interest. Depending on the optics of the instrument used, 40 \times , 25 \times , and 10 \times objectives

can be used for imaging the whole HF. For optimal cellular resolution with 40× objective, use 1,024 × 1,024 pixels and the slice spacing of 0.5–1 μm. For lower magnification objectives, larger slice spacing (>1 μm) might be optimal.

6. Photomultiplier gain, offset, and laser power will depend on the microscope and on the fluorescence of the sample. For larger HFs, the gain can be adjusted through the z-stack to ensure that the deepest cells are detected. If required, perform frame averaging.
7. After observation and data collection, remove the top cover glass gently and collect the HF with fine forceps. The HF can be kept in a 96-well plate in PBS at 4 °C for further analysis.

4 Notes

1. For maximum efficiency, we recommend using albino mice (Balb/c): the lack of pigments will improve the fluorescent imaging of the HFs (22).
2. If the skin presents darker patches, it means that the HF is not in telogen, and therefore this zone will not be synchronous with the remaining area (6).
3. Incubate with X-Gal at 30 °C, rather than at 37 °C, to reduce background staining (23).
4. For fluorescent samples, it is not necessary to remove the layer of muscles and subcutaneous fat after fixation. This can be done during the microdissection of the clones.

Acknowledgments

This work was supported by the Institut Pasteur and by the French Agence National de la Recherche n°10-01 (DEV-Process to I.S. and J.F.N). All experiments were carried out in accordance with the national guidelines for care and use of laboratory animals.

References

1. Fuchs E (2009) The tortoise and the hair: slow-cycling cells in the stem cell race. *Cell* 137:811–819
2. Legué E, Sequeira I, Nicolas J-F (2012) Hair follicle stem cells. In: Hayat MA (ed) *Stem cells and cancer stem cells*, vol 3. Springer, New York, pp 35–47
3. Fuchs E, Horsley V (2008) More than one way to skin. *Genes Dev* 22:976–985
4. Legué E, Sequeira I, Nicolas J-F (2010) Hair follicle renewal: authentic morphogenesis that depends on a complex progression of stem cell lineages. *Development* 137:569–577
5. Millar SE (2002) Molecular mechanisms regulating hair follicle development. *J Invest Dermatol* 118:216–225
6. Müller-Röver S, Handjiski B, van der Veen C et al (2001) A comprehensive guide for the accurate classification of murine hair follicles

- in distinct hair cycle stages. *J Investig Dermatol* 117:3–15
7. Stenn KS, Paus R (2001) Controls of hair follicle cycling. *Physiol Rev* 81:449–494
 8. Legué E, Nicolas J-F (2005) Hair follicle renewal: organization of stem cells in the matrix and the role of stereotyped lineages and behaviors. *Development* 132:4143–4154
 9. Feil R, Brocard J, Mascrez B et al (1996) Ligand-activated site-specific recombination in mice. *Proc Natl Acad Sci U S A* 93:10887–10890
 10. Soriano P (1999) Generalized lacZ expression with the ROSA26 Cre reporter strain. *Nat Genet* 21:70–71
 11. Vooijs M, Jonkers J, Berns A (2001) A highly efficient ligand-regulated Cre recombinase mouse line shows that LoxP recombination is position dependent. *EMBO Reports* 2:292–297
 12. Metzger D, Chambon P (2001) Site- and time-specific gene targeting in the mouse. *Methods* 24:71–80, San Diego, Calif
 13. Indra AK, Warot X, Brocard J et al (1999) Temporally-controlled site-specific mutagenesis in the basal layer of the epidermis: comparison of the recombinase activity of the tamoxifen-inducible Cre-ER(T) and Cre-ER(T2) recombinases. *Nucleic Acids Res* 27:4324–4327
 14. Jaks V, Barker N, Kasper M et al (2008) Lgr5 marks cycling, yet long-lived, hair follicle stem cells. *Nat Genet* 40:1291–1299
 15. Snippert HJ, Haegerbarth A, Kasper M et al (2010) Lgr6 marks stem cells in the hair follicle that generate all cell lineages of the skin. *Science* 327:1385–1389
 16. Li M, Indra AK, Warot X et al (2000) Skin abnormalities generated by temporally controlled RXRalpha mutations in mouse epidermis. *Nature* 407:633–636
 17. Kawamoto S, Niwa H, Tashiro F et al (2000) A novel reporter mouse strain that expresses enhanced green fluorescent protein upon Cre-mediated recombination. *FEBS Lett* 470:263–268
 18. Srinivas S, Watanabe T, Lin CS et al (2001) Cre reporter strains produced by targeted insertion of EYFP and ECFP into the ROSA26 locus. *BMC Dev Biol* 1:4
 19. Muzumdar MD, Tasic B, Miyamichi K et al (2007) A global double-fluorescent Cre reporter mouse. *genesis* 45:593–605
 20. Livet J, Weissman TA, Kang H et al (2007) Transgenic strategies for combinatorial expression of fluorescent proteins in the nervous system. *Nature* 450:56–62
 21. Snippert HJ, van der Flier LG, Sato T et al (2010) Intestinal crypt homeostasis results from neutral competition between symmetrically dividing Lgr5 stem cells. *Cell* 143:134–144
 22. Sequeira I, Nicolas J-F (2012) Redefining the structure of the hair follicle by 3D clonal analysis. *Development* 139:3741–3751
 23. Bonnerot C, Nicolas JF (1993) Clonal analysis in the intact mouse embryo by intragenic homologous recombination. *Comptes rendus de l'Académie des sciences, Série III. Sciences de la vie* 316:1207–1217

Isolation and Characterization of a Stem Cell Side-Population from Mouse Hair Follicles

Paula L. Miliani de Marval, Sun Hye Kim,
and Marcelo L. Rodriguez-Puebla

Abstract

The mouse skin is composed of at least three differentiating epithelial compartments: the epidermis, the hair follicle, and the associated glands such as the sebaceous glands. Proliferation of these epithelial cells takes place in the keratinocytes' layer or basal cell layer; in the periphery of the sebaceous gland (the basal layer of the gland) and in specific cell compartments around the hair follicle. In mouse skin, an epithelial stem cell population is thought to localize to the bulge region of the hair follicle, a segment that does not undergo regression during the hair cycle. In addition, several other putative stem cells and/or progenitors have been identified in different regions of the hair follicle. Using the Hoechst exclusion technique, originally described in the hematopoietic system, it has been possible to isolate a mouse keratinocyte cell population with characteristics of stem cells (side-population, SP). One of the main features of these SP is their ability to efflux antimetabolic drugs as well as some specific dyes. This characteristic allows for SP cells to be isolated based upon their capacity to efflux the dye Hoechst 33342, through a mechanism driven by a membrane transporter, the breast cancer resistance protein (BCRP1/ABCG2). In this chapter, we described the isolation of SP stem cells from adult mouse hair follicles utilizing the Hoechst exclusion technique by flow cytometry analysis.

Keywords: Side-population, Keratinocyte stem cells, Bulge, Hair follicle, BCRP1/ABCG2, Hoechst 33342, FACS

1 Introduction

Skin stem cells have been identified in the interfollicular epidermis (IFE), the hair follicle bulge region and the sebaceous gland (1–2, 8–10). Numerous molecular markers such as CD34, keratin 15 (K15), Blimp1, and $\alpha 6$ integrin allow distinguishing hair follicle stem cells of the bulge region from keratinocytes (3, 5, 11, 12). In addition, several other putative stem cells and/or progenitors have been identified in different regions of the hair follicle, although their exact role in maintaining epidermal homeostasis and hair follicle morphogenesis is not well understood (4, 13, 14).

A subset of cells, termed the side-population (SP), with characteristics of adult stem cells (SCs) has been identified in several

tissues including: mouse epidermis, cell lines, as well as human and experimental tumors (15–17). The main feature of these cell populations is their high efflux capability of antimitotic drugs. This characteristic allows the isolation of the SP based upon their capacity to efflux the dye Hoechst 33342 (6). The membrane transporter “breast cancer resistance protein” (BCRP1/ABCG2), which belongs to the multidrug resistance proteins (MDRPs) family, is responsible for the efflux of Hoechst 33342 (18). In agreement with the high efflux capacity of the SP, high expression of the BCRP1/ABCG2 was observed in the SP from hematopoietic stem cells and other types of cells (19). Remarkably, the SP has characteristics of adult stem cells such as long-term repopulating capacity, undifferentiated phenotype, and colony forming potential (6). However, the role of the SP in tumorigenesis is controversial, though a role as cancer stem cells has been reported (20–22). Therefore, further studies on the role of these putative stem cell populations seems to be necessary to define their main characteristics and differences with adult stem cells and to determine the potential application in regenerative medicine and oncology.

In this chapter, we describe a method to isolate SP from the mouse hair follicle. This methodology produces a side-population with characteristics of hair follicle progenitors such as the high expression of the BCRP1/ABCG2 transporter which expression can be confirmed by qRT-PCR.

2 Materials

2.1 Solutions

Prepare all the solutions in sterile conditions, under a laminar flow hood.

1. Solution A: 0.25 % Trypsin, without EDTA, without phenol red (Sigma, St. Louis, MO, USA), cool to 4 °C.
2. Chelex Serum: Fetal bovine serum (FBS) (Gemini Bio-products, West Sacramento, CA, USA) chelated with Analytical grade Chelex 100 resin (Cat. # 142-2832, Bio-Rad, Munich, Germany). See Note 1.
3. Solution B: William’s Medium E (GIBCO, Life Technologies, Darmstadt, Germany) + 10 % Chelex serum + Penicillin–Streptomycin (P/S) (Mediatech Inc, Manassas, VA, USA), cool to 4 °C.
4. Phosphate-buffered saline (PBS) containing 2 % FBS (chelated), cool to 4 °C.

2.2 Instruments and Supplies

1. Sterile dissecting forceps.
2. Sterile dissecting scissors.

3. Stainless steel razor blades, Gem Single-Edge Blade (American Safety Razor 94-0451) or #20 Blade stainless steel scalpel.
4. Electric shaver or equivalent.
5. Nair hair remover lotion.
6. Q-tips Cotton-tipped applicators, Single-tipped wood stick applicators (Cat. # NC9586484, Fisher Scientific).
7. 15 and 50-mL polypropylene conical tubes (BD Falcon, Franklin Lakes, NJ).
8. 40- μ M and 100- μ M nylon cell strainers (Cat. # 08-771-1 and 08-771-19, BD Falcon, Franklin Lakes, NJ).
9. 5-mL cell strainer round-bottom cap tubes (Cat. # 08-771-23, BD Falcon, Franklin Lakes, NJ).
10. Tissue culture dish, 100 \times 20 mm (BD Falcon, Franklin Lakes, NJ).
11. Sterile 50-mL beaker.
12. Sterile stir bar.
13. Laminar flow hood (NuAIR, Plymouth, MN).
14. Sterile and disposable 5-, 10-, and 25-mL tissue culture pipettes (Genesee Scientific, San Diego, CA).

2.3 Reagents

1. Hoechst 33342 (Cat. # B-2261, Sigma, St. Louis, MO).
2. Verapamil (Cat. # V-4629, Sigma, St. Louis, MO).
3. Propidium Iodide (Cat. # P-4170, Sigma, St. Louis, MO).

2.4 Mice

1. Three to five 7–9-weeks-old FBV/NCr mice (NCI/Frederick National Laboratory). Isolation of SP can be achieved with mice from any other common laboratory strains. See Note 2.

3 Methods

3.1 Epidermal Cell Isolation from Mouse Epidermis

Perform all procedures under sterile conditions, under the laminar flow hood preferable.

1. Euthanized mice according to the IACUC approved methods.
2. Shave the entire back of the mouse using an electric shave. Avoid forceful pressure of the shaver against the back of the mouse which could damage the skin.
3. Remove the remaining hair by evenly distributing the Nair depilatory cream on the dorsal skin with a cotton Q-tip or with a Lymtech Clean Room Swabs, (Foam Tip Width 1/2", Tip Length 1", Plastic Handle 4"). Allow the cream to work for 2–3 min.

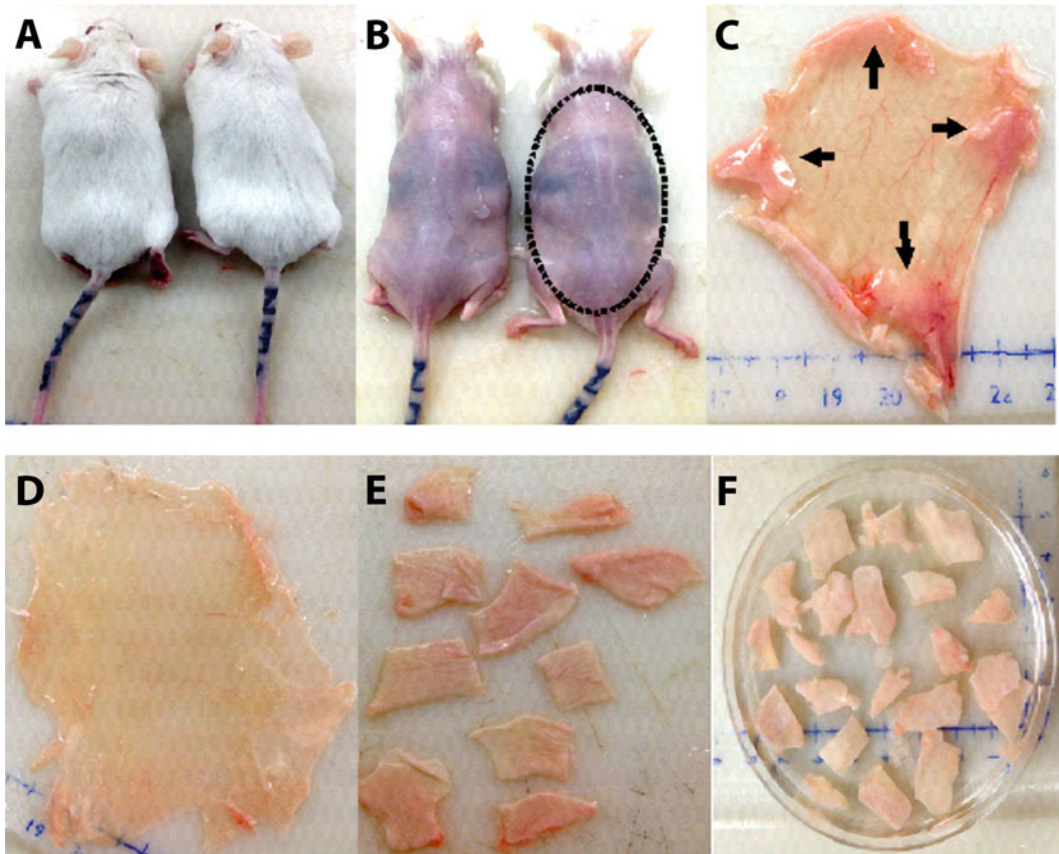


Fig. 1 Stepwise procedure for obtaining epidermis from adult mice. (a) Euthanize mice according to laboratory approved procedures, shave dorsal skin, and remove remaining hair with Nair depilatory cream. *Dashed dotted line* indicates the area of the skin to be removed. (b) Flat skin showing the dermis—shiny side up and fat pads (*arrows*). (c) Dermis shiny side up after fat removal. (d) Skin cut into 1 × 1.5 cm to extend the surface exposed to trypsin. (e) Cell culture dish with skins dermis side down floating in trypsin solution (Solution a)

4. Rinse off the Nair lotion and hair thoroughly under running water.
5. Rinse once with 70 % (vol/vol) Ethanol to remove any residual hair (Fig. 1a, b). Pat the skin dry with tissue.
6. Carefully make an incision into the hypodermis with scissors while holding the skin up with forceps and cut off the dorsal skin from the back of the head to right before the beginning of the tail (Fig. 1b, dash line).
7. Dissect the skin in one piece and place it dermal side up (which is the shiny side that contains fat tissue) on a 100-mm tissue culture dish (Fig. 1c).
8. Scrape off all the fat and muscle with a scalpel or razor blade without damaging the underlying epidermis tissue (Fig. 1d).

9. Cut the skin into 1×1.5 cm strips using sterile scalpel blade and float the strips with the dermis (shiny side) down on a 100 mm tissue culture dish containing 10-mL of cold Solution A (Fig. 1e, f). Make sure that the epidermis side of the skin does not come into contact with the trypsin. Incubate the floating skin pieces overnight at 4 °C or 2 h at 37 °C. See Note 3.
10. Prepare 50-mL conical tubes, scalpel blades, forceps, 40- μ M and 100- μ M nylon cell strainers, 25-mL tissue culture pipettes. After the incubation time with Solution A, perform all the rest of procedures on ice unless otherwise indicated.
11. Place the dish containing the skins floating on Solution A on ice while you process each piece.
12. Transfer one of the floating skin strips from the Solution A plate and place it into a 100 mm microbiology dish, on ice, (do not use tissue culture grade dish since cells tend to adhere to it) with the dermis, shiny side up. Gently scrape off and discard any remaining fat from this side.
13. Flip the skin over to its epidermal side and gently, remove the interfollicular epidermis (opaque side of the tissue) by scraping five times using a scalpel. Discard this material.
14. Move the scraped skin to a new 100 mm microbiology dish containing 2 mL of Solution B, and continue scraping off the epidermis until the shiny dermis is exposed. Discard the scrapped skin strip.
15. Repeat steps #12–14 for the rest of the tissues. Add Solution B as needed.
16. Transfer all the cellular material from all the tissue strips into one small beaker.
17. Pipette the solution up and down at least ten times with a 10-mL tissue culture pipette.
18. Add enough solution B into the beaker containing the cells to complete 25–30 mL total volume.
19. Add a small sterile stir bar and rotate slowly for 30 min at 4 °C.
20. Pipette the solution up and down at least ten times with a 10 mL tissue culture pipette.
21. Transfer and filter the solution through a 100- μ M nylon cell strainer into a new 50-mL conical tube with a ten tissue culture pipette.
22. Add 5-mL of Solution B to the mesh to wash off any remaining cell.
23. Filter the solution through a 40 μ M nylon cell strainer into a new 50-mL conical tube.
24. Spin at 4 °C at $200 \times g$ in a cell culture centrifuge for 7 min.

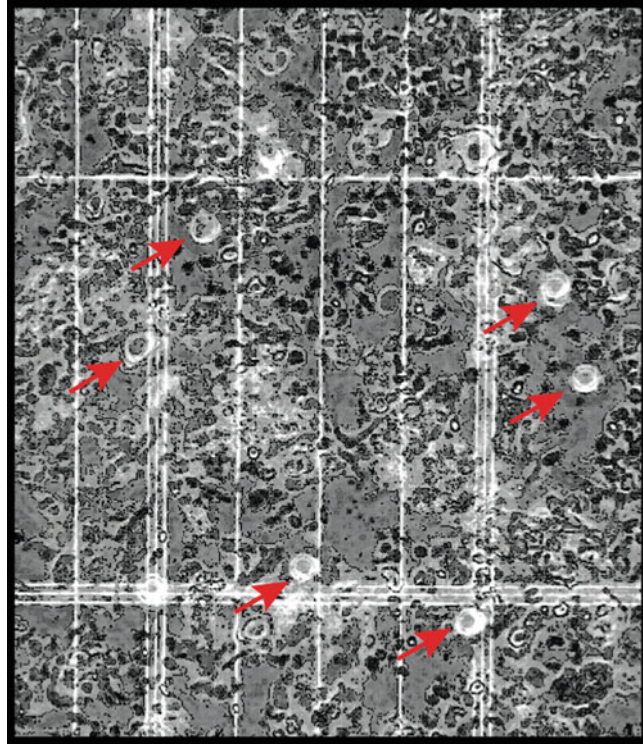


Fig. 2 Phase contrast image of freshly prepared cell fractions from epidermis of adult FBV/NCr mice. *Red arrow* points to keratinocytes

25. Remove the supernatant carefully and resuspend cells with 1 mL of PBS/2 % Chelex serum, by gently pipetting.
26. Count round-shaped cells in Neubauer chamber (Fig. 2).
27. Adjust the final volume in order to resuspend 1×10^6 cells per 1 mL of PBS/2 % Chelex serum.

3.2 Epidermal Cell Staining for FACS Analysis

See Tables 1 and 2 for the recommended working samples and dilutions.

Hoechst staining

1. Perform a control with verapamil to identify the SP by FACS analysis (Note 4). Incubate a 15-mL conical tube containing 1×10^6 cells/mL with Verapamil (50 μ M final concentration) for 20 min at room temperature, before proceeding with the Hoechst staining.
2. Incubate the verapamil control tube and an additional 15-mL conical tube containing 1×10^6 cells/mL with 5 μ g/mL of Hoechst 33342 at 37 °C for 90 min. (Shake tubes frequently during incubation). Note: do not wash the verapamil pretreated tube before incubation with Hoechst 33342. An additional

Table 1
Suggested sample set for setup and experiment

Sample set		Number of cells
1	Unstained negative control with Propidium Iodide (PI)	1×10^6
2	Hoechst 33342	1×10^6
3	Verapamil + Hoechst 33342	1×10^6

Table 2
Required dye concentrations for cell sample labeling

	Final concentration ($\mu\text{g/mL}$)
Hoechst 33342	5
Verapamil	50
Propidium iodide (PI)	2

control of live cells can be achieved by staining 1×10^6 cells/mL with add $2 \mu\text{g/mL}$ of Propidium iodine (PI) (Table 1, sample 1).

3. Add 5-mL cold PBS, and spin stained cells at 200 g , $4 \text{ }^\circ\text{C}$ for 7 min. Discard the supernatant and resuspend the cellular preparation in $200 \mu\text{L}$ of PBS/2 % FBS Chelex serum (keep cells at $4 \text{ }^\circ\text{C}$ to prohibit leakage of the Hoechst dye).
4. Perform FACS analysis using a DAKO Cytomation MoFlo Ultra-High Speed Cell Sorter or similar system. Set UV laser at 350 nm to excite Hoechst dye and measure using a $450/20\text{-nm}$ and 670 band-pass filters (Hoechst blue and red). Cells are analyzed and sorted within PI-negative cells, which represents a living population, and the SP is displayed in a Hoechst blue versus Hoechst red dot plot (Fig. 3a).
5. The side-population gate is chosen by a direct comparison against the verapamil-treated cells. The SP consists of 1–2 % of the total living cells found in the bulge region. The SP and the main population (MP) can be isolated and further analysis of mRNA expression can be performed by qRT-PCR analysis. Figure 3b shows high expression of the ABCG2 transporter in the SP, but no other markers of the bulge stem cells such as CD34, keratin 15 (K15), LRIG1, and integrin $\alpha 6$ are found in this particular population.

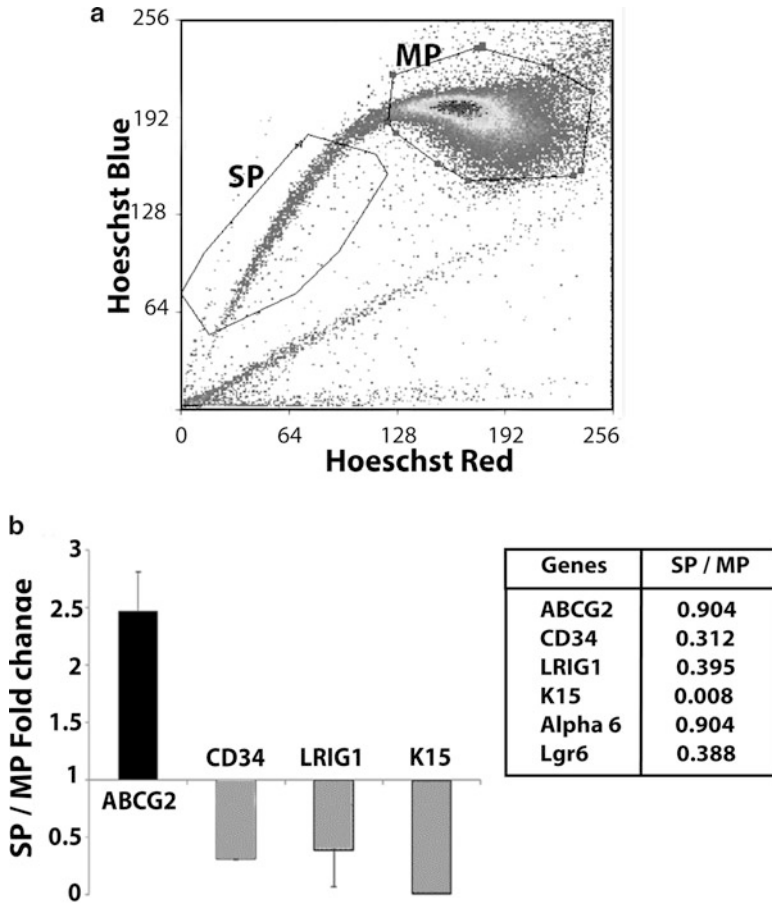


Fig. 3 Identification of side-population (SP) from mouse hair follicles. Dual wavelength FACS analysis shows keratinocytes from the hair follicle incubated with Hoechst 33342. **(a)** SP cells consist of 1.62 % of total living cells. **(b)** Total RNA extracted from FACS-sorted side-population (SP) and keratinocyte main-population (MP) were used for qRT-PCR analysis of ABCG2/Bcrp1, CD34, integrin α 6, LRIG1, LGR6, Keratin 15 (K15), and CD71. Values >1 represent higher expression on side-population, whereas $1 > \text{values} >0$ represent low expression in SP compared to keratinocytes MP

4 Notes

1. Removal of calcium from Fetal Bovine Serum using analytical grade 100 Chelex resin, (BioRad Chelex 100 Resin #142-2832): Rinse 500 g of resin to remove contaminants through extensive washes by stirring with ddH₂O at room temperature by 20–30 min. Stop stirring and allow the resin to settle down for 20 min. Repeat the washes two more times. Resuspend resin in ddH₂O and set the pH between 7.0 and 7.4 with HCl. Remove the water from the resin using a Buchner funnel with Whatman paper. Add 2 L of Fetal Bovine Serum to the

clean chelex resin and cover with foil. Stir for 4–5 h at 4 °C. Stop stirrer and allow chelex to settle. Bring the serum to the cell culture hood and filter through a 500 mL capacity 0.22 µM filter unit. Aliquot serum into 50 mL tubes and store at –20 °C. Calcium concentration after chelexing ranges between 20–140 µM.

2. We use 7–9-weeks-old mice during the second resting phase or telogen allowing for more reproducible results. One way to ensure that mice's hair cycle is indeed in telogen is by clipping their dorsal hair, wait between 48 and 72 h and select those mice with no hair growth (23).
3. Use one 100 mm dish every two mice whole skin. Do not overload the dishes with skins during this step since it will impair the ability of the trypsin to digest the skin properly making it difficult to achieve good isolation of the epidermis from the dermis. Both incubation times (ON at 4° or 2 h at 37°) work equally well.
4. Verapamil is a prototypical phenylalkylamine that blocks the activity of the ABCG2/BCRP1 transporter allowing gating of the SP by direct comparison with the non-verapamil sample (Table 1).

Acknowledgment

This work was supported by National Cancer Institute/NIH grant RO1 CA116328.

References

1. Watt FM (1998) Epidermal stem cells: markers, patterning and the control of stem cell fate. *Philos Trans R Soc Lond B Biol Sci* 353:831–837
2. Sun TT, Cotsarelis G, Lavker RM (1991) Hair follicular stem cells: the bulge-activation hypothesis. *J Invest Dermatol* 96:77S–78S
3. Horsley V, O'Carroll D, Tooze R, Ohinata Y, Saitou M, Obukhanych T et al (2006) Blimp1 defines a progenitor population that governs cellular input to the sebaceous gland. *Cell* 126:597–609
4. Jensen KB, Collins CA, Nascimento E, Tan DW, Frye M, Itami S et al (2009) Lrig1 expression defines a distinct multipotent stem cell population in mammalian epidermis. *Cell Stem Cell* 4:427–439
5. Morris RJ, Liu Y, Marles L, Yang Z, Trempe C, Li S et al (2004) Capturing and profiling adult hair follicle stem cells. *Nat Biotechnol* 22:411–417
6. Goodell MA, Brose K, Paradis G, Conner AS, Mulligan RC (1996) Isolation and functional properties of murine hematopoietic stem cells that are replicating in vivo. *J Exp Med* 183:1797–1806
7. Dunnwald M, Tomanek-Chalkley A, Alexandrunas D, Fishbaugh J, Bickenbach JR (2001) Isolating a pure population of epidermal stem cells for use in tissue engineering. *Exp Dermatol* 10:45–54
8. Cotsarelis G, Sun TT, Lavker RM (1990) Label-retaining cells reside in the bulge area of pilosebaceous unit: implications for follicular stem cells, hair cycle, and skin carcinogenesis. *Cell* 61:1329–1337
9. Miller SJ, Burke EM, Rader MD, Coulombe PA, Lavker RM (1998) Re-epithelialization of

- porcine skin by the sweat apparatus. *J Invest Dermatol* 110:13–19
10. Taylor G, Lehrer MS, Jensen PJ, Sun TT, Lavker RM (2000) Involvement of follicular stem cells in forming not only the follicle but also the epidermis. *Cell* 102:451–461
 11. Trempus CS, Morris RJ, Bortner CD, Cotsarelis G, Faircloth RS, Reece JM et al (2003) Enrichment for living murine keratinocytes from the hair follicle bulge with the cell surface marker CD34. *J Invest Dermatol* 120:501–511
 12. Trempus CS, Morris RJ, Ehinger M, Elmore A, Bortner CD, Ito M et al (2007) CD34 expression by hair follicle stem cells is required for skin tumor development in mice. *Cancer Res* 67:4173–4181
 13. Jensen UB, Yan X, Triel C, Woo SH, Christensen R, Owens DM (2008) A distinct population of clonogenic and multipotent murine follicular keratinocytes residing in the upper isthmus. *J Cell Sci* 121:609–617
 14. Nijhof JG, Braun KM, Giangreco A, van Pelt C, Kawamoto H, Boyd RL et al (2006) The cell-surface marker MTS24 identifies a novel population of follicular keratinocytes with characteristics of progenitor cells. *Development* 133:3027–3037
 15. Shimano K, Satake M, Okaya A, Kitanaka J, Kitanaka N, Takemura M et al (2003) Hepatic oval cells have the side population phenotype defined by expression of ATP-binding cassette transporter ABCG2/BCRP1. *Am J Pathol* 163:3–9
 16. Yano S, Ito Y, Fujimoto M, Hamazaki TS, Tamaki K, Okochi H (2005) Characterization and localization of side population cells in mouse skin. *Stem Cells* 23:834–841
 17. Challen GA, Little MH (2006) A side order of stem cells: the SP phenotype. *Stem Cells* 24:3–12
 18. Zhou S, Schuetz JD, Bunting KD, Colapietro AM, Sampath J, Morris JJ et al (2001) The ABC transporter Bcrp1/ABCG2 is expressed in a wide variety of stem cells and is a molecular determinant of the side-population phenotype. *Nat Med* 7:1028–1034
 19. Kim M, Turnquist H, Jackson J, Sgagias M, Yan Y, Gong M et al (2002) The multidrug resistance transporter ABCG2 (breast cancer resistance protein 1) effluxes Hoechst 33342 and is overexpressed in hematopoietic stem cells. *Clin Cancer Res* 8:22–28
 20. Patrawala L, Calhoun T, Schneider-Broussard R, Zhou J, Claypool K, Tang DG (2005) Side population is enriched in tumorigenic, stem-like cancer cells, whereas ABCG2+ and ABCG2- cancer cells are similarly tumorigenic. *Cancer Res* 65:6207–6219
 21. Chiba T, Kita K, Zheng YW, Yokosuka O, Saisho H, Iwama A et al (2006) Side population purified from hepatocellular carcinoma cells harbors cancer stem cell-like properties. *Hepatology* 44:240–251
 22. Haraguchi N, Utsunomiya T, Inoue H, Tanaka F, Mimori K, Barnard GF et al (2006) Characterization of a side population of cancer cells from human gastrointestinal system. *Stem Cells* 24:506–513
 23. Muller-Rover S, Handjiski B, van der Veen C, Eichmuller S, Foitzik K, McKay IA et al (2001) A comprehensive guide for the accurate classification of murine hair follicles in distinct hair cycle stages. *J Invest Dermatol* 117:3–15

Multiscale Mathematical Modeling and Simulation of Cellular Dynamical Process

Shinji Nakaoka

Abstract

Epidermal homeostasis is maintained by dynamic interactions among molecules and cells at different spatiotemporal scales. Mathematical modeling and simulation is expected to provide clear understanding and precise description of multiscale dynamics in tissue homeostasis under systems perspective. We introduce a stochastic process-based description of multiscale dynamics. Agent-based modeling as a framework of multiscale modeling to achieve consistent integration of definitive subsystems is proposed. A newly developed algorithm that particularly aims to perform stochastic simulations of cellular dynamical process is introduced. Finally we review applications of multiscale modeling and quantitative study to important aspects of epidermal and epithelial homeostasis.

Keywords: Multiscale mathematical modeling, Stochastic simulation algorithm, Agent-based models, Quantitative biology, Epidermal homeostasis

1 Introduction

1.1 Systems Perspective on Epidermal Homeostasis

The skin tissue is composed of different types of cells that form a complex structure. Since the skin tissue directly faces the external environment of the body, several biological functions are equipped to support maintenance of homeostasis. Repair process in wound healing and barrier function against invasion is two important machineries to maintain homeostatic state of the skin tissue. Barrier function of the skin tissue prevents invasion of physical, chemical, and biological substances. Recent studies have been highlighting the importance of the role of the skin tissue as a first defense line for the invasion of pathogens (1). Abnormal response to nonharmful antigen can induce the onset and progression of chronic inflammatory disorders such as psoriasis vulgaris (2). Resilience refers to the ability of a tissue to return to its original state after injury. For tissue repair, recent studies identified several roles of epidermal stem cells on recovery from tissue injury via active and quick recruitment of stem cells (3). Tata et al. recently reported that lineage-committed cells dedifferentiate to regain self-renewal ability during injury repair (4).

For some diseases, single genetic mutation can induce the breakdown of homeostasis. In such cases, lack or gain of function of key molecules or cells is an essential determinant of pathogenesis. On the other hand, systems perspective is required for the cases where a single causal factor does not trigger a deviation from a stable homeostatic state. Several genes are known to perform the same role in some biological function such as metabolism. Genetic redundancy is one possible mechanism to confer robustness of a system that operates to compensate for the lack of an important function (5). In general, biological functions such as barrier and repair mechanisms are maintained by spatiotemporal dynamic interactions of agents (molecular, genes, cells) across different levels. Significant biological concepts such as robustness and resilience are the property that should be inherently equipped with barrier and repair systems. Understanding and precise description of multiscale nature is an inevitable task to clarify these important concepts. A theoretical framework that deals with multiscale nature under systems perspective needs to be developed.

Mathematical modeling and simulation studies offer a powerful tool to provide clear and constitutive explanations to dynamical behavior of molecular and cellular interactions. One of the most challenging problems in mathematical description of multiscale nature is consistent integration of essential components. In the following subsections, we discuss mathematical modeling and simulation of multiscale dynamical processes.

1.2 Multiscale Mathematical Modeling and Simulation

Mathematical representation of dynamical processes at different spatiotemporal levels is called multiscale mathematical modeling (6, 7). A multiscale mathematical model is often composed of subsystems as its modules, each representing different dynamical process at a particular time- and spatial-scale. In this subsection, we emphasize and discuss the following three aspects of multiscale mathematical modeling that must be considered to ensure logical consistency and universality.

1.2.1 Verifiability

Verification of the theory has been a central issue in science. The power of mathematical modeling and simulation can be substantially useful if theoretical predictions are validated by experiments. Experimental or clinical data available for the validation of mathematical models are often obtained from a designed plan that aims to clarify some specific aspects of molecular or cellular behaviors at particular time points. Hence verification of a whole model is almost impossible. For this reason, verifiability in multiscale modeling refers to validation of subsystems via experiment or observation. For substantial verification, an appropriate choice of modeling formalism and dataset is essential. We consider this issue in the next two subsections in more details.

1.2.2 Coherency

Coherency refers to the well fitness of all the model ingredients if they are together. Coherency becomes indispensable in multiscale modeling since verification can be made only for subsystems.

There are numerous types of coherency that should be equipped with any of multiscale mathematical models. A common problem frequently faces in the integration of subsystems is that it is not evident whether subsystems can be integrated in a consistent way without violating the mathematical prerequisites presumed for each subsystem. Scale coherency in time and space is fundamental in maintaining causality. It must be carefully treated if dynamical processes of two different spatial or time scales are simultaneously considered. Context coherency refers to consistency of logical context dependence of molecular/cellular interactions in mathematical formulation. A subsystem is often designed as a closed system: A molecular/cellular behavior is completely described by given components (variables in a system of equations). If interdependence exists, unexpected context dependence can emerge when combining two subsystems. In general, argument on coherency is a context-sensitive matter. Careful consideration should be made on a case-by-case basis.

1.2.3 Emergent Complexity

We emphasize emergent complexity as an important feature to be incorporated in multiscale modeling of biological phenomena, although it might not be necessarily essential in general multiscale modeling. Emergent complexity is a concept that new rules or properties emerge from interactions of components at lower levels (8). Collective self-organized behavior is a well-known typical emergent behavior as exemplified by chemoattractant cell motion that shapes self-organized group formation (9). Homeostasis, robustness, or resilience of a tissue/body can be regarded as important cellular/tissue functioning that emerges as a consequence of complicated molecular and cellular interactions. One of the major goals of multiscale modeling and simulation is to represent and identify system functioning conferred by the integration of subsystems. Although several theoretical models have been proposed to identify basic mechanisms underlying the emergence and self-organization of complex system, most of existing theoretical models are rather abstract (8). Exploration of emergent complexity with multiscale modeling and simulation can provide a concrete explanation and understanding to emergent property on the basis of molecular/cellular interactions.

1.3 Phenomenological vs. Mechanistic

We discuss what is a feasible choice of description method to achieve reliable multiscale modeling. To start with, distinction should be made on the formalism of mathematical modeling. Mathematical modeling can be classified into two types: phenomenological (also referred as descriptive or empirical) or mechanistic (10). A phenomenological mathematical model is formulated by relating several empirical observations and knowledge of a phenomenon of interest. Phenomenological models often qualitatively reproduce observed phenomena irrespective of underlying

molecular/cellular mechanisms. In other words, manner of interactions among model ingredients is determined based on knowledge on qualitative observations, rather than actual molecular/cellular mechanistic interactions. The advantage of adopting phenomenological modeling is its usability: Modeling is possible even though mechanistic understandings and knowledge are lacking. On the other hand, phenomenological models can only end up with simply a translation of observations if no insights or emergent properties are derived from them. An important point that should be noticed in adopting phenomenological modeling is that derivation of arbitrary interpretation from arbitrarily chosen model ingredients and assumptions is an abuse of mathematical modeling.

A mechanistic mathematical model is often formulated as a representation of some principle. In physics, conservation of mass or energy is exploited as a principle to formalize mathematical equations (6). Mechanistic description of dynamical process provides common understanding that does not depend on arbitrary interpretations. Quantitative measurement rather than qualitative observation therefore provides a definitive guide to validate modeling and simulation study. However, only a few substantial basic principles such as the central dogma of molecular biology are accepted in biology at the moment. Moreover, measurement of quantitative data used for validation of mechanistic models is challenging in terms of technical difficulty and labor. This fact hampers the development of dependable mechanistic models.

1.4 Specification to Stochastic Process-Based Agent-Based Modeling

A challenging issue in multiscale modeling is to incorporate both merits of phenomenological and mechanistic formalisms: Flexible and versatile modeling framework is required to integrate subsystems, while subsystems are willing to be described by mechanistic modeling that enables verification with experimental data.

Agent-based simulation is based on an implementation of a set of rules governing a manner of interactions and state transitions of agents. Agent-based modeling provides a versatile and flexible framework to integrate different aspects of a whole dynamics. This property is suitable to combine several dynamical processes at different spatiotemporal multiscales. Extensive applications of agent-based models are found in the field of ecology and sociology in which representation of complex social behavior is often imperative (11). Number of software have already been released that support construction and simulation of agent-based models (for example, NetLogo (12)).

In agent-based modeling, a variety of model ingredients and rules need to be defined to complete formulation. Because mechanistic understanding is often lacking, lack of information must be altered with knowledge, qualitative observations, or feasible assumptions. Hence agent-based models themselves are generically highly phenomenological. It is therefore difficult to ensure the

feasibility and validity of theoretical predictions from agent-based modeling and simulations. To avoid this potential risk, incorporation of mechanistic subsystems on the basis of quantitative data validation is essential.

We emphasize the importance of the specification of agent-based modeling to stochastic process-based description in the following reasons. First, probabilistic description of molecular/cellular behavior seems to agree with recent findings. Recent progress of experimental measurement technology enables us to quantify gene expression profiles at the single cell level. Quantitative studies indicate that there exists significant heterogeneity in gene expression even in a genetically identical cell population. More precisely, heavy right-tail distributions such as lognormal or gamma are commonly measured in the gene expression profile of a population (13). Moreover, transcription of mRNA itself is revealed to be a stochastic event, leading to the speculation that a small number of molecules in a cell could contribute to significant molecular/cellular function (14). Second, most of the stochastic processes describe a simple but fundamental biological process. For instance, Yule distribution, also known as Pareto or power-law distribution, reflects heterogeneity measured by some quantity that exhibits heavy right-tail distribution in a population. The Yule distribution can be represented as a distribution of the Yule process, which is also known as preferential attachment process (15). It is well known that the resulting distribution of preferential attachment process has a power law property (16). This fact implies the possibility that feasible cell behavior can be inferred from a measured distribution. Third, incorporation of existing mathematical models is possible under stochastic process-based description. Differential equations have been used to represent molecular and cellular dynamics. There exists a theory that bridges stochastic process and differential equations. In case of chemical reactions, differential equations for chemical kinetic reactions can be derived from the Poisson stochastic counting process as thermodynamics limit under appropriate conditions (17–19). Fourth, recent rapid development of computational power enables us to carry out massive computations by in-house computers regardless of the fact that implementation of stochastic simulations is in general computationally heavy task. Moreover, parallel computational technique and facilities can be used to accelerate stochastic simulations that usually require several independent runs to obtain stable outcomes. In conclusion, specification of an agent-based model that fully incorporates stochastic process description as its subsystems has advantages not only in keeping versatility and flexibility as a general framework for multi-scale modeling but also in enabling verifiability of subsystems via quantitative measurement.

1.5 Organization

The organization of this chapter is as follows. In the next section, we discuss the Poisson stochastic process as a standard counting process that describes molecular/cellular dynamics. Following a brief introduction to the original Gillespie algorithm, individual-based Gillespie algorithm is introduced to integrate stochastic processes into an agent-based model. In Section 3, we discuss several hallmark studies on epidermal and epithelial biology in which mathematical approach is employed to investigate several important aspects of epidermal homeostasis: quantitative research on population dynamics of epidermal stem cells, mechanics of epithelia, and skin inflammatory disease.

2 Material and Method

2.1 Poisson Process

Poisson process is a basic stochastic counting process that describes the number of events occurs within a given time period under the assumption that events occur independently of each other. We used the notion of biological events for molecular/cellular activities that affect the increase or decrease of the number of a population. If a population of protein is considered, synthesis and degradation of protein can be considered as events. For cell populations, cell division and death are events. Let $X(t)$ denote the number of biological events that will occur till present time t . Then nonhomogeneous (time-dependent rate) Poisson processes must satisfy the following four conditions.

1. $P(X(0) = 0) = 1$.
2. $P(X(t+h) - X(t) = \pm 1) = \lambda(t)h + o(h)$, where $o(h)$ represents the first-order infinitesimal.
3. $P(X(t+h) - X(t) \geq 2) = o(h)$.
4. For any $t_1 < \dots < t_n$, increments $X(t_2) - X(t_1), \dots, X(t_n) - X(t_{n-1})$ are independent of each other.

Note that if the number of event incidence per unit of time follows Poisson distribution with rate parameter λ , time-interval ΔT representing waiting-time of event incidence follows exponential distribution with rate parameter λ .

2.2 Gillespie Algorithm

We briefly introduce the Gillespie algorithm, known as the direct method (19–21). The Gillespie algorithm was proposed to carry out stochastic simulations of chemical kinetic reactions (20). It is a numerical representation of the Poisson process composed of calculation of waiting-time of event incidence, and selection of an event that actually occurs.

Assume that dynamical process of interest can be fully described by R events. Let $\hat{P}(\tau, \kappa)d\tau$ denote the probability that κ th event \mathbf{R}_κ

will occur within an infinitesimal interval $(t + \tau, t + \tau + d\tau)$ ($0 \leq \tau < \infty$ and $\kappa = 1, 2, \dots, R$). The state of the system at present time t is given by $\mathbf{x}(t) = (x_1(t), \dots, x_M(t))$, where $x_i(t)$ represents the number of cells/molecules in population i (i in $\{1, 2, \dots, M\}$). Let $p_n(t, \mathbf{x})\delta t$, referred as propensity function, denote the probability that n th event \mathbf{R}_n will occur within infinitesimal interval δt . Note that $P(\tau, \kappa)$ is given by

$$P(\tau, \kappa) = p_\kappa(t, \mathbf{x}) \exp \left[- \sum_{n=1}^R p_n(t, \mathbf{x}) \tau \right]. \tag{1}$$

The Gillespie direct method consists of the following three steps. Each step is given as follows.

1. Determine time step ΔT after which one of the events will occur (waiting-time).
2. Select an event that actually occurs from the total R events.
3. Update the population number of the system according to the type of the selected event: In the case of cell populations, $+1$ for cell division and -1 for cell death.

We define the cumulative sum of propensity functions up to the K th event by $\Gamma_K(t, \mathbf{x})$ (K in $\{1, 2, \dots, R\}$). More precisely,

$$\Gamma_K(t, \mathbf{x}) = \sum_{n=1}^K p_n(t, \mathbf{x}). \tag{2}$$

Let $\Gamma_0(t, \mathbf{x})$ denote the total sum of propensity functions:

$$\Gamma_0(t, \mathbf{x}) = \sum_{n=1}^R p_n(t, \mathbf{x}). \tag{3}$$

In the first and second steps of the direct method, a couple of stochastic variables (τ, κ) is determined by generating two uniform random variables r_1 and r_2 . The waiting-time for the next event τ is given by

$$\tau = \frac{1}{\Gamma_0(t, \mathbf{x})} \log \left(\frac{1}{r_1} \right). \tag{4}$$

The event that will occur in the next time step is given by index κ . Then corresponding event \mathbf{R}_κ satisfies the following inequality:

$$\frac{\Gamma_{\kappa-1}(t, \mathbf{x})}{\Gamma_0(t, \mathbf{x})} < r_2 \leq \frac{\Gamma_\kappa(t, \mathbf{x})}{\Gamma_0(t, \mathbf{x})}. \tag{5}$$

In the third step of the direct method, for each event \mathbf{R}_k whether it increases or decreases the number of a population must be specified in advance.

2.3 Individual-Based Gillespie Algorithm

The assumption of randomness of event incidence prescribed in the Poisson process should be carefully examined in simulating cell dynamics. Single cell-based tracking in vitro experiments on lymphocyte clones exhibit nonexponential distribution for cell death (22, 23). Mathematical theory and framework as well as a computational algorithm that cover recent quantitative experimental findings need to be developed. In this subsection, we consider an algorithm that covers such requirement.

The individual-based Gillespie algorithm is a generalization of the original Gillespie algorithm developed in (24). The individual-based Gillespie algorithm is designed to simulate a specific type of individual-based model. The assumption that prescribed in the conventional Gillespie algorithm is that individuals in a group must be kinetically homogeneous. This assumption can be violated for a population of cells if heterogeneous gene expression profile is valid. Hence the conventional method is not directly applicable to perform stochastic simulations in particular for such cell populations.

A concise summary of the individual-based Gillespie algorithm is as follows. In the algorithm, an individual is characterized by a set of operations and variables. The latter is referred as individual state variables (*i*-state variables). Operation represents an individual behavior that is associated with population dynamics. For cell populations, execution of cell division or death is a typical operation. Propensity function is defined for an event that describes the probability of occurrence. One of typical *i*-state variables is age of an individual. For cells, the time after division is assumed as age that might be associated with the time of the next division or cell death. Age distribution of a cell population can be measured by recording times of cell division and death at the single cell level. By employing the idea of the theory for physiologically structured population models, any *i*-state variable can be considered as a function of time. Then any operation that incorporates effects of the *i*-state variable is also described as a function of time. Due to this property, the individual-based Gillespie algorithm almost resembles as an algorithmic representation of inhomogeneous Poisson processes except for the feature that the number of total events varies at every time step. In other words, a variety of nonexponential distribution for waiting-time can be represented as a time-dependent exponential distribution in the algorithm. More detailed and comprehensive description for the individual-based Gillespie algorithm can be found in (24). Schematic representation of the algorithm with remark and explanation is found in Fig. 1.

2.4 Implementation of Algorithm: Scheme

An individual needs to be assigned with one of data structures that allow having a set of individual state variables. In modern programming architectures, the simplest way for this purpose is to define a class for individual. Populations are represented as a vector/list of individuals. The algorithm itself is a variant of the conventional

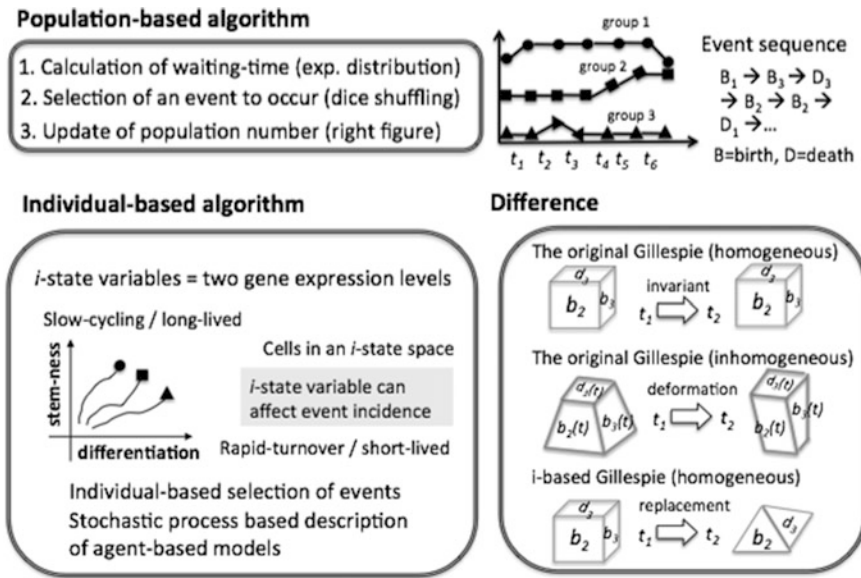


Fig. 1 Schematic representation of Gillespie algorithm. For instance, consider population dynamics of three groups each having cell division (birth) and death as events. An event sequence (*top-right*) corresponds to the type and order of events occurred (B_1 : cell division occurred in group 1, D_3 : cell death occurred in group 3). Selection of an event is determined by the second step of the Gillespie algorithm (*top-left*) which is equivalent to shuffling of an irregular-shaped dice. Each face of an R -indexed dice represents the propensity for event incidence that is proportional to the probability of the corresponding event to occur. Homogeneous Poisson processes consider constant rates of event incidence, leading to invariance of a dice in shape. On the other hand, inhomogeneous Poisson processes consider time-varying rates of event incidence that are represented by deformation of a dice. In the setting of the individual-based Gillespie algorithm, heterogeneity in a population is represented by different values of *i*-state variables. Consider a situation that self-renewal and commitment to a specific cell type via differentiation is fully determined by two master regulators (transcription factors). Self-renewal and differentiation of cells can be described as trajectories in an *i*-state space (*down-left*). If the rate of cell division is associated with differentiation process, gene expression levels of the two master regulators should be incorporated with the propensity for cell division. In the formalism of the individual-based Gillespie algorithm, the total number of events varies according to the increase or decrease of cells (groups). This variability is schematically represented as replacement of a dice: If death of a cell among the three occurs, then a four-indexed dice is used in the next selection (*down-right*)

Gillespie algorithm. Calculation of waiting-time and event selection is as same as for the conventional Gillespie algorithm. Individual states are updated every time step according to a given rule. For more details, example programming codes for C++ and python are available in Github https://github.com/petadimension/i_based_Gillespie.git.

3 Concrete Examples and Potential Applications

We introduce three topics in epidermal biology to which multiscale mathematical modeling and quantitative study are applied.

3.1 Epidermal Stem Cell Population Dynamics: Long-Term Lineage Tracing

The epidermis is composed of several layers organized by differentiated cells. Epidermal stem cells exist at the basal layer that divides the dermis and epidermis. An epidermal stem cell can produce a copy of itself by self-renewal and a progenitor cell by differentiation. Progenitor cells that have a limited number of cell division capability are called transiently amplifying cells (25). Transiently amplifying cells are believed to stay at the basal cell layer that becomes a source of differentiated epidermal cells (see (3, 25)).

Recently, inducible conditional knockout system in combination with fluorescent imaging has been used to track behavior of epidermal stem and progenitor cells in vivo for a long-term period (lineage tracing). Genetically modified mouse systems enable to obtain time-series fluorescent images of a particular cell type (having stem cell marker) upon tamoxifen administration. In (26), a new hypothesis was proposed that challenges a conventional view of epidermal stem cell biology. The authors carried out in vivo lineage tracing of epidermal stem cells at the mouse-tail. By employing a Poisson stochastic process modeling and estimation of kinetic parameters from quantitative data, the authors showed that there exists only a single progenitor cell type. Moreover, fate of stem cells in self-renewal and differentiation is demonstrated to be stochastic in (26). The probability of commitment to differentiated cells and self-renewal is kept constant in a probabilistic manner that in turn maintains epidermal homeostasis. In the following paper (27), the authors showed the same consequence in (26) for murine ear epidermis (27). In (26, 28), all cycling cells referred as committed progenitor (CP) cells that are kinetically identical and having self-renewal ability. Detailed theoretical aspects of Poisson stochastic process models are further investigated in (29–32). Quantitative lineage tracing study revealed the contribution of stochasticity in cell fate determination and maintenance of epidermal homeostasis (applications of lineage tracing on several types of stem cell compartments are summarized in a review paper (33)).

In contrast to the consequences in (26, 27) which stand for existence of a single kinetically identical cell type, existence of two distinct proliferative cell types was demonstrated by quantitative lineage tracing technique in addition to two inducible conditional knock-out mouse systems (34). On the other hand, consistent conclusion is made for stochastic fate of stem cells. In (35), the authors tested several existing hypotheses including (26, 34) by comparing simulation results produced from agent-based models. Populational asymmetry model is an alternative equivalent representation of experimental observations in (26), while populational asymmetry with stem cells (PAS) model considers the scenario demonstrated in (34). In (35), it is concluded that the hypothesis leading to the PAS model is the most feasible mechanism to represent self-renewal property of epidermal stem cells. In terms of multi-scale modeling and simulation, these studies demonstrate the

importance of stochastic cell fate as a basic mechanism underlying maintenance of epidermal homeostasis.

3.2 Repair and Mechanical Process Study

Wound healing after tissue injury is an essential dynamical process to maintain homeostasis of the tissue state. A collective motion of epithelial cells that direct to the injury site to undergo active proliferation is indicated in several experimental studies ((36) and the references therein). Emergence of collective behavior of epithelial cells under several concentrations of calcium was quantitatively analyzed in (36). A cellular potts model is employed in (36) to represent Ca^{2+} dependent spread of cells occurred within a monolayer sheet on a culture dish. In (37), maintenance mechanism of epidermal homeostasis after radiation was theoretically investigated. Histological and cell kinetics data obtained in their experiments are used in the formulation and validation of a multiscale computational model to investigate proliferative response of epidermal cells to irradiative perturbation.

Quantitative description of mechanics of the epidermis is a substantial step to precisely define skin barrier integrity (see a review paper summarizing mechanics of the epidermis (38)). However, it is in general impossible to directly measure the mechanical force among neighboring cells via noninvasive way. Statistical inference method can be used to estimate mechanical force and tension from quantitative data. In (39, 40), Bayesian statistical inference method is applied to estimate mechanical force at the epithelium tissue of *Drosophila* on the basis of noninvasive quantitative measurement. In (41), live imaging with genetic perturbation and Bayesian inference method were applied to investigate the mechanism underlying the formation and regulation of hexagonal cell packing, commonly observed at many epithelial tissues. It was shown that mechanical anisotropy in the tissue promotes ordering in hexagonal cell packing. In terms of multiscale mathematical modeling, literature introduced in this subsection provide useful computational methods to quantitatively describe epidermal mechanics by cellular dynamical and mechanical processes.

3.3 Skin Inflammatory Disease and Gene Regulatory Network Study

Atopic dermatitis is a skin inflammatory disease that is triggered by barrier dysfunction and impaired immune responses. Filaggrin is a major source of natural moisture factors that exist at the stratum corneum. After the finding of filaggrin genetic deficiency as a major factor of the onset and progression of atopic dermatitis, dysfunction of epidermal barrier function is considered as a primary step that leads to skin barrier defect (42). Claudin is one of the major integral transmembrane components of tight junctions formed at the second layer of stratum granulosum (43). Over-expression of claudin 6 is shown to induce abnormal terminal differentiation of the epidermis, and dysfunction of epidermal permeability barrier (43–45). Over-expression of kallikrein (KLK), a member of the

serine protease family, is suggested to be a major triggering factor that induces disruption of the skin barrier by promoting desquamation of the stratum corneum layer. PAR2 is a member of the proteinase-activated receptor (PAR) family that induces immune response characterized by Th2 type allergic reaction. Over-activation of PAR2 and thymic stromal lymphopoietin (TSLP) via hyper-activation of KLK5 is reported on patients of the Netherton syndrome (46), a recessive genetic deficiency lacking SPINK5 as an inhibitor of KLK5 (47). Hence activation of KLK, PAR2, and TSLP is suggested to play a role in the pathogenesis of atopic dermatitis.

A mathematical model describing KLK and PAR2 interactions is proposed to investigate the onset and progression of atopic dermatitis (48). A system of ordinary differential equations is employed to represent an abrupt change of the skin tissue toward disease state. This abrupt change is explained by positive feedback regulation of KLK activity. The model proposed in (48) is further extended to include cellular dynamics at the tissue level (49). Dynamics of KLK activity studied in (48) is combined with tissue dynamics to investigate the effect of cellular level dynamics on the tissue level dynamics. A variable at the tissue level model is used as a measure of skin barrier integrity. Effects of excess protease activity and inflammation on the skin barrier integrity are examined by numerical computations.

Maintenance of homeostasis and disease progression can be regarded as two sides of the same coin: disruption or impairment of machinery underlying the maintenance of homeostasis results in abnormal tissue state. The literature introduced in this subsection show the importance of systems perspective on the onset of atopic dermatitis: switching is given risen from interactions among key genes and molecules. The idea of genetic circuit and network motif is extensively used to interpret gene regulatory network in the research field of systems biology. Although careful consideration should be made whether an abnormality in a gene regulatory network directly triggers disruption of the skin barrier, simple and clear explanation can help to demystify inherently complex disease progression.

4 Concluding Remarks and Future Perspectives

Multiscale modeling and simulations provide theoretical prediction on dynamical process at the tissue level by integrating several dynamical processes at different spatiotemporal time scales. Specification to a stochastic process-based agent-based modeling is emphasized to ensure verifiability of subsystems with quantitative data. Multiscale modeling and simulation aiming to discover emergent complexity at the tissue level is expected to bring understanding of homeostasis that is generically determined by system behavior rather than by a single molecule or cell behavior.

To understand the onset of disease as a structural change in a system, it is crucial to identify predisposing factors that would initiate and trigger deviation from a stable normal state. A theory for dynamical network biomarkers can be applied to detect pre-disease state that characterizes the critical transition from health to disease state (50). A time-series dataset for gene expression profile is adopted to identify a set of genes that is significantly up- or downregulated at the pre-disease state. Application of multiscale modeling and simulation is expected to fill a gap between predisposing factors and actual dynamical transition to a disease state. Molecular, cellular, or biological functions of the genes screened via the application of dynamical network biomarker theory can be used to make a working hypothesis for modeling and simulation. In terms of atopic dermatitis study, dynamical process of barrier impairment due to excessive protease activity is an important target of this approach.

Applications of multiscale mathematical modeling and simulation have a long history in cancer research (7). An emergence property was identified by interdisciplinary experimental and computational work on self-organized spatial group formation of tumor infiltrating macrophages that is shaped by inhibitory effects of tumor producing lactose on macrophage survival (51). Although all existing literature introduced in Section 3 are directly or in part related to multiscale modeling and simulations in epidermal biology, more research activities are necessary to cover another important aspects of skin tissue homeostasis. Integration of experimental works on the basis of multiscale modeling and simulation could provide a unified understanding of the biological role of the epidermis in health and disease. Promotion of this research direction requires substantial collaborative works aiming to solve specific biological problems in epidermal biology that in turn facilitate construction of dependable multiscale mathematical models.

Acknowledgment

This research was partly supported by Aihara Innovative Mathematical Modelling Project, JSPS through its “Funding Program for World-Leading Innovative R&D on Science and Technology (FIRST Program)” and “Grant-in-Aid for Young Scientists B25871132.”

References

1. Gallo RL, Hooper LV (2012) Epithelial antimicrobial defence of the skin and intestine. *Nat Rev Immunol* 12:503–516
2. Nestle FO, Kaplan DH, Barker J (2009) Psoriasis. *New Engl J Med* 361:496–509
3. Blanpain C, Fuchs E (2009) Epidermal homeostasis: a balancing act of stem cells in the skin. *Nat Rev Mol Cell Biol* 10:207–217
4. Tata PR, Mou H, Pardo-Saganta A, Zhao R, Prabhu M, Law BM, Vinarsky V, Cho JL,

- Breton S, Sahay A, Medoff BD, Rajagopal J (2013) Dedifferentiation of committed epithelial cells into stem cells in vivo. *Nature* 503:218–223
5. Kitano H (2007) Towards a theory of biological robustness. *Mol Syst Biol* 3:137
 6. Weinan E (2011) Principles of multiscale modeling. Cambridge University Press, Cambridge
 7. Cristini V, Lowengrub J (2010) Multiscale modeling of cancer: an integrated experimental and mathematical modeling approach. Cambridge University Press, Cambridge
 8. Jensen HJ (1998) Self-organized criticality: emergent complex behavior in physical and biological systems. Cambridge University Press, Cambridge
 9. Greenfield D, McEvoy AL, Shroff H, Crooks GE, Wingreen NS, Betzig E, Liphardt J (2009) Self-organization of the *Escherichia coli* chemotaxis network imaged with super-resolution light microscopy. *PLoS Biol* 7:e1000137
 10. Ellner SP, Guckenheimer J (2006) Dynamic models in biology. Princeton University Press, Princeton
 11. Railsback SF, Grimm V (2011) Agent-based and individual-based modeling: a practical introduction. Princeton University Press, Princeton
 12. Wilensky U (1999) NetLogo: center for connected learning and computer-based modeling. Northwestern University, Evanston
 13. Taniguchi Y, Choi PJ, Li GW, Chen H, Babu M, Hearn J, Emili A, Xie XS (2010) Quantifying *E. coli* proteome and transcriptome with single-molecule sensitivity in single cells. *Science* 329:533–538
 14. Kaern M, Elston TC, Blake WJ, Collins JJ (2005) Stochasticity in gene expression: from theories to phenotypes. *Nat Rev Genet* 6:451–464
 15. Hamilton DT, Handcock MS, Morris M (2008) Degree distributions in sexual networks: a framework for evaluating evidence. *Sex Transm Dis* 35:30–40
 16. Barabasi A-L, Albert R (1999) Emergence of scaling in random networks. *Science* 286:509–512
 17. Gillespie DT (1992) A rigorous derivation of the chemical master equation. *Physica A* 188:404–425
 18. Gillespie DT (2000) The chemical Langevin equation. *J Chem Phys* 113:297–306
 19. Gillespie DT (2007) Stochastic simulation of chemical kinetics. *Annu Rev Phys Chem* 58:35–55
 20. Gillespie DT (1976) A general method for numerically simulation the stochastic time evolution of coupled chemical reactions. *J Comput Phys* 22:403–434
 21. Gillespie DT (1977) Exact stochastic simulation of coupled chemical reactions. *J Phys Chem* 81:2340–2360
 22. Hawkins ED, Turner ML, Dowling MR, van Gend C, Hodgkin PD (2007) A model of immune regulation as a consequence of randomized lymphocyte division and death times. *Proc Natl Acad Sci U S A* 104:5032–5037
 23. Hawkins ED, Markham JF, McGuinness LP, Hodgkin PD (2009) A single-cell pedigree analysis of alternative stochastic lymphocyte fates. *Proc Natl Acad Sci U S A* 106:13457–13462
 24. Nakaoka S, Aihara K (2013) Stochastic simulation of structured skin cell population dynamics. *J Math Biol* 66:807–835
 25. Blanpain C, Horsley V, Fuchs E (2007) Epithelial stem cells: turning over new leaves. *Cell* 128:445–458
 26. Clayton E, Doupé DP, Klein AM, Winton DJ, Simons BD, Jones PH (2007) A single type of progenitor cell maintains normal epidermis. *Nature* 446:185–189
 27. Doupé DP, Jones PH (2012) Interfollicular epidermal homeostasis: dicing with differentiation. *Exp Dermatol* 21:249–253
 28. Doupé DP, Klein AM, Simons BD, Jones PH (2010) The ordered architecture of murine ear epidermis is maintained by progenitor cells with random fate. *Dev Cell* 18:317–323
 29. Klein AM, Doupé DP, Jones PH, Simons BD (2007) Kinetics of cell division in epidermal maintenance. *Phys Rev E Stat Nonlin Soft Matter Phys* 76:021910
 30. Klein AM, Doupé DP, Jones PH, Simons BD (2008) Mechanism of murine epidermal maintenance: cell division and the voter model. *Phys Rev E Stat Nonlin Soft Matter Phys* 77:031907
 31. Antal T, Krapivsky PL (2010) Exact solution of a two-type branching process: clone size distribution in cell division kinetics. *J Stat Mech Theor Exp* 2010, P07028
 32. Antal T, Krapivsky PL (2011) Exact solution of a two-type branching process: models of tumor progression. *J Stat Mech Theor Exp* 2010, P08018
 33. Blanpain C, Simons BD (2013) Unravelling stem cell dynamics by lineage tracing. *Nat Rev Mol Cell Biol* 14:489–502
 34. Mascré G, Dekoninck S, Drogat B, Youssef KK, Brohéé S, Sotiropoulou PA, Simons BD, Blanpain C (2012) Distinct contribution of stem

- and progenitor cells to epidermal maintenance. *Nature* 489:257–262
35. Li X, Upadhyay AK, Bullock AJ, Dicolandrea T, Xu J, Binder RL, Robinson MK, Finlay DR, Mills KJ, Bascom CC, Kelling CK, Isfort RJ, Haycock JW, MacNeil S, Smallwood RH (2013) Skin stem cell hypotheses and long term clone survival—explored using agent-based modelling. *Sci Rep* 3:1904
 36. Hirashima T, Hosokawa Y, Iino T, Nagayama M (2013) On fundamental cellular processes for emergence of collective epithelial movement. *Biol Open* 2:660–666
 37. Cucinotta F (2013) Epidermal homeostasis and radiation responses in a multiscale tissue modeling framework. *Integr Biol (Camb)* 6:76–89
 38. Guillot C, Lecuit T (2013) Mechanics of epithelial tissue homeostasis and morphogenesis. *Science* 340:1185–1189
 39. Ishihara S, Sugimura K (2012) Bayesian inference of force dynamics during morphogenesis. *J Theor Biol* 313:201–211
 40. Ishihara S, Sugimura K, Cox SJ, Bonnet I, Bellaïche Y, Graner F (2013) Comparative study of non-invasive force and stress inference methods in tissue. *Eur Phys J E Soft Matter* 36:9859
 41. Sugimura K, Ishihara S (2013) The mechanical anisotropy in a tissue promotes ordering in hexagonal cell packing. *Development* 140:4091–4101
 42. Irvine AD, McLean WHI, Leung DYM (2011) Filaggrin mutations associated with skin and allergic diseases. *N Engl J Med* 365:1315–1327
 43. Kubo A, Nagao K, Amagai M (2012) Epidermal barrier dysfunction and cutaneous sensitization in atopic diseases. *J Clin Invest* 122(2):440–447
 44. Turksen K, Troy T-C (2002) Permeability barrier dysfunction in transgenic mice overexpressing claudin 6. *Development* 129:1775–1784
 45. Troy T-C, Arabzadeh A, Larivière NMK, Enikanolaiye A, Turksen K (2009) Dermatitis and aging-related barrier dysfunction in transgenic mice overexpressing an epidermal-targeted Claudin 6 tail deletion mutant. *PLoS ONE* 4(11):1–10
 46. Briot A, Deraison C, Lacroix M, Bonnart C, Robin A, Besson C, Dubus P, Hovnanian A (2009) Kallikrein 5 induces atopic dermatitis-like lesions through PAR2-mediated thymic stromal lymphopoietin expression in Netherton syndrome. *J Exp Med* 206:1135–1147
 47. Hachem J-P, Wagberg F, Schmuth M, Crumrine D, Lissens W, Jayakumar A, Houben E, Mauro TM, Leonardsson G, Brattsand M, Egelrud T, Roseeuw D, Clayman GL, Feingold KR, Williams ML, Elias PM (2006) Serine protease activity and residual LEKTI expression determine phenotype in Netherton syndrome. *J Invest Dermatol* 126:1609–1621
 48. Tanaka RJ, Ono M, Harrington HA (2011) Skin barrier homeostasis in atopic dermatitis: feedback regulation of kallikrein activity. *PLoS One* 6:e19895
 49. Domínguez-Hütinger E, Ono M, Barahona M, Tanaka RJ (2013) Risk factor-dependent dynamics of atopic dermatitis: modelling multi-scale regulation of epithelium homeostasis. *Interface Focus* 3:20120090
 50. Chen L, Liu R, Liu Z-P, Li M, Aihara K (2012) Detecting early-warning signals for sudden deterioration of complex diseases by dynamical network biomarkers. *Sci Rep* 2:342
 51. Carmona-Fontaine C, Bucci V, Akkari L, Deforet M, Joyce JA, Xavier JB (2013) Emergence of spatial structure in the tumor microenvironment due to the Warburg effect. *Proc Natl Acad Sci U S A* 110:19402–19407

Erratum to: Differentiation of Human Induced Pluripotent Stem Cells into a Keratinocyte Lineage

Igor Kogut, Dennis R. Roop, and Ganna Bilousova

Erratum to: Methods in Molecular Biology
DOI: 10.1007/7651_2013_64

Please note the correction to the above mentioned chapter:

The stock and working concentrations of human BMP4 were erroneously indicated as 25 $\mu\text{g}/\mu\text{l}$ and 25 $\text{ng}/\mu\text{l}$ respectively. The correct stock concentration should be 25 $\mu\text{g}/\text{mL}$, and the final working concentration of BMP4 in DKSFM for differentiation should be 25 ng/mL .

As a result of this error, the following corrections should be made:

- In section “**2.3 Differentiation of iPSCs with RA and BMP4**”, Subsection 2. should read: “2. 25 $\mu\text{g}/\text{mL}$ stock solution of human BMP4 (R&D Systems) reconstituted in sterile 4 mM HCL containing 0.1% BSA.”
- In section “**3.3 Differentiation of iPSCs with RA and BMP4**”:

Subsection 2 should read: “2. Add 5 mL of prewarmed DKSFM from the previous step to a 15 mL conical tube, add 5 μL of 1 mM RA to achieve 1 μM final working concentration and 5 μL of 25 $\mu\text{g}/\text{mL}$ BMP4 to achieve 25 ng/mL final working concentration, mix well.”

Subsection 3 should read: “3. Aspirate off N2B27 medium from the dish with plated iPSCs, wash once with 4 mL of 1 x PBS, and add 4 mL of DKSFM containing 1 μM RA and 25 ng/mL BMP4 from the step above. This is day 1 of differentiation procedure.”

Subsection 5 should read: “5. Replace the medium with fresh DKSFM containing 1 μM RA and 25 ng/mL BMP4 after 48 h of incubation. Transfer the cell to the incubator for another 48 h.”

We apologize for any confusion caused by this error.

Erratum to: Reactive Oxygen Species (ROS) Protection via Cysteine Oxidation in the Epidermal Cornified Cell Envelope

Wilbert P. Vermeij and Claude Backendorf

Erratum to: Methods in Molecular Biology
DOI: 10.1007/7651_2013_51

Name and affiliation for the first author, Dr. Wilbert P. Vermeij, are missing in the online version.

The missing details are:

Department of Genetics, Erasmus University Medical Center,
Dr. Molewaterplein 50, 3015GE Rotterdam, The Netherlands

Erratum to: Human Keratinocyte Cultures in the Investigation of Early Steps of Human Papillomavirus Infection

Laura M. Griffin, Louis Cicchini, Tao Xu, and Dohun Pyeon

Erratum to: Methods in Molecular Biology
DOI: 10.1007/7651_2013_49

The name and affiliation of the first three authors are missing in the online version.
The missing details are:

Laura M. Griffin, Louis Cicchini and Tao Xu

Department of Microbiology, University of Colorado
School of Medicine, Aurora, CO, 80045, USA

INDEX

A

- Activin 18
- Adenovirus vectors
 - arginine–glycine–aspartic acid 43–44
 - coxsackie and adenovirus receptor 43–44
 - keratinocyte transgene delivery 43–44
 - cell seeding and infection 45–46
 - materials 44–45
 - reagents 44–45
 - reporter gene expression detection 46
- Affymetrix arrays 66, 67, 69–71, 79, 80, 92
- Agent-based modeling 278, 280
 - Gillespie algorithm 274
 - stochastic simulation algorithm 272–273
- Anatomically complete autologous cultured epidermis (A-CEA) 1
 - biopsy procedures 214
 - to chronic wounds 214–215
 - clinical performance 215
 - formation 211–212
 - post-production procedures 214
- Anoikis 187, 188
- ArrayExpress 67–69
- Atopic dermatitis 280
- Autogenic co-culture (ACC) system 17–19
- Autografts
 - CEAs 204, 211–213
 - serum-free medium (*see* Serum-free medium)

B

- Basal nutrient medium, HECK-109 208–209
- Bone-morphogenetic protein-4 (BMP4) 2, 3, 5–7

C

- Calcitriol 99
- Caveolae 134
- Caveolin 134, 135, 139
- CE *See* Cornified cell envelope (CE)
- Cell aggregates
 - embedded in collagen gel 184, 186, 187
 - experimental procedure 186
 - immunocytochemical analysis 189
 - morphological appearance 188
 - preparation 184–186
 - staining 185
- Chemically defined medium 204
- Chromatin extraction, MNase 53–55

- Chronic wounds, A-CEA to 214–215
- Clonal growth 212–214
- Collagen type I (Coll), iPSCs on 2–4
- Cornified cell envelope (CE)
 - oxidation-selective cysteine labeling 164–165
 - preparation 165
 - ROS and (*see* Reactive oxygen species (ROS))
- Coxsackie and adenovirus receptor (CAR) 43–44
- CreER^T transgenic mice, hair follicles 247–248, 250–251
- Cremophor[®] EL, 4-hydroxy-tamoxifen in 239, 242–244
- Cre-recombinase, hair follicles 248, 250, 252–253
- Cultured epidermal autografts (CEAs) 204, 211–213

D

- Darier's disease (DD) 192, 197–198
- Database for Annotation Visualization and Integrated Discovery (DAVID) program 82, 92
 - analysis 83
 - Functional Annotation Chart 89–90
 - outputs from 85–88
 - tools 84
 - transcription factor binding 83
- De-epidermalized dermis (DED)
 - preparation 173–175
 - skin reconstitution on 173, 176–177
- Detergent-resistant membranes, in epithelial keratinocytes 133–141

DNA

- collection, mononucleosomal 53–54, 56
- precipitation, MNase 53, 55–56

E

- Embryonic stem cell (ESC) 1
- Enzymes
 - serial cultivation of epithelial cells without 23–25
 - cultivation 23–25
 - monolayer culture 23–24, 28, 29, 31, 32
 - mucosa keratinocyte culture 30
 - pop-up cells 24
 - primary culture 25–28
 - reconstituted cultivation 28
 - serial cultivation 26, 28–30
 - suspension culture 23–24
 - serine proteases 153
- Epidermal homeostasis
 - aspects 274

Epidermal homeostasis (*cont.*)
 maintenance 278–279
 systems perspective on 269–270

Epidermal stem cells 278–279

Epidermis 111–113

 differentiation
 DNA microarray 63
 from hESC (*see* Human embryonic stem cell-derived keratinocytes (hESCs-Kert))
 three-dimensional cell culture (*see* Three-dimensional cell culture)

 experimental procedure
 and lipid extraction 127
 and phospholipids extraction 122–124

 keratinocytes 204

 layers, separation 64

 phosphatidic acid 113, 122, 125

 phosphatidylglycerol production
 measurement 127–128

 phospholipase D 113–115
 materials for 116–117

 primary keratinocyte preparation
 materials for 115–116
 from mouse 117–120
 from tail of adult mouse 120–122

 reconstruction
 Darier's disease 192, 197–198
 histological analysis of 194, 197, 199
 in-house production 192
 on polycarbonate filter 194
 protein extraction 194, 198–199
 RNA extraction 197–198

 schematic representation 111–113

 thin-layer chromatography 124–127

 transcriptional profiling (*see* Transcriptional profiling, in human epidermis)

Epithelial keratinocytes, lipid raft isolation of 133–137

 antibodies 138

 buffers 138

 caveolae 134

 caveolin 134, 135, 139

 cell culture 139

 cholesterol depletion 139

 disruption of caveolin association 139

 equipment 138

 membrane microdomains 133

 preparation 139–140

 proteins characterization 140–141

 reagents 138

 scaffolding domain peptide 139

F

FACS analysis, epidermal cell staining for 264–266

Filaggrin 279

Fluorescent protein
 GFP 43, 44, 46, 47, 222
 reporter gene detection 255

Formaldehyde treatment, MNase 52, 54

G

GCOS and RMAExpress, integrating results 76–78

Gelatinase 145

Gelatin zymography 146–148

Geltrex, coating tissue culture dishes with 3, 4

Gene Expression Omnibus (GEO) 67

Gene regulatory network study 279–280

Genetic redundancy 270

Gillespie algorithm 274–275
 implementation 276–277
 individual-based 276
 schematic representation 277

Green fluorescent protein (GFP) 43, 44, 46, 47, 222

H

HaCaT keratinocytes 221, 225, 229

 in collagen gels 187

 growth and differentiation 33–34
 basal, verification 37–39
 calcium induction 34, 37
 cell culture components 34–35
 induction 36–37
 low-calcium conditions 35–36
 phenotype verification components 35

Hair follicles (HFs)

 BCRP1/ABCG2 260

 bulge region 259, 265

 epidermal cell
 isolation from mouse epidermis 261–263
 staining for FACS analysis 264–266

 for lineage tracing
 clonal analysis 247, 252–253
 CreER^T transgenic mice 247–248, 250–251
 Cre-recombinase 248, 250–253
 fluorescent protein 255
 LacZ clones observation 256–257
 microdissection 255
 mouse anaesthesia 247–248, 251
 Rosa26^{CreERT2} 250–251
 sample biopsies and fixation 253–254
 synchronization cycles 251–252
 tools and equipment 249–250
 treatment with 4-OHT 252–253
 X-Gal 248–249, 254–255

 side-population from 259
 epidermal cell isolation 261–263
 FACS analysis 264–266
 Hoechst staining 264–266
 instruments and supplies 260–261

reagents 261
solutions 260

HFKs *See* Human foreskin keratinocytes (HFKs)

Hoechst staining 264–266

HPVs *See* Human papillomaviruses (HPVs)

Human embryonic stem cell-derived keratinocytes
(hESCs-Kert) 13

 activin 18

 autogenic microenvironment for 17

 cell culture and differentiation 14, 16–18

 differentiation and characterization 19

 flow cytometry 14–16, 19–21

 immunofluorescence staining 14–16, 19–21

 phase-contrast images 17

 real-time RT-PCR 14, 18–20

 reverse transcriptase-polymerase chain reaction
analysis 14, 18–20

Human foreskin keratinocytes (HFKs) 221–223, 227

Human keratinocytes 191

 in HECK 109 serum-free medium 212–214

 human papillomaviruses

 gene knockdown and overexpression 225–226,
229–232

 HaCaT cells 225

 lentiviruses for transducing 225–226, 229–231

 NIKS 221, 223–225, 227–229

 primary human foreskin keratinocytes 222–223,
227

 transduction 226, 231

 transfection 226, 231–232

 primary culture 193–195

 reconstructed human epidermis

 Darier’s disease 192, 197–198

 histological analysis of 194, 197, 199

 in-house production 192

 on polycarbonate filter 194

 protein extraction 194, 198–199

 RNA extraction 197–198

Human papillomaviruses (HPVs) 219

 infectivity assay 226–227, 232–234

 keratinocyte

 gene knockdown and overexpression 225–226,
229–232

 HaCaT cells 225

 lentiviruses for transducing 225–226, 229–231

 NIKS 221, 223–225, 227–229

 primary human foreskin keratinocytes 222–223,
227

 transduction 226, 231

 transfection 226, 231–232

 puromycin-resistant cells selection 226, 232

4-Hydroxy-tamoxifen 239

 in Cremophor® EL 239, 242–244

 injected according to mouse weight 242, 243

injection solution

 high-dose 242

 low-dose 241

 preparation 241

iv/ip injection 241–244

materials 240

 stock solution preparation 240–241

Hypercalcemia 99

I

Induced pluripotent stem cells (iPSCs)

 on collagen type I 2–4

 differentiation of BMP4 3, 5–7

 into keratinocytes 1–2

 coating tissue culture dishes with Geltrex and
ColI 3, 4

 differentiation of RA and BMP4 3, 5–7

 equipment 3

 plating for differentiation 3–5

 rapid attachment and culturing 3, 7–9

 RA differentiation of 3, 5–7

K

Keratinocytes 183

 basal layer, isolation 64

 chromatin structure by MNase (*see* Micrococcal nuclease
(MNase), keratinocytes chromatin structure) 29

 cobblestone 29

 cultivation 23–25

 reconstituted 28

 serial 26, 28–30

 differentiation 188

 growth and isolation 63

 HaCaT 221, 225, 229

 HPV16-LucF infectivity 220

 human papillomaviruses

 gene knockdown and overexpression 225–226,
229–232

 HaCaT cells 225

 lentiviruses for transducing 225–226, 229–231

 NIKS 221, 223–225, 227–229

 primary human foreskin keratinocytes 222–223,
227

 transduction 226, 231

 transfection 226, 231–232

 iPSCs into (*see* Induced pluripotent stem cells (iPSCs),
into keratinocytes) 65–66

 isolation of β 4+ and β 4- 145–154

 MMP-2,-9 and TIMP-1,-2 assays in 28–30

 passaging 28

 pop-up 25–28

 primary culture 25–28

 proliferative potential 214

Keratinocytes 183 (*cont.*)
 surface area 31
 transgene delivery, adenovirus vectors 43–44
 cell seeding and infection 45–46
 polycation 44
 reagents 44–45
 reporter gene expression detection 46
 transduction efficiency 46
 viral vectors 44

L

Lentivirus
 infection 222
 packaging plasmids 225
 for transducing keratinocytes 225–226, 229–231
 Lineage tracing, hair follicles for
 clonal analysis 247, 252–253
 CreER^T transgenic mice 247–248, 250–251
 Cre-recombinase 248, 250–253
 detection of reporter gene
 fluorescent protein 255
 X-Gal staining 254–255
 fluorescent protein 255
 LacZ clones observation
 with brightfield microscope 256
 with confocal microscope 256–257
 microdissection 255
 mouse anaesthesia 247–248, 251
 Rosa26^{CreERT2} 250–251
 sample biopsies and fixation 253–254
 synchronization cycles 251–252
 tools and equipment 249–250
 treatment with 4-OHT 252–253
 X-Gal
 preparation 248–249
 staining 254–255
 Lipid rafts
 adhesion proteins and 136
 biochemical techniques for 137
 in epithelial keratinocytes 133
 antibodies 138
 buffers 138
 caveolae 134
 caveolin 134, 135, 139
 cell culture 139
 cells 139
 cholesterol depletion 139
 disruption of caveolin association 139
 equipment 138
 membrane microdomains 133
 preparation 139–140
 proteins characterization 140–141
 reagents 138
 scaffolding domain peptide 139
 Lists2Networks algorithm 90

M

Mallory's trichrome-staine 213
 Matrix metalloproteinases (MMPs)-2,-9 145–146
 gelatin zymography 146–148
 reverse zymography 146, 148–149
 Western blotting analysis 146–147, 149–151
 Mechanistic mathematical model 271–272
 Membrane microdomains 133
 Methyl- β -cyclodextrin (M β CD) 134, 135
 Micrococcal nuclease (MNase), keratinocytes
 chromatin structure 49–52
 chromatin extraction 53–55
 cross-linking 52–54
 digestion 53, 55
 DNA precipitation 53, 55–56
 formaldehyde treatment 52, 54
 high-throughput sequencing 53–54, 56
 mononucleosomal DNA collection 53–54, 56
 nucleosomes 49–52, 57
 proteinase 53, 55–56
 RNase treatment 53, 55–56
 Mouse hair follicles (HFs)
 See Hair follicles (HFs)
 Multiscale mathematical modeling
 agent-based simulation 272–273
 atopic dermatitis 280
 epidermal homeostasis
 aspects 274
 maintenance 278–279
 systems perspective on 269–270
 gene regulatory network study 279–280
 Gillespie algorithm 274–275
 implementation 276–277
 individual-based 276
 schematic representation 277
 long-term lineage tracing 278
 mechanical process study 279
 organization 274
 phenomenological *vs.* mechanistic 271–272
 poisson process 273, 274, 276–278
 quantitative biology 272–274, 276–279
 repair process 269, 279
 and simulation
 coherency 270–271
 emergent complexity 271
 perspectives 280–281
 verifiability 270
 skin inflammatory disease 279–280

N

NIKS *See* Normal immortalized keratinocytes (NIKS)
 Nonfat dried milk solution (NFDMS) 38
 Nonparametric approach 81

Normal immortalized keratinocytes (NIKS) 221,
 223–225, 227–229
 Nucleosomes, MNase 49–52, 57
 Nutrient basal medium, HECK-109 208–209

O

Ontological categories 82–84, 89
 Orbitrap tandem mass spectrometry 164
 Oxidation-sensitive cysteine residues 159
 in isolated CEs 164–165
 in purified proteins 163–164
 Oxidative stress 157

P

Phenomenological mathematical model 271–272
 Phosphatidic acid (PA) 113, 122, 125
 Phosphatidylglycerol, production measurement 127–128
 Phospholipase D (PLD) 113–115
 activity assay 122–127
 experimental procedure
 and extraction of phospholipids 122–124
 and lipid extraction 127
 in keratinocytes 114–115
 materials for 116–117
 PA 113, 122, 125
 phosphatidylglycerol production
 measurement 127–128
 primary keratinocyte preparation
 materials for 115–116
 from mouse 117–120
 from tail of adult mouse 120–122
 thin-layer chromatography
 lipids separation 124–127
 separation 127–128
 Poisson process 273, 274, 276–278
 Polycarbonate filter, RHE *See* Reconstructed human
 epidermis (RHE)
 Primary epidermal keratinocyte propagation 173,
 175–176
 Primary keratinocyte culturing
 compound screening and transcriptional
 profiling 99–102
 calcitriol 99
 confirmatory quantitative real-time PCR... 105–106
 cultivation 102–103
 cytotoxicity assessment 104
 cytotoxicity evaluation 100
 hypercalcemia 99
 materials 102
 microarray assessment 105
 MTT assay 104
 RNA isolation from 104–105
 SFM medium 102, 103
 splitting, passaging, and eventual
 cryopreservation 103

with sub-toxic compound doses 104
 RNA isolation from 104–105
 Proteinase, MNase 53, 55–56
 Puromycin-resistant cells 226, 232

R

RA *See* Retinoic acid (RA)
 RankProd, meta-analysis using 81–82
 Reactive oxygen species (ROS) 157–158
 CE preparation 165
 in-solution tryptic digestion for MS analysis 165
 oxidation-sensitive cysteine residues 159
 in isolated CEs 164–165
 in purified proteins 163–164
 redox state
 imaging 158–159
 sensitive protein interaction 160, 165–166
 in situ imaging of skin specimens 160–161
 SPRR protein 158
 production 159, 162
 purification 159, 162–163
 tryptic digestion 159–160
 Real-time reverse transcriptase-polymerase chain reaction
 (RT-PCR) 14, 18–20, 105–106
 Reconstructed human epidermis (RHE)
 Darier's disease 192, 197–198
 histological analysis of 194, 197, 199
 in-house production 192
 on polycarbonate filter 194
 protein extraction 194, 198–199
 RNA extraction 197–198
 Redox state
 imaging 158–159
 sensitive protein interaction 160, 165–166
 in situ imaging of skin specimens 160–161
 Retinoic acid (RA) 2, 3, 5–7
 Reverse zymography 146, 148–149
 RHE *See* Reconstructed human epidermis (RHE)
 RMAExpress 71–74, 76–78
 RNA isolation 64, 66, 104–105
 RNase treatment 53, 55–56
 ROS *See* Reactive oxygen species (ROS)
 Rosa26^{CreERT2}, hair follicles 250–251

S

Serial cultivation of epithelial cells 23–25
 keratinocytes
 cultivation 23–25
 primary culture 25–28
 reconstituted cultivation 28
 serial cultivation 26, 28–30
 monolayer culture 23–24, 28, 29, 31, 32
 mucosa keratinocyte culture 30
 pop-up cells 24
 suspension culture 23–24

Serum-free medium205, 207, 211, 216
 A-CEA
 biopsy procedures 214
 to chronic wounds214–215
 clinical performance 215
 formation211–212
 post-production procedures 214
 adult skin samples205
 beta-TGF 205, 211, 216
 biological dressings 203–204
 chemicals source 205
 clonal growth assay method 212–214
 HECK 109
 human keratinocytes212–214
 preparation205–209
 insulin-like growth factor-1205, 207, 211, 216
 primary cultures
 freezing keratinocyte cells from..... 210
 preparation209–210
 secondary cultures preparation..... 210–211
 Side-population from hair follicles259
 Hoechst staining 264–266
 instruments and supplies 260–261
 reagents261
 solutions260
 3-D skin equivalents 171–172
 Skin inflammatory disease..... 279–280
 Skinomics63
 Small proline-rich (SPRR) proteins 158
 production 159, 162
 purification159, 162–163

T

Tamoxifen *See* 4-Hydroxy-tamoxifen
 Thin-layer chromatography (TLC)
 lipids separation..... 124–127
 separation..... 127–128
 Three-dimensional cell culture
 advantage 184
 analyses 184
 antibody analysis 185
 cell aggregates
 embedded in collagen gel 184, 186
 experimental procedure 186
 immunocytochemical analysis 189
 morphological appearance 188
 preparation184–186
 staining of 185

 histochemical analysis..... 187–188
 Western blotting analysis184–185, 187
 Tissue inhibitors of metalloproteinases
 (TIMPs)-1,-2 145–146
 gelatin zymography 146–148
 reverse zymography146, 148–149
 Western blotting analysis 146–147, 149–151
 Transcriptional profiling, in human epidermis61–63
 Affymetrix arrays 66, 67, 69–71, 79, 80, 92
 ArrayExpress67–69
 bioinformatics..... 62
 data files, downloading71–76
 data subsets, selecting 80
 DAVID program82–90
 DNA microarray 62
 empty cells 80
 GCOS76–78
 gene lists
 annotation82–90
 clustering and comparison90–92
 comparing regulated 90
 growth of keratinocytes 63
 isolation
 of basal layer keratinocytes 64
 of keratinocytes 63
 of β 4+ and β 4- keratinocytes from skin 65–66
 of total RNA.....64, 66
 Lists2Networks algorithm 90
 meta-analysis
 cross-referencing and merging79–80
 public repositories for67–71
 MIAMI rules 62
 negative numbers 80
 oPOSSUM analysis92–93
 preparation of labeled probes, and hybridization ... 64
 promoter analysis92–95
 provenance and maintenance 65
 RankProd, meta-analysis using..... 81–82
 RMAExpress71–74, 76–78
 separation of epidermal layers 64

W

Western blotting analysis 146–147, 149–151,
 184–185, 187

X

X-Gal..... 248–249, 254–255